# Catalyst and Monomer Design: Targeting Polymer Properties *via* Organic Catalysed Ring Opening Polymerisation

Richard Todd, MChem

A thesis submitted in partial fulfilment
of the requirements for the degree of:

Doctor of Philosophy in Chemistry

October 2013

THE UNIVERSITY OF
WARWICK

# Table of Contents

# List of Figures

# List of Schemes

# List of Tables

# Abbreviations

| | |
|---|---|
| ACE | Activated chain end mechanism |
| AIBN | Azobisisobutyronitrile |
| AM | Activated monomer mechanism |
| $\delta$ | Chemical shift |
| BEMP | 2-Tert-Butylimino-2-diethylamino-1,3-dimethylperhydro-1,3,2-diazaphosphorine |
| *bis*-MPA | Bis(hydroxylmethyl)propionic acid |
| β-Me7CC | 5-Methyl-1,3-dioxepan-2-one |
| CDI | 1,1'-Carbonyliimidazole |
| CL | $\varepsilon$-Caprolactone |
| DBU | 1,8-Diazabicyclo[5.4.0]undec-7-ene |
| DCM | Dichloromethane |
| DLA | *D*-Lactide |
| $Đ_M$ | Dispersity |
| DMAP | 4-Dimethylaminopyridine |
| DMF | Dimethyl formamide |
| dMMLABz | [R,S]-4-benzylcarbonyl-3,3-dimethyl-2-oxetanone |
| DMSO | Dimethyl sulfoxide |

| | |
|---|---|
| DP | Degree of polymerisation |
| DPP | Diphenyl phosphate |
| DRI | Differential refractive index |
| DSC | Differential scanning calorimetry |
| $f$ | Molar fraction of monomer in the feed |
| $F$ | Molar fraction of monomer in the polymer |
| GPC | Gel permeation chromatography |
| HOTf | Trifluoromethanesulfonic acid |
| ICD | β-Isocupreidine |
| $k$ | Rate constant |
| $k_{app}$ | Apparent rate constant |
| LA | Lactide |
| lacOCA | 5-Methyl-1,3-dioxolane-2,4-dione |
| LLA | *L*-Lactide |
| $M_n$ | Number-averaged molecular weight |
| $M_w$ | Weight-averaged molecular weight |
| MAC | 5-Methyl-5-allyloxycarbonyl-1,3-dioxan-2-one |
| MALDI-ToF MS | Matrix-assisted laser desorption ionisation time-of-flight mass spectrometry |

| | |
|---|---|
| malOCA | Benzyl 2-(2,5-dioxo-1,3-dioxolan-4-yl)acetate |
| m-CPBA | *meta*-Chloroperoxybenzoic acid |
| $Me_6$TREN | Tris[2-(dimethylamino)ethyl]amine |
| MMA | Methyl methacrylate |
| mPEG | Methoxypolyethylene glycol |
| MSA | Methanesulfonic acid |
| MTBD | 7-Methyl-1,5,7-triazabicyclo[4.4.0]dec-5-ene |
| NHC | *N*-Heterocyclic carbene |
| NMR | Nuclear magnetic resonance |
| $P_1$-*t*-Bu | N'-*tert*-Butyl-N,N,N',N',N'',N''-hexamethylphosphorimidic triamide |
| $P_2$-*t*-Bu | 1-*tert*-Butyl-2,2,4,4,4-pentakis(dimethylamino)-$2\lambda^5$,$4\lambda^5$-catenadi(phosphazene) |
| $P_4$-*t*-Bu | 1-*tert*-Butyl-4,4,4-tris(dimethylamino)-2,2-bis[tris(dimethylamino)-phosphoranylidenamino]-$2\lambda^5$,$4\lambda^5$-catenadi(phosphazene) |
| PCC | Poly(9,9-dimethyl-2,4,8,10-tetraoxaspiro[5.5]undecan-3-one) |
| PCL | Poly(*ε*-caprolactone) |
| PDLA | Poly(*D*-lactide) |

| | |
|---|---|
| PEO | Poly(ethylene oxide) |
| PLA | Poly(lactide) |
| PLLA | Poly(*L*-lactide) |
| $P_m$ | Probability of isotactic enchainment |
| PMAC | Poly(5-Methyl-5-allyloxycarbonyl-1,3-dioxan-2-one) |
| PMMA | Poly(methyl methacrylate) |
| PPTO | Poly(9-phenyl-2,4,8,10-tetraoxaspiro[5,5]undecan-3-one) |
| PS | Poly(styrene) |
| PTMC | Poly(trimethylene carbonate) |
| PTSA | p-Toluenesulfonic acid |
| PVDC | Poly(9-vinyl-2,4,8,10-tetraoxaspiro[5.5]undecan-3-one) |
| *r* | Reactivity ratio |
| *rac*-LA | Racemic lactide |
| ROP | Ring opening polymerisation |
| TACN | 1,4,7-Trimethyl-1,4,7-triazacyclononane |
| TEA | Triethylamine |
| $T_g$ | Glass transition temperature |

| | |
|---|---|
| $T_m$ | Melting transition temperature |
| TBD | 1,5,7-Triazabicyclo[4.4.0]dec-5-ene |
| THF | Tetrahydrofuran |
| TMC | Trimethylene carbonate |
| TU | 1-(3,5-Bis(trifluoromethyl)phenyl)-3-cyclohexylthiourea |
| UV | Ultraviolet |
| VDC | 9-Vinyl-2,4,8,10-tetraoxaspiro[5.5]undecan-3-one |
| *w* | Weight fraction of monomer in polymer |

# Acknowledgments

First off I must thank my supervisor Dr. A. P. Dove for giving me the opportunity to undertake a PhD in his group. What I have learnt under his tutelage is sure to stay with me no matter where my future takes me. Of course the work undertaken within this thesis could not have been performed without funding and so I must thank my "secret" backer, the EPRSC. Many thanks must also go to Dr Ivan Prokes who allowed me run so many NMR samples over the course of my PhD and for not mentioning anything about my excessive "Ozric" booking.

To all those that made the lab a pleasant place to work during these past four years, thank you. In particularly Robin and Mike who from the very beginning made the lab an enjoyable place to work, and could still manage a laugh even when the chemistry was getting the best of us. Danny, the most knowledgeable post-doc I had the luck to work with, always willing to listen and offer good advice. Chatting with Andy was always a breath of fresh air which I now sadly miss. Although Gabi's time in the lab was short, his extremely loose trousers will be a memory that I will unfortunately not be able to forget.

I am sure that my family has had no idea what I have been doing for the past four years, and so I must thank them for their blind support.

Finally I must thank my partner Sarah. I had the great pleasure of working beside Sarah in the lab and was able to experience her Swedish Nobel Peace Prize winning super model drawing skills first hand! While I do not know what the future holds for me, I am at least lucky enough to know that it will be with her by my side.

# Declaration

Experimental work contained within this thesis is original research carried out by the author, unless otherwise stated, in the Department of Chemistry at the University of Warwick, between October 2009 and October 2013. No material contained herein has been submitted for any other degree, or at any other institution.

Results from other authors are referenced in the usual manner throughout the text.

Signed: _____ Date: _____

Richard Todd

## Abstract

The work undertaken in this thesis focuses on the synthesis of biodegradable materials with desirable properties *via* the organic catalysed ring opening polymerisation (ROP) of cyclic monomers. Influence over the resulting polymer properties is obtained either through the careful design of catalyst or monomer.

Chapter 1 reviews organic catalysts that have been developed for ring opening polymerisation, focussing on particular advantages and disadvantages of each and providing an overview of compatible types of cyclic monomers.

(-)-Sparteine in conjunction with a co-catalyst is capable of synthesising isotactic PLA with very few stereoerrors, but its sudden commercial unavailability has led to a need for a replacement. Chapter 2 therefore focuses on the synthesis of benzyl bispidine, a (-)-sparteine analogue, demonstrating its almost identical behaviour as a ring opening polymerisation catalyst to produce polymers with optimal properties from lactide.

Post-polymerisation provides access to functionalities not compatible with ROP, and allowing careful tailoring of polymer properties. Whilst a range of cyclic carbonate monomers have been designed to provide this ability after ROP, poly(carbonate)s with only low glass transition have been obtained. Chapter 3 describes the synthesis of 9-vinyl-2,4,8,10-tetraoxaspiro[5.5]undecan-3-one (VDC), a sterically bulky, vinyl functional cyclic carbonate and its subsequent ROP and thiol-ene functionalisation to yield functional poly(carbonate)s with improved thermal properties.

In Chapter 4, work is undertaken to tailor the glass transition temperature of functional poly(carbonate)s. Copolymers of VDC with the allyl functional cyclic carbonate allyl 5-methyl-2-oxo-1,3-dioxane-5-carboxylate (MAC) are synthesised to demonstrate the ability to produce poly(carbonate)s with a predetermined glass transition temperature after post-polymerisation functionalisation depending on the initial monomer feed ratio.

In Chapter 5 the results from the previous chapters are discussed, with the experimental data obtained for these chapters provided in Chapter 6.

# Chapter One

## Biodegradable Polymers *via* Organic Catalysed Ring Opening Polymerisation

THE UNIVERSITY OF
WARWICK

## 1.1 Introduction

In just over a decade the field of organocatalysis in the ring opening polymerisation (ROP) of cyclic monomers has grown significantly.[1-5] While well defined polymers from cyclic monomers could traditionally only be obtained using metal based catalysts,[6-9] a wide range of organic catalysts can be used nowadays. In addition, most organic catalysts are commercially available and easily removed through simple washing steps as a result of their basic or acidic nature. The metal-free ROP of cyclic monomers therefore has a significant advantage over metal catalysts, especially in applications where trace metals can have negative effects.

The application of organic catalysts in ROP reaches further than commercially available monomers such as lactide and ε-caprolactone, with a continuous development of more specialised cyclic monomers for targeted applications.[10, 11] Although there is no "universal" organocatalyst for all types of cyclic monomers, through careful selection well defined biodegradable polymers can be synthesised. Herein the development and use of organocatalysts for the ROP of a range of cyclic monomers will be discussed.

## 1.2 Cyclic Monomers

A range of cyclic monomers exist that are capable of undergoing ROP to yield aliphatic biodegradable polymers and while there has been a great focus on cyclic esters such as lactide and lactones, cyclic carbonates and cyclic phosphates have received increased interest recently.

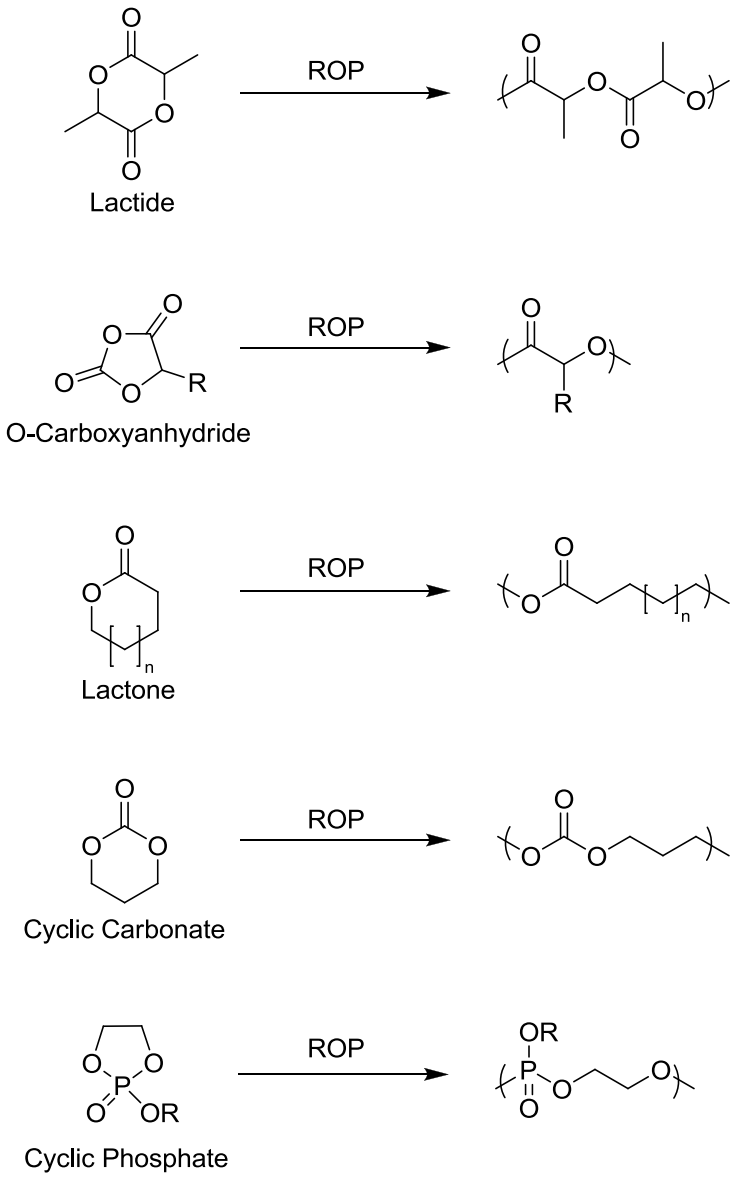


**Scheme 1.1** Cyclic monomers and their resulting polymers upon ROP.

### 1.2.1 Commercially Available Monomers

Commercially available cyclic monomers include glycolide, lactide, ε-caprolactone, δ-valerolactone, pentadecalactone, trimethylene carbonate and β-propiolactone which result in degradable aliphatic poly(ester)s or poly(carbonate)s with highly controlled molecular parameters upon ROP. Due to their availability

much research has been directed towards their development, especially in improving mechanical properties, hydrophilicity and degradability profiles through copolymerisations and synthesising different architectures such as stars, brushes, cycles, cross linked materials and hyper branched polymers.[12-15] Tailoring the properties of biodegradable polymers for many applications is therefore very challenging using just these cyclic monomers, requiring the development of new functional cyclic monomers that can introduce desired functionality throughout the polymer backbone and imparting improved properties.

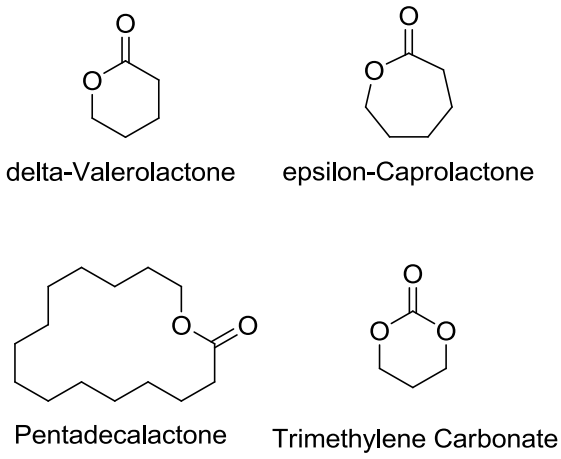


**Figure 1.1** Lactone monomers for ROP.

### 1.2.2 Lactide

Lactide is possibly the most well-known cyclic ester, with applications of the resulting poly(lactide) (PLA) ranging from food packaging to medical sutures. As lactide (LA) has two stereocentres, there are three possible stereoisomers, *LL*- (*L*-lactide), *DD*- (*D*-lactide) and *DL*- (*meso*-lactide). Both *L*-lactide and *D*-lactide are commercially available on a large scale, while *meso*-lactide has just recently become

commercially available. Depending on the choice of LA monomer it is possible to synthesise PLA with a range of microstructures. The ROP of stereopure LA results in isotactic PLA whereas the ROP of *meso*-lactide can potentially result in either syndiotactic (alternating stereocentres), heterotactic (doubly alternating) or atactic (random distribution of stererocentres) PLA. A 50:50 combination of *L*-lactide and *D*-lactide (i.e. *rac*-lactide) can theoretically result in a range of microstructures depending on the catalyst (Scheme 1.2). The need to negate epimerisation is important in lactide polymerisations as changes to the microstructure of PLA have a large effect on the polymers resulting properties. Isotactic PLA synthesised from stereopure monomers with a lack of epimerisation is highly crystalline and exhibits a melting point ranging from 170-190 °C.[16] However, when epimerisation occurs during the polymerisation stereroerrors are introduced into the PLA chains when the epimerised monomers are incorporated. The crystallinity and melting point are thus reduced and when over 10-12% stereoerrors are present the resulting PLA is amorphous.

The thermal properties of isotactic PLA can be improved further by forming stereocomplexes between PDLA and PLLA.[17] Stereocomplexation results in an increased crystallinity due to alignment of the two different polymer chains forming a structure with increased stability and higher melting point (approximately 230-240 °C). The degradation temperatures of stereocomplexed PLLA/PDLA were explored by Endo and co-workers who found that residual catalyst had a large effect.[18] Without effectively removing their catalysts, $Sn(Oct)_2$, an onset degradation temperature of 220 °C was measured by thermogravimetric analysis (TGA), finishing around 290 °C. In comparison when complete removal of the metal catalyst (<10 ppm Sn content) was performed, an improved onset degradation temperature of

260 °C was measured by TGA (finishing around 320 °C). The benefits that organic catalysts can bring to the ROP of lactide are therefore clear, but the need to keep epimerisation to a minimum is key. Epimerisation occurs more readily in the presence of acids or bases and increases significantly when combined with high temperatures. The careful choice of catalyst system for the ROP of lactide is therefore important to obtain stereopure (isotactic) PLA.

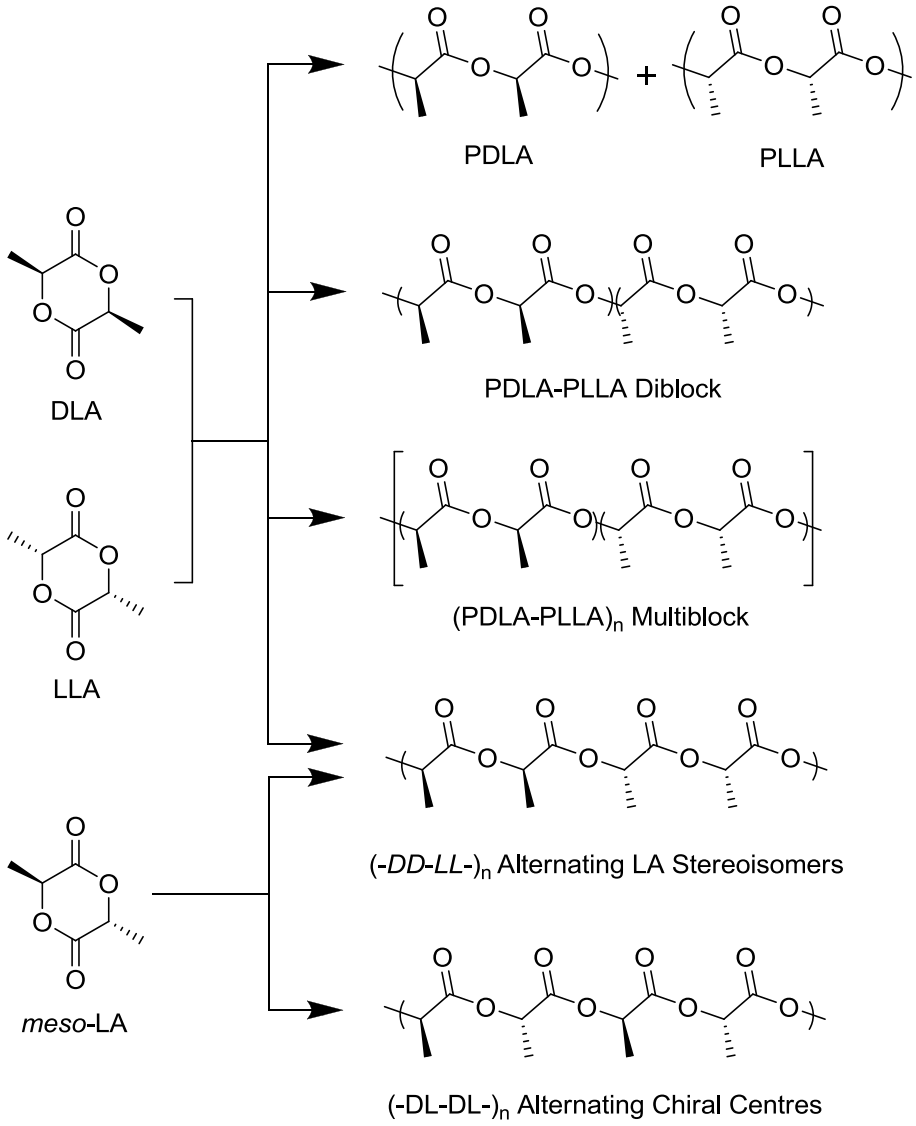


**Scheme 1.2** Possible PLA microstructures from the stereocontrolled ROP of *rac*-lactide or *meso*-lactide.

### 1.2.3 Functional Cyclic Esters

The success of commercially available monomers such as lactide and ε-caprolactone has led to research focussing on the development of functional analogues. The most common reported procedures to synthesise functional cyclic diester monomers are either *via* the self condensation of α-hydroxy acids catalysed/cracking of oligoesters or the step by step condensation of an α-hydroxy acid and an α-haloacyl halide with subsequent base-mediated cyclisation. A range of functional diesters have been designed, synthesised and subsequently polymerised with the aim to improve on the thermal properties of PLA by introducing sterically bulky side groups,[19] improving degradability *via* pendant carboxylic groups (*via* deprotection after ROP),[20] introducing water solubility with poly(ethylene glycol) side chains[21] or allowing post-polymerisation functionalisation *via* pendant alkyne groups.[22]

In comparison to functional cyclic diesters where ring closure is usually time consuming and extremely low yielding, functional caprolactones can be synthesised through the simple ring-expansion of their corresponding cyclohexanones *via* a Bayer-Villiger oxidation with *meta*-chloroperoxybenzoic acid (mCPBA) (Scheme 1.3). This has led to a larger range of functional cyclic esters produced through this method.[11] ROP of these monomers have resulted in polymers exhibiting various properties like tailored polymer degradability, improved mechanical properties or are capable of undergoing further modification *via* the imparted functional group on the polymer backbone.

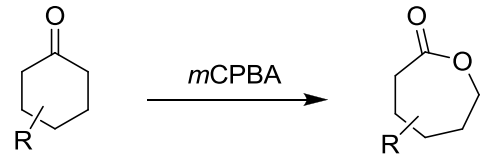


**Scheme 1.3** General synthesis of functional caprolactones *via* Bayer-Villiger oxidation of a cyclohexanone

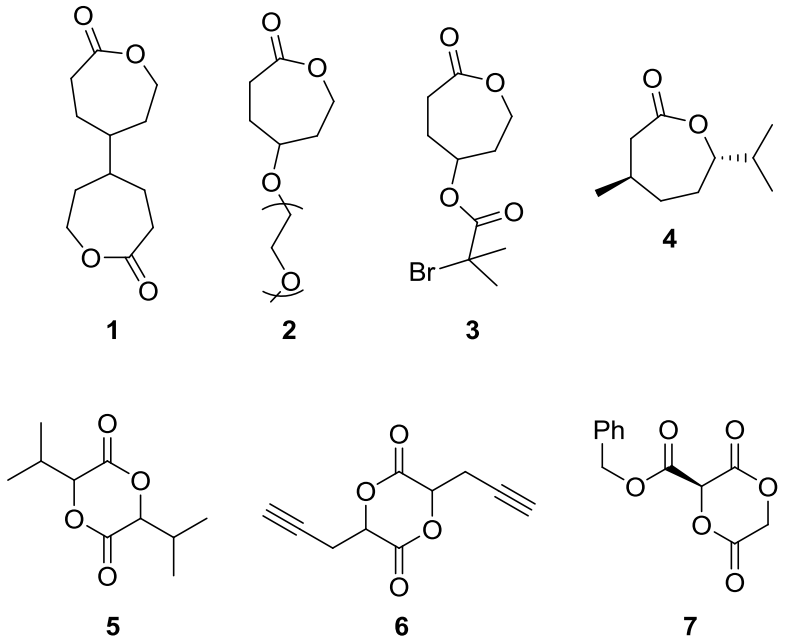


**Figure 1.2** Examples of functional cyclic diesters and lactones.[11, 19- 22]

### 1.2.4 Cyclic Carbonates

There has been an increased interest in aliphatic poly(carbonates) synthesised *via* ROP of cyclic carbonates recently.[10] In addition to being biocompatible and biodegradable poly(carbonate)s tend to be more stable compared to aliphatic polyesters such as PLA and poly(caprolactone) under basic and acidic conditions. The degradation of poly(ester)s results in the formation of carboxylic acid terminated

chains causing further degradation due to the reduced local pH environment. Poly(trimethylene carbonate) (PTMC), in comparison, is virtually non-degradable in buffers ranging from pH 1 to 13 in the absence of enzymes.[23, 24] Poly(carbonate) degradation results in carbonic acid monoester groups, that due to their inherent instability subsequently degrade further releasing $CO_2$, forming a primary alcohol. The lack of acidic degradation products means that poly(carbonate)s are less likely to cause inflammatory responses in biomedical applications.

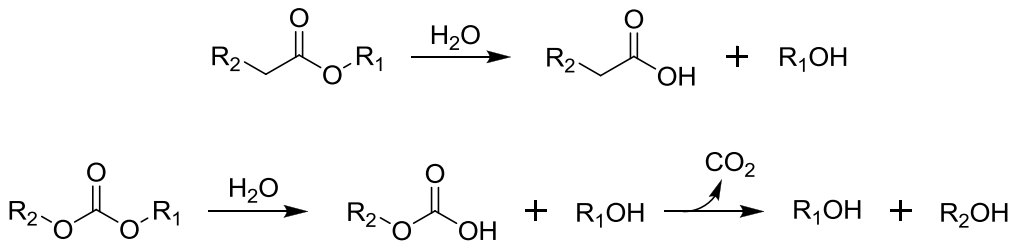


**Scheme 1.4** Hydroylsis of an ester versus carbonate.

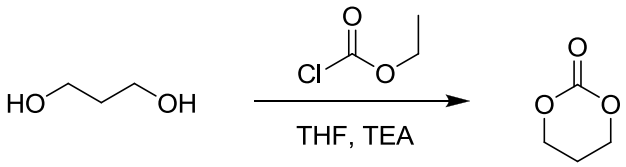


**Scheme 1.5** Formation of TMC using ethyl chlorformate.

While the ROP of cyclic carbonates of different ring sizes (5, 6 and 7) have been reported, most published work has focused on 6-membered cyclic carbonates due to their facile synthesis, ease to introduce functionality and controlled

polymerisation.[25, 26] Several methods of forming 6-membered cyclic carbonates have been reported in literature, mostly including ring closure of 1,3-diols using phosgene derivatives such as ethyl chloroformate (Scheme 1.4).[27] Typical yields for the cyclisation of sterically unhindered 1,3-diols are around 70%. The facile monomer synthesis has resulted in a large range of reported functional cyclic carbonate monomers with resulting polymers used in a applications such as gene transfection and targeted drug delivery.[28, 29]

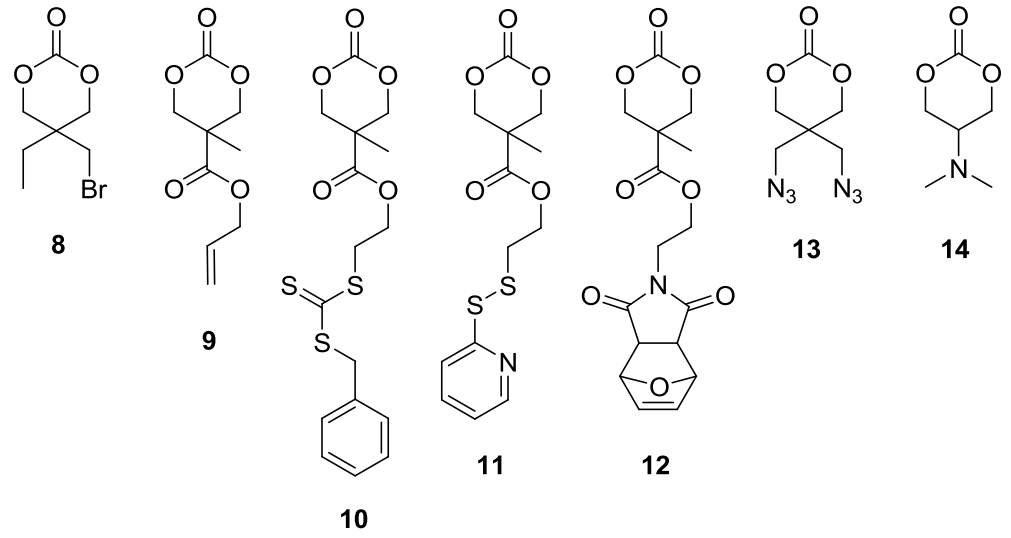


**Figure 1.3** Examples of cyclic carbonates that have been successfully polymerised in literature.[10]

### 1.2.5 Cyclic Phosphates

Cyclic phosphates are another class of cyclic monomers of which the ROP results in the formation of aliphatic poly(phosphoester)s which have a structure similar to that of nucleic and teichoic acids. Due to this similarity of polyphosphoesters to natural products along with their low cycotoxicity and

degradation through hydrolysis and possible enzymatic digestion under physiological conditions, they have the potential to be used for a range of biological and pharmaceutical applications.[30]

Functional cyclic phosphates can be easily synthesised through the condensation of commercially available 2-chloro-2-oxo-1,3,2-dioxaphospholane (COP) and an alcohol (Scheme 1.5).[31-33] Although the number of reported cyclic phosphates and there corresponding polymers are limited in literature, the easy monomer synthesis and potential to produce poly(phosphoester)s with a range chemical properties and structures will undoubtedly lead to their use in a range of applications.

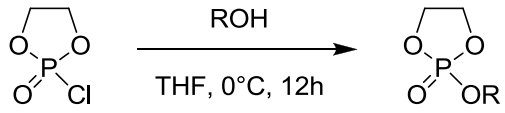


**Scheme 1.6** Functional cyclic phosphate synthesis from COP.

## 1.3 Organic Catalysts

### 1.3.1 4-(Dimethylamino)pyridine Catalysed ROP

The first organocatalytic approach to the living ROP of LA was reported by Hedrick and co-workers in 2001 using 4-(dimethylamino)pyridine (DMAP).[34] Using one equivalent of DMAP to alcohol initiator in dichloromethane high monomer conversions were obtained at room temperature. The resulting polymers had low dispersities ($Đ_M$) (<1.15), but the system proved to be particularly slow with a degree

of polymerisation (DP) of 30 taking 60 h to reach completion. Polymerisation times could be reduced to 24 hours by increasing the number of equivalents of DMAP to four. However, considerably faster reaction times could be achieved by performing the polymerisation in bulk at 135 °C. The synthesis of a DP100 PLA took only 20 minutes when performed in bulk while still maintaining a low $Đ_M$ (1.14). Exposing a solution of PLA to catalytic quantities of DMAP for an extended period (24 hours) resulted in no change in the GPC of the PLA trace suggesting low amounts or no transesterification whilst $^{13}C$ NMR spectroscopy of PLA synthesised using DMAP also showed no observable epimerisation. While well defined PLA is produced using this catalyst system, due to its slow polymerisation rate in the ROP of lactide it has been superseded by other organocatalysts.

For DMAP catalysed ROP of LA, a mechanism involving nucleophilic attack of DMAP on LA to produce a zwitterionic alkoxide was initially proposed.[34] The subsequent reaction of the zwitterionic alkoxide with an alcohol then produces a ring opened monomer with an alcohol chain end that upon repeating the process multiple times results in an increase the chain length (Scheme 1.6). Recently, computational investigations undertaken by Bourissou and co-workers suggest that an alcohol activation mechanism is also possible wherein DMAP acts as a bifunctional activator.[35] DMAP provides hydrogen-bonding through its basic nitrogen to the alcohol initiator/propagating chain end in the proposed mechanism while its acidic *ortho*-hydrogen atom activates the LA carbonyl *via* hydrogen-bonding (Scheme 1.7). Both nucleophilic attack and alcohol activation pathways are energetically possible and while the latter is of a lower energy and thus more favourable, nucleophilic attack is still likely to occur when no alcohol is present or at extremely low concentrations (i.e. for high [M]/[I]).

DMAP has also been used to catalyse the ROP of alkyl substituted LA monomers and while high monomer conversions were achieved, the high temperatures that were required (110 °C for 1 hour) resulted in larger dispersities (1.48) compared to LA polymerisations at 35 °C.

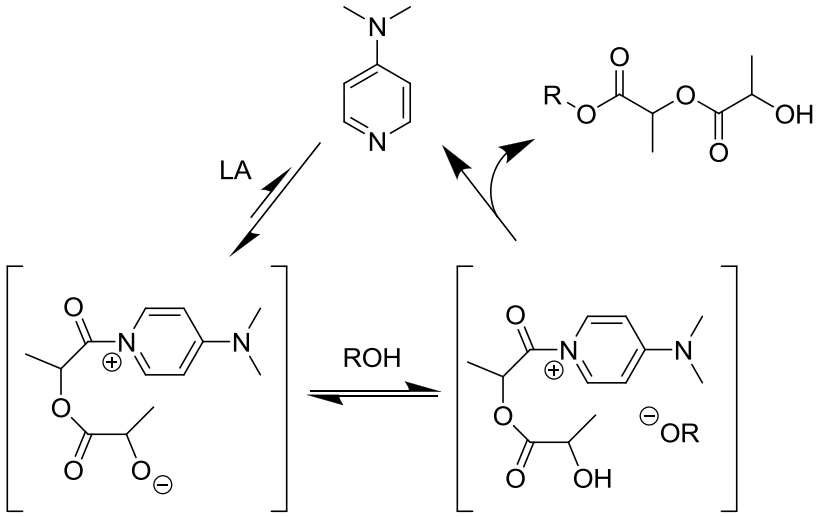


**Scheme 1.7** Nucleophilic mechanism for the ROP of lactide by DMAP.

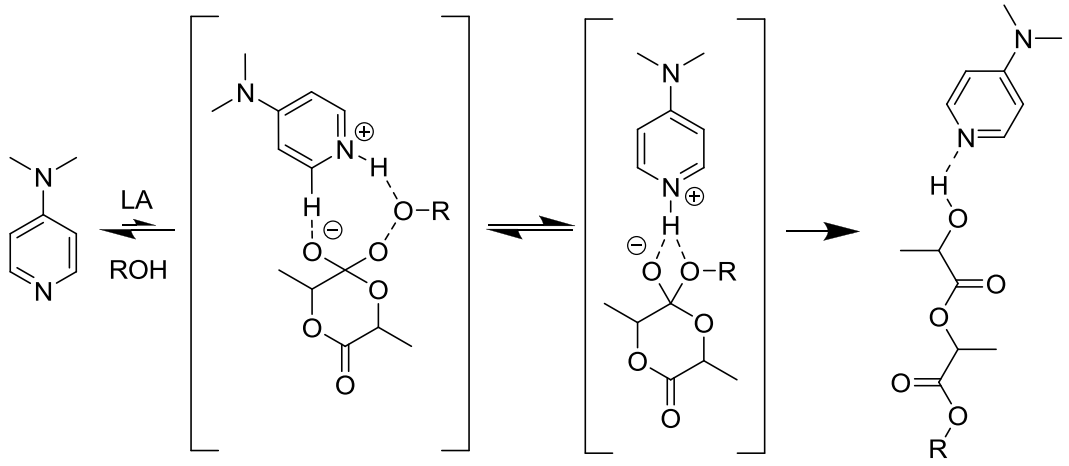


**Scheme 1.8** Hydrogen-bonding mechanism for the ROP of lactide by DMAP.

Another group of cyclic monomers that can undergo DMAP catalysed ROP are O-carboxyanhydrides (OCAs). Their smaller ring size results in a larger the ring strain and therefore an increased reactivity compared to LA. OCA's have received more interest as monomers than α-lactones as the latter are far too reactive to be used practically in ROP. In addition, the liberation of a molecule of $CO_2$ per monomer unit upon ROP of OCA's provides a considerable increase in reactivity. ROP of 5-methyl-1,3-dioxolane-2,4-dione (lacOCA) results in structurally identical polymers to that of the ROP of lactide but the polymerisation is considerably faster. The increased reactivity was demonstrated by Bourissou and co-workers who reported that ROP of lacOCA by DMAP in the presence of an alcohol reached full conversion in just 5 minutes at room temperature (lacOCA/DMAP/ROH = 20/1/1), whereas under the same conditions the ROP of lactide took 4 days to reach 93% monomer conversion (lactide/DMAP/ROH = 10/1/1).[36] Varying the ratio of lacOCA to initiator produced PLA with degrees of polymerisation closely matching initial [M]/[I] ratios and low polymer dispersities (<1.3). The combination of control with successful chain extension experiments demonstrated the living nature of lacOCA ROP catalysed by DMAP. Homonuclear decoupled $^1$H NMR spectroscopy of the synthesised PLA also showed no evidence of epimerisation. The same two reaction mechanisms are proposed for the DMAP catalysed ROP of lacOCA as for LA, but computational investigations have suggested that one pathway is no more favourable than the other.[35]

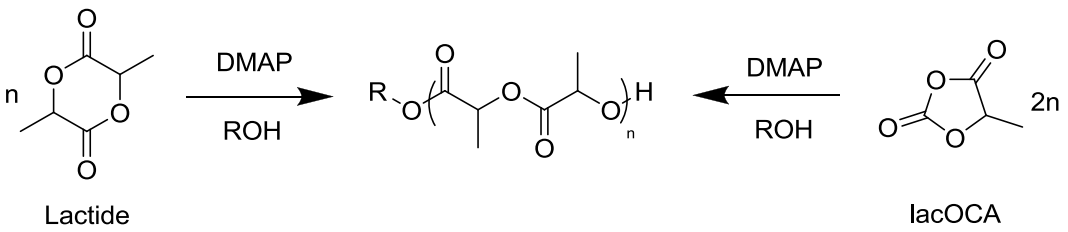


**Scheme 1.9** PLA synthesised by DMAP catalysed ROP of LA or lacOCA.

Relatively few examples of other functional OCAs have been reported (which might be due to undesirable side reactions occurring).[37, 38] The DMAP catalysed ROP of malOCA resulted in the production of polymers with a number of impurities due to the deprotection of the acidic methine proton of the monomer by DMAP.[38] The use of less basic pyridines such as 4-methoxypyridine as the catalyst resulted in a reduction of most impurities, but MALDI-ToF spectra still showed evidence that ring opening occurred at both OCA carbonyls resulting in polymers with carboxylic acid chain ends as well as those with an alcohol chain ends. DFT studies agreed with this evidence proposing a 9 to 1 ratio in favour of ring opening occurring at the most electrophilic OCA carbonyl. Through tailoring the basicity of the pyridine catalyst, ROP of malOCA could be achieved in a living manner resulting in relatively well defined polymers.

### 1.3.2 *N*-Heterocyclic Carbene Catalysed ROP

With *N*-heterocyclic carbenes (NHCs) having already been shown to be potent nucleophilic catalysts for transesterification reactions, Hedrick and co-

workers explored their use for the ROP of cyclic monomers in 2002.[39] They reported that significantly increased polymerisation rates compared to DMAP catalysed ROP of LA in solution were observed with DP100 PLA synthesised in just 2 hours at room temperature using 1.5 equivalents of 1,3-bis-(2,4,6-trimethylphenyl)imidazol-2-ylidene, **15**, with respect to alcohol initiator. Polymer dispersities below 1.15 were achieved for PLA with a range of DPs and the system exhibited all the features of a living polymerisation without any observable epimerisation of the LA. The catalyst was also shown to be active for the ROP of ε-caprolactone and *β*-butyrolactone, although the quantitative conversion of ε-caprolactone resulted in increased dispersites (1.33) due to transesterification. Reducing the steric effects of the NHC along with the basicity (e.g. **16** and **17**) resulted in reduced polymer dispersities in the ROP of lactones (1.16-1.32).[40] Due to the high activity of active NHCs, quenching of the polymerisation is always necessary to prevent undesirable transesterification once high monomer conversion is achieved. Since their first report as a catalyst for ROP, NHCs have been applied to a wide range of monomers such as lactones, cyclic carbonates, epoxides, cyclic siloxanes and even acrylates.[41-45]

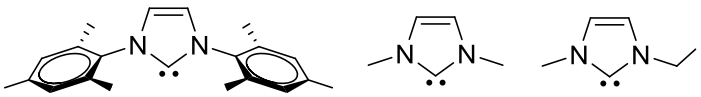


**15** **16** **17**

**Figure 1.4** Examples of NHC organic catalysts.

For the NHC catalysed ROP of cyclic esters and cyclic carbonates a similar nucleophilic mechanism is proposed as for DMAP, where the NHC ring opens the

monomer to yield a zwitterionic alkoxide (Scheme 1.10). Computational investigations have suggested that NHCs are capable of hydrogen-bonding to alcohols, meaning that an activated alcohol mechanism of ROP is possible (Scheme 1.11).[46] In the absence of an alcohol, NHCs have been demonstrated to result in macrocycles rather than linear polymers, providing support to the nucleophilic mechanism.[47] In the presence of an alcohol initiator it is likely that both mechanisms occur with nucleophilic activation more prevalent at higher [M]/[I] ratios.

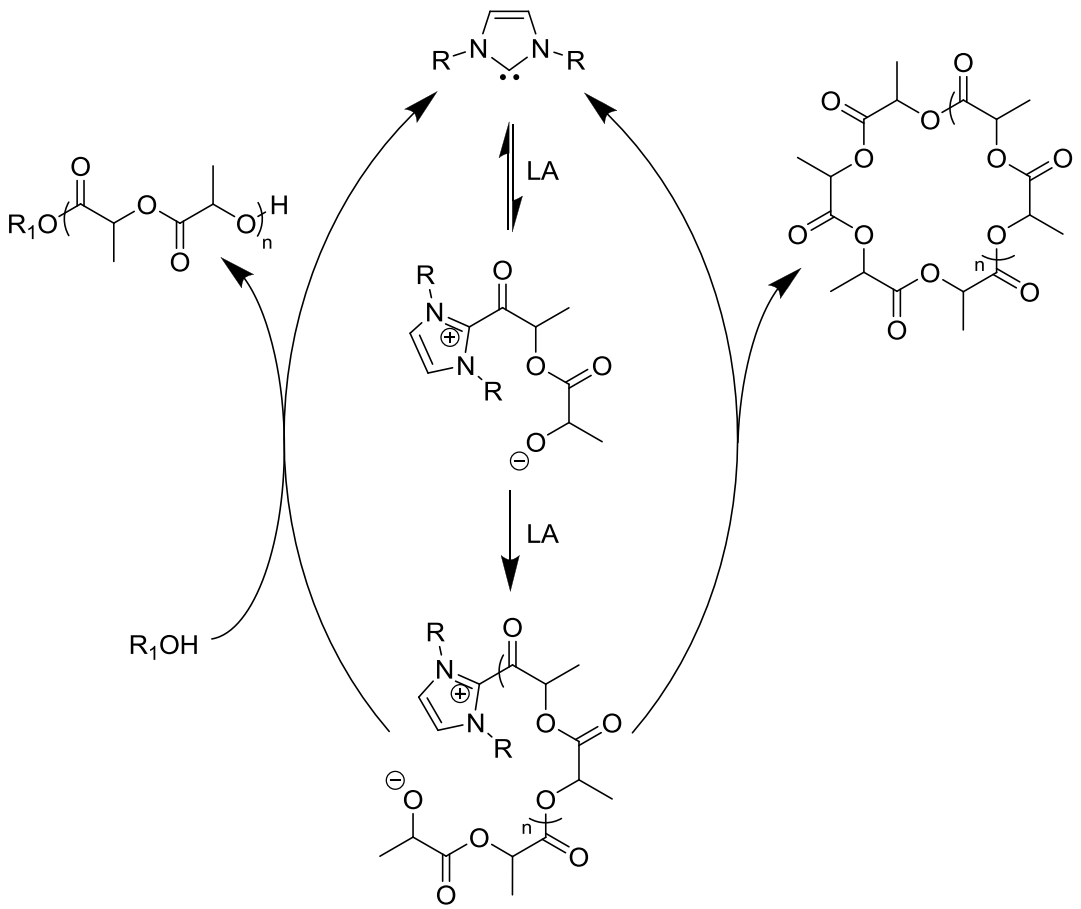


**Scheme 1.10** Formation of linear or cyclic PLA *via* the NHC catalysed ROP of LA.

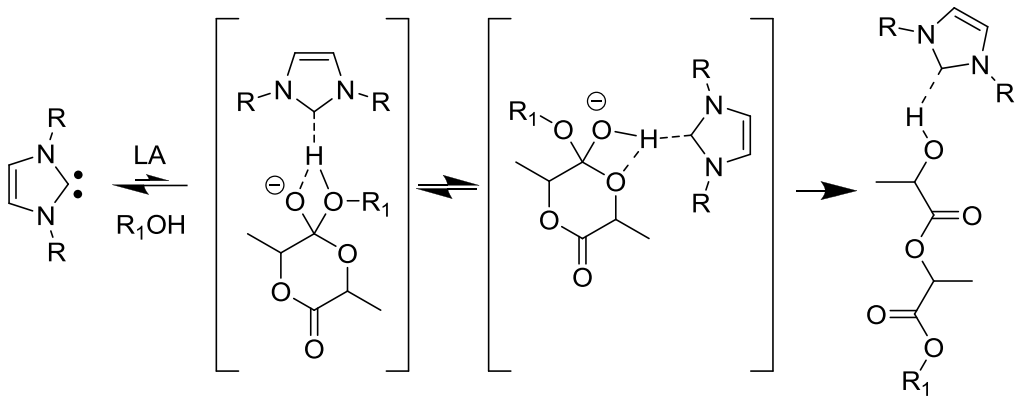


**Scheme 1.11** H-bonding monomer activation mechanism for NHC catalysed ROP.

Due to inherent stability problems and the extreme air and water sensitivity of NHCs such as **1-3**, methods were developed to prepare NHCs *in situ*. These new NHC's include those formed their respective acid salts as well as thermally activated NHCs.[48-50] Commercially available 1,3,4-triphenyl-4,5-dihydro-1*H*-1,2-triazol-5-ylidene carbine for example only shows low conversions of LA at room temperature after 100 hours, whilst elevating the temperature to 90 $^{o}$C results in the quantitative polymerisation of LA (DP70) within 50 hours.[48] At higher temperatures the catalyst dissociates into an alcohol and an active carbene. The reversible nature of this dissociation results in a reduced concentration of active carbenes compared to the first generation NHC's and therefore slower polymerisation rates, but transesterification is also suppressed due to this lower active NHC concentration.

The use of NHCs, either first or second generation, allows the synthesis of polymers with unique macromolecular structures and these type of catalysts posses the ability to polymerise less active monomers making them useful tools in the field of organic catalysed ROP.

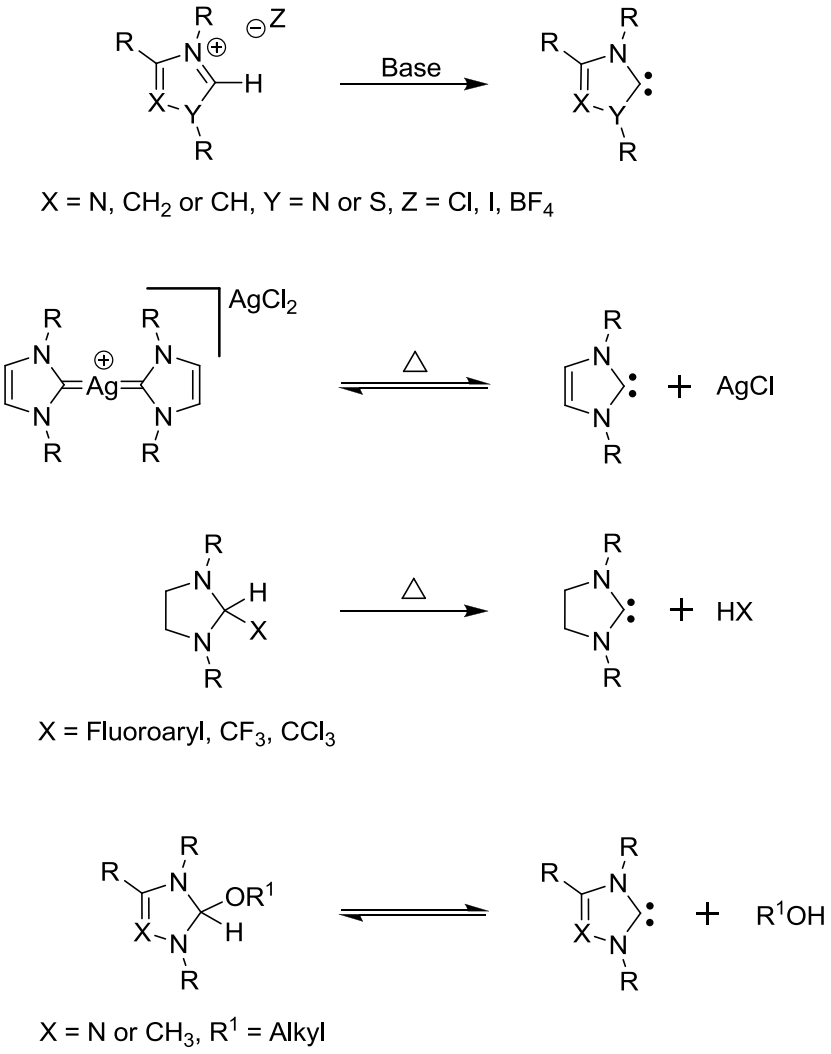


**Scheme 1.12** In situ generation of NHCs.

### 1.3.3 Anionic ROP catalysts

Phosphazene bases with the general structure $(R_2N)_3P{=}N-R$ have been shown to be able to facilitate the ROP of a number of cyclic monomers. The catalysts 2-tert-butylimino-2-diethylamino-1,3-dimethylperhydro-1,3,2-diazaphosphorine (BEMP) and N'-tert-butyl-N,N,N',N',N'',N''-hexamethylphosphorimidic triamide ($P_1$-*t*-Bu) are more basic than either DBU or

MTBD and have both been used in the ROP of lactide and δ-valerolactone.[51] The polymerisation of lactide using an alcohol initiator in toluene with either catalyst (0.5-2 mol% to monomer) yields PLA with low dispersities (<1.1), although an increase in dispersity was observed (<1.2) at higher conversions (>90%) suggesting small amounts transesterification. Increased transesterfication was also observed at higher catalyst loadings. Polymerisations of lactide were not exceptionally fast with the polymerisation using a [M]/[I] ratio of 100 taking 66 hours to reach 97% monomer conversion. $^{13}$C NMR spectroscopy of PLA synthesised with stereopure lactide showed little observable evidence of epimerisation occurring despite the strongly basic nature of BEMP and P$_1$-*t*-Bu. Polymerisations of *δ*-valerolactone in bulk at room temperature also yields well defined polymers ($Đ_M$'s <1.2). The polymerisation of *ε*-caprolactone, however was reported to be remarkably slow even at elevated temperatures (14% monomer conversion after 240 hours at 80 °C (bulk), DP100). The mechanism proposed for phosphazene bases is one wherein the alcohol initiator/propagating chain end is activated allowing nucleophilic attack of the monomer, resulting in its ring opening to form an alkoxide chain end (Scheme 1.13).

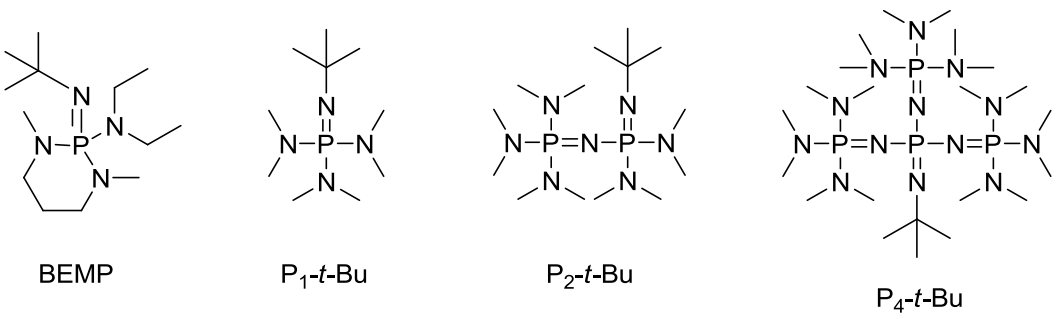


**Figure 1.5** Phosphazene catalysts.

Phosphazenes have recently proved successful in the ROP of β-lactones, the ROP of these monomers having previously been relatively unsuccessful when other organic catalysts were used. The polymerisation of the *β*-lactone [R,S]-4-benzylcarbonyl-3,3-dimethyl-2-oxetanone (dMMLABz) using 1-tert-Butyl-2,2,4,4,4-pentakis(dimethylamino)-2λ5,4λ5-catenadi(phosphazene) (**P**$_2$-*t*-Bu) as the catalyst was reported to achieve relatively good control by Dubois and co-workers in 2012.[52] A carboxylic acid was used as an initiator for the polymerisation and it was proposed that the phosphazene reacts with the carboxylic acid initiator to form a phosphazenium carboxylate active species that can then ring open the β-lactone monomer *via* "O-alkyl" scission. Improved activity for the ROP of dMMLABz could be achieved *via* the application of a stronger phosphazene base in the order of: P$_1$-*t*-Bu < P$_2$-*t*-Bu < P$_4$-*t*-Bu. The increase in basicity correlates directly to the increasing number of phosphorus atoms which results from an increase of the delocalization of the charge on the conjugated phosphazenium cation.

Six-membered cyclic carbonates have also been shown to undergo controlled ROP using phosphazene bases. Examples so far have been restricted to the bulk polymerisation of TMC between 60-150 °C from an alcohol initiator by BEMP, resulting in moderately low dispersities (<1.6) using a range of catalyst loadings.[53] Seven-membered cyclic carbonates proved to be less active towards ROP by BEMP, with polymerisations only occurring over 100 °C using a ratio 100/1/1 of monomer/ROH initiator/BEMP. Although complete conversion was reached after 60 minutes for the ROP of 5-methyl-1,3-dioxepan-2-one (*β*-Me7CC).[54]

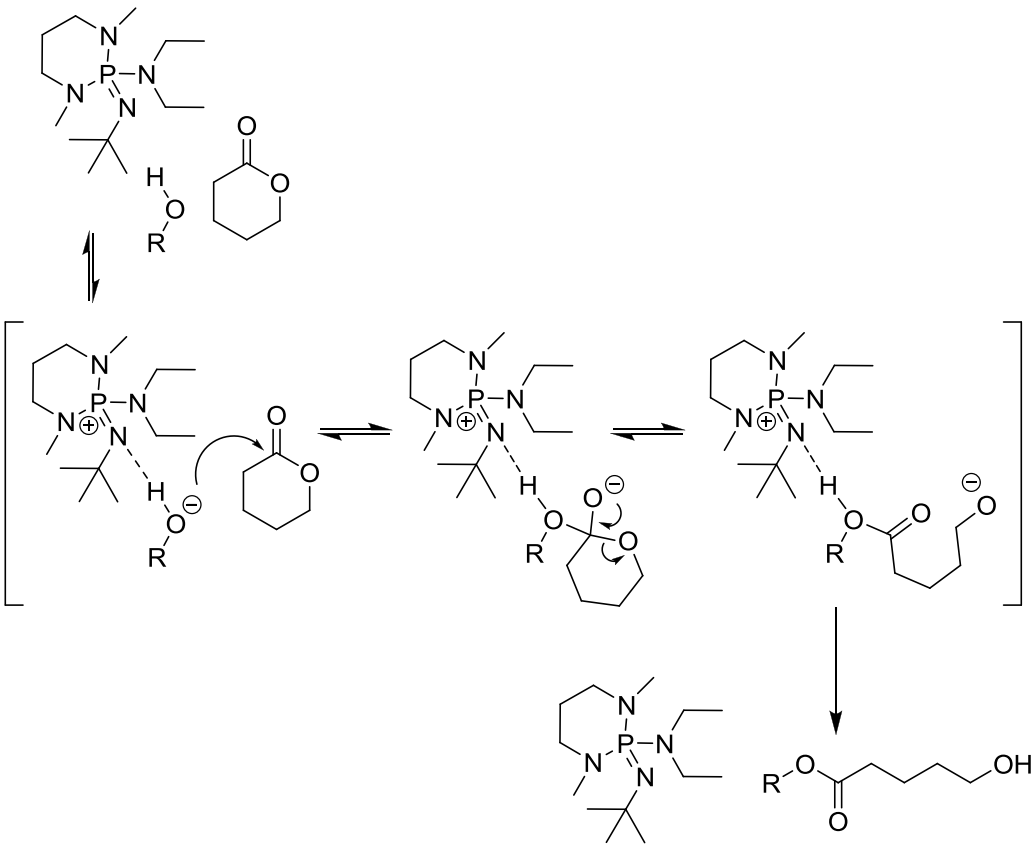

**Scheme 1.13** BEMP catalysed ROP mechanism of valerolactone.

Recently the ability of phosphazenes to catalyse the anionic polymerisation of methyl methacrylate (MMA), known since the early 1990's,[55, 56] was combined with ROP. In 2012 Zhang and co-workers demonstrated the ability of $P_4$-*t*-Bu to polymerise both methacrylate and lactone monomers together in a "hybrid polymerisation" producing a novel material (Scheme 1.14).[57] Copolymerisation of MMA and ε-caprolactone using a ratio of monomers/ROH initiator/$P_4$-*t*-Bu of 100/1/1 was demonstrated by NMR spectroscopy to result in the incorporation of both monomers into polymer chains. The synthesis of statistical copolymers rather than block copolymers was backed up by the observation of only a single glass

transition temperature ($T_g$) for the copolymers with the $T_g$'s matching those predicted by the Fox equation for copolymers. Polymer dispersities were found to be typically lower than 2.0 for the copolymers, but the GPC traces exhibited bimodality. Careful fractional precipitation of a bimodal copolymer showed that both distributions had almost identical monomer compositions, but different molecular weights, most likely from nucleophilic attack on the carbonyl group of MMA for one of the distributions.

While considerable work in the area of anionic ROP to obtain biodegradable materials has focused on the use of phosphazenes as organic catalysts, which is unsurprising due to their unusual catalytic abilities, the use of Brederecks's reagent must also be noted. Although originally envisioned as an alternative method of forming N-hetereocyclic carbenes *in situ*, Bredereck's reagent was found to reversibly form an alkoxide at elevated temperatures that can ring open LA *via* an anionic mechanism.[58] During propagation the formed formamidinium counterion can reversibly capture the propagating anion, acting as a shuttle system resulting in deactivated and active growing chains during the polymerisation (Scheme 1.15). While this remains a hypothesis, the ROP of LA catalysed by Bredereck's reagent at elevated temperatures (70 °C) in tetrahydrofuran resulted in high monomer conversion after 3 hours (DP70) with considerably faster reaction times (10 min) when performed under vacuum.

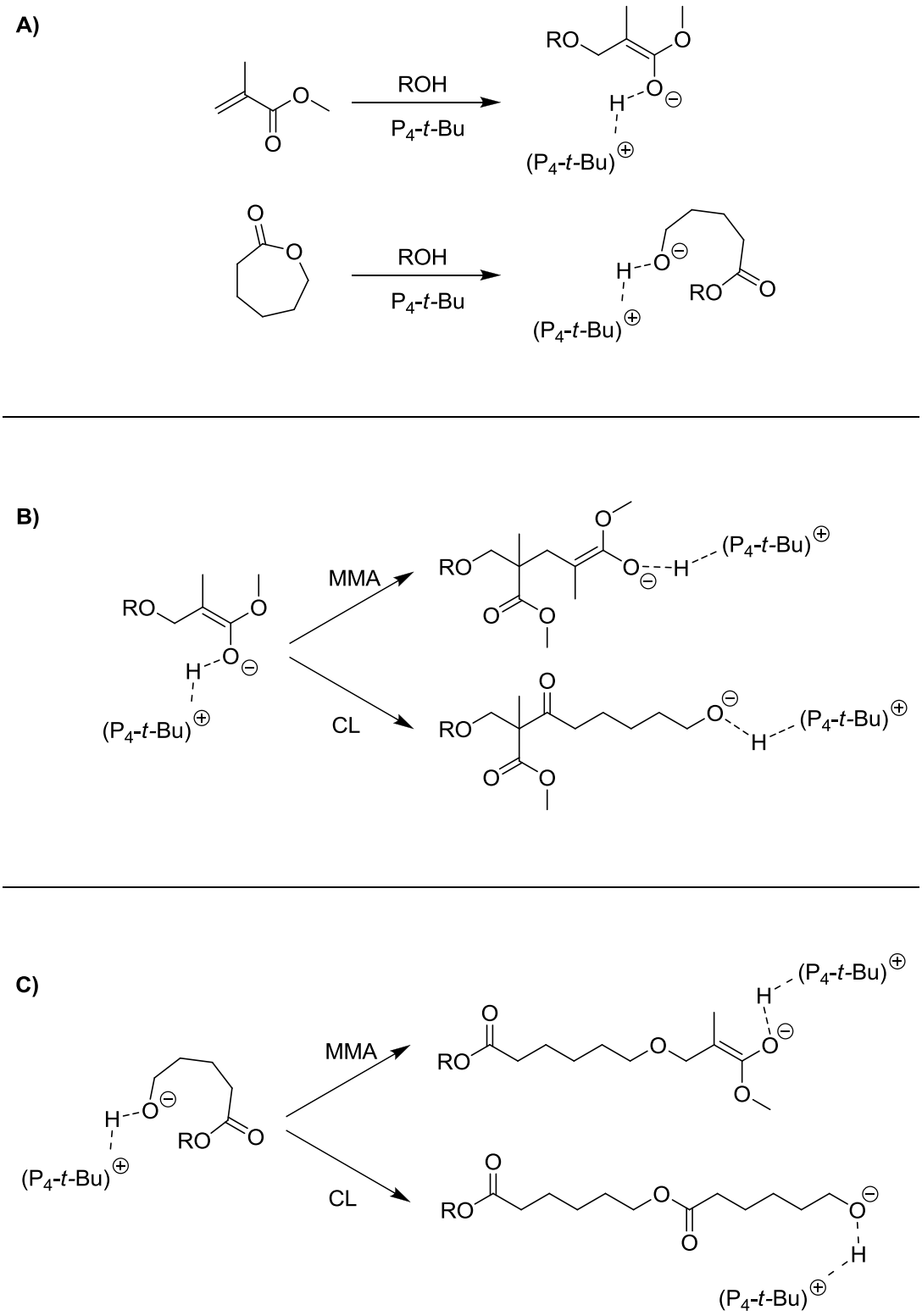


**Scheme 1.14** Possible initiation and propagation mechanisms for the CL/MMA phosphazene catalysed copolymerisation. A) Initiation. B) Propagation from MMA. C) Propagation from CL.

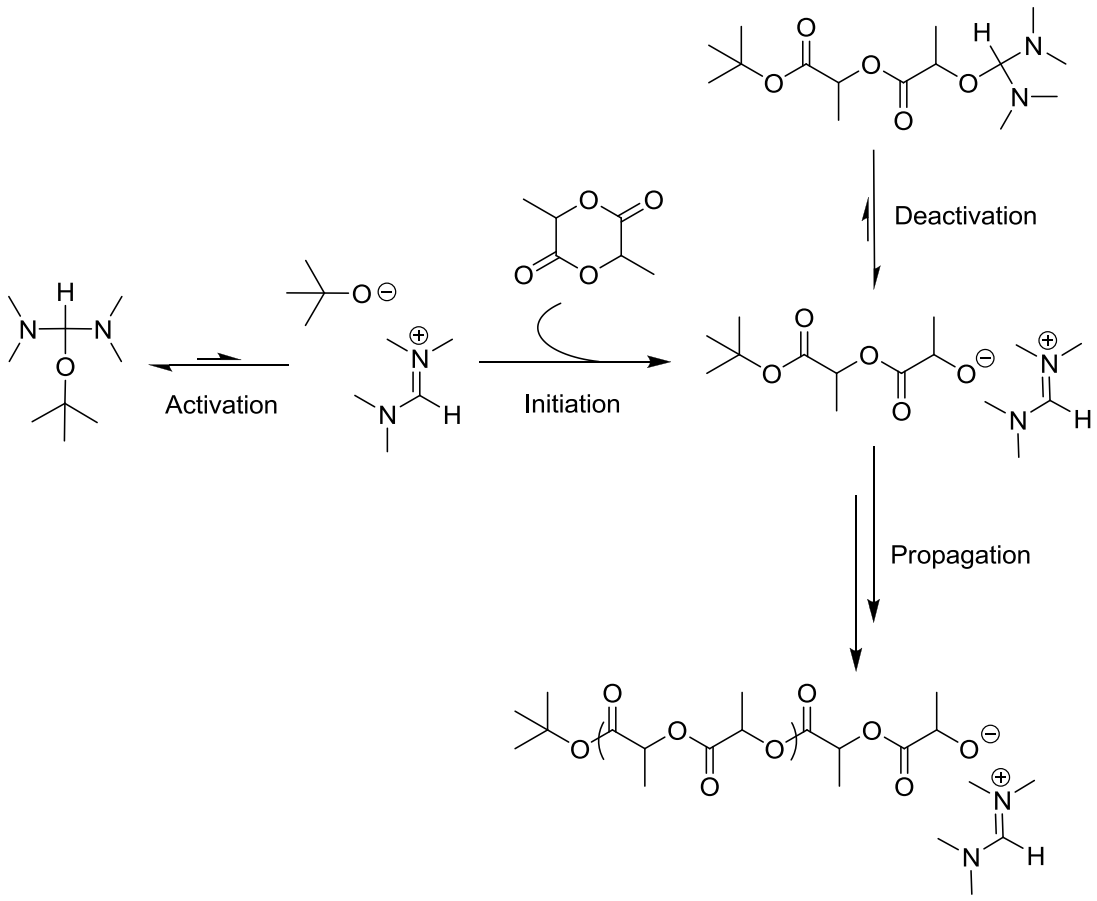


**Scheme 1.15** Anionic ROP of lactide catalysed by Bredereck's reagent.

### 1.3.4 Acid Catalysed ROP

A number of organic acids have been utilised as catalysts for the cationic ring opening polymerisation of cyclic monomers. While there have been a few examples of organic acids for use in the ROP of lactide, most literature focuses on their use in the ROP of lactones. Endo and co-workers demonstrated the ability of HCl•$OEt_2$, in the presence of an alcohol initiator, to polymerise both ε-caprolactone and δ-valerolactone in a controlled manner.[59] Aliphatic polymers were synthesised with low polymer dispersities (<1.17) using equal amounts of initiator to HCl in

dichloromethane, but required long polymerisations times (24 hours for a DP75). Increasing equivalents HCl did not result in reduced (polymer) molecular weights, suggesting that HCl does not act as an initiator but solely provides activation to promote ROP. Star polymers could also be synthesised using pentaerythritol as the initiator using this catalyst system or other acids such as fumaric, maleic, trichloroacetic acid or trifluoroacetic acid under bulk conditions.[60] A large number of carboxylic acids have subsequently been shown to be effective catalysts for the ROP of ε-caprolactone.[61]

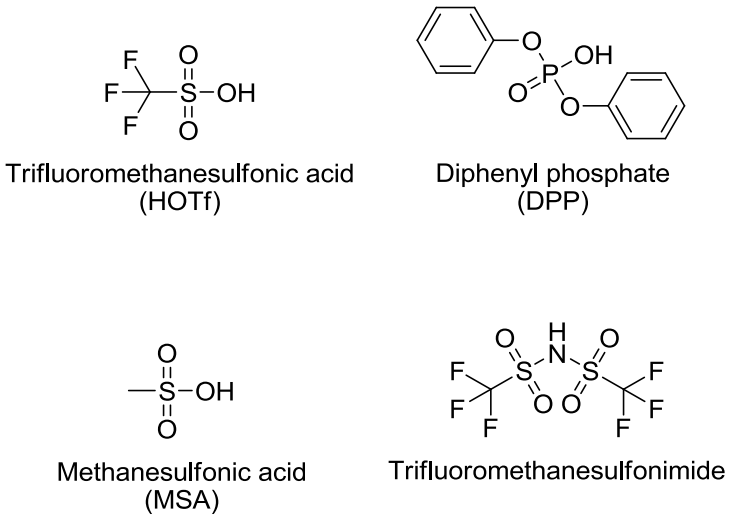


**Figure 1.6** Various acidic ROP catalysts.

To be able to successfully undertake the polymerisation of lactide, a stronger acid such as trifluoromethanesulfonic acid (HOTf) is required.[62-64] Initiating from either water or an alcohol, polymerisations take several hours to reach high monomer conversion (DP50 reaching >96% monomer conversion using 1:1 ratio of initiator to acid at room temperature) whilst maintaining moderately low polymer dispersities

(<1.5). The living character of ROP catalysed by HOTf was demonstrated by the linear relationship between the monomer to initiator ratio and molecular weights obtained of the synthesised PLA by GPC. Additionally, a lack of any epimerisation was found by homonuclear decoupled $^{1}$H NMR spectroscopy. Lacombe *et al* proposed a mechanism where the protonation of the LA carbonyl by HOTf results in its activation towards ROP *via* nucleophilic addition of the alcohol initiator/alcohol chain end. However, computational investigations undertaken by Maron and co-workers found evidence for a bifunctional mechanism where both the monomer and alcohol initiator/propagating chain end are activated, with the acid catalyst then acting as a proton shuttle after nucleophilic addition (Figure 1.7).[65]

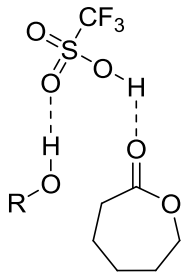


**Figure 1.7** Proposed dual activation of alcohol and *ε*-caprolactone by HOTf

While HOTf has also been demonstrated to be active for the ROP of *ε*-caprolactone, it was found to be detrimental when larger equivalents were used relative to the alcohol initiator.[66] ROP of ε-caprolactone using a 1:1 ratio of HOTf to initiator, targeting a DP40 in toluene at room temperature required 90 minutes to reach completion. The less acidic catalyst methanesulfonic acid (MSA) also took 90 minutes to reach completion under the same conditions, but the MSA to initiator

ratio could be increased to 3:1 reducing the polymerisation time to 30 minutes.[66] Increasing the HOTf to initiator ratio to three resulted in a reduction in monomer conversion down to 33%. This reduction was proposed to be a result of excess amounts of strong acid deactivating the alcohol initiator/chain end, whereas for weaker acids such as MSA will only result in further monomer activation.

Another strong acid which merits note is trifluoromethanesulfonimide ($HNTf_2$) whose highly acidic nature has allowed lower quantities of catalyst to be used compared to HOTf or MSA.[67] In the ROP of δ-valerolactone a 1:0.1 ratio of alcohol initiator to $HNTf_2$ was shown to be effective, with a polymerisation with [M]/[I] = 100 taking 9 h to reach 95% monomer conversion in dichloromethane at room temperature.[68] Good control was achieved with low dispersities (<1.16) found for the synthesised polymers, as well as a linear relationship between molecular weight and monomer conversion.

Use of the highly acidic catalysts applied in ROP of lactide unfortunately leads to undesirable side reactions when applied in the ROP of cyclic carbonates. Work carried out by Bourissou and co-workers demonstrated that the polymerisation of TMC catalysed by HOTf resulted in undesirable decarboxylation whereas with MSA no decarboxylation was observed even at elevated temperatures (80 °C).[69] While the polymerisation of TMC catalysed by MSA using water as an initiator yielded monomodal GPC traces, bimodal traces were observed when using *n*-pentanol. Following a single polymerisation catalysed by MSA (TMC/ROH = 40/1) showed that after 30% monomer conversion there was no longer a linear correlation between the monomer conversion and the molecular weights obtained by GPC. At higher monomer/initiator ratios the resulting PTMC showed a greater deviation from

the expected molecular weights. It was proposed that these observations result from two separate competing mechanisms, an activated monomer (AM) mechanism and an active chain end (ACE) mechanism (Scheme 1.16).

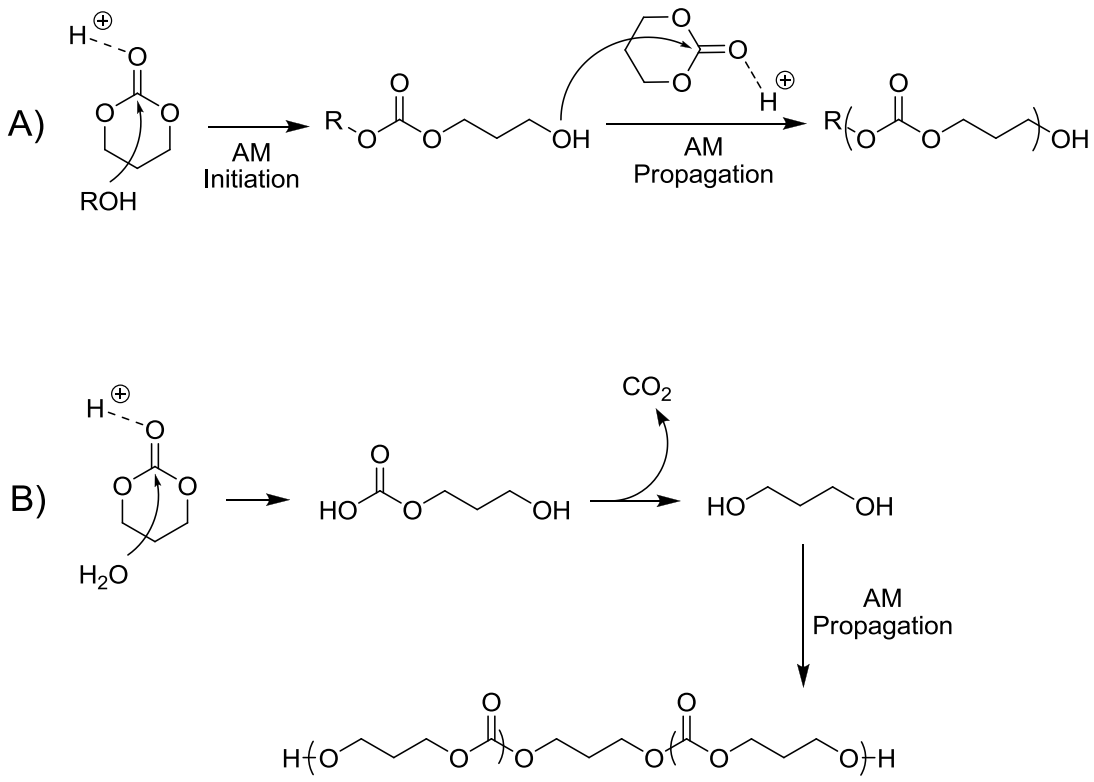


**Scheme 1.16** Proposed activated monomer (AM) mechanism for the ROP of TMC. A) Initiated from an alcohol. B) Initiated from water.

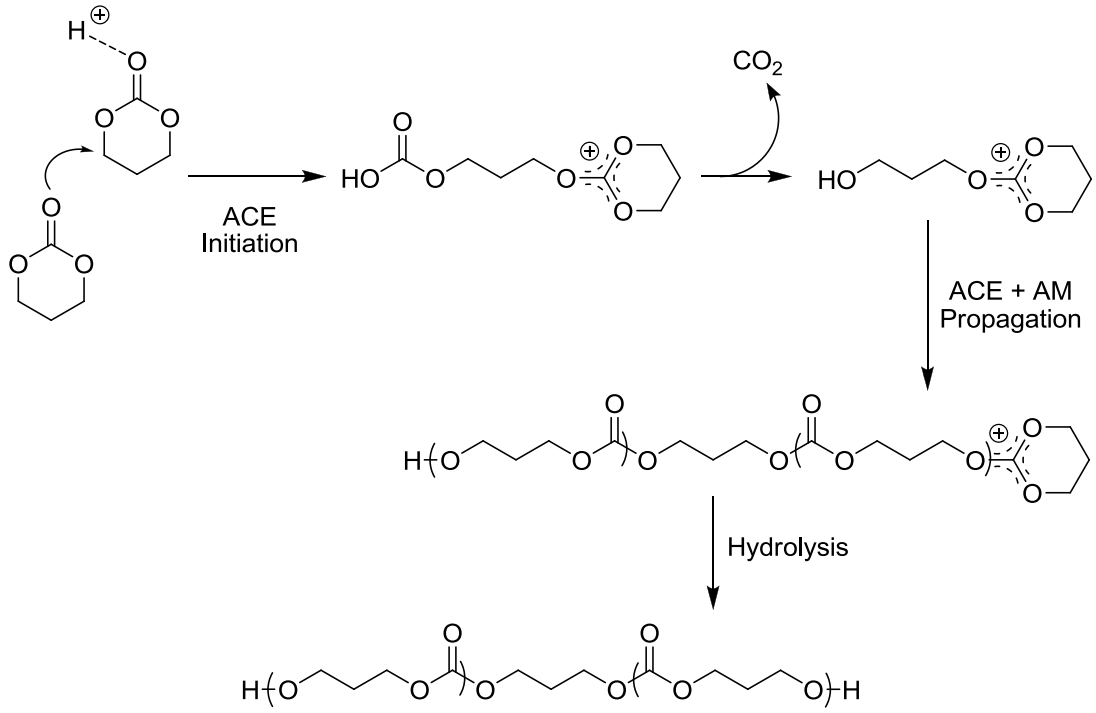


**Scheme 1.17** Proposed activated chain end (ACE) mechanism for the ROP of TMC.

In the AM mechanism the carbonyl of the monomer is activated by the acid catalyst which then allows for nucleophilic attack by an alcohol resulting in ring opening of the monomer. The ACE mechanism is similar, but a monomer unit undertakes nucleophilic attack on the activated monomer rather than an alcohol. Spontaneous decarboxylation then results in a bifunctional molecule with a terminal hydroxyl group at one end and an oxanium group at the other. While the hydroxyl chain end can continue to grow *via* an AM mechanism, the oxonium group can facilitate further growth through the ACE mechanism where further monomer units can undergo nucleophilic attack on the oxonium group. The oxonium group would be easily hydrolysed either during the polymerisation or work up, resulting in a

poly(carbonate) hydroxyl terminated chain ends. Unfortunately the final product from the ACE mechanism is identical to a polymer chain initiated from residual water that has gone through the AM mechanism, making it difficult to determine the actual ROP pathway.[70] Undertaking polymerisations where the monomer/initiator ratio was kept below 10 (via multiple monomer feeds), molecular weights of the final polymers were found to match the theoretical values, and therefore show a reduction in the ACE mechanism.[69]

In comparison, the ROP of TMC catalysed by diphenyl phosphate (DPP) resulted in a linear correlation between monomer conversion and molecular weight measured by GPC with the observation of only monomodal GPC traces demonstrating an improved living character for DPP catalysed cyclic carbonate polymerisations.[71] While it was previously postulated that for DPP only an activated monomer mechanism takes place, molecular modelling carried out by Hedrick and co-workers into the mechanistic pathways found that an ACE mechanism was energetically unfavourable for all acids.[72] The computational investigations along with the known difficulty of drying sulfonic acids (due to their ability to absorb moisture) led to the conclusion that rather than being caused by an ACE mechanism, bimodaility in GPC traces was caused by the initiation from residual water through a mechanism similar to the AM mechanism. The development of acidic catalysts for the ROP of cyclic carbonates has now advanced sufficiently to allow the polymerisation of base sensitive cyclic carbonates in a controlled manner, which was not previously possible *via* other organic catalysts. DPP has also been used successfully to catalyse the ROP of ε-caprolactone and δ-valerolactone, achieving low dispersities (<1.09) for DPs up to 300. The lower acidity of DPP compared to

HOTf prevented undesirable transesterification even at high monomer conversions, with the polymerisations displaying living characteristics.[73]

### 1.3.5 Nitrogen bases

The structurally similar bases N-methylated TBD (MTBD) and 1,8-diaza[5.4.0]bicyloundec-7-ene (DBU) are effective catalysts for the ROP of LA. Both catalysts are capable of achieving quantitative LA conversion in approximately one hour for polymerisations with [M]/[I] = 100 and resulting polymers have low dispersitities (1.05), although at high monomer conversions the catalysts need to be quenched to prevent undesirable transesterification. DBU and MTBD are relatively inert to cyclic monomers and instead work *via* an alcohol activation mechanism (Figure 1.8).[74]

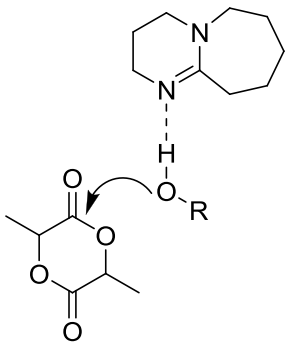


**Figure 1.8** DBU catalysed ROP of LA

Polymerisations of LA catalysed by DBU in the absence of an alcohol initiator have been shown to result in the production of polymer, suggesting an alternative/competing mechanism (Scheme 1.18).[75] Careful MALDI-ToF analysis of

low molecular weight PLA produced in this manner revealed distributions belonging to both linear and cyclic polymers. It was therefore postulated that DBU can also act as a nucleophilic initiator forming a zwitterion upon ring opening of a LA molecule. The resulting zwitterion can react in two ways. The first results in the addition of further LA to the alkoxide of the zwitterion to give larger chains that when are long enough attack the acyl amidinium to form a cyclic polymer, releasing the DBU. The alternative pathways results in the deprotection of the zwitterion to yield a ketene aminal that in the presence of an excess of DBU undergoes chain growth. The chain extended ketene aminal can then either cyclise to produce cyclic polymers or the ketene acetal could be removed upon workup yielding linear PLA chains.

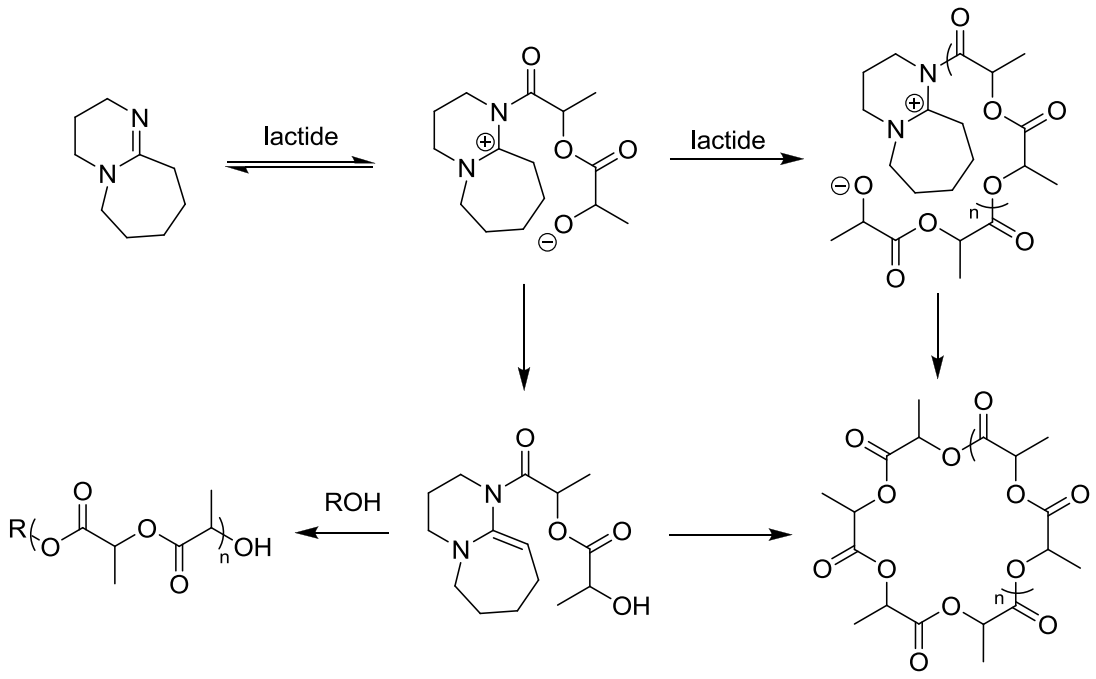


**Scheme 1.18** Proposed mechanism for the ROP of lactide by DBU in the absence of an initiator.

It must also be noted that the method of quenching DBU or MTBD catalysed polymerisations is important. In 2011 Hedrick and co-workers showed that the benzoic acid salt of either of DBU or MTBD was able to catalyse the polymerisation of lactide, albeit with decreased activity.[76] Experimental and computational results pointed to a dual activation mechanism where the aminium ion interacts with the carbonyl of the LA *via* hydrogen bonding with the negatively charged carboxylate of the benzoic acid anion hydrogen bonding to the initiator/propagating chain end alcohol (Figure 1.9). The addition of a further equivalent of benzoic acid blocks this secondary interaction, completely retarding any further polymerisation, demonstrating the need of an excess of acid to quench DBU polymerisation.

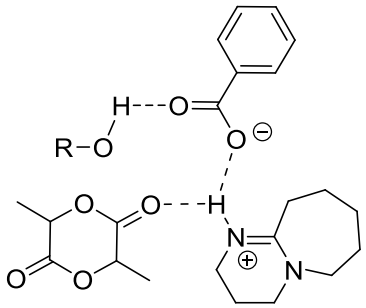


**Figure 1.9** Dual activation by the benzoic acid salt of DBU

While DBU and MTBD are active catalysts for the ROP of LA and cyclic carbonates, they have proven to be ineffective for the polymerisation of lactones. DBU has been used as a catalyst in the preparation of poly(carbonate)s and poly(phosphoester)s showing moderate control except at high monomer conversions where a loss of control results in large polymer dispersities.

### 1.3.6 Bifunctional Activation

The previous examples of organic catalysts take place primarily through a monomer or alcohol activating mechanism. A number of organic catalyst systems also exist where both monomer and alcohol are activated to make ROP possible. Such activation has already been successfully applied in a number of organic reactions for small molecule formation. Investigations have led to a variety of catalyst systems to be developed, focussing on hydrogen-bonding to activate both monomer and initiator either using unimolecular or bimolecular systems.

#### 1.3.6.1 Thiourea/Amine dual catalysis.

In 2005 the first example of a bifunctional organocatalyst for the ROP of LA was reported by Dove *et al.*[77] Thiourea-amine catalyst **18** activates both LA and alcohol initiator through hydrogen-bonding to produce PLAs with DPs up to 200 and low $Đ_M$ values (1.05) suggesting negligible transesterfication even after extended reaction times (48 hours to reach 97% conversion for DP100). $^{13}C$ NMR spectroscopy demonstrated that no observable epimerisation occurred during the polymerisation.

The mechanism for LA ROP catalysed by **18** proposes activation of the carbonyl group of LA by the thiourea group while the tertiary amine of the catalyst activates the initiating/propagating alcohol simultaneously. The dual activation helps to facilitate nucleophilic attack of the initiator. This mechanism was later confirmed by Prat and co-workers who conducted experiments in which the catalyst was essentially split into its active parts, **19** and **20** (Figure 1.10).[78] Polymerisations

undertaken with either **19** or **20** failed to result in any monomer conversion. Further confirmation of the proposed mechanism was the lack of polymerisation observed when **18** was used in tetrahydrofuran, as the solvent disrupts the hydrogen bonding activation of the catalyst. When both thiourea co-catalyst **20** and tertiary amine **19** were used together to catalyse the ROP of LA, similar rates and control were observed as for **18**.

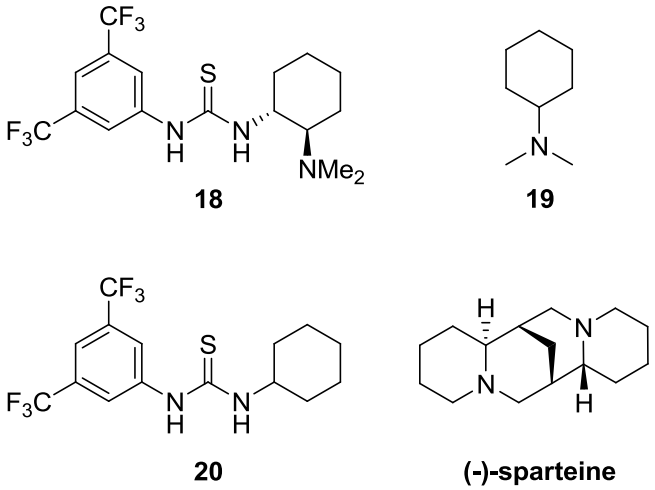


**Figure 1.10** Structures of thiourea-amine **3**, thiourea **4** and amine **5**.

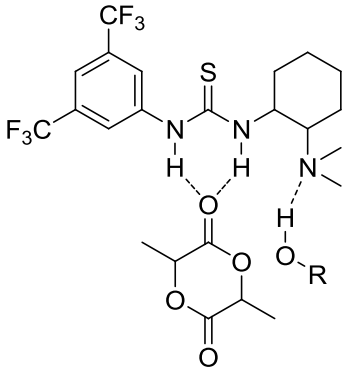


**Figure 1.11** Dual activation of lactide and an alcohol initiator by a thiourea-tertiary amine catalyst.

Further improvements to polymerisation rates were obtained when **20** was used in combination with various commercially available tertiary amines.[78] A forty fold increase in polymerisation rate was observed whilst retaining low dispersities ($Đ_M$ = 1.05) when (-)-sparteine was used as catalyst in combination with **20**, $[M]_0/[I]_0$ = 100 polymerisations reaching full conversion within 24 hours. The increased activity of (-)-sparteine has been assigned to its two nitrogen atoms positioned towards each other allowing for both to partake in hydrogen-bonding to one hydroxyl group and therefore providing increased activation. The (-)-sparteine/**20** catalyst system displayed low levels of monomer epimerisation which was quantified to be ~4% by homonuclear decoupled $^1$H NMR spectoscopy. The (-)-sparteine/**20** binary catalyst system has also been shown to effectively catalyse the ROP of trimethylene carbonate (TMC), producing PTMC with narrow dispersities (<1.07).[45] The catalyst system has since been used with great success in the ROP of cyclic carbonates with a wide range of functionalities.[79-81]

### 1.3.6.2 Alternative Monomer Activators

While thoiurea catalyst **20** is used in conjunction with (-)-sparteine to catalyse the ROP of LA, functional glycolides and cyclic carbonates in most reports, the investigation of other co-catalysts capable of activating cyclic monomers *via* hydrogen bonding has been undertaken (Figure 1.12). Bibal and co-workers have demonstrated that the combination of structurally similar amido-indole (**21**) and (-)-sparteine is capable of catalysing the ROP of LA ([M]/[I] = 20) quantitatively in 24 hours.[82] The same result was obtained when (-)-sparteine/**20** was used under the same conditions with similar molecular properties for both ($Đ_M$ = 1.07-1.10). While

the method of synthesis provided a simple route to produce a range of co-catalysts based on the amido-indole structure, all tested catalysts resulted in lower catalyst activity compared to **20**, resulting from undesirable co-catalyst dimerisation and/or increased hydrogen-bonding between co-catalyst and (-)-sparteine.[83]

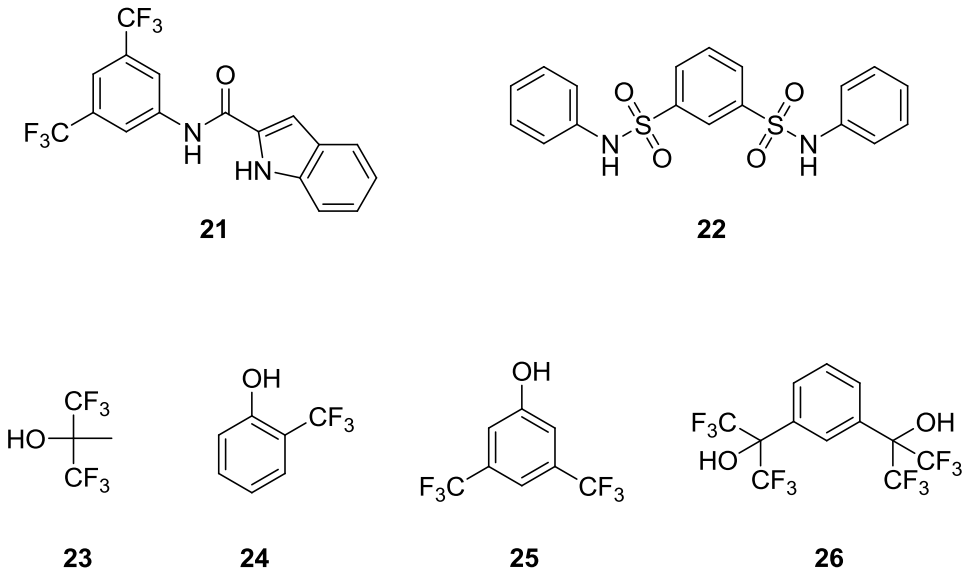


**Figure 1.12** Alternative hydrogen-bond donors

The use of alcohol containing co-catalysts as hydrogen-bond donors has also been used effectively as an alternative to thioureas in ROP. The addition of bulky electron-withdrawing fluorinated groups was found necessary to increase the acidity of the alcohol to aid hydrogen bonding while the sterically bulky groups prevent initiation from the hydroxyl group. Use of fluorinated diol **26** with (-)-sparteine provided control in LA polymerisations yielding PLA with low dispersities.[84] No evidence of stereoerrors in the produced PLA was found by $^{13}C$ NMR spectroscopy. The use of **26**/(-)-sparteine in ROP was even able to yield low molecular weight

poly(β-butyrolactone). Fluorinated phenols **24-25** were shown to be efficient hydrogen-bonding co-catalysts yielding well defined polymers when used in conjunction with (-)-sparteine.[85] MALDI-ToF analysis of the final polymers demonstrated that no initiation from the alcohol containing co-catalyst had taken place and initiation had occurred only from the desired alcohol initiator. The commercial availability and in some cases the low expense of these fluorinated co-catalysts make them an attractive alternative to thiourea **20**.

In comparison to other hydrogen-bonding co-catalysts, bis-sulfonamide **22** displayed a higher activity in the ROP of LA when used in conjunction with DMAP rather than (-)-sparteine.[86] The reduced activity observed when used with (-)-sparteine possibly results from the combined steric effects of (-)-sparteine and the bis-sulfonamides. A mechanism where the two amides of the bis-sulfonamide provide hydrogen-bonding to the carbonyl of LA and DMAP activates the alcohol initiator/chain end was proposed, although long polymerisation times were found experimentally ([M]/[I] = 100, 85% monomer conversion after 156 hours). The system was, however found to display living characteristics and result in PLA with low dispersities.

### 1.3.6.3 DBU/TU and MTBD/TU

While both DBU and MTBD are able to catalyse the ROP of LA and cyclic carbonates, they are ineffective for lactones such as caprolactone or valerolactone even at high catalyst loadings (20 mol% to monomer). However, when used in combination with a thiourea co-catalyst (**20**), the polymerisation of these lactones readily occurs resulting in well defined polymers ($Đ_M$ < 1.07).[74] Although the

MTBD/**20** and DBU/**20** binary catalyst systems are considerably less active than TBD for δ-valerolactone and ε-caprolactone, requiring days to reach high monomer conversion for ε-caprolactone, they have the advantage that polymerisations can be easily quenched to prevent transesterification. Improved kinetics have been achieved by performing polymerisations in bulk, but this was found to be detrimental to the control of the polymerisation.

In comparison, the DBU/**20** binary catalyst system has proven to be effective for the ROP of a wide range of cyclic monomers. A number of functional poly(carbonate)s have been synthesised using this catalyst system due to the resulting fast polymerisation times and the low DBU concentration that prevents undesirable transesterification. For example, ROP of the propargyl functional cyclic carbonate (5-methyl-5-propargyloxycarbonyl-1,3-dioxan-2-one) (MPC), reported by Dove and co-workers, took 24 hours with a [M]/[I] ratio of 20 using 5 mol% (-)-sparteine and 10 mol% **20**.[79] Whereas polymerisations with a [M]/[I] ratio of 100 using 1 mol% DBU and 5 mol% **20** resulted in 90% monomer conversion after just 6 hours and a low $Đ_M$ of 1.11 for the resulting PMPC. The DBU/**20** binary catalyst system has also been shown to result in poly(phosphoester)s with high monomer conversion, whereas when using DBU alone plateaus of around 60% monomer conversion were reported.[87, 88]

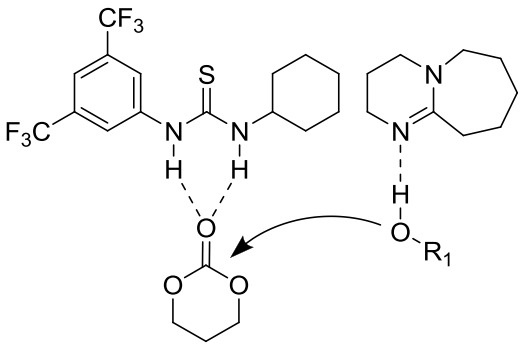


**Figure 1.13** Dual activation of TMC and iniator/propagating chain end by DBU and a thiourea.

### 1.3.6.4 1,5,7–Triazabicyclododecane (TBD)

In 2006, Lohmeijer and co-workers reported the use of 1,5,7-triazabicylo-[4.4.0]dec-5-ene (TBD) as a catalyst for the polymerisation of LA.[74] The strong basicity of TBD ($pK_a$ = 26.0 in acetonitrile *vs* $pK_a$ = 21.66 for (-)-sparteine) combined with its ability to act as an activator for both the monomer and initiator resulted in a vast improvement to the polymerisation rate. PLLA with a DP of 100 and a PDI of 1.19 could be synthesised in less than 20 seconds. However, while TBD has a higher selectivity for the ROP of LA than for transesterfication, at high monomer conversion transesterification takes over. The resulting increase in $Đ_M$ can be avoided by quenching the catalyst with an acid upon completion. In comparison to DBU, where the 1:1 DBU/benzoic acid salt is an active ROP catalyst, the TBD/benzoic acid salt has been found unable to act as an ROP catalyst.[76]

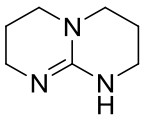

**Figure 1.14** Structure of TBD

TBD has also been used as a catalyst in the ROP of δ-valerolactone and ε-caprolactone.[74] Relatively low catalyst loadings (0.5 mol% to monomer), good end group fidelity, low dispersities (<1.16) and quick polymerisation times (DP100 polyvalerolactone, 30 min) were achieved when ROP was undertaken in toluene. Recently it was also shown that TBD is also capable of polymerising ω-pentadecalactone, a monomer for which only enzymatic or metal based catalysis had previously proven efficient due to the reduced ring strain of this monomer. Again, while good control was reported with TBD in bulk or solution, removal of the catalyst was shown to be vital to obtain well defined polymers.

Other cyclic monomers that have undergone ROP catalysed by TBD are cyclic phosphates, where higher monomer conversion values and shorter time reaction times were achieved compared to DBU catalysed polymerisations. Using DBU, a DP50 poly(2-isopropoxy-2-oxo-1,3,2-dioxaphospholane) (PIPP) was synthesised in 300 minutes whereas when TBD was used as a catalyst a similar molecular weight PIPP was obtained in just 20 minutes whilst obtaining a low dispersity (1.06).[87] The increased activity of TBD over DBU is not unexpected due the dual activation mechanism of TBD, but surprisingly even at high monomer

conversion (99%) relatively low dispersities can be achieved (<1.2) for polyphosphoesters.

TBD is known to form a stable acyl-TBD intermediate upon reaction with vinyl acetate, which in the presence of an excess of an alcohol will acylate to regenerate TBD and form an ester. It was therefore first proposed that TBD catalysed ROP of cyclic monomers proceeds by a similar mechanism, with acylation of TBD by the cyclic monomer. The subsequent activation of the alcohol initiator/propagating chain end *via* hydrogen bonding from the adjacent nitrogen atom then facilitates the displacement of the acylated TBD, releasing the hydroxyl terminated ring opened monomer (Scheme 1.19).[74, 89] While this bifunctional nucleophilic mechanism has proven to be feasible by computational investigations, an alternative mechanism was found to be more favourable.[90, 91] In this mechanism simultaneous activation of the monomer and alcohol are achieved in method analogous to that of a thiourea/amine binary catalyst system (Scheme 1.20).

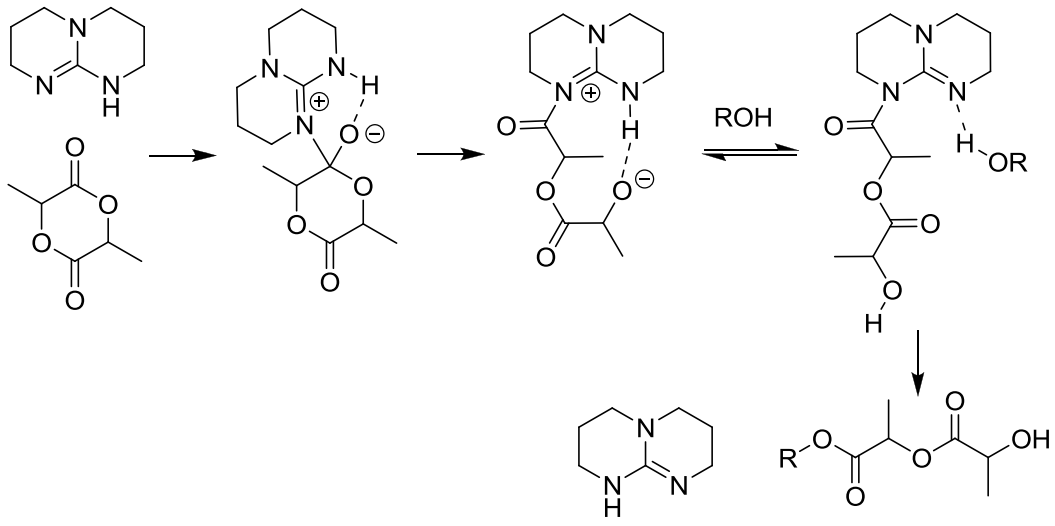


**Scheme 1.19** Nucleophilic mechanism for the ROP of LA catalysed by TBD.

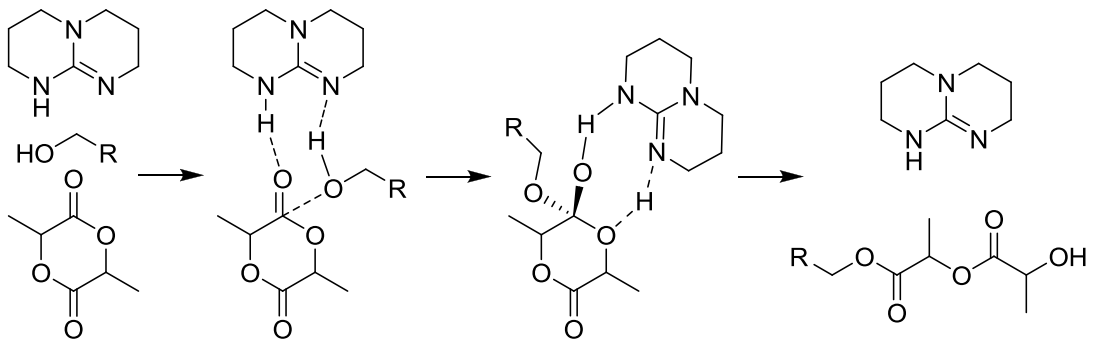

**Scheme 1.20** Generalised hydrogen bonding mechanism for ROP of lactide with TBD.

### 1.3.7 Stereoselective ROP of LA

As discussed in the beginning of this chapter, the microstructure of PLA plays an important role on the polymers properties. While ROP of stereopure LA in an absence of epimerisation results in isotactic PLA, ROP of *rac*-lactide produces atactic PLA unless the catalyst system possesses the ability to control the insertion of different stereoisomers of LA into the polymer chain. A range of metal based catalysts are capable of this, producing isotactic and even heterotactic PLA from *rac*-lactide.[16] In comparison there have been relatively few reports of organic catalysts able to provide control the stereochemistry of PLA.

Phosphazene catalyst $P_2$-t-Bu has been shown to yield crystalline PLA *via* the polymerisation of *rac*-lactide at very low temperatures.[92] At 20 °C the catalyst resulted in a probability of isotactic enchainment ($P_m$) of 0.72 with MALDI-ToF analysis demonstrating a large degree of transesterification, but at -75°C a $P_m$ of 0.95 was measured with no observable transesterfication by MALDI-ToF. For the PLA

synthesised at -75 °C, a melting point of 201 °C was measured by DSC which suggests the formation of stereocomplexation between PDLA and PLLA chains formed during ROP. As $P_2$-t-Bu catalyses the ROP of cyclic monomers *via* an alcohol activation mechanism, both stereoisomers are ring opened equally during the first turnover. The alcohol initiator does not direct any stereoselectivity onto the catalyst (although there have been no reports studying the effect of chiral alcohol initiators), but once a single LA has been ring opened the stereochemistry adjacent to the propagating alkoxide chain end influences the bulky catalyst making preferential addition of the same stereoisomer again. At extremely low temperatures the mobility of the catalyst/alkoxide chain end is reduced, resulting in the observed enhanced stereoselectivity.

NHC catalysts are also capable of polymerising *rac*-lactide to form isotactic PLA, but only if they are sterically bulky.[93] As for the phosphazene catalyst, at room temperature NHC catalyst **27** demonstrates only a slight preference towards stereocontrol ($P_m$ = 0.59), but polymerisations undertaken at -70 °C resulted in a significant enhancement in stereocontrol ($P_m$ of 0.90). It has been demonstrated that chiral metal catalysts are capable of polymerising one particular stereoisomer of LA. Introducing chiral groups into the NHC catalyst in the hopes that a stereopure catalyst would also preferentially ring open just one LA stereoisomer has however not resulted in improvements in stereoselectivity. As for the phosphazene catalyst, it therefore seems that steric congestion of the active propagating chain end is the major factor in improving stereoselectivity for the NHC catalysts.

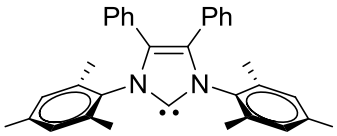


**27**

**Figure 1.15** Sterically bulky NHC.

While both phosphazene and NHC catalysts can produce stereoblock PLA from rac-LA at extremely low temperatures, it would be an obvious advantage to achieve the same stereoselectivity at room temperature. The (-)-sparteine/**6** binary catalysts system results in moderate stereoselctivity at room temperature, with $P_m$ values of 0.77 reported.[94] This increased stereocontrol, possibly due to the chiral nature of (-)-sparteine has led to the investigation of another chiral hydrogen bonding catalyst, β-isocupreidine (ICD), but only stereoselectivities similar to (-)-sparteine/TU are observed ($P_m$ = 0.64-0.75) with the catalyst requiring extremely long polymerisation times ([M]/[I] = 100, [M] = [I], 90% monomer conversion after 60 hours).

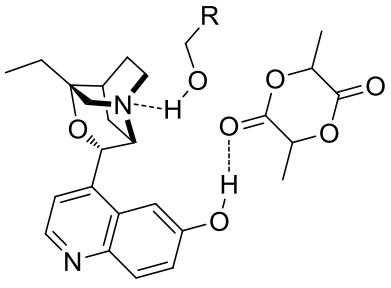


**Figure 1.16** Dual activation of lactide and an alcohol initiator by β-isocupreidine.

## 1.4 Concluding Remarks

As stated at the beginning of this chapter, no one organic catalyst is capable of producing well defined polymers from all types of cyclic monomers, meaning that careful choice of organic catalyst based on the monomer and polymer application are required. Acid organocatalysts are capable of producing polymers from small lactones in a controlled manner within reasonable reaction times with more reactive organocatalysts such as TBD required for less activated macrolactones. While TBD and NHCs are highly active resulting in their ability to polymerise a range of cyclic monomers, they can result in a loss of control if not properly monitored. Although NHCs can be utilised to produce unusual macromolecular architectures. DBU is highly active for the ROP of LA and only results in a small quantity of epimerisation, making it a useful catalyst when perfect control of the PLA microstructure is not required. The (-)-sparteine/TU binary catalyst system is useful to obtain PLA with negligible stereoerrors from stereopure LA while phosphazenes provide the ability to produce highly isotactic PLA from *rac*-LA. The copolymerisation of cyclic monomers with methacrylates by phosphazenes has the potential to produce completely novel materials.

While organic catalysts have advanced far enough over the past decade to be able to now compete with metal catalysed ROP, there are still some challenges that exist. The organic catalysed ROP of LA under industrial conditions (i.e. bulk) is still not possible, due to the lower thermal stability of organic catalysts and the inability to avoid epimerisation at higher temperatures. Stereoselectivity by organic catalysts has only been achieved at extremely low temperatures, where the ability to produce isotactic PLA from *rac*-LA at ambient temperatures or above is highly desirable.

The number and type of cyclic monomers that undergo ROP to yield biodegradable materials continues to grow and diversify. Through the combination of these monomers with the capabilities of organic catalysts, polymers with a range of interesting and useful properties can be designed and synthesised.

## 1.5 References


1. M. Fevre, J. Pinaud, Y. Gnanou, J. Vignolle and D. Taton, *Chem. Soc. Rev.*, 2013, **42**, 2142-2172.
2. D. Bourissou, S. Moebs-Sanchez and B. Martín-Vaca, *C. R. Chim.*, 2007, **10**, 775-794.
3. N. E. Kamber, W. Jeong, R. M. Waymouth, R. C. Pratt, B. G. G. Lohmeijer and J. L. Hedrick, *Chem. Rev.*, 2007, **107**, 5813-5840.
4. M. K. Kiesewetter, E. J. Shin, J. L. Hedrick and R. M. Waymouth, *Macromolecules*, 2010, **43**, 2093-2107.
5. A. P. Dove, *ACS Macro Lett.*, 2012, **1**, 1409-1412.
6. H. R. Kricheldorf, M. Berl and N. Scharnagl, *Macromolecules*, 1988, **21**, 286-293.
7. B. J. O'Keefe, M. A. Hillmyer and W. B. Tolman, *Dalton Trans.*, 2001, 2215-2224.
8. A.-C. Albertsson and I. K. Varma, *Biomacromolecules*, 2003, **4**, 1466-1486.
9. S. Dutta, W.-C. Hung, B.-H. Huang and C.-C. Lin, in *Synthetic Biodegradable Polymers*, eds. B. Rieger, A. Künkel, G. W. Coates, R. Reichardt, E. Dinjus and T. A. Zevaco, Springer Berlin Heidelberg, 2012, vol. 245, pp. 219-283.
10. S. Tempelaar, L. Mespouille, O. Coulembier, P. Dubois and A. P. Dove, *Chem. Soc. Rev.*, 2013, **42**, 1312-1336.
11. R. J. Pounder and A. P. Dove, *Polym. Chem.*, 2010, **1**, 260-271.
12. J. M. Becker, R. J. Pounder and A. P. Dove, *Macromol. Rapid Commun.*, 2010, **31**, 1923-1937.
13. J. K. Oh, *Soft Matter*, 2011, **7**, 5096-5108.

14. M. A. Woodruff and D. W. Hutmacher, *Prog. Polym. Sci.*, 2010, **35**, 1217-1256.

15. H. Kweon, M. K. Yoo, I. K. Park, T. H. Kim, H. C. Lee, H.-S. Lee, J.-S. Oh, T. Akaike and C.-S. Cho, *Biomaterials*, 2003, **24**, 801-808.

16. M. J. Stanford and A. P. Dove, *Chem. Soc. Rev.*, 2010, **39**, 486-494.

17. H. Tsuji, *Macromol. Biosci.*, 2005, **5**, 569-597.

18. Y. Fan, H. Nishida, Y. Shirai, Y. Tokiwa and T. Endo, *Polym. Degrad. Stab.*, 2004, **86**, 197-208.

19. M. Yin and G. L. Baker, *Macromolecules*, 1999, **32**, 7711-7718.

20. R. J. Pounder and A. P. Dove, *Biomacromolecules*, 2010, **11**, 1930-1939.

21. X. Jiang, E. B. Vogel, M. R. Smith and G. L. Baker, *J. Polym. Sci. A Polym. Chem.*, 2007, **45**, 5227-5236.

22. X. Jiang, E. B. Vogel, M. R. Smith and G. L. Baker, *Macromolecules*, 2008, **41**, 1937-1944.

23. K. J. Zhu, R. W. Hendren, K. Jensen and C. G. Pitt, *Macromolecules*, 1991, **24**, 1736-1740.

24. E. Bat, J. e. A. Plantinga, M. C. Harmsen, M. J. A. van Luyn, Z. Zhang, D. W. Grijpma and J. Feijen, *Biomacromolecules*, 2008, **9**, 3208-3215.

25. Y. Shibasaki, F. Sanda and T. Endo, *Macromol. Rapid Commun.*, 1999, **20**, 532-535.

26. M. Azechi, K. Matsumoto and T. Endo, *J. Polym. Sci. A Polym. Chem.*, 2013, **51**, 1651-1655.

27. J. Matsuo, K. Aoki, F. Sanda and T. Endo, *Macromolecules*, 1998, **31**, 4432-4438.

28. E. I. Geihe, C. B. Cooley, J. R. Simon, M. K. Kiesewetter, J. A. Edward, R. P. Hickerson, R. L. Kaspar, J. L. Hedrick, R. M. Waymouth and P. A. Wender, *Proc. Natl. Acad. Sci. USA*, 2012, **109**, 13171-13176.

29. F. Suriano, R. Pratt, J. P. K. Tan, N. Wiradharma, A. Nelson, Y.-Y. Yang, P. Dubois and J. L. Hedrick, *Biomaterials*, 2010, **31**, 2637-2645.

30. Y.-C. Wang, Y.-Y. Yuan, J.-Z. Du, X.-Z. Yang and J. Wang, *Macromol. Biosci.*, 2009, **9**, 1154-1164.

31. S. Zhang, J. Zou, F. Zhang, M. Elsabahy, S. E. Felder, J. Zhu, D. J. Pochan and K. L. Wooley, *J. Am. Chem. Soc.*, 2012, **134**, 18467-18474.

32. Y. H. Lim, G. S. Heo, S. Cho and K. L. Wooley, *ACS Macro Lett.*, 2013, **2**, 785-789.

33. S. Zhang, H. Wang, Y. Shen, F. Zhang, K. Seetho, J. Zou, J.-S. A. Taylor, A. P. Dove and K. L. Wooley, *Macromolecules*, 2013, **46**, 5141-5149.

34. F. Nederberg, E. F. Connor, M. Möller, T. Glauser and J. L. Hedrick, *Angew. Chem. Int. Ed*, 2001, **40**, 2712-2715.

35. C. Bonduelle, B. Martín-Vaca, F. P. Cossío and D. Bourissou, *Chem. Eur. J.*, 2008, **14**, 5304-5312.

36. O. Thillaye du Boullay, E. Marchal, B. Martin-Vaca, F. P. Cossío and D. Bourissou, *J. Am. Chem. Soc.*, 2006, **128**, 16442-16443.

37. O. Thillaye du Boullay, C. Bonduelle, B. Martin-Vaca and D. Bourissou, *Chem. Commun.*, 2008, 1786-1788.

38. R. J. Pounder, D. J. Fox, I. A. Barker, M. J. Bennison and A. P. Dove, *Polym. Chem.*, 2011, **2**, 2204-2212.

39. E. F. Connor, G. W. Nyce, M. Myers, A. Möck and J. L. Hedrick, *J. Am. Chem. Soc.*, 2002, **124**, 914-915.

40. G. W. Nyce, T. Glauser, E. F. Connor, A. Möck, R. M. Waymouth and J. L. Hedrick, *J. Am. Chem. Soc.*, 2003, **125**, 3046-3056.

41. J. Raynaud, C. Absalon, Y. Gnanou and D. Taton, *J. Am. Chem. Soc.*, 2009, **131**, 3201-3209.

42. S. Naumann, S. Epple, C. Bonten and M. R. Buchmeiser, *ACS Macro Lett.*, 2013, **2**, 609-612.

43. M. Rodriguez, S. Marrot, T. Kato, S. Stérin, E. Fleury and A. Baceiredo, *J. Organomet. Chem.*, 2007, **692**, 705-708.

44. J. Raynaud, N. Liu, Y. Gnanou and D. Taton, *Macromolecules*, 2010, **43**, 8853-8861.

45. F. Nederberg, B. G. G. Lohmeijer, F. Leibfarth, R. C. Pratt, J. Choi, A. P. Dove, R. M. Waymouth and J. L. Hedrick, *Biomacromolecules*, 2006, **8**, 153-160.

46. C.-L. Lai, H. M. Lee and C.-H. Hu, *Tetrahedron Lett.*, 2005, **46**, 6265-6270.

47. W. Jeong, E. J. Shin, D. A. Culkin, J. L. Hedrick and R. M. Waymouth, *J. Am. Chem. Soc.*, 2009, **131**, 4884-4891.

48. O. Coulembier, B. G. G. Lohmeijer, A. P. Dove, R. C. Pratt, L. Mespouille, D. A. Culkin, S. J. Benight, P. Dubois, R. M. Waymouth and J. L. Hedrick, *Macromolecules*, 2006, **39**, 5617-5628.

49. S. Csihony, D. A. Culkin, A. C. Sentman, A. P. Dove, R. M. Waymouth and J. L. Hedrick, *J. Am. Chem. Soc.*, 2005, **127**, 9079-9084.

50. A. P. Dove, R. C. Pratt, B. G. G. Lohmeijer, D. A. Culkin, E. C. Hagberg, G. W. Nyce, R. M. Waymouth and J. L. Hedrick, *Polymer*, 2006, **47**, 4018-4025.

51. L. Zhang, F. Nederberg, R. C. Pratt, R. M. Waymouth, J. L. Hedrick and C. G. Wade, *Macromolecules*, 2007, **40**, 4154-4158.

52. J. De Winter, O. Coulembier, P. Gerbaux and P. Dubois, *Macromolecules*, 2010, **43**, 10291-10296.

53. M. Helou, O. Miserque, J.-M. Brusson, J.-F. Carpentier and S. M. Guillaume, *Chem. Eur. J.*, 2010, **16**, 13805-13813.

54. P. Brignou, M. Priebe Gil, O. Casagrande, J.-F. o. Carpentier and S. M. Guillaume, *Macromolecules*, 2010, **43**, 8007-8017.

55. T. Pietzonka and D. Seebach, *Angew. Chem. Int. Ed*, 1993, **32**, 716-717.

56. N. Miyamoto, Y. Inoue, S. Koizumi and T. Hashimoto, *J. Appl. Crystallogr.*, 2007, **40**, s568-s572.

57. H. Yang, J. Xu, S. Pispas and G. Zhang, *Macromolecules*, 2012, **45**, 3312-3317.

58. S. Csihony, T. T. Beaudette, A. C. Sentman, G. W. Nyce, R. M. Waymouth and J. L. Hedrick, *Adv. Synth. Catal.*, 2004, **346**, 1081-1086.

59. Y. Shibasaki, H. Sanada, M. Yokoi, F. Sanda and T. Endo, *Macromolecules*, 2000, **33**, 4316-4320.

60. F. Sanda, H. Sanada, Y. Shibasaki and T. Endo, *Macromolecules*, 2001, **35**, 680-683.

61. E. Oledzka and S. S. Narine, *J. Appl. Polym. Sci.*, 2011, **119**, 1873-1882.

62. D. Bourissou, B. Martin-Vaca, A. Dumitrescu, M. Graullier and F. Lacombe, *Macromolecules*, 2005, **38**, 9993-9998.

63. M. Baśko and P. Kubisa, *J. Polym. Sci. A Polym. Chem.*, 2010, **48**, 2650-2658.

64. M. Baśko and P. Kubisa, *J. Polym. Sci. A Polym. Chem.*, 2006, **44**, 7071-7081.

65. N. Susperregui, D. Delcroix, B. Martin-Vaca, D. Bourissou and L. Maron, *J. Org. Chem.*, 2010, **75**, 6581-6587.

66. S. p. Gazeau-Bureau, D. Delcroix, B. Martín-Vaca, D. Bourissou, C. Navarro and S. p. Magnet, *Macromolecules*, 2008, **41**, 3782-3784.

67. K. Makiguchi, S. Kikuchi, T. Satoh and T. Kakuchi, *J. Polym. Sci. A Polym. Chem.*, 2013, **51**, 2455-2463.

68. R. Kakuchi, Y. Tsuji, K. Chiba, K. Fuchise, R. Sakai, T. Satoh and T. Kakuchi, *Macromolecules*, 2010, **43**, 7090-7094.

69. D. Delcroix, B. Martín-Vaca, D. Bourissou and C. Navarro, *Macromolecules*, 2010, **43**, 8828-8835.

70. J. M. Campos, M. R. Ribeiro, M. F. Ribeiro, A. Deffieux and F. Peruch, *Macromol. Chem. Phys.*, 2013, **214**, 85-93.

71. K. Makiguchi, Y. Ogasawara, S. Kikuchi, T. Satoh and T. Kakuchi, *Macromolecules*, 2013, **46**, 1772-1782.

72. D. J. Coady, H. W. Horn, G. O. Jones, H. Sardon, A. C. Engler, R. M. Waymouth, J. E. Rice, Y. Y. Yang and J. L. Hedrick, *ACS Macro Lett.*, 2013, **2**, 306-312.

73. K. Makiguchi, T. Satoh and T. Kakuchi, *Macromolecules*, 2011, **44**, 1999-2005.

74. B. G. G. Lohmeijer, R. C. Pratt, F. Leibfarth, J. W. Logan, D. A. Long, A. P. Dove, F. Nederberg, J. Choi, C. Wade, R. M. Waymouth and J. L. Hedrick, *Macromolecules*, 2006, **39**, 8574-8583.

75. H. A. Brown, A. G. De Crisci, J. L. Hedrick and R. M. Waymouth, *ACS Macro Lett.*, 2012, **1**, 1113-1115.

76. D. J. Coady, K. Fukushima, H. W. Horn, J. E. Rice and J. L. Hedrick, *Chem. Commun.*, 2011, **47**, 3105-3107.

77. A. P. Dove, R. C. Pratt, B. G. G. Lohmeijer, R. M. Waymouth and J. L. Hedrick, *J. Am. Chem. Soc.*, 2005, **127**, 13798-13799.

78. R. C. Pratt, B. G. G. Lohmeijer, D. A. Long, P. N. P. Lundberg, A. P. Dove, H. Li, C. G. Wade, R. M. Waymouth and J. L. Hedrick, *Macromolecules*, 2006, **39**, 7863-7871.

79. S. Tempelaar, I. A. Barker, V. X. Truong, D. J. Hall, L. Mespouille, P. Dubois and A. P. Dove, *Polym. Chem.*, 2013, **4**, 174-183.

80. S. Onbulak, S. Tempelaar, R. J. Pounder, O. Gok, R. Sanyal, A. P. Dove and A. Sanyal, *Macromolecules*, 2012, **45**, 1715-1722.

81. S. Tempelaar, L. Mespouille, P. Dubois and A. P. Dove, *Macromolecules*, 2011, **44**, 2084-2091.

82. S. Koeller, J. Kadota, A. Deffieux, F. Peruch, S. Massip, J. M. Leger, J. P. Desvergne and B. Bibal, *J. Am. Chem. Soc.*, 2009, **131**, 15088-+.

83. S. Koeller, J. Kadota, F. Peruch, A. Deffieux, N. Pinaud, I. Pianet, S. Massip, J. M. Leger, J. P. Desvergne and B. Bibal, *Chem. Eur. J.*, 2010, **16**, 4196-4205.

84. O. Coulembier, D. R. Sanders, A. Nelson, A. N. Hollenbeck, H. W. Horn, J. E. Rice, M. Fujiwara, P. Dubois and J. L. Hedrick, *Angew. Chem. Int. Ed*, 2009, **48**, 5170-5173.

85. C. Thomas, F. Peruch, A. Deffieux, A. Milet, J. P. Desvergne and B. Bibal, *Adv. Synth. Catal.*, 2011, **353**, 1049-1054.

86. A. Alba, A. Schopp, A. P. D. Delgado, R. Cherif-Cheikh, B. Martin-Vaca and D. Bourissou, *J. Polym. Sci. A Polym. Chem.*, 2010, **48**, 959-965.

87. Y. Iwasaki and E. Yamaguchi, *Macromolecules*, 2010, **43**, 2664-2666.

88. B. Clément, B. Grignard, L. Koole, C. Jérôme and P. Lecomte, *Macromolecules*, 2012, **45**, 4476-4486.

89. R. C. Pratt, B. G. G. Lohmeijer, D. A. Long, R. M. Waymouth and J. L. Hedrick, *J. Am. Chem. Soc.*, 2006, **128**, 4556-4557.

90. L. Simón and J. M. Goodman, *J. Org. Chem.*, 2007, **72**, 9656-9662.

91. A. Chuma, H. W. Horn, W. C. Swope, R. C. Pratt, L. Zhang, B. G. G. Lohmeijer, C. G. Wade, R. M. Waymouth, J. L. Hedrick and J. E. Rice, *J. Am. Chem. Soc.*, 2008, **130**, 6749-6754.

92. L. Zhang, F. Nederberg, J. M. Messman, R. C. Pratt, J. L. Hedrick and C. G. Wade, *J. Am. Chem. Soc.*, 2007, **129**, 12610-12611.

93. A. P. Dove, H. B. Li, R. C. Pratt, B. G. G. Lohmeijer, D. A. Culkin, R. M. Waymouth and J. L. Hedrick, *Chem. Commun.*, 2006, 2881-2883.

94. A. P. Dove, R. C. Pratt, B. G. G. Lohmeijer, R. M. Waymouth and J. L. Hedrick, *J. Am. Chem. Soc.*, 2005, **127**, 13798-13799.

# Chapter Two

## A Novel Organic Catalyst for the Ring Opening Polymerisation of Lactide

THE UNIVERSITY OF
WARWICK

## 2.1 Introduction

The last decade has led to many advances in organocatalytic ring-opening polymerisation (ROP) of several cyclic monomers, most commonly including esters and carbonates.[1-8] On account of their facile access, commercial availability and efficient nature, organic catalysts have become a valuable addition to this field. While several simple species have been reported to mediate these processes, 1,8-diazabicyclo[5.4.0]undec-7-ene (DBU), triazabicyclodecene (TBD) and *N*-heterocyclic carbenes are amongst the most active,[9-14] the bifunctional catalyst system containing both a thiourea and tertiary amine (Figure 2.1), has been reported to proceed with an almost absence of transesterification and epimerization side reactions, and thus provides a critical method for the production of precisely defined polymers. The high selectivity towards polymerisation in preference to deleterious side reactions is attributed to the supramolecular recognition (and concurrent activation) of the cyclic ester monomers in preference to the linear esters by the thiourea moiety.[15, 16] Critically however, it was demonstrated that the thiourea and the amine need not be conjoined and in turn this has led to the discovery of more active analogues, most notably the combination of 1-(3,5-bis(trifluoromethyl)phenyl)-3-cyclohexylthiourea (TU) and (-)-sparteine, a naturally occurring alkaloid, which finds the optimum balance between activity and selectivity.[16] The increased rate of polymersation (25 fold increase) can be assigned to the two tertiary amines of (-)-sparteine being forced into close proximity as a consequence of the fixed rigid backbone with the lone pairs being oriented towards each other in such a way to promote hydrogen bonding. Concurrently, the weakly basic nature of (-)-sparteine (p$K_a$ = 21.66),[17] maintains the high selectivity towards ROP *vs.* transesterification and epimerisation. This concept has since been extended

to a wide range of hydrogen bond acceptors and donors that maintain the simultaneous activation of both the carbonyl group of the monomer and the initiating/propagating alcohol.[18-22]

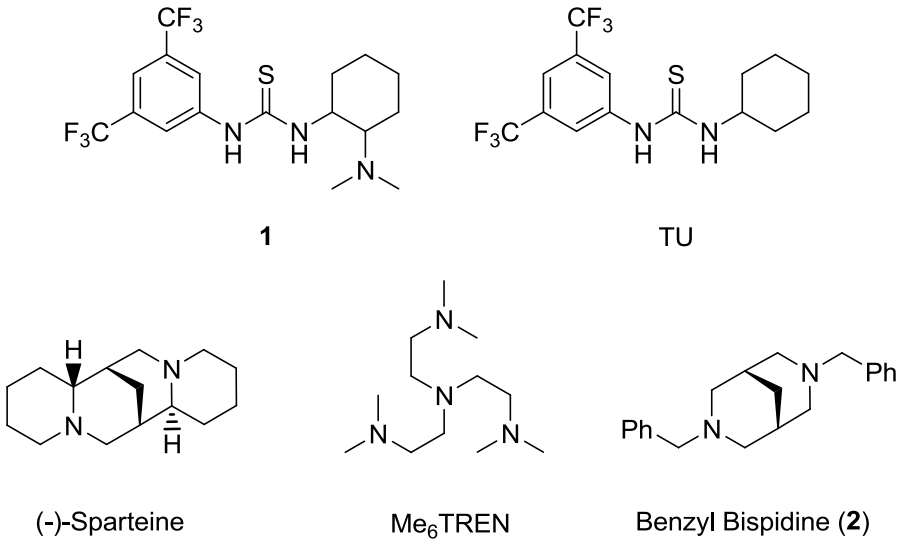


**Figure 2.1** Ring opening-polymerisation catalysts.

In addition to its uses in ROP, (-)-sparteine has a number of other uses such as a chiral ligand in asymmetric deprotonations, substitutions and metalations.[23-26] Despite this widespread use and utility, (-)-sparteine has become increasingly difficult to acquire through commercial sources. Several potential routes to obtain (-)-sparteine exist including isolation from the abundant Scotch Broom (*Cytisus scoparius*),[27] or total synthesis *via* a multistep route that has varying overall yields.[28, 29] Furthermore, the derivation of synthetic replacements may enable more highly active and stereoselective analogues to be realised.

These challenges in obtaining (-)-sparteine have led to the investigation of synthetically simple analogues. Aided by computational modelling, Hedrick and co-workers recently identified several commercially available tertiary amines that displayed similar nitrogen–nitrogen spacing (approximately 3 Å) and lone pair orientations to (-)-sparteine.[30] Of the tertiary amines selected, tris[2-dimethylamino)ethyl]amine ($Me_6$TREN) and 1,4,7-trimethyl-1,4,7-triazacyclononane (TACN), in combination with TU, proved the most effective catalysts in the ROP of lactide. While TACN displayed comparable polymerization kinetics to (-)-sparteine, transesterification was noted to occur rapidly upon complete conversion of the monomer. Application of $Me_6$TREN led to less transesterification than TACN, albeit at a longer polymerisation time.

Herein the improved synthesis of a dibenzyl-functional bispidine is reported, chosen for its identical backbone and similar basicity ($pK_a$ = 21.25) to (-)-sparteine.[17] Its ability to catalyse the ROP of lactide, comparing directly to that of (-)-sparteine and $Me_6$TREN, is explored. Extension of the application of this species with a range of co-catalysts and other monomer feedstocks is also demonstrated.

## 2.2 Results and Discussion

### 2.2.1 Bispidine Synthesis

The synthesis of a range of bispidine compounds has been reported previously. Most work has focused on their chelation to metal atoms as a consequence of their favourable rigidity imparted by the bispidine backbone or their use in antiarrhythmic agents. There are two synthetic routes that have been utilised for the synthesis of bispidines. The first involves a double Mannich reaction of a functional 4-piperidone with an amine to form a bispidone, followed by a Wolff–Kishner reduction with hydrazine to remove the ketone group, forming a bispidine (Scheme 2.1).[31]

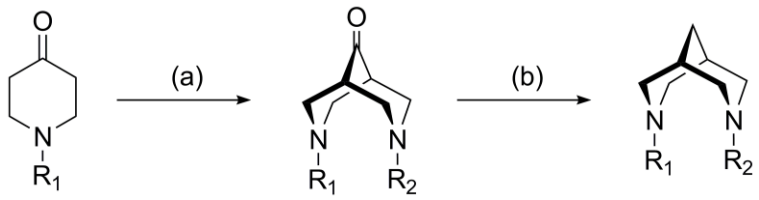


**Scheme 2.1** Two step synthesis of bispidines: (a) Paraformaldehyde, $NH_2R$, acetic acid, MeOH; (b) Hydrazine hydrate.

The second route reported by Gogoll *et al.* contains a larger number of synthetic steps, the functionality is only imparted to the bispidine on the final step, allowing for the facile synthesis of a range of bispidine compounds in just one step from a common precursor if so required.[17, 32] For this reason this longer synthetic route was chosen.

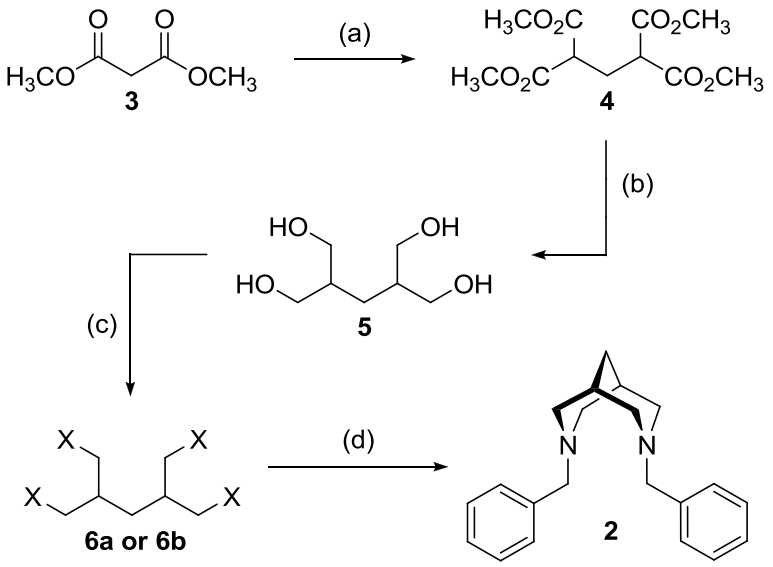


**Scheme 2.2** Alternative benzyl bispidine synthesis: (a) Paraformaldehyde, KOH, 95 °C; (b) $LiAlH_4$, THF; (c) **6a** (X = I): $I_2$, $P_{red}$, 120 °C; **6b** (X = Br): $PBr_3$, 100 °C; (d) benzylamine, toluene, reflux.

The first of a four step synthetic route involves a simple Knoevenagel condensation of dimethyl malonate, **3**, with paraformaldehyde at 95 °C as reported previously by Gogoll *et al*.[32] After heating for a further 16 h, the remaining starting material was removed under high vacuum and the pure product, **4**, was obtained in a 96% yield after the removal of volatiles *in vacuo* and purification by column chromatography. Compound **4** was then reduced using $LiAlH_4$ under reflux in tetrahydrofuran, with isolation of the resulting tetra-alcohol species **5** in a 40% yield *via* soxhlet extraction. Iodination of **5**, which had been previously reported by Gogoll *et al.*,[32] proved to be problematic on a large scale due to the exothermic and unpredictable nature of the reaction. As an alternative, the tetra-bromo species **6b** was synthesised in an analogous manner to that previously reported for a structurally similar tetra-bromo compound.[33] After bromination of tetra-alcohol **5** by $PBr_3$ at 100

°C, the crude product was extracted, purified by passing through silica and recrystallised yielding **6b** as white crystals in a 61% yield.

Benzyl bispidine, **2**, was finally synthesised by refluxing tetra-bromo species **6b** with benzylamine and toluene under a nitrogen atmosphere in an ampoule. After several washing and extraction steps, **2** was further purified by column chromatography using conditions reported by Toom *et al.*[17] An alternative faster method of purification was developed wherein **2** was purified by passing the crude mixture through a short silica plug using DCM/MeOH (90:10), successfully removing all byproducts in a single step, followed by flushing the silica plug with DCM/MeOH/TEA (80:10:10) giving **2** in a 31% yield. In comparison, Toom *et al.* reported a 40% yield of **2** when using the tetra-iodine species **6a**.[17] The change to the synthetic procedure provides a slight reduction in yield, but overall provides a more streamlined synthesis that can be achieved on a larger scale. Representative $^{1}$H NMR spectra of **6b** and **2** are shown in Figure 2.2. The central bridge protons of **6b** appear as a triplet at $\delta$ = 1.64 ppm, with the neighbouring two protons appearing as a multiplet at $\delta$ = 2.08 ppm. These do not shift significantly in upon the formation of **2**, while the protons now adjacent to the tertiary amine in the two 6-membered rings show a large shift from two doublet of doublets at $\delta$ = 3.6 and 3.46 ppm to $\delta$ = 2.80 and 2.33 ppm. The clear doublet and two triplets at $\delta$ = 7.44, 7.31 and 7.23 ppm and the singlet at $\delta$ = 3.47 ppm are characteristic of benzyl groups, which demonstrates the successful synthesis of **2**.

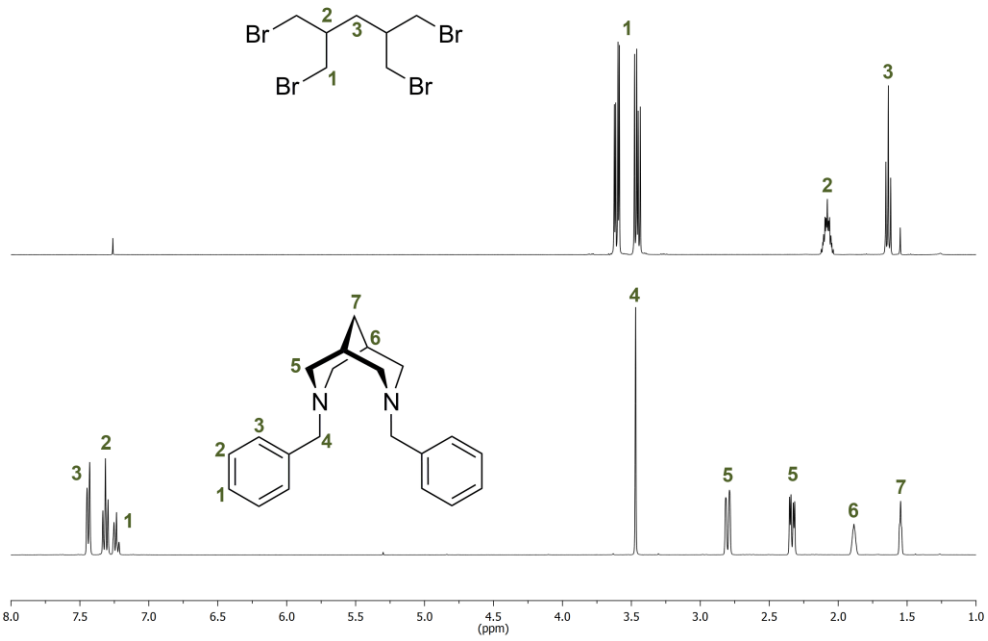


**Figure 2.2** $^{1}$H NMR spectra of **6b** (top) and **2** (bottom) (400 MHz, $CDCl_3$).

### 2.2.2 ROP of Lactide

The ROP of *L*-lactide, LLA, using 10 mol% TU and 5 mol% **2**, was studied in $CDCl_3$ ($[LA]_0$ = 0.7 M) at ambient temperature using 1-phenylethanol as the initiator at a monomer-to-initiator ratio of 50 ($[M]_0/[I]_0$ = 50). Monitoring the polymerisation by $^{1}$H NMR spectroscopy revealed that 87% monomer conversion was reached in 81 min. The resultant PLLA was precipitated into a stirred solution of hexanes, redissolved in $CH_2Cl_2$ and then precipitated into hexanes once again. Analysis of the pure polymer by gel-permeation chromatography (GPC) revealed a well controlled polymerisation with a number average molecular weight ($M_n$) of 13.4 kg mol$^{-1}$ and a narrow dispersity ($Đ_M$) of 1.08. The theoretical molecular weight of the resulting PLLA (7.2 kg mol$^{-1}$) differs from the experimental value obtained by GPC due to the use of polystyrene calibrants to determine the $M_n$. In comparison, under the same

conditions, the polymerisation of *L*-LA with (-)-sparteine resulted in 93% monomer conversion after 66 min. Very similar molecular parameters were observed from the GPC results, with a number average molecular weight ($M_n$) of 14.9 kg mol$^{-1}$ and a narrow dispersity ($Đ_M$) of 1.08. While these initial results provide evidence for the close similarity of **2** and (-)-sparteine in the ROP of lactide, the scope of the comparison was extended to also include the recently reported $Me_6$TREN as a catalyst. Although recent work by Hedrick suggests $Me_6$TREN is a good alternative to (-)-sparteine in the ROP of lactide, with polymerisations only taking marginally longer, these polymerisations were undertaken using significantly higher concentrations (in 2.3 M DCM with $[M]_0/[I]_0$ = 100). Under these conditions the polymerisation with 5 mol% (-)-sparteine and 5 mol% TU proceeds too rapidly to be monitored by $^1$H NMR spectroscopy, the point of completion could therefore not be accurately obtained. For a more precise comparison between polymerisations catalysed using **2**, (-)-sparteine and $Me_6$TREN, the ROP of LLA using 10 mol% TU and 5 mol% $Me_6$TREN was also studied in 0.7 M $CDCl_3$ at ambient temperature using 1-phenylethanol as the initiator with a $[M]_0/[I]_0$ = 50. After 450 min, 92% conversion of LLA was observed, this being a considerable increase in polymerisation time compared to that of (-)-sparteine. Again, similar molecular parameters by GPC were achieved with a number average molecular weight ($M_n$) of 12.1 kg mol$^{-1}$ and a narrow dispersity ($Đ_M$) of 1.09.

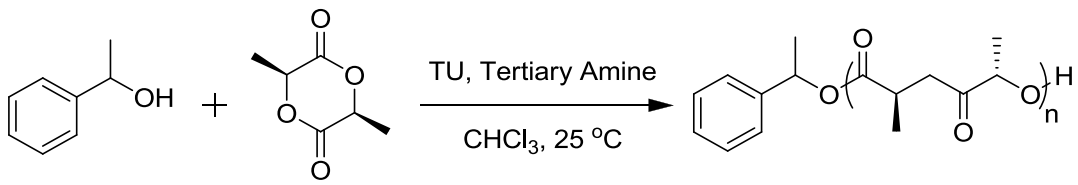


**Scheme 2.3** ROP of *L*-lactide using TU, and a tertiary amine co-catalyst.

**Table 2.1** Comparison of PLLA synthesised using various tertiary amines.

| Catalyst[a] | Conversion[b] (%) | Time (min) | $M_n$[c] (g mol$^{-1}$) | $Đ_m$[c] | $k_{app}$ (h$^{-1}$) |
|---|---|---|---|---|---|
| (-)-Sparteine | 93 | 66 | 14,900 | 1.08 | 2.53 |
| **2** | 87 | 81 | 13,400 | 1.08 | 1.35 |
| $Me_6$TREN | 92 | 450 | 12,100 | 1.09 | 0.38 |

[a] Conditions: 1 ml of $CDCl_3$ at room temperature; [L-LA] = 0.7 M; 1-phenylethanol as initiator; 5 mol% tertiary amine; 10 mol% of TU; $[M]_0/[I]_0 = 50$.[b] Determined by $^1$H NMR spectroscopy by comparing the integral values of the CH resonance of the monomer to the CH resonance of the polymer.[c] Determined by GPC analysis in $CHCl_3$ calibrated against polystyrene standards.

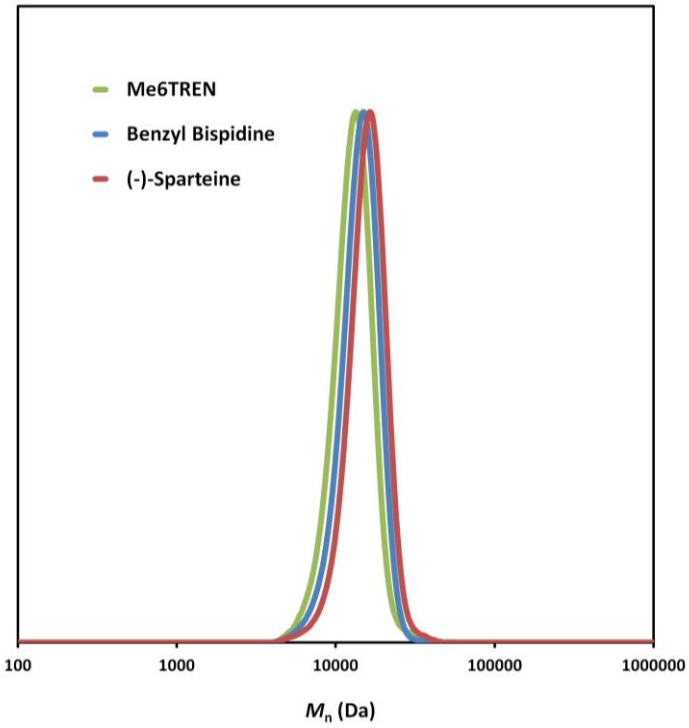


**Figure 2.3** GPC traces of PLLA synthesised using various tertiary amines/TU ($[M]_0/[I]_0 = 50$). Analysed by chloroform GPC.

To more precisely compare catalyst reactivities, kinetic studies of LA ROP for each catalyst system were investigated in triplicate. Polymerisations using each of the tertiary amine catalysts were undertaken using the same conditions and followed closely by $^{1}$H NMR spectroscopy. As shown in Figure 2.4, each catalyst resulted in the polymerisation reaching a plateau around 95% LA conversion and for $Me_6$TREN a slight induction period could be observed at the start of the polymerisation. First order kinetic plots of $ln([M]_0/[M]_t)$ against time reveal a linear correlation, with apparent rate constants ($k_{app}$) calculated as 1.35 $h^{-1}$, 2.53 $h^{-1}$ and 0.38 $h^{-1}$ for **2**, (-)-sparteine and $Me_6$TREN in combination with TU respectively. Under these conditions, while **2** catalyses lactide ROP at a lower rate than (-)-sparteine, the polymerisation occurs almost four times faster than when $Me_6$TREN is applied.

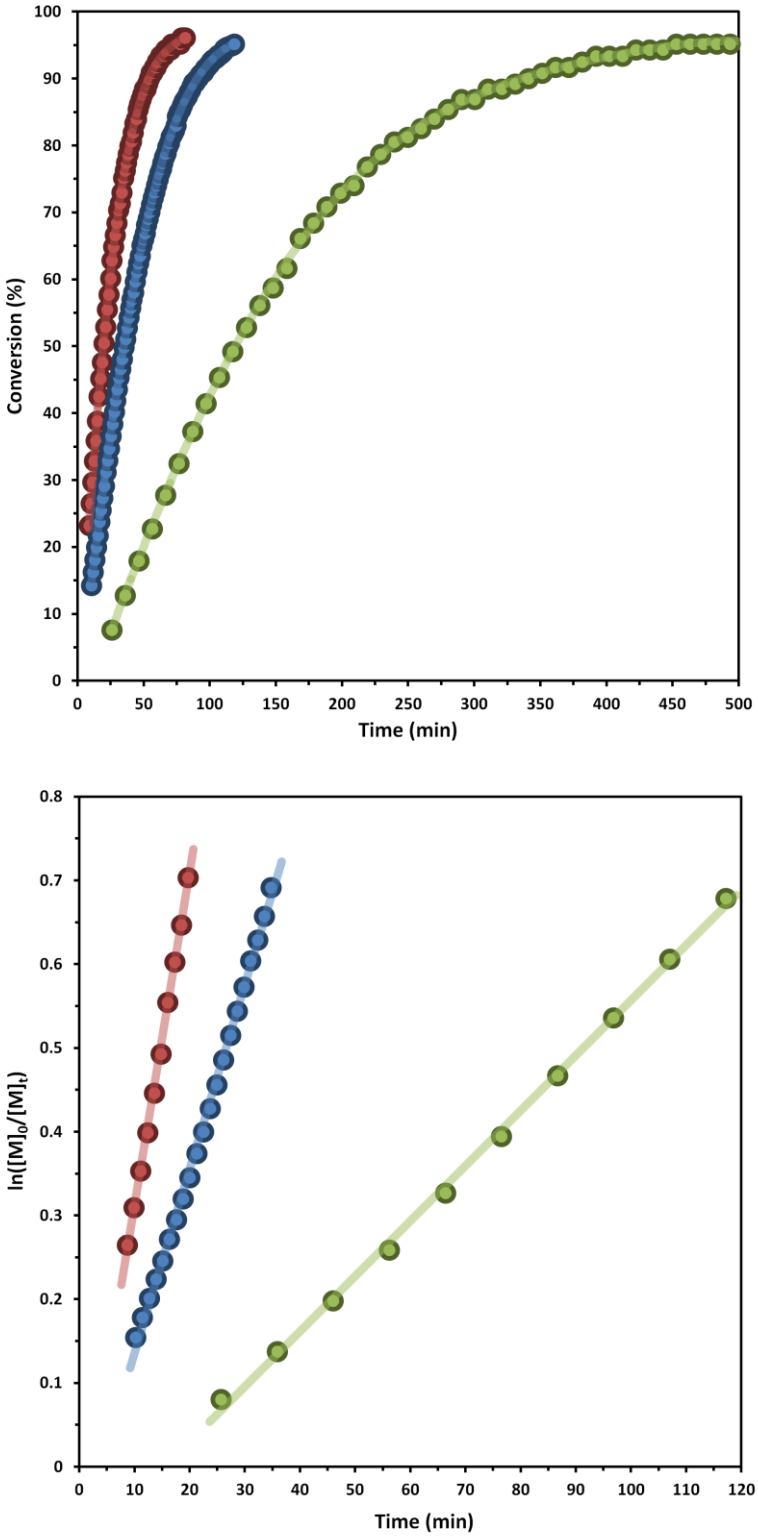


**Figure 2.4** Variation of tertiary amine catalyst. (Top) Plot of time versus LLA conversion. (Bottom) Semi-log kinetic plot. (Red = (-)-sparteine/TU, Blue = **2**/TU and Green = $Me_6$TREN/TU).

### 2.2.3 Controlled Nature of Lactide ROP

The controlled nature of the benzyl bispidine-catalysed polymerisation was further verified by the linear correlation between $M_n$ values obtained by GPC and the [M]/[I] ratio (Figure 2.6a) and the monomer conversion (Figure 2.6b) as determined by $^1$H NMR spectroscopy. The resultant PLAs all displayed narrow dispersities (1.18–1.03, Table 2.2) which indicates that minimal transesterification is occurring. Further analysis of the resultant polymers by matrix-assisted laser desorption ionisation time of flight mass spectrometry (MALDI-ToF MS) revealed only a single distribution with spacings of 144 *m*/*z* between neighbouring peaks (Figure 2.7). The absence of a second distribution with spacings of 72 *m*/*z* is consistent with the absence of transesterification side reactions. The peak masses of the distribution correspond to the equation: ($M_n$ = DP(144.1) + 122.2 + 23), where DP is the degree of polymerisation (number of lactide molecules incorporated into polymer), which shows that all chains are successfully initiated from 1-phenylethanol.

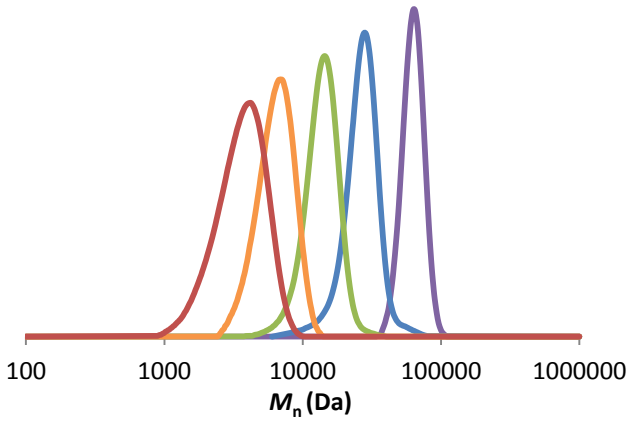


**Figure 2.5** GPC traces of PLLA synthesised using the **2**/TU binary catalyst system, with from left to right: $[M]_0/[I]_0$ = 10, 20, 50, 100, 250. Analysed by chloroform GPC.

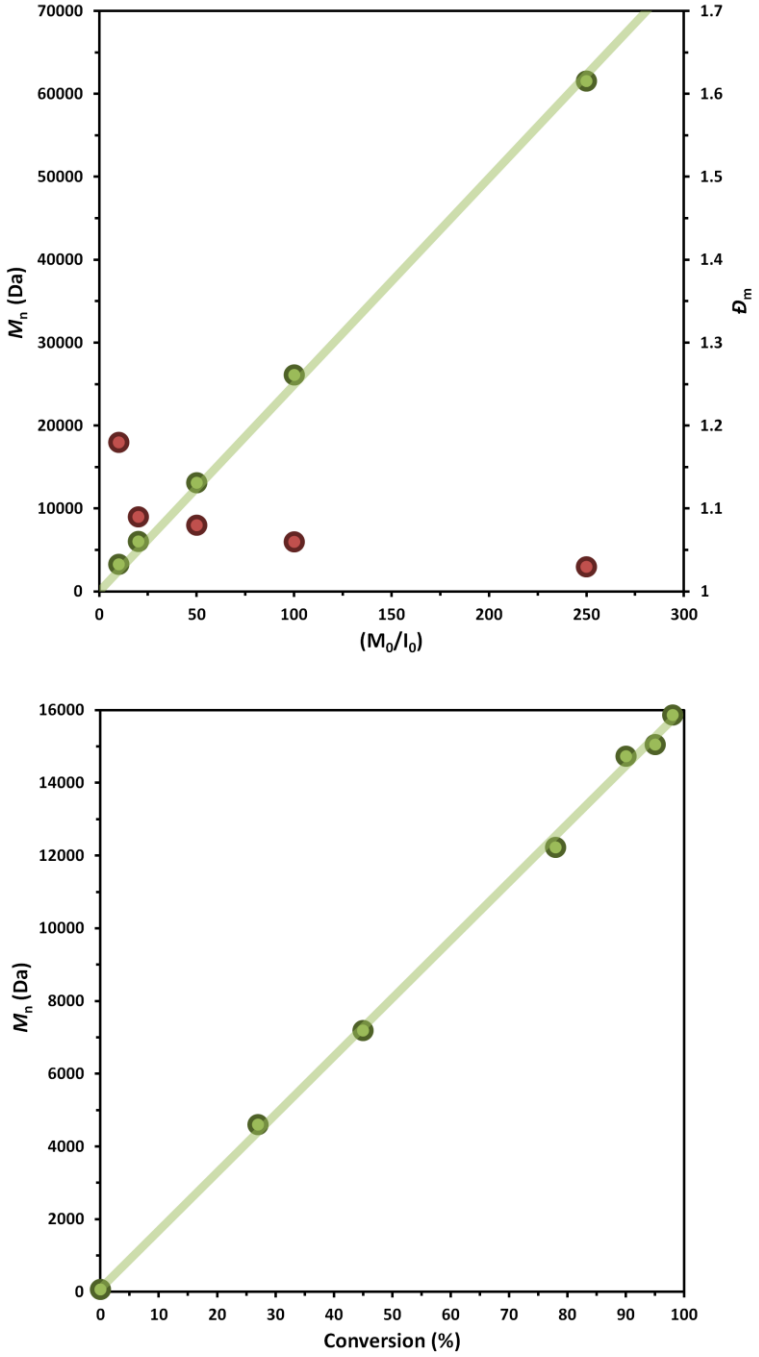


**Figure 2.6** (a) Number-average molecular weight ($M_n$) against % monomer conversion and (b) number-average molecular weight ($M_n$) and dispersity ($Đ_M$) against initial monomer-to-initiator ratio ($[M]_0/[I]_0$) for the ROP of L-LA using TU and **2**.

**Table 2.2** Variation in $[M]_0/[I]_0$ with the **2**/TU binary catalyst system[a]

| [M]/[I] | Conversion[b] (%) | Time (min) | $M_n$[c] (g mol$^{-1}$) | $Đ_m$[c] |
|---|---|---|---|---|
| 10 | 90 | 21 | 3,280 | 1.18 |
| 20 | 94 | 43 | 6,050 | 1.09 |
| 50 | 92 | 75 | 13,200 | 1.08 |
| 100 | 89 | 137 | 26,150 | 1.06 |
| 250 | 90 | 366 | 61,600 | 1.03 |

[a]Conditions: 1 ml of $CDCl_3$ at room temperature; [L-LA] = 0.7 M; 1-phenylethanol as initiator; 5 mol% of **2**; 10 mol% of TU. [b]Determined by $^1$H NMR spectroscopy. [c]Determined by GPC analysis in $CHCl_3$.

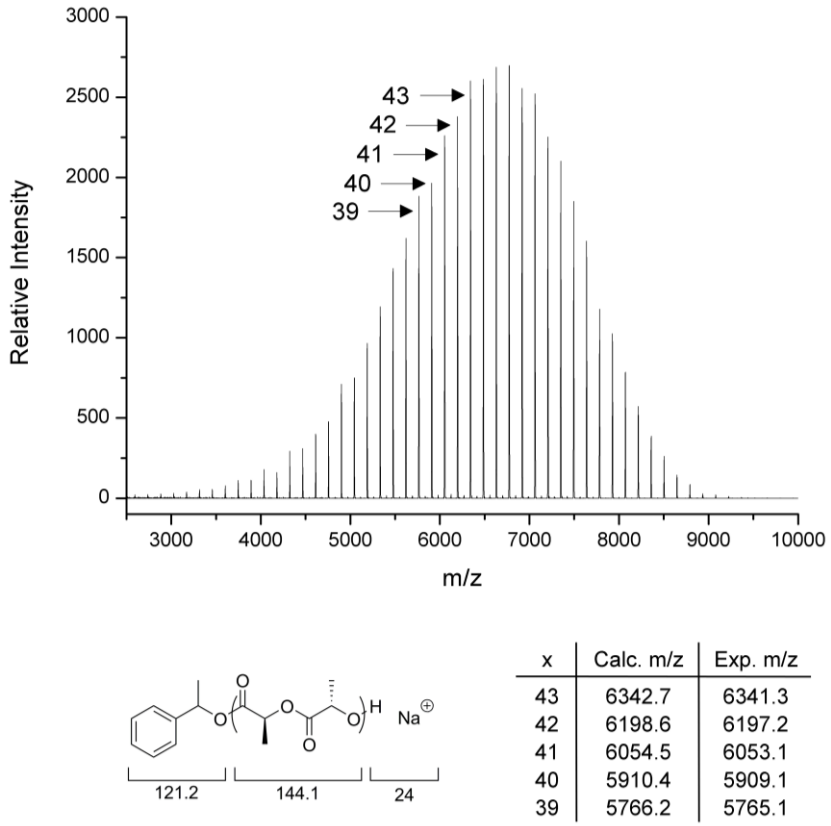


**Figure 2.7** MALDI-ToF MS spectrum of PLLA synthesised using the **2**/TU binary catalyst system.

### 2.2.4 Extent of Epimerisation

Epimerisation can occur during the polymerisation of lactide, resulting in the inversion of one or both of the chiral centres of the lactide monomer. For *L*-lactide, epimerisation results in the formation of *meso*- or possibly (*D*)-lactide, with the former being more likely due to only one chiral centre being inverted, compared to two per molecule for the formation of *D*-lactide. If epimerisation occurs, the inverted chiral centres will be incorporated into the PLLA resulting in stereoerrors along the backbone, causing a reduction in packing of the polymer chains, resulting in a decrease on $T_m$ that can be measured by differential scanning calorimetry (DSC). To assess whether epimerisation was taking place, thermal analysis was performed on PLLAs (DP = 100) synthesised using both **2**/TU and (-)-sparteine/TU binary catalytic systems (Figure 2.8).

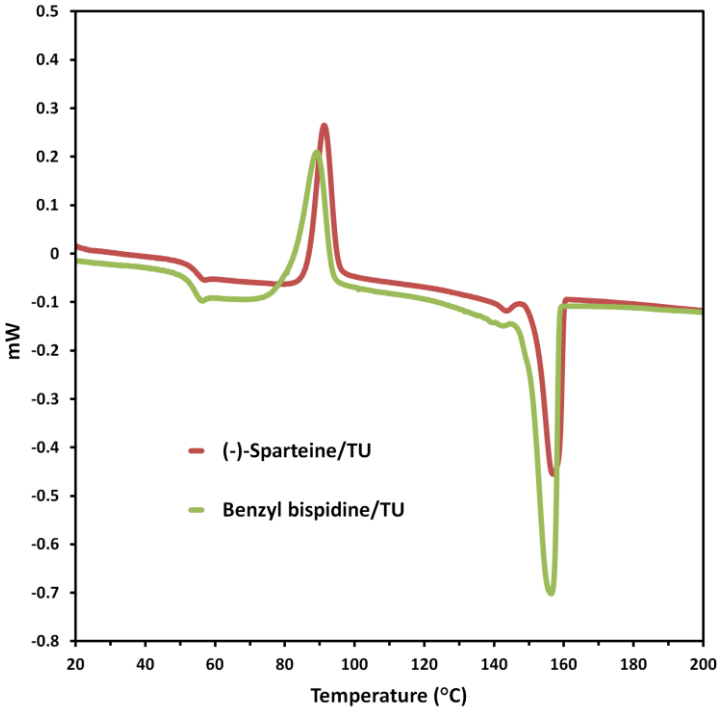


**Figure 2.8** DSC thermogram of PLLA synthesised using (-)-sparteine/TU and **2**/TU.

For PLLAs prepared using both **2**/TU and (-)-sparteine/TU, a clear glass transition temperature ($T_g$) of 54 and 55 °C were respectively measured by DSC and similar crystallisation peaks were observed. A $T_m$ of 156 °C for PLLA synthesised using **2**/TU as the binary catalyst system and of 158 °C for (-)-sparteine/TU, matching previously reported melting points for isotactic PLLA prepared using (-)-sparteine.[34, 35] This shows that the use of **2** as a catalyst results in similar low levels of epimerisation in the PLLA as when (-)-sparteine is used as a catalyst in lactide ROP.

To further investigate the levels of epimerisation that occur during ROP, homonuclear decoupled $^1$H NMR spectroscopy was undertaken. A $^1$H NMR spectrum of pure PLLA consists of two peaks (ignoring end groups), a quartet at $\delta$ = 5.16 ppm corresponding to the methine proton and a doublet at $\delta$ = 1.58 ppm corresponding to the methyl hydrogens, the splitting a result of their coupling. Removing the coupling between these hydrogens was achieved by focusing the decoupling pulse at the methyl region (at around $\delta$ = 1.6 ppm), which produces a homonuclear decoupled $^1$H NMR spectrum where the methine proton now exists as a singlet resonance at $\delta$ = 5.2 ppm. The two spectra for PLLAs synthesised using **2**/TU and (-)-sparteine/TU were found to be very similar, both having one major singlet resonance. The neighbouring smaller peaks at $\delta$ = 5.20 and 5.21 ppm indicate a small percentage of stereoerrors in both PLLAs, resulting from very low levels of epimerisation during polymerisation.[36-38] Finally this result was confirmed by the $^{13}$C NMR spectra of the PLLA samples, wherein for both polymers the signal at $\delta$ = 69 ppm only shows one major peak with some small baseline peaks resulting from a small number stereoerrors and therefore negligible epimerisation.

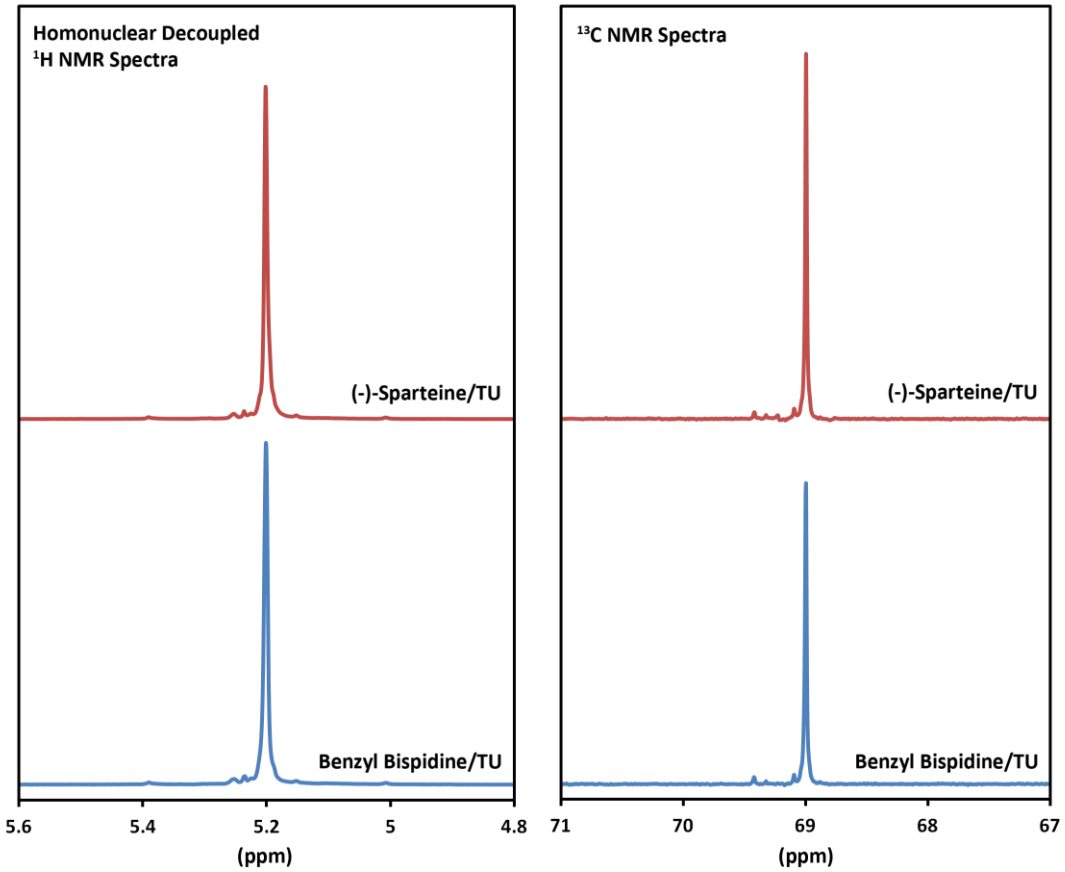


**Figure 2.9** Homonuclear decoupled $^{1}H$ NMR spectra (left) and $^{13}C$ NMR spectra (right) of PLLA synthesised using the (-)-sparteine/TU or benzyl bispidine/TU binary catalyst systems ($CDCl_3$).

### 2.2.5 Stereoselectivity of Binary Catalyst System

In addition to the determination of the extent of epimerisation in the ROP of LLA by homonuclear decoupled $^{1}$H NMR spectroscopy, the stereoselectivity of the catalyst in the ROP of *rac*-lactide could also be determined using the same NMR process. To that end, the ROP of *rac*-lactide (*rac*-LA) was undertaken to determine if any stereoselectivity would be observed using the catalyst combination of TU and **2**. Homonuclear decoupled $^{1}$H NMR spectra of poly(*rac*-lactide) were run on a 400 MHz NMR machine using $CDCl_3$ as solvent. The decoupling pulse was focused in the methyl region, at around $\delta$ = 1.6 ppm, with the resulting spectra resolved by using NMR software deconvolution algorithms, the peaks assigned according to literature.[36-38]

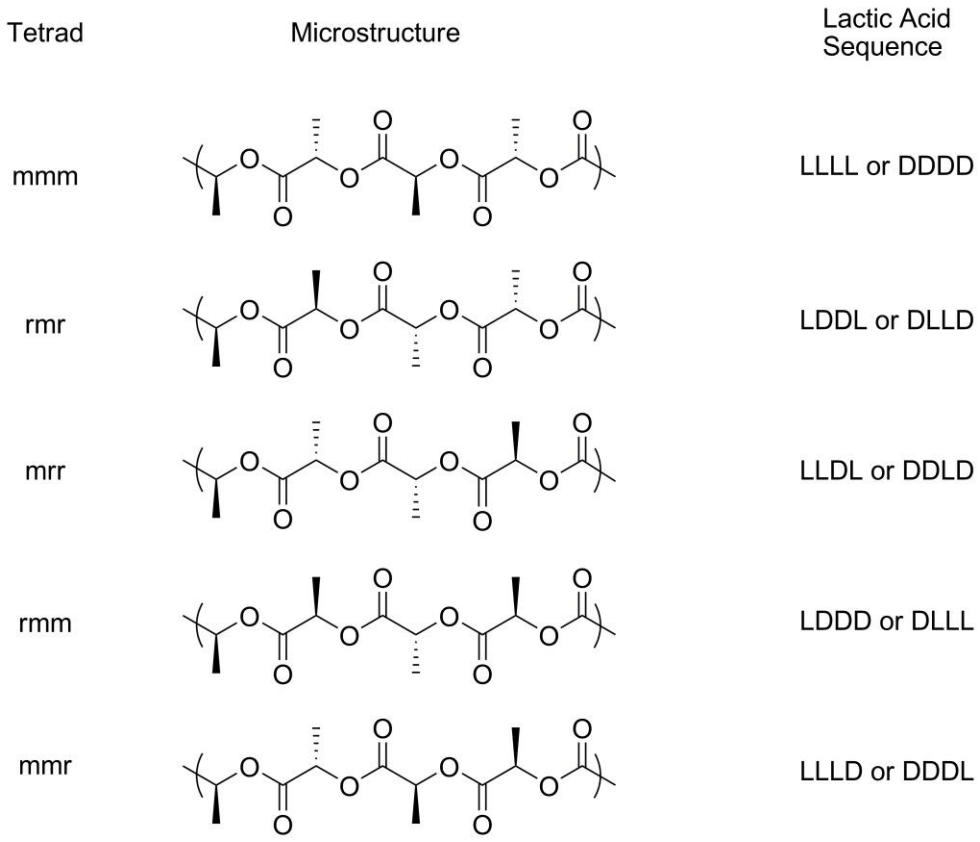


**Figure 2.10** Tetrads arising from poly*(rac*-lactide)

In a homonuclear decoupled $^{1}$H NMR spectrum of poly(*rac*-lactide) there are theoretically five peaks, each arising from a possible tetrad found in the polymers microstructure (Figure 2.10). Each tetrad is made up of two repeat units of lactide (four lactic acid units), and depending on how these four stereocentres are arranged with respect to each other determines the tetrad and therefore the ppm shift of the methine signal. Assuming the polymerisation of *rac*-LA is undertaken with zero stereoselectivity occurring, the probability of each tetrad in the polymer can be predicted (Table 2.3). For different isotactic enchainment probabilities, the intensity ratios of the five tetrad NMR peaks can be calculated and then compared to experimental values using a least square method to ascertain the correct $P_m$ value for the catalytic system. Despite the absence of stereogenic centres in **2**, unlike (-)-sparteine, the probability of isotactic enchainment ($P_m$) of the DP100 poly(*rac*-lactide)s was found to be the same for both catalytic systems ($P_m$(**2**/TU) = $P_m$((-)-sparteine/TU) = 0.74). The results clearly demonstrate a preference to produce isotactic PLA from the racemic monomer mixture in both cases. Furthermore these values are comparable to previously reported *rac*-LA ROP catalysed by (-)-sparteine/TU ($P_m$ = 0.77).[16]

**Table 2.3** Probability equations for each possible tetrad in poly(rac-lactide) where $P_m + P_r = 1$ (calculated according to Bernoullian statistics).

| Tetrad | Probability |
|---|---|
| mmm | $(P_m)^2 + 0.5P_rP_m$ |
| mmr | $0.5P_rP_m$ |
| rmm | $0.5P_rP_m$ |
| rmr | $0.5(P_r)^2$ |
| mrm | $0.5((P_m)^2 + P_rP_m)$ |

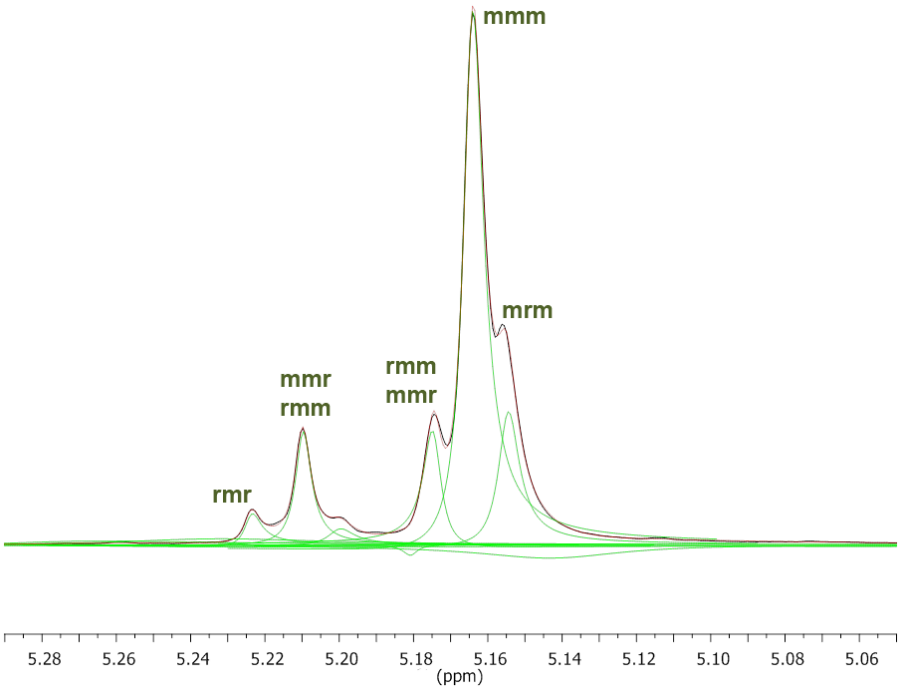


**Figure 2.11** Homonuclear decoupled $^1$H NMR spectra (in $CDCl_3$, focussed around methine region) of poly(rac-lactide) synthesised using **2**/TU at room temperature.

**Table 2.4** Calculated $P_m$ values for the binary catalyst systems **2**/TU and (-)-sparteine/TU

| Catalyst | | | rmr | rmm | mmr | mmm | mrm | Difference of Squares |
|---|---|---|---|---|---|---|---|---|
| **Benzyl Bispidine + TU** | **Experimental Intensities** | | 0.0301 | 0.0967 | 0.0913 | 0.6430 | 0.1388 | |
| | $P_m$ | **0.73** | 0.0365 | 0.0986 | 0.0986 | 0.6315 | 0.1350 | 0.0180 |
| | | **0.74** | 0.0338 | 0.0962 | 0.0962 | 0.6438 | 0.1300 | 0.0046 |
| | | **0.75** | 0.0313 | 0.0938 | 0.0938 | 0.6563 | 0.1250 | 0.0219 |
| **(-)-Sparteine + TU** | **Experimental Intensities** | | 0.0252 | 0.0994 | 0.0723 | 0.6456 | 0.1575 | |
| | $P_m$ | **0.73** | 0.0365 | 0.0986 | 0.0986 | 0.6315 | 0.1350 | 0.0300 |
| | | **0.74** | 0.0338 | 0.0962 | 0.0962 | 0.6438 | 0.1300 | 0.0154 |
| | | **0.75** | 0.0313 | 0.0938 | 0.0938 | 0.6563 | 0.1250 | 0.0280 |
| **Benzyl Bispidine + TU (0 °C)** | **Experimental Intensities** | | 0.0254 | 0.1031 | 0.0911 | 0.6299 | 0.1506 | |
| | $P_m$ | **0.72** | 0.0392 | 0.1008 | 0.1008 | 0.6192 | 0.1400 | 0.0197 |
| | | **0.73** | 0.0365 | 0.0986 | 0.0986 | 0.6315 | 0.1350 | 0.0094 |
| | | **0.74** | 0.0338 | 0.0962 | 0.0962 | 0.6438 | 0.1300 | 0.0263 |

### 2.2.6 Variation of the Hydrogen Bond Donor Co-Catalyst

Several hydrogen bond donor alternatives to the cyclohexyl thiourea co-catalyst (TU) have been reported in recent years (Figure 2.12).[18-22] While all have been successfully used in conjunction with (-)-sparteine for the ROP of lactide, the conditions used have always varied and therefore a direct comparison between the hydrogen bond donor co-catalysts has not been possible. As **2** has been shown to be a good alternative to (-)-sparteine, polymerisations were undertaken using these alternative co-catalysts under the same conditions with the aim of providing an accurate comparison between them.

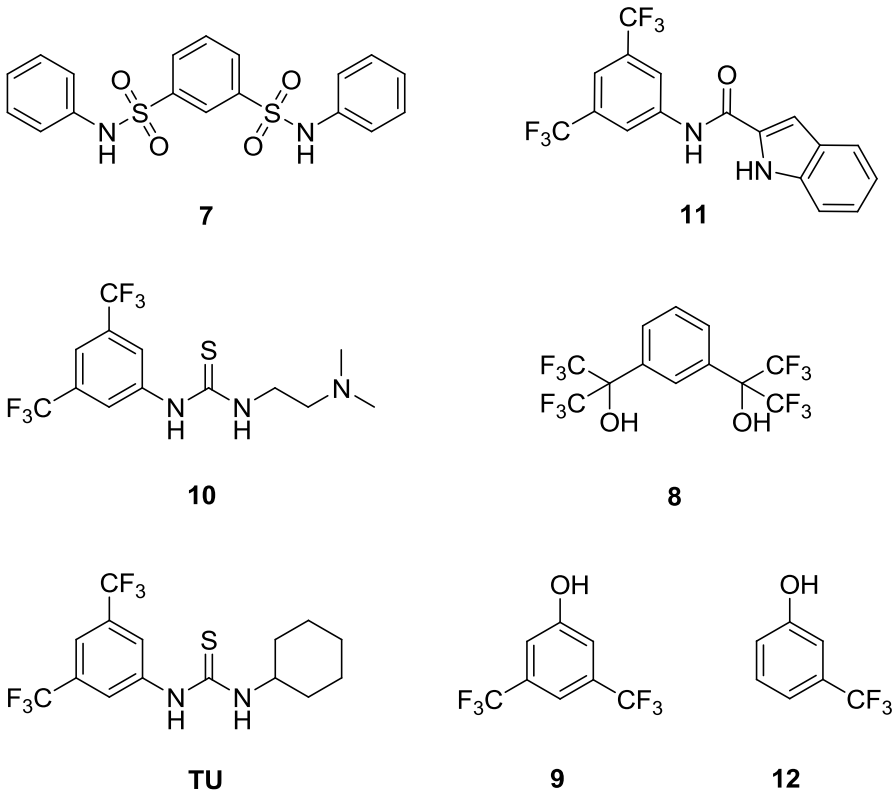


**Figure 2.12** Hydrogen bond donor co-catalysts.

The ROP of L-lactide, LLA, using 5 mol% **2** with 10 mol% hydrogen bond donor co-catalyst was again studied in $CDCl_3$ ($[LLA]_0$ = 0.7 M) at ambient temperature using 1-phenylethanol as the initiator at a monomer-to-initiator ratio of 50 ($[M]_0/[I]_0$ = 50). The limited solubility of **11** in chloroform required its application at the lower molar ratio of 5 mol% (in preference to the standard 10 mol%). To provide an accurate comparison, polymerisations using co-catalyst TU were also undertaken at 5 mol% loading. Kinetic studies for each catalyst system were investigated in triplicate by monitoring monomer conversion against time using $^1$H NMR spectroscopy. First order kinetic plots of $\ln([M]_0/[M]_t)$ against time (Figure 2.13) enabled the determination of $k_{app}$ values (Table 2.5). The tested catalysts

demonstrated a broad range of activities, with $k_{app}$ values ranging from 0.138 $h^{-1}$ for **12** to 0.03 $h^{-1}$ for **10**, but none displayed a polymerisation rate close to that of TU (1.35 $h^{-1}$). The co-catalyst with the most similar rate to TU is *m*-trifluoromethylphenol, **12,** with a $k_{app}$ approximately an order of magnitude lower than that observed for TU. Notably, the amide catalyst **11** (5 mol% loading) remained highly active with the measured $k_{app}$ value approximately 6 times lower than that TU at the reduced 5 mol% loading, whilst polymerisation using co-catalyst **7** displayed an extremely low reaction rate under these conditions, with <5% monomer conversion being observed after one week and therefore no $k_{app}$ value being measured.

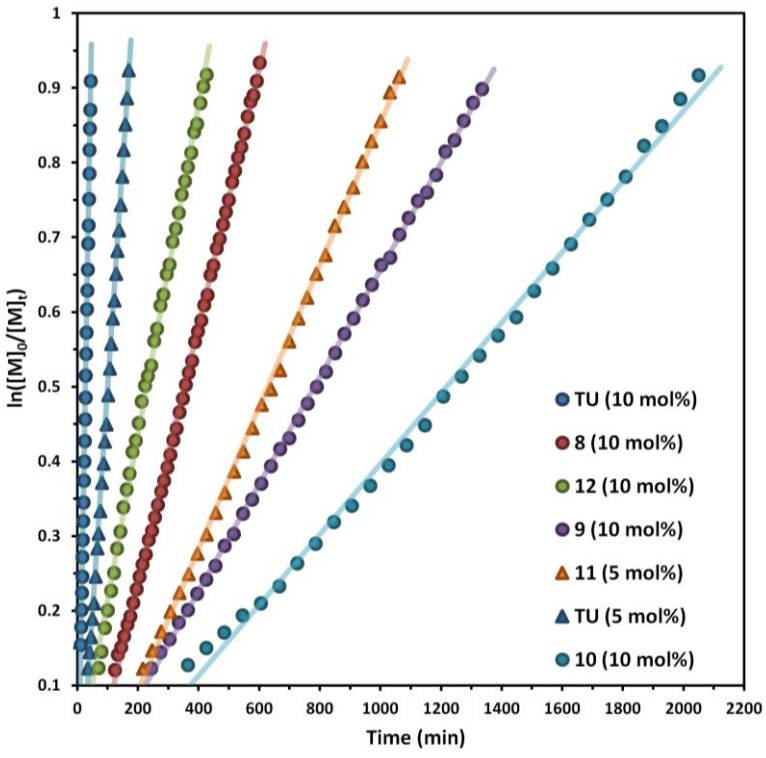


**Figure 2.13** Kinetic plots resulting from variation in hydrogen bond donor co-catalyst.

**Table 2.5** Variation in hydrogen bond donor co-catalyst

| Co-Catalyst | [M]/[I] | Conversion[c] (%) | Time (min) | $M_n$[d] (g mol$^{-1}$) | $Đ_M$[d] | $k_{app}$ (h$^{-1}$) |
|---|---|---|---|---|---|---|
| TU[a] | 50 | 86 | 75 | 13,500 | 1.08 | 1.354 ± 0.053 |
| TU[b] | 50 | 90 | 350 | 12,750 | 1.07 | 0.391 ± 0.027 |
| 8[a] | 50 | 86 | 1220 | 8,450 | 1.06 | 0.103 ± 0.001 |
| 9[a] | 50 | 91 | 3240 | 9,090 | 1.11 | 0.044 ± 0.002 |
| 10[a] | 50 | 86 | 4200 | 10,300 | 1.08 | 0.029 ± 0.001 |
| 11[b] | 50 | 92 | 2710 | 11,900 | 1.08 | 0.063 ± 0.007 |
| 12[a] | 50 | 93 | 1470 | 4,010 | 1.20 | 0.138 ± 0.007 |

[a]Conditions: 1 ml of $CDCl_3$ at room temperature; [L-LA] = 0.7 M; 5 mol% **2**; 10 mol% co-catalyst; 1-phenylethanol as initiator. [b]Conditions: 1 ml of $CDCl_3$ at room temperature; [L-LA] = 0.7 M; 5 mol% **2**; 5 mol% co-catalyst; 1-phenylethanol as initiator. [c]Determined by $^1$H NMR spectroscopy. [d]Determined by GPC analysis in $CHCl_3$.

In each case, analysis of the molecular parameters of the resultant polymers revealed low dispersity values which suggests that the polymerisations were well controlled (Table 2.5). Notably however, co-catalyst **12** resulted in PLLA with lower molecular weight than predicted from the $[M]_0/[I]_0$ ratio. MALDI-ToF MS analysis of this polymer revealed two distinct distributions, both displaying the expected 144 *m*/*z* spacing for the monomer repeat unit but with a molecular weight difference of ~40 *m*/*z* between the distributions (Figure 2.14). One of these distributions revealed values that correspond to sodium-charged polymer chains initiated from 1-phenylethanol as expected, the observed peak masses obeying the equation: ($M_n$ = DP(144.1) + 122.2 + 23), however the other distribution revealed values that match

up to to sodium-charged polymer chains initiated from the co-catalyst **12**, the peak masses corresponding to the altered equation: ($M_n$ = DP(144.1) + 162.2 + 23). This unintended dual initiation most likely contributes to the relatively high rate of polymerisation for the **2/12** binary catalyst system. In the case of **9**, in which two $CF_3$ substituents are present on the phenol ring, co-catalyst initiation was not observed, with the MALDI-ToF MS peak masses following the equation: ($M_n$ = DP(144.1) + 122.2 + 23), corresponding to successful initiation from 1-phenylethanol. This suggests that the phenol in **9** is appropriately activated to only undertake hydrogen bonding and not serve as a source of initiation in the polymerisation.

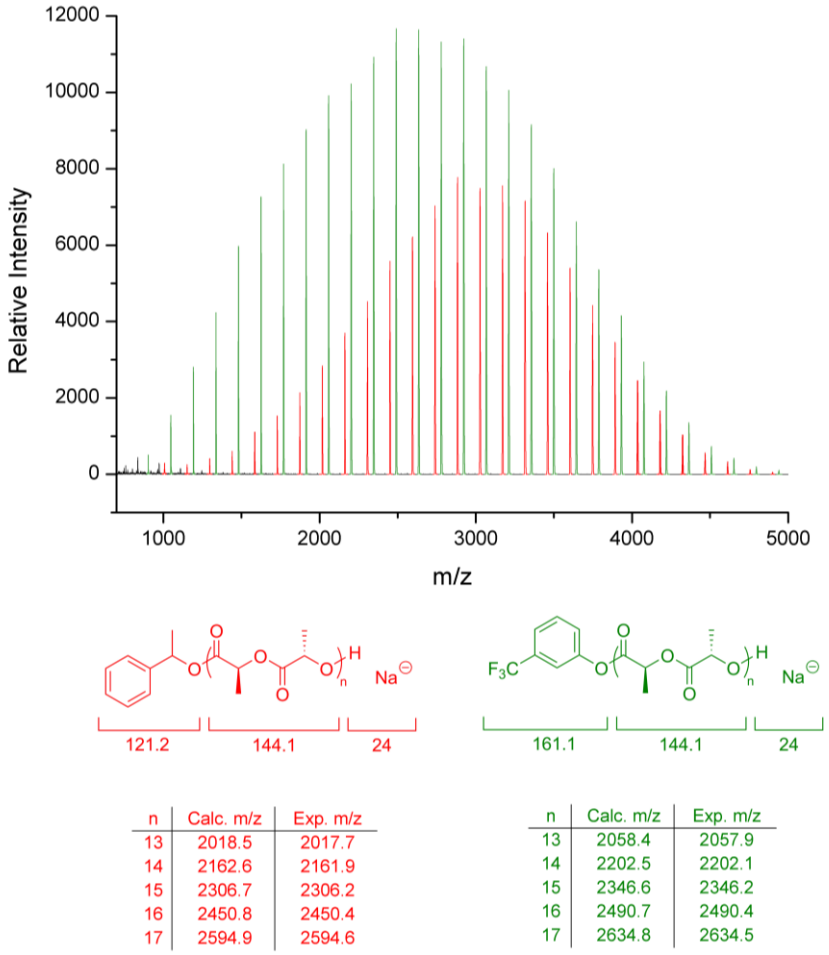


| n | Calc. m/z | Exp. m/z |
|---|---|---|
| 13 | 2018.5 | 2017.7 |
| 14 | 2162.6 | 2161.9 |
| 15 | 2306.7 | 2306.2 |
| 16 | 2450.8 | 2450.4 |
| 17 | 2594.9 | 2594.6 |

| n | Calc. m/z | Exp. m/z |
|---|---|---|
| 13 | 2058.4 | 2057.9 |
| 14 | 2202.5 | 2202.1 |
| 15 | 2346.6 | 2346.2 |
| 16 | 2490.7 | 2490.4 |
| 17 | 2634.8 | 2634.5 |

**Figure 2.14** Colour coded MALDI-ToF MS of PLLA synthesised using **2**/**12**. Red = PLLA chains initiated from 1-phenylethanol. Green = PLLA chains initiated from **12**.

Interestingly, $^{1}$H NMR spectroscopic analysis of the polymer produced using **2**/**8** as co-catalysts for the ROP of L-LA revealed a number of overlapping quartets in the range of $\delta$ = 5.10–5.25 ppm, consistent with the epimerisation of the monomer during polymerisation (Figure 2.15). Despite the previous report of the ROP of L-LA using (-)-sparteine/**8** proceeding in the absence of epimerisation,[22] repeating the experiment with (-)-sparteine resulted in comparable $^{1}$H NMR spectra of the resultant polymers for both catalytic systems.

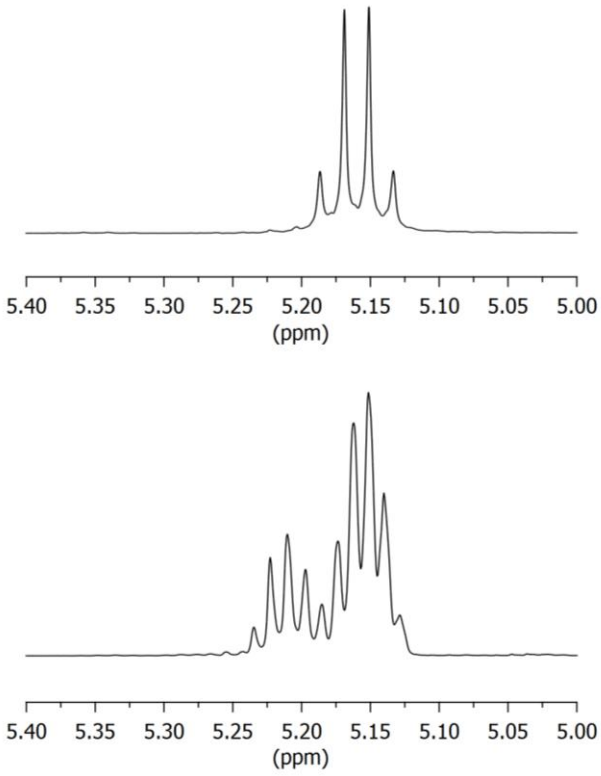


**Figure 2.15** $^{1}$H NMR spectra ($CDCl_3$, 400 MHz, focussed around the methine region) of PLLA synthesised using **2**/**8** (Bottom) and **2**/TU (Top).

### 2.2.7 ROP of Cyclic Carbonates

To further investigate the versatility of the **2**/TU binary catalyst system, polymerisations were undertaken of the 6-membered cyclic carbonates, trimethylene carbonate (TMC) and 5-methyl-5-allyloxycarbonyl-1,3-dioxan-2-one (MAC) of which the (-)-sparteine/TU system has previously demonstrated well controlled homopolymerisation.[39-41] Polymerisations were carried out under conditions previously reported,[40] using both **2** and (-)-sparteine in combination with TU as catalysts with a target $[M]_0/[I]_0 = 50$ for TMC and 20 for MAC. The ROP of TMC was performed using 5 mol% of **2** or (-)-sparteine with 5 mol% TU. After *ca.* 70 h $^1$H NMR spectroscopic analysis of the polymerisation mixtures revealed monomer conversions >90% (Table 2.6). GPC analysis of the resultant poly(TMC)s showed that similar $M_n$ values resulted from polymerisations using both catalysts with narrow dispersities observed. MALDI-ToF analysis of the poly(TMC) synthesised using **2**/TU revealed a single distribution with the desired spacing of 102 *m*/*z*, the peak masses corresponding to the equation: ($M_n$ = DP(102.1) + 107.1 + 24) showing sodium charged chains only initiated from benzyl alcohol (Figure 2.18). No secondary distributions were observed in the MALDI-ToF spectra.

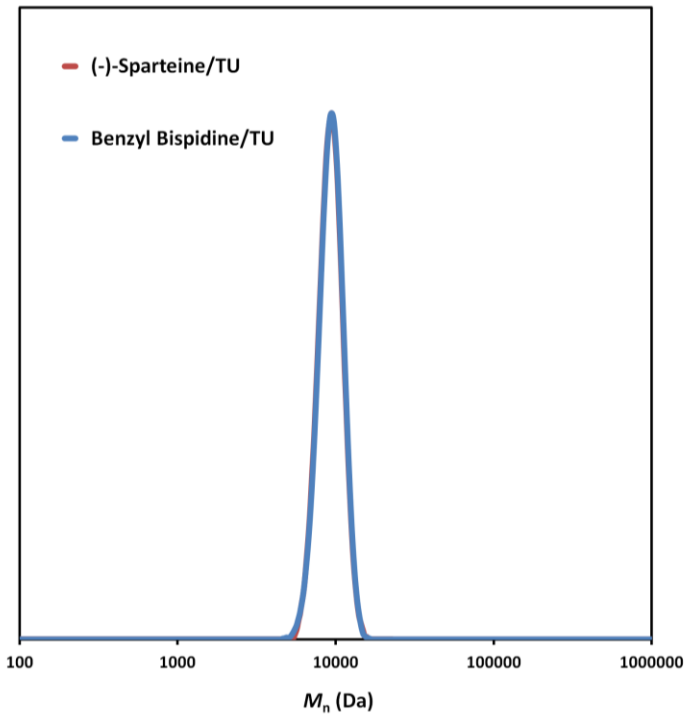


**Figure 2.16** Two overlapping GPC traces of poly(TMC) ($[M]_0/[I]_0$ = 50) synthesised using **2**/TU and (-)-sparteine/TU, initiated from benzyl alcohol in $CDCl_3$ (2.0 M). Analysed by chloroform GPC.

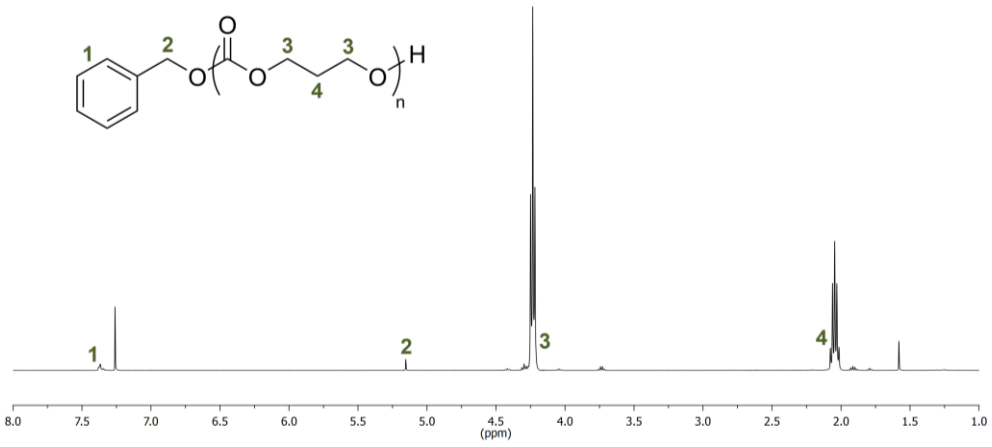


**Figure 2.17** $^1H$ NMR spectrum ($CDCl_3$, 400 MHz) of PTMC synthesised using **2**/TU.

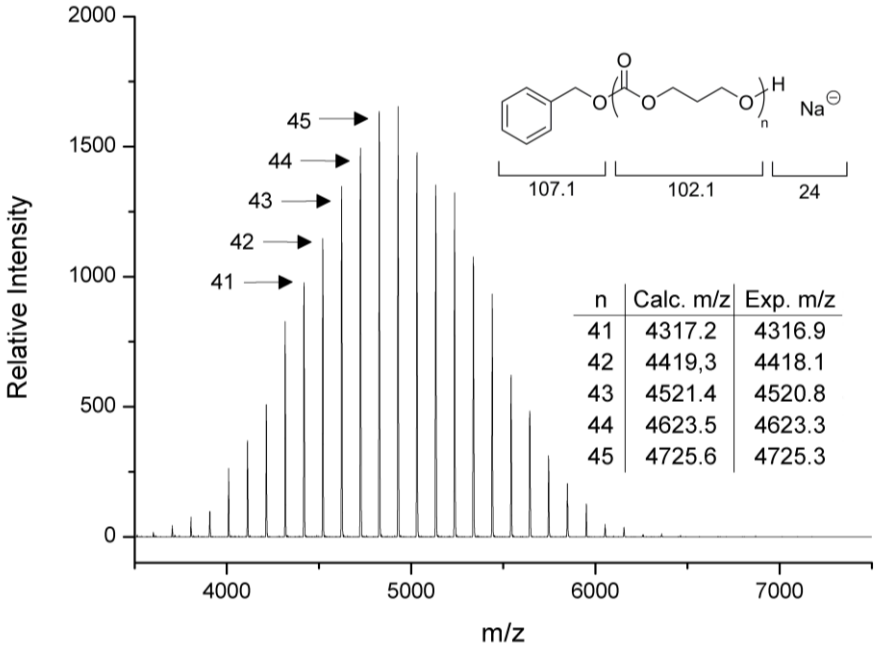


**Figure 2.18** MALDI-ToF MS of PTMC synthesised using **2**/TU.

**Table 2.6** Comparison of catalysts for the ROP of cyclic carbonates

| Monomer | Catalyst | $[M]_0/[I]_0$ | Conversion[c] (%) | Time (min) | $M_n$ (g mol$^{-1}$) | $Đ_M$ |
|---|---|---|---|---|---|---|
| TMC[a] | (-)-Sparteine | 50 | 92 | 4280 | 9,100[d] | 1.03[d] |
| TMC[a] | **2** | 50 | 90 | 4750 | 9,100[d] | 1.03[d] |
| MAC[b] | (-)-Sparteine | 20 | 90 | 400 | 6,400[e] | 1.11[e] |
| MAC[b] | **2** | 20 | 90 | 410 | 6,200[e] | 1.10[e] |
| MAC[b] | $Me_6$TREN | 20 | 89 | 45 days | 6,100[e] | 1.13[e] |

[a]Conditions: 0.5 ml of $CDCl_3$ at room temperature; [TMC] = 2.0 M; 5 mol% tertiary amine; 5 mol% TU; benzyl alcohol as initiator. [b]Conditions: 0.5 ml of $CDCl_3$ at room temperature; [MAC] = 0.5 M; 5 mol% tertiary amine; 10 mol% TU; benzyl alcohol as initiator. [c]Determined by $^1$H NMR spectroscopy. [d]Determined by GPC analysis in $CHCl_3$. [e]Determined by GPC analysis in DMF.

The polymerisations of MAC were undertaken using 5 mol% of **2** or (-)-sparteine with 10 mol% TU, as reported recently. Targeting a DP of 20, polymerisations catalysed by TU in combination with **2** or (-)-sparteine achieved 90% monomer conversion after 410 and 400 min respectively. Notably these results demonstrate the comparable activity of both bispidine co-catalysts for the ROP of cyclic carbonates. In both cases, GPC analysis revealed that the molecular weights and dispersities for the resulting poly(MAC) were within error and MALDI-ToF MS analysis revealed only the desired single distribution with the predicted spacing of 200 *m*/*z* that corresponds to the molecular weight of the repeat unit (Figure 2.20). The observed peak masses correspond to the equation: ($M_n$ = DP(200.2) + 107.1 + 24), showing sodium charged chains only initiated from benzyl alcohol. Interestingly, the application of 10 mol% TU with 5 mol% $Me_6$TREN revealed a much slower polymerisation with 89% conversion only after 45 days. GPC analysis of the resultant polymer revealed molecular weights and dispersities in close agreement to (-)-sparteine and **2**.

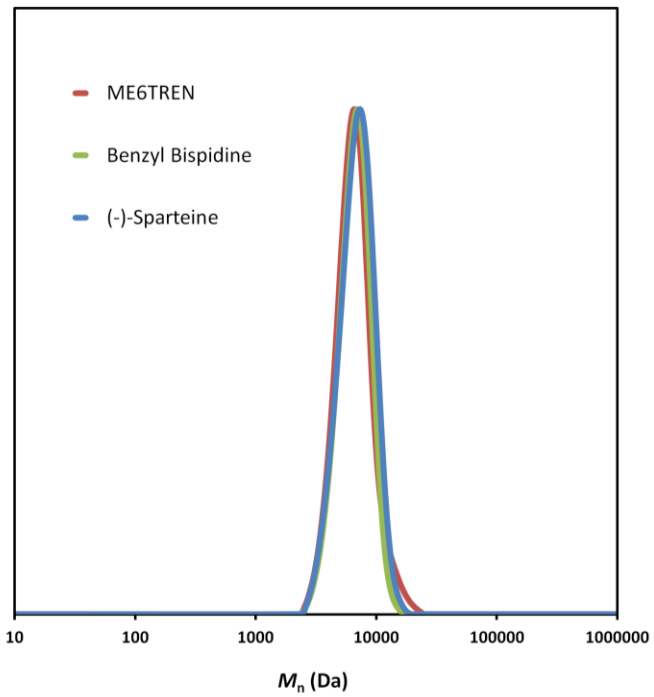


**Figure 2.19** Three overlapping GPC traces of poly(MAC) ($[M]_0/[I]_0$ = 20) synthesised using **2**/TU, $Me_6$TREN/TU and (-)-sparteine/TU, initiated from benzyl alcohol in $CDCl_3$ (0.5 M). Analysed by DMF GPC.

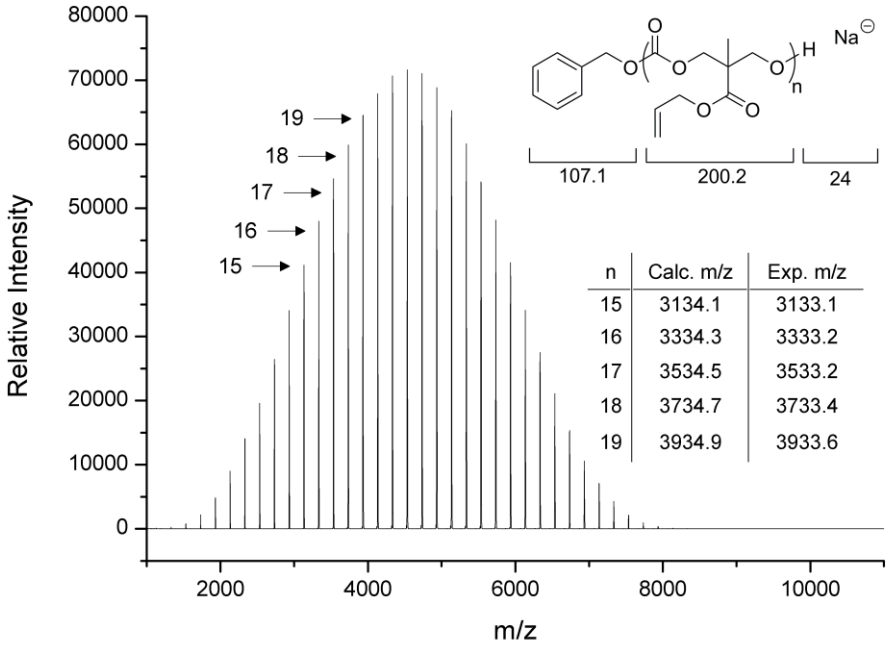


**Figure 2.20** MALDI-ToF MS of poly(MAC) synthesised using **2**/TU.

## 2.3 Conclusions

From this work it is demonstrated that, in conjunction with a hydrogen bond donor co-catalyst, the dibenzyl-functional bispidine, **2**, is an excellent replacement for (-)-sparteine in the ROP of lactide, producing well controlled polymers in the absence of observable transesterification and epimerisation. Additionally the ROP of *rac*-lactide revealed similar stereoselectivities for **2** and (-)-sparteine, with a $P_m$ of 0.74 calculated for both catalyst systems. A study of different reported co-catalysts revealed that 1-(3,5-bis(trifluoromethyl)phenyl)-3-cyclohexylthiourea (TU) resulted in the highest observed polymerisation rates and good control. In addition, the ROP of cyclic carbonates with **2** was explored achieving rates almost identical to those observed using (-)-sparteine whilst the control over the molecular weight and dispersity was maintained. In conclusion, benzyl bispidine has proven to be a versatile catalyst and an excellent replacement for (-)-sparteine.

## 2.4 References


1. D. Bourissou, S. Moebs-Sanchez and B. Martin-Vaca, *C. R. Chim.*, 2007, **10**, 775-794.
2. N. E. Kamber, W. Jeong, R. M. Waymouth, R. C. Pratt, B. G. G. Lohmeijer and J. L. Hedrick, *Chem. Rev.*, 2007, **107**, 5813-5840.
3. M. K. Kiesewetter, E. J. Shin, J. L. Hedrick and R. M. Waymouth, *Macromolecules*, 2010, **43**, 2093-2107.
4. J. M. Becker, R. J. Pounder and A. P. Dove, *Macromol. Rapid Commun.*, 2010, **31**, 1923-1937.
5. A. P. Dove, *ACS Macro Lett.*, 2012, **1**, 1409-1412.
6. O. Coulembier, P. Degee, J. L. Hedrick and P. Dubois, *Prog. Polym. Sci.*, 2006, **31**, 723-747.
7. G. Rokicki, *Prog. Polym. Sci.*, 2000, **25**, 259-342.
8. S. Tempelaar, L. Mespouille, O. Coulembier, P. Dubois and A. P. Dove, *Chem. Soc. Rev.*, 2013, **42**, 1312-1336.
9. E. F. Connor, G. W. Nyce, M. Myers, A. Mock and J. L. Hedrick, *J. Am. Chem. Soc.*, 2002, **124**, 914-915.
10. A. P. Dove, H. B. Li, R. C. Pratt, B. G. G. Lohmeijer, D. A. Culkin, R. M. Waymouth and J. L. Hedrick, *Chem. Commun.*, 2006, 2881-2883.
11. A. P. Dove, R. C. Pratt, B. G. G. Lohmeijer, D. A. Culkin, E. C. Hagberg, G. W. Nyce, R. M. Waymouth and J. L. Hedrick, *Polymer*, 2006, **47**, 4018-4025.
12. B. G. G. Lohmeijer, R. C. Pratt, F. Leibfarth, J. W. Logan, D. A. Long, A. P. Dove, F. Nederberg, J. Choi, C. Wade, R. M. Waymouth and J. L. Hedrick, *Macromolecules*, 2006, **39**, 8574-8583.

13. R. C. Pratt, B. G. G. Lohmeijer, D. A. Long, R. M. Waymouth and J. L. Hedrick, *J. Am. Chem. Soc.*, 2006, **128**, 4556-4557.

14. M. Fevre, J. Pinaud, A. Leteneur, Y. Gnanou, J. Vignolle, D. Taton, K. Miqueu and J. M. Sotiropoulos, *J. Am. Chem. Soc.*, 2012, **134**, 6776-6784.

15. A. P. Dove, R. C. Pratt, B. G. G. Lohmeijer, R. M. Waymouth and J. L. Hedrick, *J. Am. Chem. Soc.*, 2005, **127**, 13798-13799.

16. R. C. Pratt, B. G. G. Lohmeijer, D. A. Long, P. N. P. Lundberg, A. P. Dove, H. B. Li, C. G. Wade, R. M. Waymouth and J. L. Hedrick, *Macromolecules*, 2006, **39**, 7863-7871.

17. L. Toom, A. Kutt, I. Kaljurand, I. Leito, H. Ottosson, H. Grennberg and A. Gogoll, *J. Org. Chem.*, 2006, **71**, 7155-7164.

18. C. Thomas, F. Peruch, A. Deffieux, A. Milet, J. P. Desvergne and B. Bibal, *Adv. Synth. Catal.*, 2011, **353**, 1049-1054.

19. S. Koeller, J. Kadota, A. Deffieux, F. Peruch, S. Massip, J. M. Leger, J. P. Desvergne and B. Bibal, *J. Am. Chem. Soc.*, 2009, **131**, 15088-+.

20. S. Koeller, J. Kadota, F. Peruch, A. Deffieux, N. Pinaud, I. Pianet, S. Massip, J. M. Leger, J. P. Desvergne and B. Bibal, *Chem. Eur. J.*, 2010, **16**, 4196-4205.

21. A. Alba, A. Schopp, A. P. D. Delgado, R. Cherif-Cheikh, B. Martin-Vaca and D. Bourissou, *J. Polym. Sci. A Polym. Chem.*, 2010, **48**, 959-965.

22. O. Coulembier, D. R. Sanders, A. Nelson, A. N. Hollenbeck, H. W. Horn, J. E. Rice, M. Fujiwara, P. Dubois and J. L. Hedrick, *Angew. Chem. Int. Ed*, 2009, **48**, 5170-5173.

23. T. A. Johnson, M. D. Curtis and P. Beak, *Org. Lett.*, 2002, **4**, 2747-2749.

24. S. D. Wu, S. Lee and P. Beak, *J. Am. Chem. Soc.*, 1996, **118**, 715-721.

25. P. Ona-Burgos, I. Fernandez, L. Roces, L. Torre-Fernandez, S. Garcia-Granda and F. Lopez-Ortiz, *Org. Lett.*, 2008, **10**, 3195-3198.

26. C. Metallinos and V. Snieckus, *Org. Lett.*, 2002, **4**, 1935-1938.

27. P. M. Dewick, in *Medicinal Natural Products*, John Wiley & Sons, Ltd, 2009, pp. 311-420.

28. J. P. R. Hermet, M. J. McGrath, P. O'Brien, D. W. Porter and J. Gilday, *Chem. Commun.*, 2004, 1830-1831.

29. N. R. Norcross, J. P. Melbardis, M. F. Solera, M. A. Sephton, C. Kilner, L. N. Zakharov, P. C. Astles, S. L. Warriner and P. R. Blakemore, *J. Org. Chem.*, 2008, **73**, 7939-7951.

30. D. J. Coady, A. C. Engler, H. W. Horn, K. M. Bajjuri, K. Fukushima, G. O. Jones, A. Nelson, J. E. Rice and J. L. Hedrick, *ACS Macro Lett.*, 2012, **1**, 19-22.

31. P. C. Ruenitz and E. E. Smissman, *J. Heterocycl. Chem.*, 1976, **13**, 1111-1113.

32. A. Gogoll, C. Johansson, A. Axén and H. Grennberg, *Chem. Eur. J.*, 2001, **7**, 396-403.

33. J. A. Landgrebe and L. W. Becker, *J. Am. Chem. Soc.*, 1968, **90**, 395-400.

34. G. M. Miyake and E. Y. X. Chen, *Macromolecules*, 2011, **44**, 4116-4124.

35. L. Zhang, F. Nederberg, J. M. Messman, R. C. Pratt, J. L. Hedrick and C. G. Wade, *J. Am. Chem. Soc.*, 2007, **129**, 12610-12611.

36. M. T. Zell, B. E. Padden, A. J. Paterick, K. A. M. Thakur, R. T. Kean, M. A. Hillmyer and E. J. Munson, *Macromolecules*, 2002, **35**, 7700-7707.

37. J. Coudane, C. UstarizPeyret, G. Schwach and M. Vert, *J. Polym. Sci. A Polym. Chem.*, 1997, **35**, 1651-1658.

38. J. E. Kasperczyk, *Polymer*, 1999, **40**, 5455-5458.

39. F. Nederberg, B. G. G. Lohmeijer, F. Leibfarth, R. C. Pratt, J. Choi, A. P. Dove, R. M. Waymouth and J. L. Hedrick, *Biomacromolecules*, 2006, **8**, 153-160.

40. S. Tempelaar, L. Mespouille, P. Dubois and A. P. Dove, *Macromolecules*, 2011, **44**, 2084-2091.

41. D. M. Stevens, S. Tempelaar, A. P. Dove and E. Harth, *ACS Macro Lett.*, 2012, **1**, 915-918.

# Chapter Three

## Synthesis and Functionalisation of Pentaerythritol Based Aliphatic Poly(Carbonate)s

THE UNIVERSITY OF WARWICK

## 3.1 Introduction

Aliphatic poly(carbonate)s have attracted a large amount of interest over the past couple of decades as biodegradable materials, particularly for biomedical applications. Their synthesis has been achieved in a number of ways; *via* copolymerisation of epoxides with carbon dioxide, ring-opening polymerisation (ROP) of cyclic carbonate monomers, condensation polymerisation of diols with phosgene or the transesterfication between diols and disubstituted carbonates.[1-6] In particular the ROP of six-membered cyclic carbonates has developed significantly in recent years, since the simplicity of the monomer synthesis has permitted the development of a plethora of monomers, allowing the formation of poly(carbonate)s with a wide range of functionalities, thermal properties and control over degradation.[7]

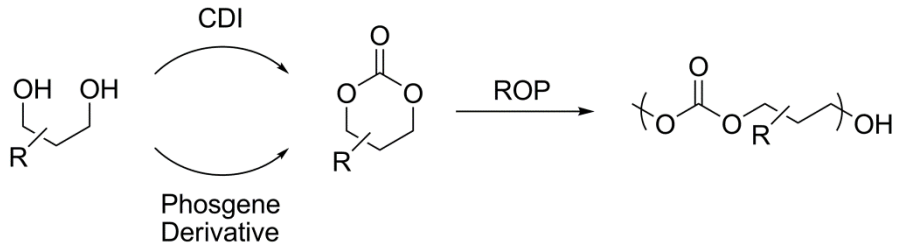


**Scheme 3.1** Generalised synthesis of six-membered cyclic carbonates and resultant poly(carbonate).

The formation of six-membered cyclic carbonate monomers can be achieved *via* the reaction of 1,3-diols with either phosgene derivatives or 1,1′-

carbonyldiimidazole (CDI). While CDI is proposed as a more environmentally friendly and less harmful reagent for carbonate formation, the phosgene derivative ethyl chloroformate is most commonly reported.[8] In some situations it has been found that these reagents are ineffective in cyclic carbonate formation. For example, Mikami *et al.* recently reported that the *trans* configuration of the two hydroxyl groups of the glucose precursor to the carbonate resulted in only monosubstituted compounds being obtained when using ethyl choroformate.[9] To successfully synthesise the cyclic carbonate, a more reactive carbonylation agent bis(pentafluorophenyl) carbonate with cesium fluoride at elevated temperatures) had to be used. Unfortunately the relatively high cost of bis(pentafluorophenyl) carbonate limits its scale of use.

ROP of cyclic carbonates has been achieved using a number of organocatalyst systems. Tertiary amines, super bases, phosphazenes, *N*-heterocyclic carbenes, and binary catalyst systems have all been proven to work effectively, either *via* nucleophilic attack of the cyclic carbonate or by activating the monomer and/or the hydroxyl chain end. Alternatively there have been several reports on organic acids as catalysts. While strong acids such as TfOH result in the decarboxylation of the carbonate group, weaker acids such as diphenyl phosphate do not suffer from the same problem achieving relatively high molecular weights whilst maintaining good control (PTMC, DP100, $M_n$ = 9,850 Da, $Đ_M$ = 1.13). Recent focus on acidic catalysts has increased the range of polymerisable cyclic carbonate monomers. For example, perfluorophenyl 5-methyl-2-oxo-1,3-dioxane-5-carboxylate (MTC-$OC_6F_5$) features an activated ester group that reacts readily with amines or alcohols under basic conditions and is therefore not compatible with basic organic catalysts.[10] Development of acidic organic catalysts has allowed the polymerisation of MTC-

$OC_6F_5$, increasing the number of poly(carbonate)s that can undergo post-polymerisation modification.[11, 12]

Post-polymerisation functionalisation provides a simple route to add groups that are not compatible with the ROP, such as hydroxyl, carboxylic acid, amine and thiol groups. Work carried out by Dove and coworkers using the bis(hydroxylmethyl)propionic acid (*bis*-MPA) scaffold to synthesise cyclic carbonates containing allyl, maleimide, norbornene or alkyne functionality, has provided several simple and effective routes to functional poly(carbonate)s through post-polymerisation functionalisation.[13-16] All can react with thiols either by a free radical mechanism or Michael addition. Alkyne and norbornene functional polymers can also react with azides *via* copper catalysed azide cycloaddition "click" reaction or thermal addition respectively. Additionally, the norbornene functionality can undergo near quantitative reactions with tetrazines without the need of an added catalyst.[16]

While these monomers provide a facile method of synthesising a wide range of functional materials, the fundamental thermal properties of the polymers remain unchanged. Most aliphatic poly(carbonate)s have a low glass transition temperature. For example, the resulting polymer synthesised from trimethylene carbonate which has no pendant functionality has a $T_g$ of -26 °C resulting from its flexible backbone. Poly(5-methyl-5-allyloxycarbonyl-1,3-dioxan-2-one) (PMAC) contains a methyl group on each repeat unit along with a pendant allyl ester group, but the same $T_g$ is observed as PTMC. Moreover, reported functionalisations of PMAC have only altered the $T_g$ marginally (-33 °C to -5.1 °C).[13]

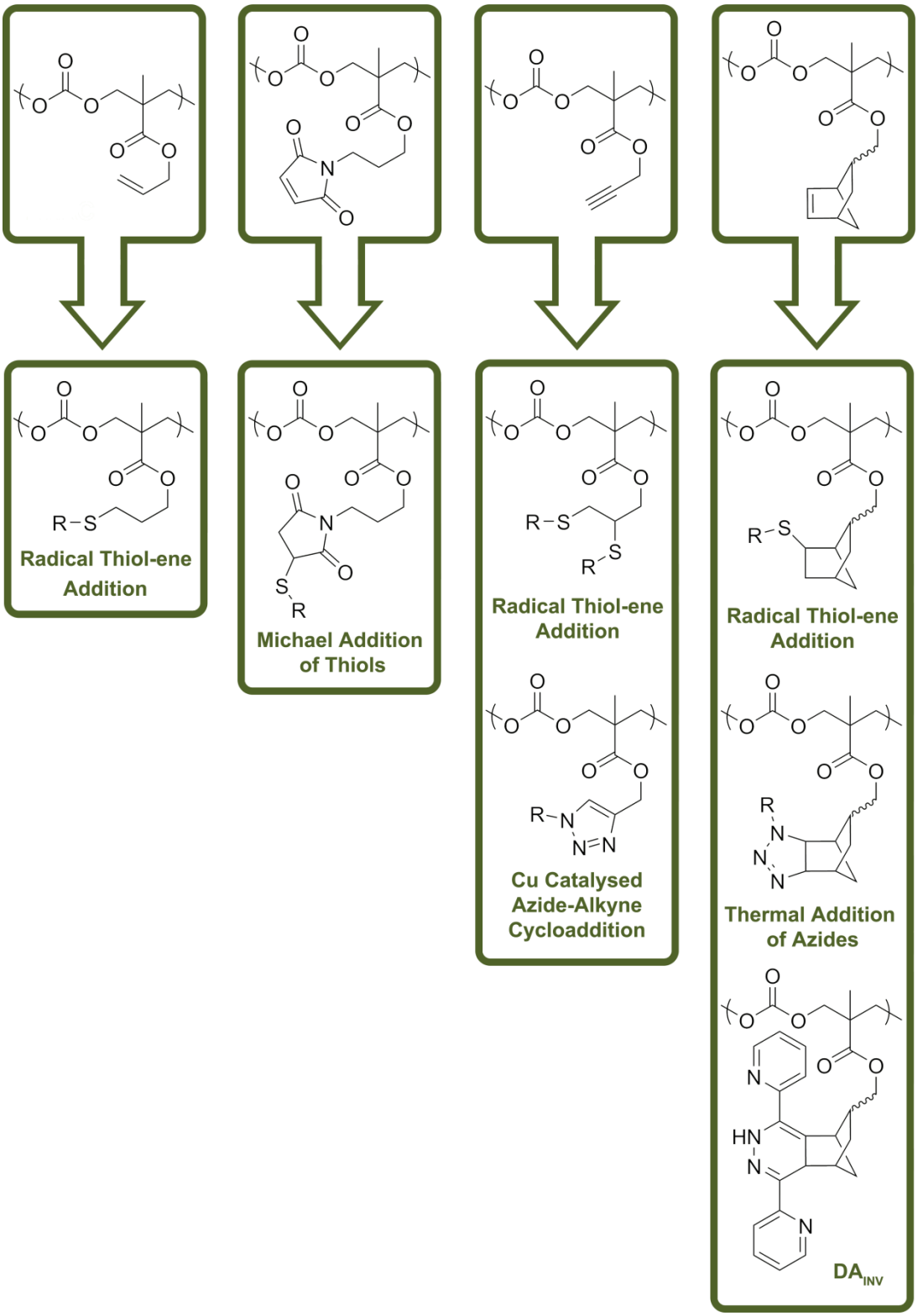


**Figure 3.1** Reported post-polymerisation functionalisations of poly(carbonate)s derived from the ROP of cyclic carbonate monomers.

A standard method of increasing glass transition temperatures is to introduce aromatic groups into the backbone of the polymer, reducing rotation and resulting in an increased rigidity. In the case of cyclic carbonate monomers, the addition of sterically bulky groups has been used to achieve the same effect. Several bicyclic carbonates have been reported previously, typically containing a secondary ring at the 5 position of the carbonate ring.[9, 17-30] Examples of such spiro carbonates include **1**-**7**, with $T_g$'s ranging from 36 to 124 °C. For the resulting polymer of **9**, which incorporates a fused 5-membered ring onto the carbonate ring, a $T_g$ of 128 °C is observed demonstrating that the fused second ring significantly increases the rigidity of the backbone.[22]

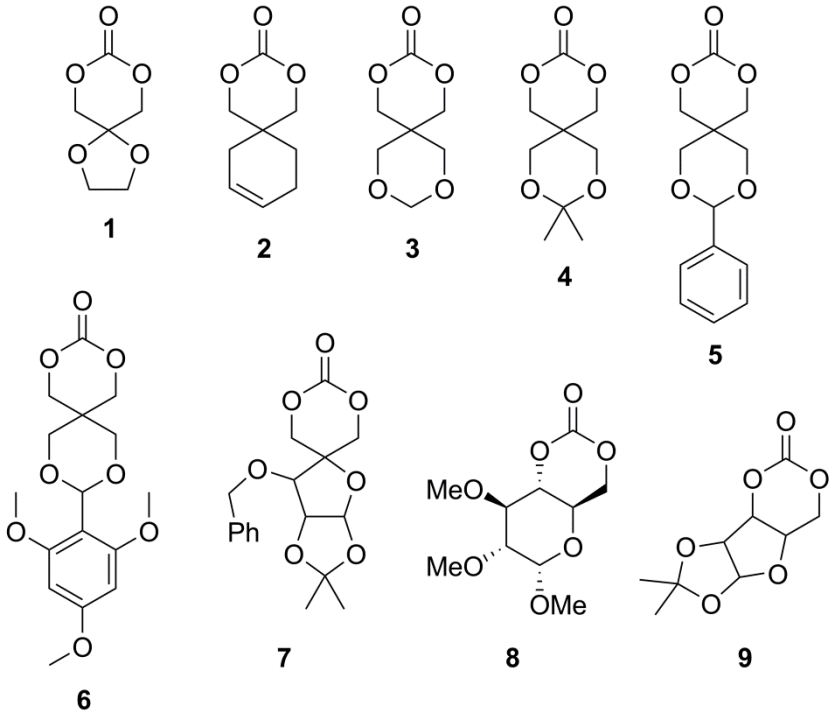


**Figure 3.2** Sterically bulky cyclic carbonate monomers.

This chapter focuses on the development of a new poly(carbonate) that can undergo post polymerisation functionalisation to yield functional poly(carbonate)s with improved thermal properties. To this end, the monomer 9-vinyl-2,4,8,10-tetraoxaspiro[5.5]undecan-3-one (VDC) was synthesised and polymerised using a range of basic organocatalysts. The controlled nature of the polymerisation was explored by GPC, NMR and MALDI-ToF analysis, with further work demonstrating the versatility of the polymerisation using a range of (macro)intitiators. Functionalistion of poly(9-vinyl-2,4,8,10-tetraoxaspiro[5.5]undecan-3-one) (PVDC) was achieved using a UV activated radical thiol-ene method, obtaining well-defined functionalised polymers.

## 3.2 Results and Discussion

### 3.2.1 Monomer Synthesis

A number of cyclic carbonates derived from pentaerythritol have been reported in literature. These monomers were prepared *via* the addition of a functional aldehyde across two of the hydroxyl groups of pentaerythritol, followed by carbonate formation using ethyl chloroformate. A procedure reported by Jing and co-workers for the preparation of the phenyl functional carbonate **5** was initially followed for the synthesis of VDC, replacing benzaldehyde with acrolein in the first step.[27] Unlike the reported procedure for the diol precursor to **5**, **10** did not precipitate. Even after extended reaction times $^{1}$H NMR spectroscopic analyses showed mostly starting material present (>90%) as well as a small amount of the diol product and a disubstituted product. With the reverse reaction being favoured when water is used as the solvent, the reaction was performed in DMF (at 100 °C). After a short reaction time, unreacted pentaerythritol could be removed by filtration upon cooling. The disubstituted product could be easily removed *via* flash chromatography in diethyl ether, while the subsequent addition of ethyl acetate resulted in the isolation of **10** in a 45% yield. Ring closure to form VDC was achieved by reaction of **10** with ethyl chloroformate in THF, achieving a yield of 74%.

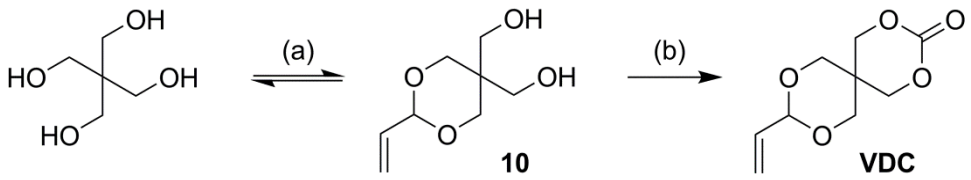


**Scheme 3.2** Synthesis of VDC: (a) Acrolein, DMF, PTSA, 100 °C; (b) Ethyl chloroformate, triethylamine, THF 0-25 °C.

Representative $^{1}$H NMR spectra of **10** and **VDC** are shown in Figure 3.3 The vinylic hydrogens of diol **10** at $\delta$ = 5.77, 5.36, and 5.22 ppm along with the resonances at $\delta$ = 4.57 and 4.47 ppm for the two hydroxyl groups clearly demonstrate the addition of one equivalent of acrolein to pentaerythritol to form diol **10**. Ring closure to form VDC results in little change in the resonances from the vinyl dioxane. A clear shift is observed for the $CH_2$ resonances of the cyclic carbonate ring, these resonances shift from $\delta$ = 3.56 and 3.18 ppm for the diol to resonances at $\delta$ = 4.53 and 4.12 ppm for the cyclic carbonate. As expected, ring closure resulted in the complete disappearance of the two hydroxyl resonances. The appearance of a resonance at $\delta$ = 148 ppm in the $^{13}$C NMR spectrum of VDC is characteristic for a carbonate carbonyl group, further demonstrating the successful synthesis of the carbonate ring.

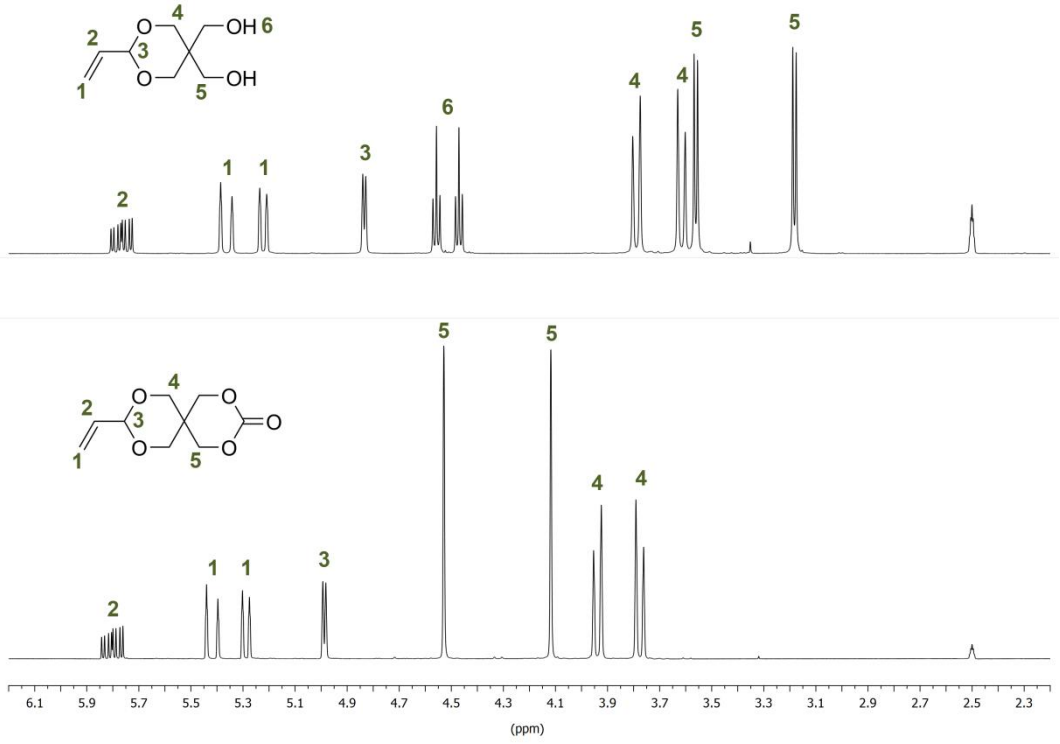


**Figure 3.3** Diol **10** and VDC $^{1}$H NMR (400 MHz) in *d*-DMSO.

### 3.2.2 ROP of VDC

The polymerisation of VDC was performed using a range of basic organic catalyst systems including (-)-sparteine/1-(3,5-bis(trifluoromethyl)phenyl)-3-cyclohexylthiourea (TU), benzyl bispidine/TU, 1,8-diazabicyclo[5.4.0]undec-7-ene (DBU)/TU and $Me_6$TREN/TU. Polymerisations were initiated from benzyl alcohol ($[M]_0/[I]_0$ = 20) using 5 mol% tertiary amine and 10 mol% TU in deuterated chloroform (0.5 M). For the DBU/TU binary system of 1 mol% DBU and 5 mol% TU were used. Polymerisations were followed by $^1$H NMR spectroscopy and upon 90% monomer conversion were directly purified by flash chromatography. Loading the polymerisation solution onto a silica column and flushing with hexanes removed the TU with diethyl ether then removing any unreacted monomer. Finally flushing with ethyl acetate resulted in the recovery of pure PVDC.

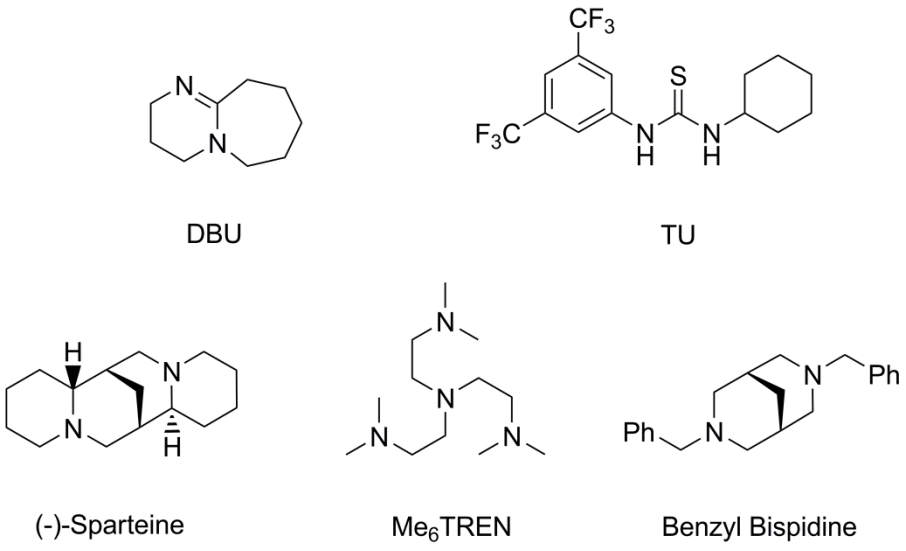


**Figure 3.4** Catalysts for the ROP of cyclic carbonates.

Almost identical GPC traces were obtained for each catalyst system, with similar molecular weights and $Đ_M$ values (1.12 - 1.13). Polymerisation of VDC catalysed by $Me_6$TREN/TU was found to reach 91% monomer conversion only after ~80 days. Benzyl bispidine/TU and (-)-sparteine/TU reached >90% monomer conversion much faster, with polymerisations taking 320 and 390 minutes respectively. The binary catalytic system of DBU/TU was found to be most active even though a reduced loading was used in comparison to the other catalyst systems (120 min). The increased kinetic rate resulting from DBU/TU combined with its good control resulted in its selection as the catalytic system for further polymerisations.

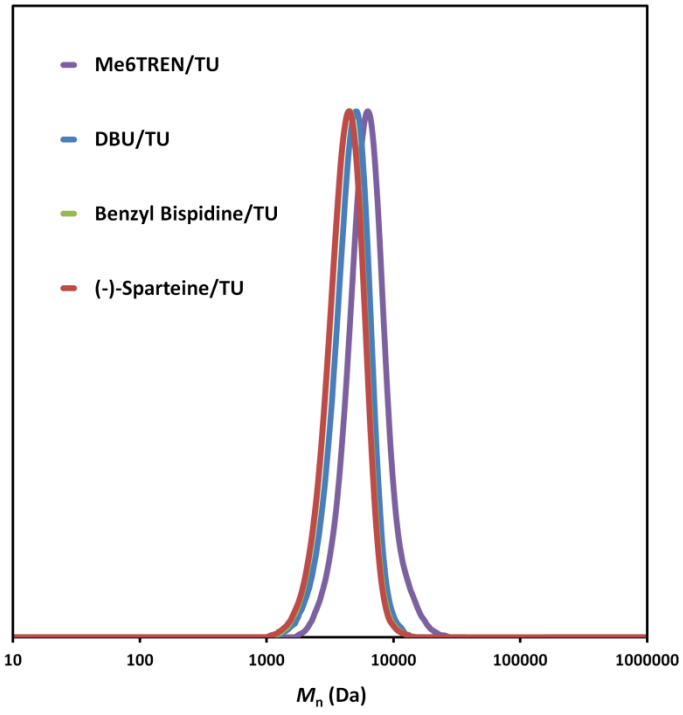


**Figure 3.5** GPC traces of PVDC catalysed by various catalytic systems, initiated from benzyl alcohol ($[M]_0/[I]_0$ = 20). Analysed by chloroform GPC against PS standards.

The $^{1}$H NMR spectrum resulting from the polymerisation of VDC initiated from benzyl alcohol ($[M]_0/[I]_0 = 20$) with the DBU/TU binary catalyst system shows a clear shift of the $CH_2$ resonances from the carbonate ring in the monomer to the polymer backbone (Figure 3.6**)**. In particular, the resonance shifting from $\delta$ = 4.61 ppm for the monomer to $\delta$ = 4.46 ppm for the polymer provided an excellent handle to monitor the polymerisation *in situ*. Although there is little change in position of the vinylic resonances of the vinyl dioxane, some broadening is observed.

A comparison of the integrals of the benzyl end group resonances at $\delta$ = 7.37 ppm and 5.16 ppm to those of the polymer backbone at $\delta$ = 4.47 ppm revealed a degree of polymerisation (DP) of 20 which corresponds to the targeted $[M]_0/[I]_0$. The degree of polymerisation could be further verified by comparing the integral values of the resonance resulting from the final repeat unit in the polymer next to the hydroxyl chain end at $\delta$ = 4.54 ppm to that of the polymer backbone. As both methods produce a DP of 20 it can be concluded that no initiation from water or other undesired side reactions have occurred.

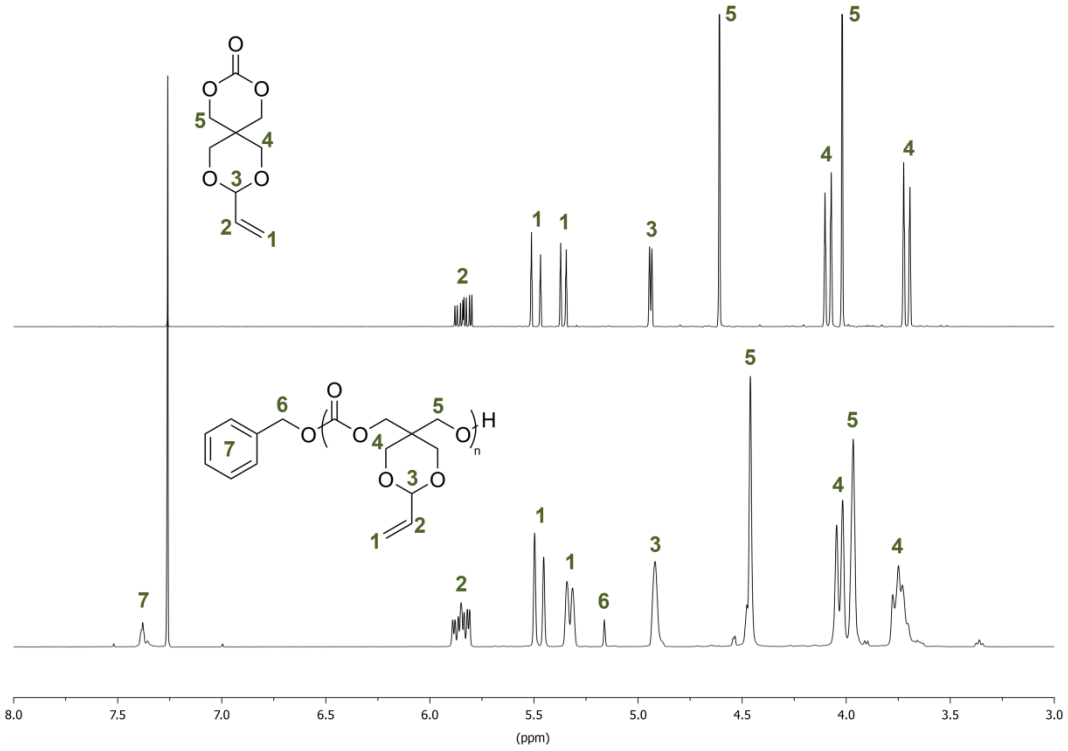


**Figure 3.6** $^{1}$H NMR spectra (400 MHz) of VDC and PVDC initiated from benzyl alcohol (DP20) in $CDCl_3$.

### 3.2.3 Controlled Nature of VDC ROP

The polymerisation of VDC initiated from benzyl alcohol ($[M]_0/[I]_0$ = 50), using the DBU/TU binary catalyst system was monitored against time by $^1$H NMR spectroscopy, revealing that a plateau was reached at 92% monomer conversion (Figure 3.7). A linear relationship between $\ln([M]_0/[M]_t)$ *vs* time revealed first order kinetics, attesting to the controlled nature of the polymerisation (Figure 3.8). To further prove the controlled nature of the polymerisation a VDC polymerisation ($[M]_0/[I]_0$ = 50) was sampled at various points through the reaction and a $M_n$ *vs* conversion graph plotted (Figure 3.9). A linear relationship between $M_n$ and conversion demonstrated that controlled growth in molecular weight is achieved as the monomer undergoes polymerisation. Further polymerisations targeting a range of DP's (10, 20, 50, 75 and 100) also demonstrated a linear evolution against $M_n$ by GPC analysis (Figure 3.10). In all cases dispersitites ($Đ_M$) of the VDC homopolymers were found to be ≤ 1.1. Only for the DP10 PVDC a higher $Đ_M$ of 1.27 was observed.

**Table 3.1** Variation in $[M]_0/[I]_0$ with the DBU/TU binary catalyst system[a]

| $[M]_0/[I]_0$ | Time (min)[b] | $M_n$ (Da)[c] | $Đ_M$[c] |
|---|---|---|---|
| 10 | 50 | 2,080 | 1.27 |
| 20 | 120 | 4,610 | 1.10 |
| 50 | 310 | 12,620 | 1.10 |
| 75 | 540 | 18,970 | 1.09 |
| 100 | 740 | 26,650 | 1.04 |

[a][VDC] = 0.5 M in chloroform, 1 mol% DBU, 5 mol% TU, initiated from benzyl alcohol; [b]Time taken to reach 90% monomer conversion as measured by $^1$H NMR spectroscopy; [c]Measured by chloroform GPC against PS standards.

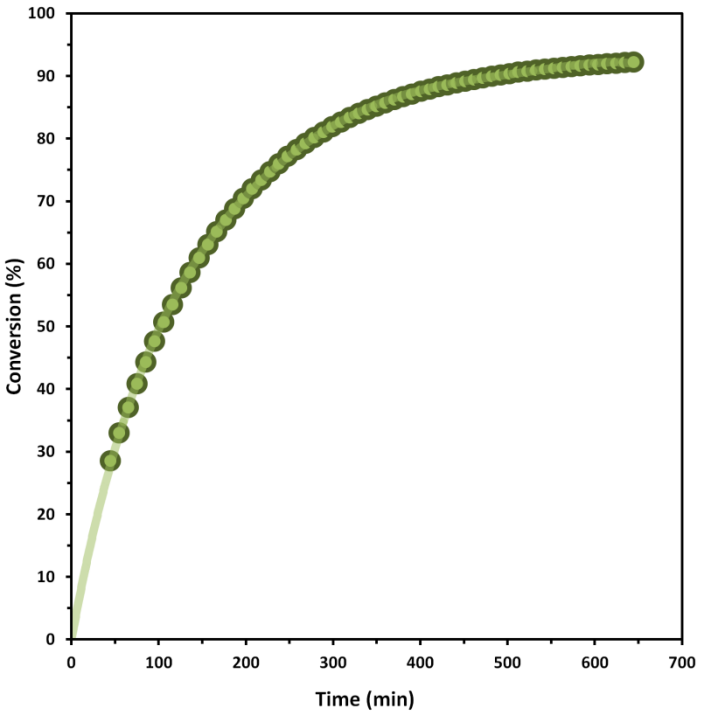


**Figure 3.7** Conversion *vs* time graph of VDC polymerisation ($[M]_0/[I]_0$ = 50).

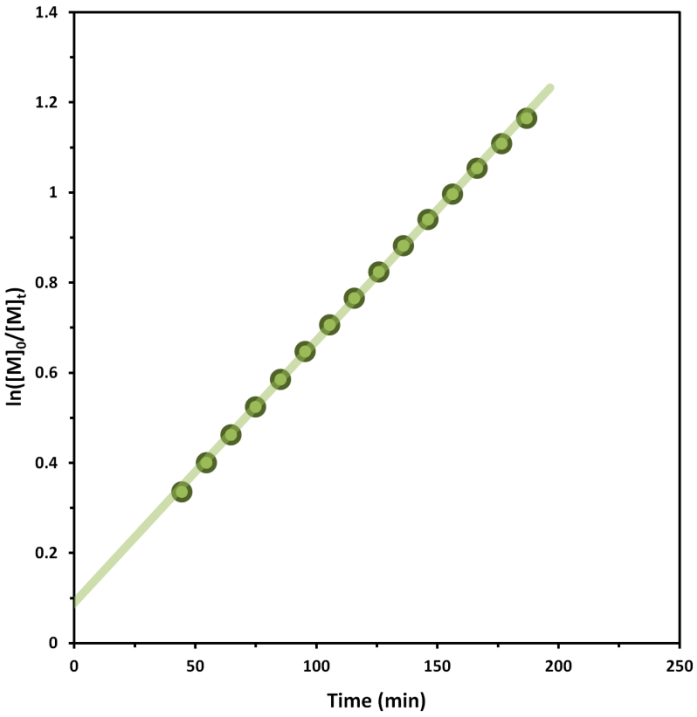


**Figure 3.8** $\ln([M]_0/[M]_t)$ vs time graph of VDC polymerisation ($[M]_0/[I]_0$ = 50).

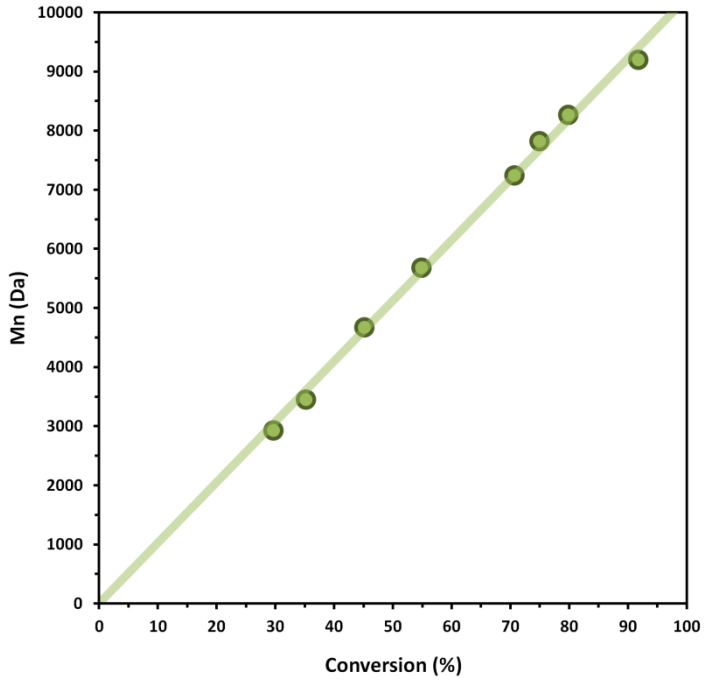


**Figure 3.9** $M_n$ *vs* conversion graph for a single VDC polymerisation.

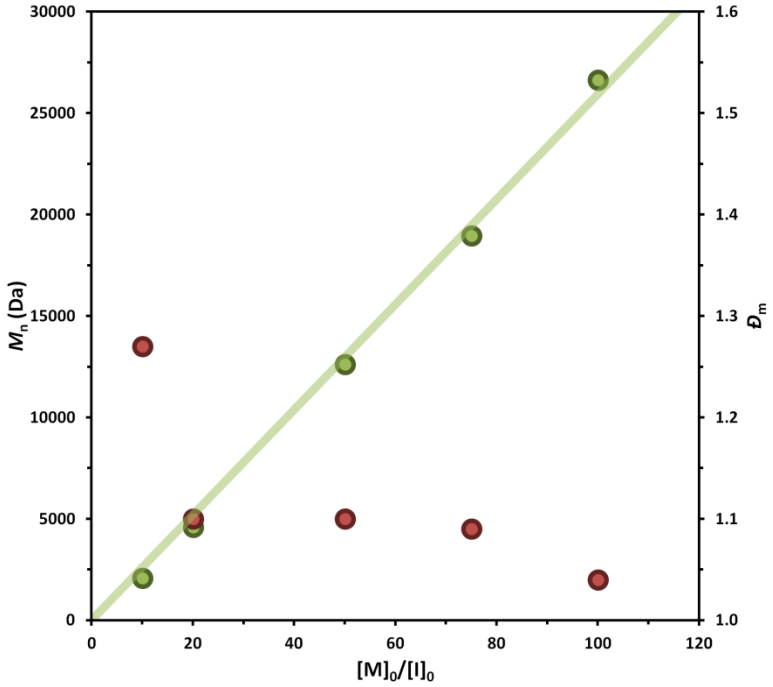


**Figure 3.10** $M_n$ *vs* $[M]_0/[I]_0$ *vs* $Đ_M$ for PVDC polymerisations.

Further analysis of the resultant polymers by matrix-assisted laser desorption ionisation time of flight mass spectrometry (MALDI-ToF MS) revealed only a single distribution with spacings of 200 *m*/*z* between neighbouring peaks (Figure 3.11). The peak masses of the distribution correspond to the equation: ($M_n$ = DP(200.2) + 107.1 + 24), where DP is the degree of polymerisation (number of VDC molecules incorporated into polymer), showing that all chains are successfully initiated from benzyl alcohol. No secondary distributions resulting from degradation of the polymer backbone or side reactions such as water initiation ($M_n$ = DP(200.2) + 174.2 + 23) are observed attesting to the controlled nature of the ROP of VDC catalysed by the binary catalytic system of DBU/TU.

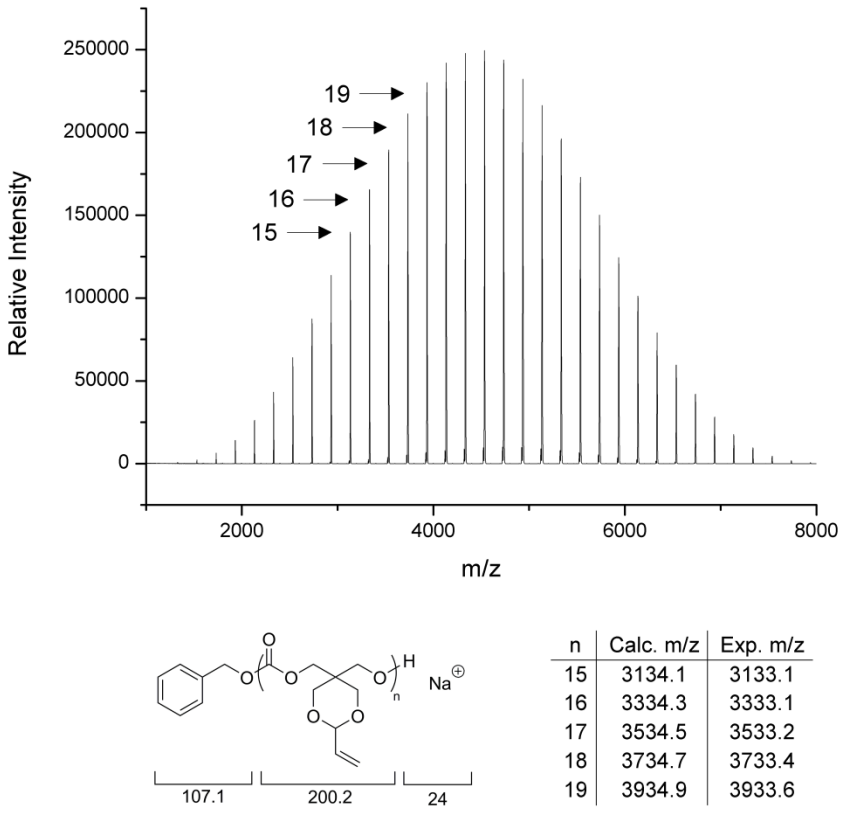


| n | Calc. m/z | Exp. m/z |
|---|---|---|
| 15 | 3134.1 | 3133.1 |
| 16 | 3334.3 | 3333.1 |
| 17 | 3534.5 | 3533.2 |
| 18 | 3734.7 | 3733.4 |
| 19 | 3934.9 | 3933.6 |

**Figure 3.11** MALDI-ToF spectrum of PVDC (DP20) initiated from benzyl alcohol.

### 3.2.4 Versatility of VDC ROP

To demonstrate initiator versatility, VDC polymerisations were undertaken with a range of initiators. Polymerisations were carried out using the same DBU/TU conditions as before using 5-norbornene-2-methanol (**12**), 1,4-butanediol (**11**) or the furan protected maleimide **13**. Polymerisations with $[M]_0/[I]_0$ ratios of 20, 100 and 200 were carried out initiating from **11**. GPC analysis of the resulting polymers gave $M_n$ values consistent with those previously initiated from benzyl alcohol as well as low $Đ_M$ values. Initiators **12** and **13** were chosen to provide further possibilities of post-polymerisation modification of PVDC. Initiating from **12** would result in PVDC that could be chain-end functionalised as well as functionalised along the backbone. PVDC initiated from **12** ($[M]_0/[I]_0$ = 20**)** resulted in a $M_n$ of 2,970 Da and a $Đ_M$ of 1.13 by GPC analysis. In addition MALDI-ToF analysis of this polymer revealed a single distribution with a spacing of 200 *m/z* between the peaks. The distribution was found to obey the formula $M_n$ = DP(200.2) + 24 + 123.2, showing that all chains are successfully initiated from **12** and sodium charged.

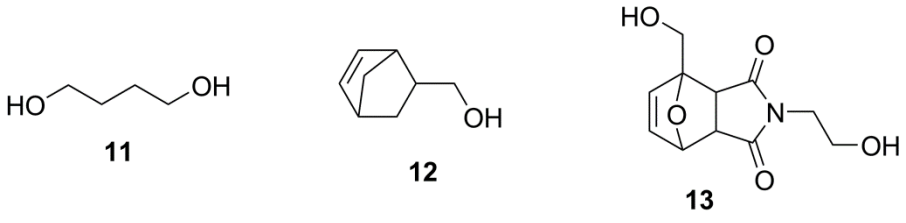


**Figure 3.12** Functional initiators used in the ROP of VDC.

**Table 3.2** Different initiators used in the ROP of VDC[a]

| Initiator | $[M]_0/[OH]_0$ | $M_n$ (Da)[b] | $Đ_M$[b] |
|---|---|---|---|
| **11** | 20 | 3,430 | 1.15 |
| **11** | 100 | 21,610 | 1.04 |
| **11** | 200 | 42,070 | 1.03 |
| **12** | 20 | 2,970 | 1.13 |
| **13** | 50 | 10,490 | 1.05 |

[a][VDC] = 0.5 M in chloroform, 1 mol% DBU, 5 mol% TU; [b]Measured by chloroform GPC against PS standards.

Finally VDC was initiated from the protected maleimide **13**, with a $[M]_0/[I]_0$ ratio of 50 being used. MALDI-ToF analysis of the resultant PVDC produced a spectrum exhibiting two distributions separated by approximately 43 m/z (Figure 3.13). Each distribution is centered on ~5,250 *m/z*, half the expected molecular mass for a DP50 polymer. While this could suggest that the diol has cleaved during polymerisation resulting in two separate polymers, GPC analysis of the same polymer resulted in a single distribution with a $M_n$ of 10,490 Da, close to the expected theoretical value for the uncleaved polymer. These observations lead to the conclusion that the polymer undergoes a retro-Diels-Alder reaction during the MALDI-ToF analysis, cleaving the polymer in two, most likely resulting from the energy imparted from the laser. Cleaving the diol results in two polymers, one containing a furan end group and the other a maleimide end group. The expected difference in molecular weight between these two polymers is 43 Da which matches the result obtained by MALDI-ToF analysis. The distributions are found to obey the formula $M_n$ = DP(200.2) + 24 + 97.1 or $M_n$ = DP(200.2) + 24 + 140.1. The first

formula corresponds to the furan terminated polymer and the latter for the maleimide terminated polymer. No additional distributions are observed, attesting to the controlled nature of the PVDC polymerisation being maintained using different initiators.

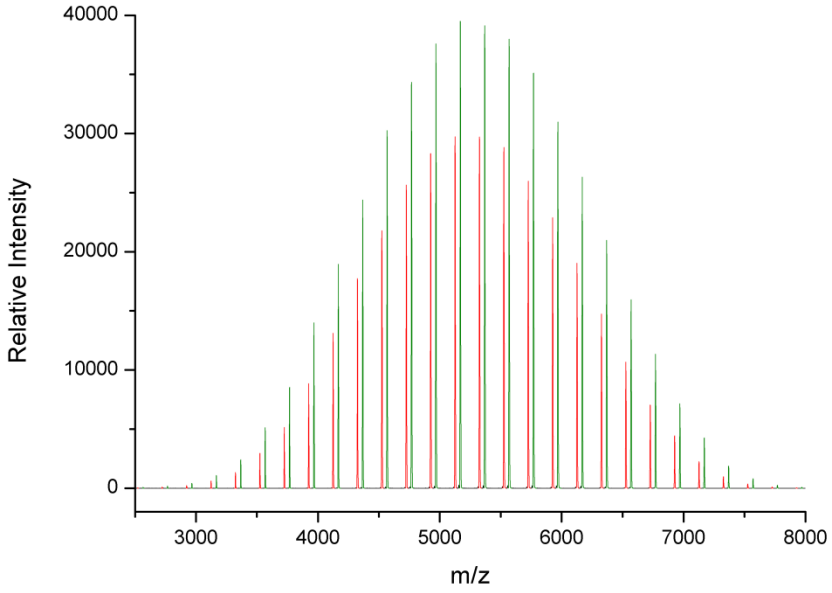


| n | Calc. m/z | Exp. m/z |
|---|---|---|
| 25 | 5126.1 | 5125.4 |
| 24 | 4925.9 | 4925.2 |
| 23 | 4725.7 | 4725.1 |
| 22 | 4525.5 | 4525.1 |
| 21 | 4325.3 | 4324.6 |

| n | Calc. m/z | Exp. m/z |
|---|---|---|
| 25 | 5169.1 | 5168.7 |
| 24 | 4968.9 | 4968.3 |
| 23 | 4768.9 | 4768.1 |
| 22 | 4568.5 | 4568.3 |
| 21 | 4368.3 | 4367.8 |

**Figure 3.13** MALDI-ToF Spectrum of PVDC initiated from the furan protected maleimide **13**.

To further demonstrate the initiator versatility, VDC was polymerised from a range of macroinitiators. Commercially available poly(caprolactone) and poly(ethylene oxide) monomethyl ether-5K were found to have a $M_n$ of 4,020 and 9,640 Da respectively when characterised by chloroform GPC against poly(styrene) standards. Chain extension of poly(ethylene oxide) with VDC resulted in a clear shift to higher molecular by GPC analysis ($M_n$ = 15,840 Da) whilst maintaining the same $Đ_M$ of 1.03 (Figure 3.14). The use of poly(caprolactone) as a macroinitator resulted in an increase of $M_n$ to 8,420 Da with a decrease in $Đ_M$ from 1.24 to 1.09 for the block co-polymer. Two further macroinitiators were synthesised *via* the ROP of L-lactide (LLA) and trimethylene carbonate (TMC). Polymerisations were undertaken using the same conditions as for VDC, initiated from benzyl alcohol using the DBU/TU catalyst system, resulting in poly(L-lactide) PLLA with a DP of 40 ($M_n$ = 9,000 Da, $Đ_M$ = 1.06) and PTMC with a DP of 30 ($M_n$ = 4,130 Da, $Đ_M$ = 1.06). Chain extension of PTMC to form $PTMC_{30}$-$PVDC_{27}$ block copolymer resulted in a shift to higher molecular weight ($M_n$ = 10,770 Da) by GPC analysis whilst maintaining the same $Đ_M$ of 1.06. The $PLLA_{40}$-$PVDC_{36}$ block copolymer exhibited a shift to higher molecular weight along with an increase in $Đ_M$ of 1.09. Additionally, to prove the living nature of the VDC polymerisation block copolymers with TMC and LLA were synthesised from a PVDC macro initiator (DP = 33, $M_n$ = 7,220 Da, $Đ_M$ = 1.11) forming $PVDC_{33}$-$PLLA_{32}$ ($M_n$ = 12,870 Da, $Đ_M$ = 1.08) and $PVDC_{33}$-$PTMC_{33}$ ($M_n$ = 10,540 Da, $Đ_M$ = 1.07) block copolymers. The $^1$H NMR spectrum of the $PVDC_{33}$-$PTMC_{33}$ block copolymer is shown in figure 3.15, exhibiting the characteristic resonances for PVDC as well as a triplet at $\delta$ = 4.13 ppm and a pentet at $\delta$ = 2.04 ppm resulting from the PTMC block. As the final monomer unit next to the hydroxyl chain end has changed from a VDC unit to a TMC unit, no resonance at $\delta$ = 4.47

ppm is observed. Instead two small resonances at δ = 4.29 ppm and 1.90 ppm are observed. The clear shift to higher molecular weight by GPC of the two block copolymers along with slight reduction in $Đ_M$ demonstrates the end group fidelity of the synthesised PVDC.

**Table 3.3** Block copolymers

| **Polymer** | **DP**[d] | $M_n$ **(Da)**[e] | $Đ_M$[e] |
|---|---|---|---|
| HO-PCL-OH[a] | 18 | 4,020 | 1.24 |
| PVDC-$PCL_{18}$-PVDC[b] | 9[f] | 8,420 | 1.09 |
| mPEG(5k)[a] | 135 | 9,640 | 1.03 |
| mPEG(5k)-VDC[b] | 29 | 15,840 | 1.03 |
| PLLA[c] | 40 | 9,000 | 1.06 |
| $PLLA_{40}$-PVDC[b] | 36 | 14,720 | 1.09 |
| PTMC[c] | 30 | 4,130 | 1.06 |
| $PTMC_{30}$-PVDC[b] | 27 | 10,770 | 1.06 |
| PVDC[c] | 33 | 7,220 | 1.11 |
| $PVDC_{33}$-PLLA[b] | 32 | 12,870 | 1.08 |
| $PVDC_{33}$-PTMC[b] | 33 | 10,540 | 1.07 |

[a]Obtained from commercial sources; [b][Monomer] = 0.5 M in chloroform, 1 mol% DBU, 5 mol% TU; [c][Monomer] = 0.5 M in chloroform, initiated from benzyl alcohol, 1 mol% DBU, 5 mol% TU; [d]Determined by $^1$H NMR spectroscopy (400 MHz); [e]Measured by chloroform GPC against PS standards. [f]Per OH group.

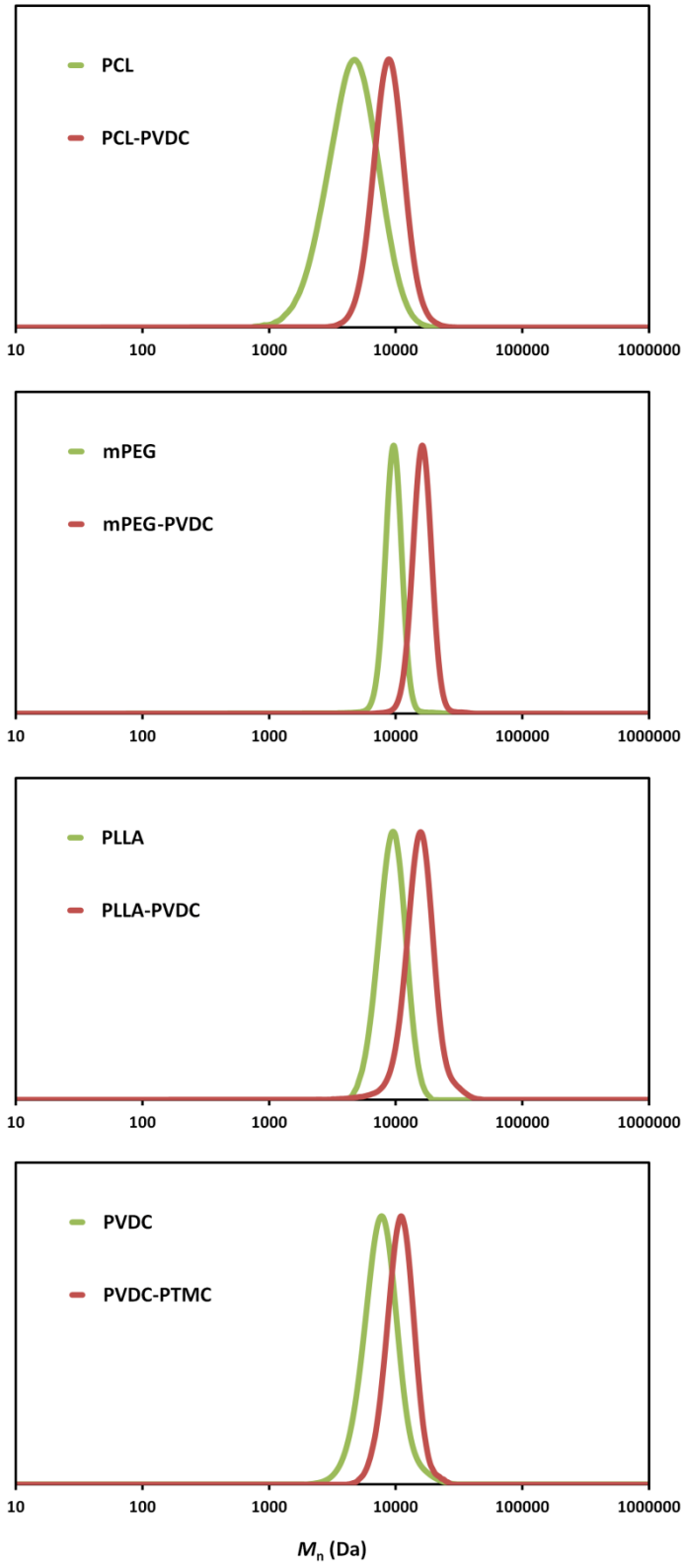


**Figure 3.14** GPC traces of assorted block copolymers. Analysed by chloroform GPC against PS standards.

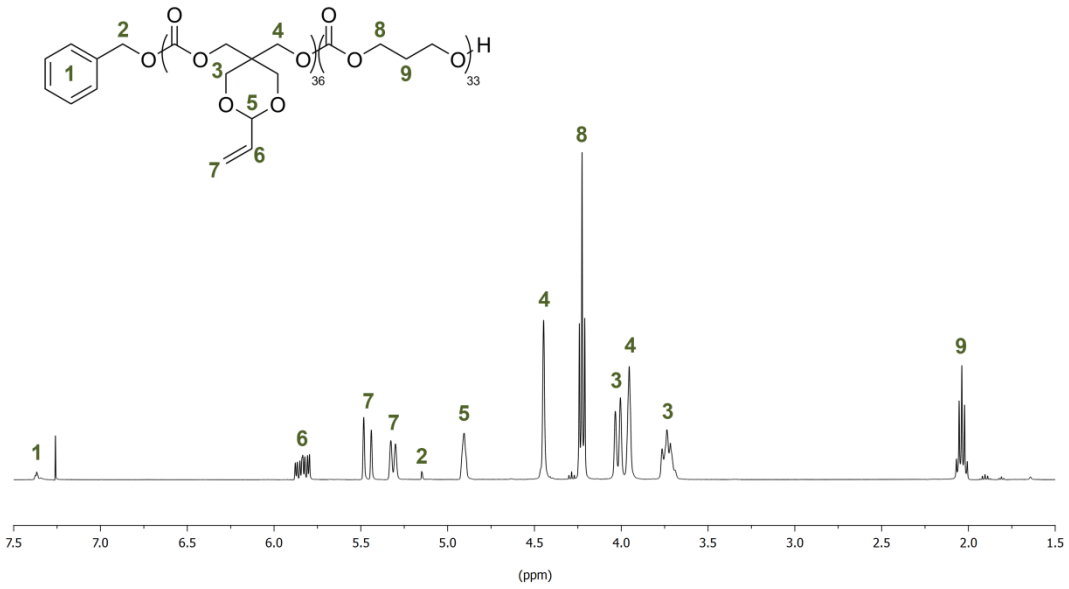


**Figure 3.15** $^{1}$H NMR spectrum (400 MHz) of PVDC-PTMC block co-polymer in $CDCl_3$.

### 3.2.5 Post-polymerisation Functionalisation of PVDC

The functionalisation of PMAC *via* a thiol-ene reaction has been reported previously using a range of thiols and azobisisobutyronitrile (AIBN) as a radical source.[13] This method requires the application of heat to produce the necessary radicals and is reported having long reaction times (24 h) to achieve full conversion. In an effort to refine the reaction further for use with PVDC, the utilisation of a photoinitiator to replace AIBN was explored. To produce the radicals required for the thiol-ene reaction a UV source would only be required, the reaction can therefore take place at room temperature. The photointiator IRGACURE® 369 was chosen due to its commercial availability and broad absorption range.

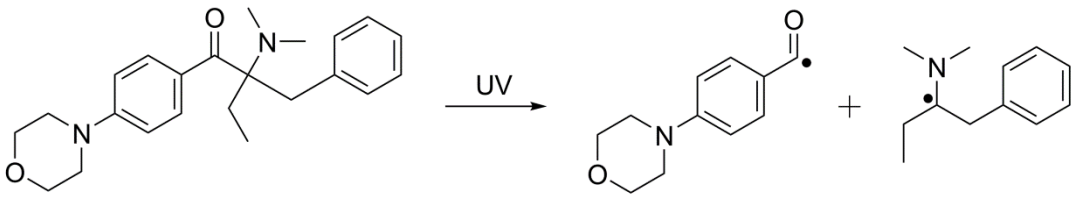


**Scheme 3.3** Structure of IRGACURE® 369.

The thiol-ene functionalisations of PVDCs with a DP of 20 ($M_n$ = 4,430 Da, $Đ_M$ = 1.13) and 100 ($M_n$ = 19,360 Da, $Đ_M$ = 1.05) initiated from benzyl alcohol and 1,4-butanediol respectively were undertaken by dissolution in 1,4-dioxane and the addition of two equivalents of 1-dodecanethiol followed by 1 mol% IRGACURE® 369 with respect to polymers vinylic groups. After 2 h exposure to UV light from a lightbox the polymers were precipitated into methanol. GPC analysis of the functionalised polymers showed that in each case a clear shift to higher molecular

weight compared to the starting PVDC GPC trace was observed. A $M_n$ of 8,810 Da with a $Đ_M$ of 1.13 was obtained for the DP20 PVDC and a $M_n$ of 35,340 Da with a $Đ_M$ of 1.07 for the DP100 (Figure 3.16 and 3.17). While a monomodal trace was observed for the DP20 functionalised polymer, the trace for the DP100 exhibited a small high molecular weight shoulder.

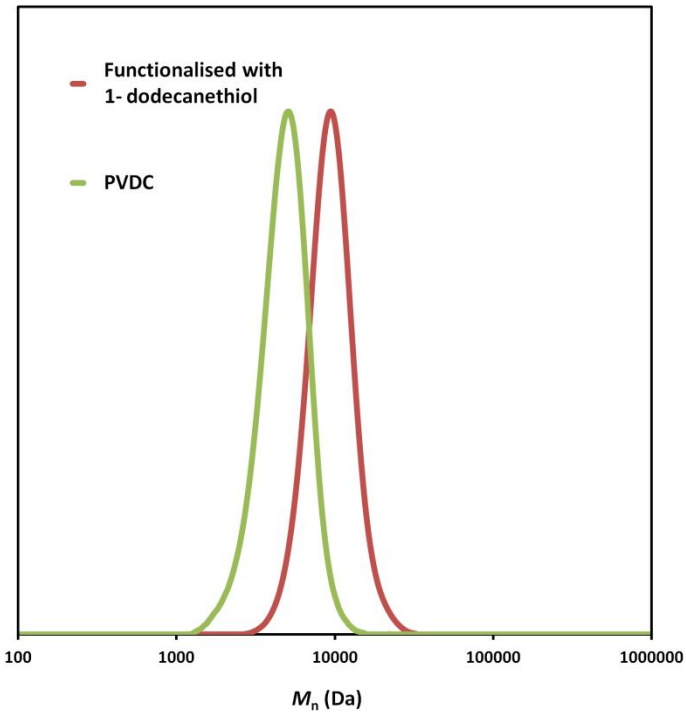


**Figure 3.16** PVDC (DP20) functionalised using 1-dodecanethiol with IRGACURE® 369. Analysed by chloroform GPC against PS standards. (Green trace $M_n$ = 4,430 Da, $Đ_M$ = 1.13; Red trace: $M_n$ = 8,810 Da, $Đ_M$ = 1.12)

The molecular weight of the shoulder can be estimated to be twice that of the main distribution, suggesting a small percentage of crosslinking has taken place between polymer chains during the thiol-ene reaction. In an effort to eradicate this undesirable side reaction the conditions used were altered by increasing the number of equivalents of thiol, reducing the concentration of the polymer or reducing the amount of photoinitiator. In each case a reduction of the high molecular weight shoulder was not achieved. The combination of all three conditions failed to achieve any improvement as well. In the reported functionalisation of PMAC using AIBN as a radical source, the resulting polymers showed no obvious sign of crosslinking by GPC analysis when two equivalents of thiol were used. The use of these conditions (50 mg of PVDC in 136 μl of 1,4-dioxane, 2 equivalents of thiol, 10 mol% AIBN, 90 °C, 24 h) was therefore tested for the functionalisation of PVDC. As can be seen in Figure 3.17, the use of AIBN actually resulted in a larger shoulder in the case of PVDC functionalisation suggesting that a higher degree of crosslinking has occurred, likely resulting from the increased polymer and radical concentration. Since no improved conditions were found, all further post-polymerisation functionalisations were carried out using the original photoinitiator conditions.

$^{1}$H NMR spectroscopic analysis of DP20 and DP100 polymers functionalised with 1-dodecanethiol using a photoinitiator revealed a complete disappearance of the vinylic resonances at $\delta$ = 5.84, 5.47 and 5.32 ppm (Figure 3.18). In addition to this, resonances corresponding to the added dodecyl group can clearly be seen at $\delta$ = 2.50, 1.57, 1.35, 1.29 and 0.88 ppm along with a shift in the resonances that previously corresponded to the vinyl group at $\delta$ = 4.63, 2.58 and 1.91 ppm. Integration of the dodecyl resonances reveal >99% conversion for the thiol-ene reaction, showing that the actual amount of crosslinking is negligible.

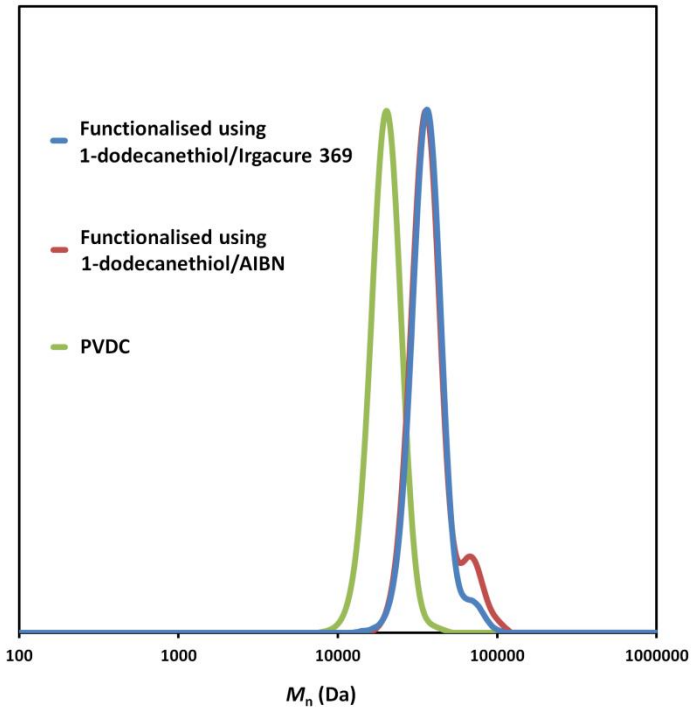


**Figure 3.17** Resulting GPC traces from the functionalisation of PVDC (DP100) with 1-dodecanethiol using AIBN or IRGACURE® 369 as the radical source in 1,4-dioxane. Analysed by chloroform GPC against PS standards. (Green trace $M_n$ = 19,360 Da, $Đ_M$ = 1.05; Blue trace: $M_n$ = 35,340 Da, $Đ_M$ = 1.07; Red trace: $M_n$ = 36,150 Da, $Đ_M$ = 1.09)

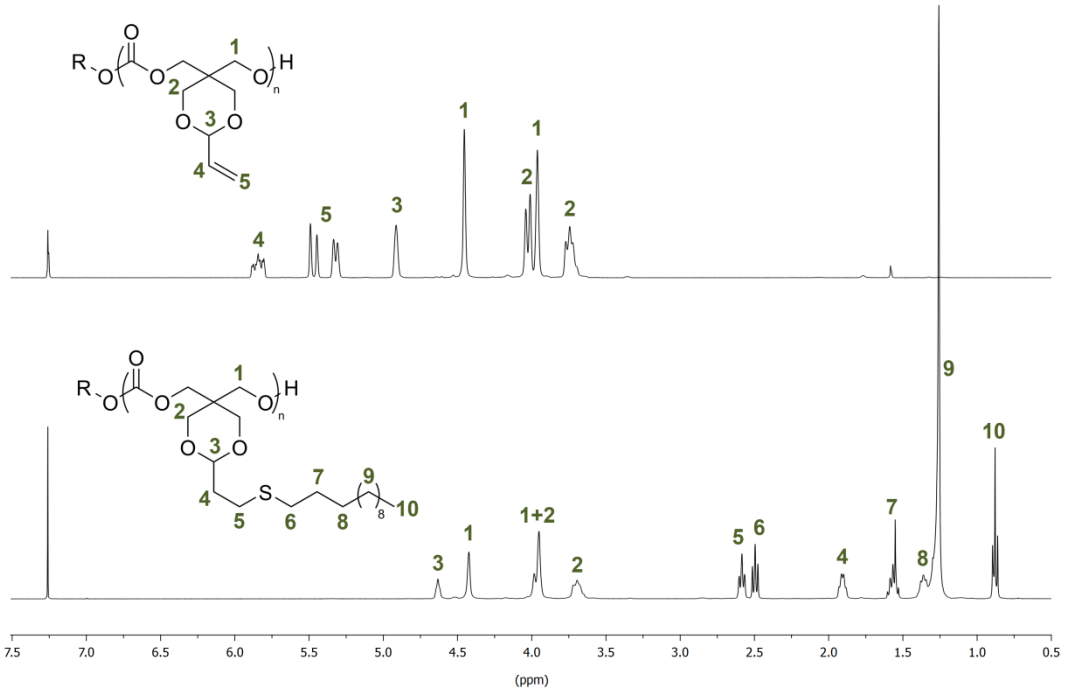


**Figure 3.18** $^{1}$H NMR spectra ($CDCl_3$, 400 MHz) of PVDC (DP100) before and after its functionalisation with 1-dodecanethiol using IRGACURE® 369.

To further demonstrate the versatility of this method, functionalisation of the DP20 and DP100 VDC homopolymers were carried out using a range of thiols, including those containing functionalities not compatible with ROP. While the functionalisation of PVDC with hexylthiol, butylthiol, mercaptoethanol, mercaptoacetic acid and 1-thioglycerol showed complete disappearance of the vinyl resonances by $^{1}$H NMR spectroscopy and the appearance of resonances consistent with those expected for the added groups, the thiol-ene reaction with benzyl mercaptan and adamantylthiol failed to reach complete conversion under the same conditions. For adamantylthiol complete conversion could be achieved by increasing

number of equivalents of the photoinitiator to two, whereas for benzyl mercaptan an increase to four equivalents was found necessary. For all functionalised polymers an increase in molecular weight was observed by GPC with dispersity remaining low in each case (Table 3.4). It must be noted that while a response was observed by GPC for the DP20 functionalised PVDC with thioglycolic acid, none was observed by the refractive index detector for the DP100 functionalised polymer, even though the polymer was completely soluble in the GPC solvent.

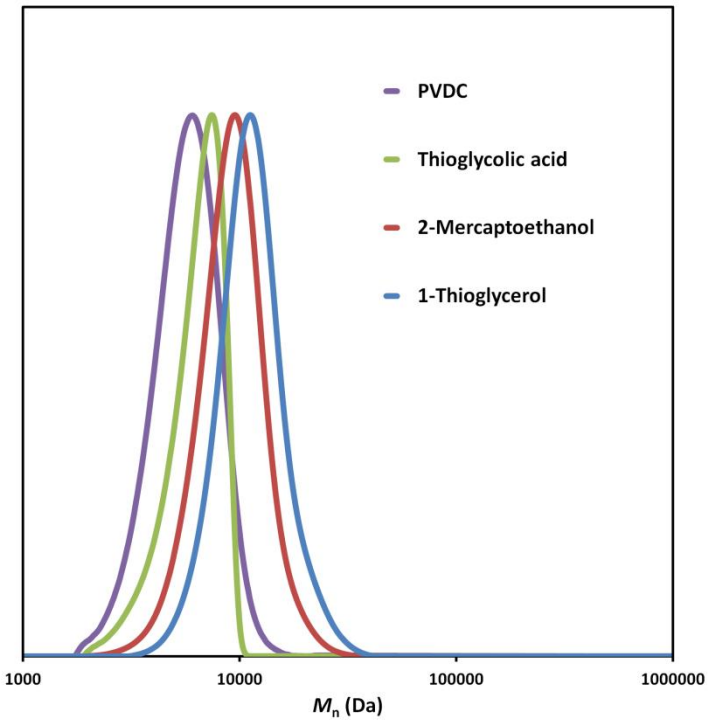


**Figure 3.19** PVDC (DP20) functionalised using different thiols. Analysed by DMF GPC against PMMA standards. (Purple trace $M_n$ = 5,240 Da, $Đ_M$ = 1.13; Green trace $M_n$ = 7,440 Da, $Đ_M$ = 1.09; Red trace $M_n$ = 8,460 Da, $Đ_M$ = 1.13; Blue trace $M_n$ = 10,480 Da, $Đ_M$ = 1.13)

**Table 3.4** Thiol-ene functionalised PVDC[a]

| DP of PVDC | Thiol | $M_n$ (Da) | $Đ_M$ |
|---|---|---|---|
| 20 | - | 4,433[b]/5,420[c] | 1.13[b]/1.13[c] |
| 100 | - | 21,620[b]/23,710[c] | 1.04[b]/1.06[c] |
| 20 | 1-dodecanethiol | 8,810[b] | 1.12[b] |
| 100 | 1-dodecanethiol | 35,340[b] | 1.07[b] |
| 20 | hexylthiol | 6,880[b] | 1.14[b] |
| 100 | hexylthiol | 28,360[b] | 1.07[b] |
| 20 | butylthiol | 6,270[b] | 1.15[b] |
| 100 | butylthiol | 28,890[b] | 1.08[b] |
| 20 | 1-adamantylthiol | 6,420[b] | 1.18[b] |
| 100 | 1-adamantylthiol | 29,900[b] | 1.17[b] |
| 20 | benzyl mercaptan | 6,570[b] | 1.18[b] |
| 100 | benzyl mercaptan | 31,000[b] | 1.55[b] |
| 20 | 1-thioglycerol | 10,480[c] | 1.13[c] |
| 100 | 1-thioglycerol | 40,200[c] | 1.09[c] |
| 20 | 2-mercaptoethanol | 8,460[c] | 1.13[c] |
| 100 | 2-mercaptoethanol | 34,840[c] | 1.09[c] |
| 20 | thioglycolic acid | 7,440[c] | 1.09[c] |
| 100 | thioglycolic acid | -[c] | -[c] |

[a]PVDC (20 mg) in 1,4-dioxane (0.25 ml), 2 equivalent of RSH, 1 mol% photoinitiator (to vinyl groups), 2 h UV exposure; [b]Measured by chloroform GPC against PS standards; [c]Measured by DMF GPC against PMMA standards.

To further demonstrate the successful thiol-ene functionalisation, MALDI-ToF analysis was undertaken on each of the functionalised PVDC (DP20) samples. While polymers containing hydroxyl or carboxylic acid groups on each repeat unit failed to show any response, polymers containing alkyl groups all displayed singular distributions (Figure 3.20). The distribution observed for the 1-dodecanethiol functionalisation follows the formula $M_n$ = DP(402.6) + 24 +107.1. The same could be determined for hexyl and adamantyl thiol functionalised polymers, obeying the following formulae respectively: $M_n$ = DP(318.4) + 24 + 107.1 and $M_n$ = DP(368.5) + 24 + 107.1. The increase in spacing from 200 *m/z* along with lack of secondary distributions in these spectra confirms the complete functionalisation of the PVDC. In the case of the benzyl mercaptan functionalised polymer, a small second distribution is observed. While the main distribution follows the formula $M_n$ = DP(324.4) + 24 + 107.1, the secondary distribution follows the formula $M_n$ = DP-1(324.4) + 202.2 + 24 + 107.1 for a polymer with all but one repeat unit functionalised. The lack of any other distributions in any of the obtained spectra shows an absence of any side reactions such as cross-linking, and confirms that no degradation of the polymer has occurred during functionalisation.

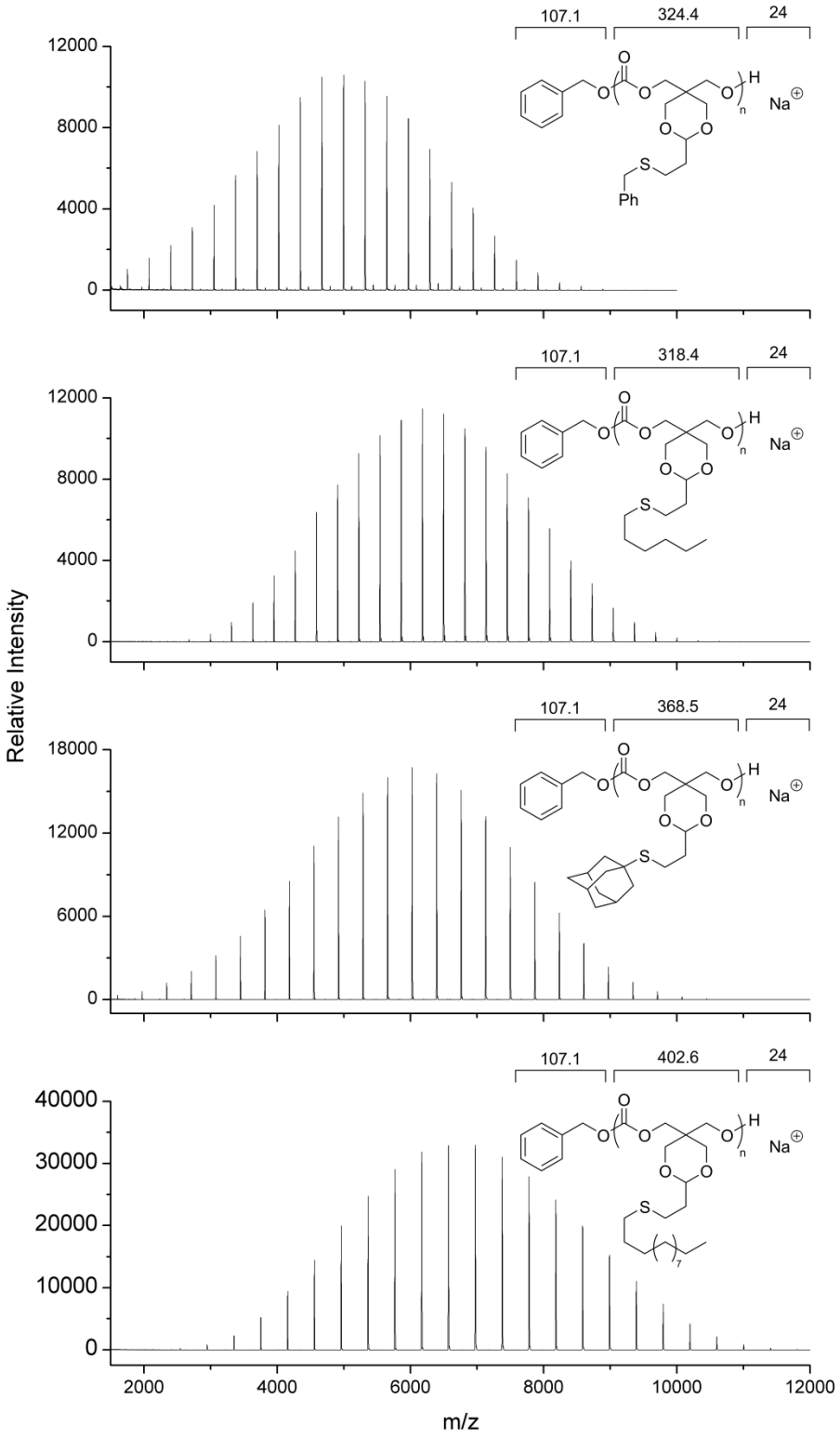


**Figure 3.20** MALDI-ToF spectra of functionalised PVDC (DP20).

### 3.2.6 Thermal Analysis of Functionalised PVDC

Analysis of the synthesised DP100 PVDC and subsequent functionalisations by differential scanning calorimetry (DSC) was undertaken to explore the effect of different groups on the thermal properties of the poly(carbonate). For a DP100 PVDC, DSC analysis revealed a glass transition temperature of 73.8 °C and no observable melting temperature, meaning that PVDC is amorphous. The $T_g$ lies between that of the structurally similar poly(carbonate)s of poly(9,9-dimethyl-2,4,8,10-tetraoxaspiro[5.5]undecan-3-one) (PCC) and poly(9-phenyl-2,4,8,10-tetraoxaspiro[5,5]undecan-3-one) (PPTO), and is considerably higher than the allyl functional poly(carbonate) PMAC ($T_g$ = -26 °C).[13, 18, 21, 27]

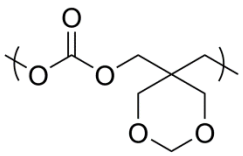

PDOXTC $T_g$ = 36 °C

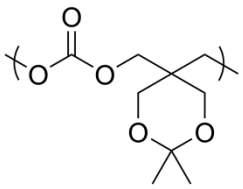

PCC $T_g$ = 99 °C Semi-crystalline; $T_g$ = 68 °C Amorphous

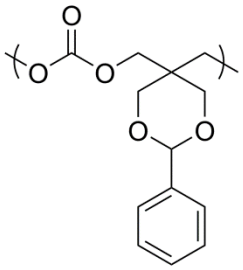

PPTO $T_g$ = 124 °C

**Figure 3.21** Poly(carbonate)s structurally similar to PVDC and their respective $T_g$'s as reported in literature.

All functionalities apart for the adamantyl functionalised PVDC resulted in a reduction in $T_g$ by DSC (Table 3.5). The bulky adamantyl group provides restriction to rotation for the polymer chains and therefore produces an increase in $T_g$. Alkyl side chains have been reported to lower the $T_g$ of polymers due to an increase in polymer flexibility with a larger effect observed for longer alkyl chains. The addition of 1-butylthiol to PVDC considerably lowers the $T_g$ to 15.6 °C, with the slightly longer chain of 1-hexylthiol reducing the $T_g$ even further to 7.7 °C.[31] It could therefore be expected that the functionalisation of PVDC with 1-dodecanthiol would result in a further reduction in $T_g$, but this is not observed. 1-Dodecanthiol results in a $T_g$ of 23.5 °C along with a melting point of 42.0 °C due to crystallisation of the dodecyl side chains.[32-34] While the functionalisation of PMAC with benzyl mercaptan is reported to result in an increase in $T_g$ from -26.4 to -5.1 °C, a reduction is observed for the same functionalisation of PVDC, the resultant polymer displaying a $T_g$ of 35.5 °C.[13]

**Table 3.5** Thermal analysis of functionalised PVDC.

| Thiol | $T_m$ (°C) | $T_g$ (°C) |
|---|---|---|
| - | - | 73.8 |
| 1-Adamantylthiol | - | 109.3 |
| 1-Dodecanethiol | 42.0 | 23.5 |
| 1-Butylthiol | - | 15.6 |
| 1-Hexylthiol | - | 7.7 |
| Benzyl Mercaptan | - | 35.5 |
| 1-Mercaptoethanol | - | 43.4 |
| 1-Thioglycerol | - | 40.6 |
| Thioglycolic acid | - | 48.3 |

[a]Glass transition temperature measured by DSC analysis of the third scan; [b]Melting point measured by DSC analysis.

## 3.3 Conclusion

In this work, the synthesis of 9-vinyl-2,4,8,10-tetraoxaspiro[5.5]undecan-3-one (VDC) has been demonstrated. The polymerisation of this bulky vinyl functional cyclic carbonate was performed with a range of basic organic catalysts with the DBU/TU binary catalyst system favoured due to its faster kinetics. The living nature of the polymerisation was proven by a linear increase in molecular weight *vs.* conversion and the synthesis of PVDC with a range of molecular weights that correspond linearly to the degree of polymerisation, whilst maintaining low dispersities. To further demonstrate the versatility of the VDC polymerisation, a range of telechelic and block copolymers were synthesised. An easier method of thiol-ene post-polymerisation functionalisation of PVDC compared to that reported for PMAC was found using the photoinitiator IRGACURE® 369. The use of a photoinitiator instead of AIBN allowed the functionalisation of PVDC in shorter reaction times with the advantage that the reaction could be performed in air, instead of under an inert atmosphere. The post-polymerisation functionalisation was undertaken using a wide range of thiols, obtaining functional poly(carbonate)s with low dispersities. Thermal analysis of the PVDC homopolymer revealed a high $T_g$ of 74 °C with the functionalised polymers displaying a range of thermal properties.

## 3.4 References


1. L. Wang, B. Xiao and G. Wang, *J. Nat. Gas Chem.*, 2010, **19**, 436-440.
2. B. Ochiai and T. Endo, *Prog. Polym. Sci.*, 2005, **30**, 183-215.
3. D. J. Darensbourg, R. M. Mackiewicz, A. L. Phelps and D. R. Billodeaux, *Acc. Chem. Res.*, 2004, **37**, 836-844.
4. D. J. Darensbourg, *Chem. Rev.*, 2007, **107**, 2388-2410.
5. G. W. Coates and D. R. Moore, *Angew. Chem. Int. Ed*, 2004, **43**, 6618-6639.
6. F. Nederberg, B. G. G. Lohmeijer, F. Leibfarth, R. C. Pratt, J. Choi, A. P. Dove, R. M. Waymouth and J. L. Hedrick, *Biomacromolecules*, 2006, **8**, 153-160.
7. S. Tempelaar, L. Mespouille, O. Coulembier, P. Dubois and A. P. Dove, *Chem. Soc. Rev.*, 2013, **42**, 1312-1336.
8. J. Mindemark and T. Bowden, *Polymer*, 2011, **52**, 5716-5722.
9. K. Mikami, A. T. Lonnecker, T. P. Gustafson, N. F. Zinnel, P.-J. Pai, D. H. Russell and K. L. Wooley, *J. Am. Chem. Soc.*, 2013, **135**, 6826-6829.
10. D. P. Sanders, K. Fukushima, D. J. Coady, A. Nelson, M. Fujiwara, M. Yasumoto and J. L. Hedrick, *J. Am. Chem. Soc.*, 2010, **132**, 14724-14726.
11. A. C. Engler, J. M. W. Chan, D. J. Coady, J. M. O'Brien, H. Sardon, A. Nelson, D. P. Sanders, Y. Y. Yang and J. L. Hedrick, *Macromolecules*, 2013, **46**, 1283-1290.
12. D. J. Coady, H. W. Horn, G. O. Jones, H. Sardon, A. C. Engler, R. M. Waymouth, J. E. Rice, Y. Y. Yang and J. L. Hedrick, *ACS Macro Lett.*, 2013, **2**, 306-312.
13. S. Tempelaar, L. Mespouille, P. Dubois and A. P. Dove, *Macromolecules*, 2011, **44**, 2084-2091.

14. S. Tempelaar, I. A. Barker, V. X. Truong, D. J. Hall, L. Mespouille, P. Dubois and A. P. Dove, *Polym. Chem.*, 2013, **4**, 174-183.

15. S. Onbulak, S. Tempelaar, R. J. Pounder, O. Gok, R. Sanyal, A. P. Dove and A. Sanyal, *Macromolecules*, 2012, **45**, 1715-1722.

16. R. J. Williams, I. A. Barker, R. K. O'Reilly and A. P. Dove, *ACS Macro Lett.*, 2012, **1**, 1285-1290.

17. X. Chen, S. P. McCarthy and R. A. Gross, *Macromolecules*, 1997, **30**, 3470-3476.

18. X. Chen, S. P. McCarthy and R. A. Gross, *J. Appl. Polym. Sci.*, 1998, **67**, 547-557.

19. X. Chen, S. P. McCarthy and R. A. Gross, *Macromolecules*, 1998, **31**, 662-668.

20. Y. Shen, X. Chen and R. A. Gross, *Macromolecules*, 1999, **32**, 3891-3897.

21. E. J. Vandenberg and D. Tian, *Macromolecules*, 1999, **32**, 3613-3619.

22. Y. Shen, X. Chen and R. A. Gross, *Macromolecules*, 1999, **32**, 2799-2802.

23. X. Chen and R. A. Gross, *Macromolecules*, 1998, **32**, 308-314.

24. R. Kumar, W. Gao and R. A. Gross, *Macromolecules*, 2002, **35**, 6835-6844.

25. L.-S. Wang, S.-X. Cheng and R.-X. Zhuo, *Macromol. Rapid Commun.*, 2004, **25**, 959-963.

26. A. N. Zelikin, P. N. Zawaneh and D. Putnam, *Biomacromolecules*, 2006, **7**, 3239-3244.

27. Z. Xie, C. Lu, X. Chen, L. Chen, Y. Wang, X. Hu, Q. Shi and X. Jing, *J. Polym. Sci. A Polym. Chem.*, 2007, **45**, 1737-1745.

28. L.-L. Mei, G.-P. Yan, X.-H. Yu, S.-X. Cheng and J.-Y. Wu, *J. Appl. Polym. Sci.*, 2008, **108**, 93-98.

29. W. Chen, F. Meng, F. Li, S.-J. Ji and Z. Zhong, *Biomacromolecules*, 2009, **10**, 1727-1735.

30. F. Suriano, R. Pratt, J. P. K. Tan, N. Wiradharma, A. Nelson, Y.-Y. Yang, P. Dubois and J. L. Hedrick, *Biomaterials*, 2010, **31**, 2637-2645.

31. H. K. Reimschuessel, *J. Polym. Sci. A Polym. Chem.*, 1979, **17**, 2447-2457.

32. E. F. J. Rettler, J. M. Kranenburg, H. M. L. Lambermont-Thijs, R. Hoogenboom and U. S. Schubert, *Macromol. Chem. Phys.*, 2010, **211**, 2443-2448.

33. L. C. E. Struik, *Polymer*, 1987, **28**, 1521-1533.

34. A. Mizuno, M. Mitsuiki and M. Motoki, *J. Agric. Food Chem.*, 1998, **46**, 98-103.

# Chapter Four

## Tailored Thermal Properties of Aliphatic Poly(Carbonate)s

THE UNIVERSITY OF WARWICK

## 4.1 Introduction

The glass transition temperature ($T_g$) of materials for biomedical applications is very important. For example, for a load bearing implants the $T_g$ needs to be higher than body temperature (37 °C) so that the chains are immobile forming a rigid material, whereas materials used for artificial skin need to be more pliable and so a $T_g$ lower than body temperature is beneficial.[1-4] For drug delivery, the materials $T_g$ has an effect on the drug release rate. A $T_g$ lower than body temperature results in a rubbery material that has a higher permeability to water, resulting in faster degradation and drug release. With a $T_g$ higher than body temperature, the material will hydrate at a greatly reduced rate, resulting in longer drug release times and polymer degradation.[5]

In Chapter Three it was demonstrated that the incorporation of a vinyl dioxane group onto a cyclic carbonate resulted in a higher $T_g$ of the resulting homopolymer, with subsequent thiol-ene reactions yielding functional polymers with higher $T_g$'s than can be obtained *via* the thiol-ene post-polymerisation functionalisation of 5-methyl-5-allyloxycarbonyl-1,3-dioxan-2-one (MAC). To extend this work further, this chapter focuses the synthesis of functional aliphatic poly(carbonate)s with variable $T_g$'s *via* the copolymerisation of VDC and MAC. Through a thorough investigation, the combination of these two monomers is shown to allow the synthesis of copolymers that after post-polymerisation functionalisation can have a predetermined glass transition temperature.

## 4.2 Results and Discussion

### 4.2.1 Copolymerisation of VDC and MAC

In order to obtain poly(carbonate)s that can be post-polymerisation functionalised whilst controlling the glass transition temperature, the copolymerisation of VDC and MAC was investigated. The homopolymerisations of VDC and MAC were undertaken in triplicate using the binary catalyst system of DBU (1 mol%) and TU (5 mol%) to determine if the monomers display similar homopolymer activity. The catalyst system has already been successfully employed in VDC polymerisations (Chapter Three) yielding well defined vinyl functional poly(carbonate)s with narrow dispersity, however the apparent rate constant was not previously determined. Polymerisations were performed in $CDCl_3$ (0.5 M) using benzyl alcohol as an initiator ($[M]_0/[I]_0$ = 50). Both homopolymerisations were followed by $^1$H NMR spectroscopy with the conversion monitored by the disappearance of monomer resonances at $\delta$ = 1.34 and 4.60 ppm for MAC and VDC and the growth of the PMAC and PVDC resonances at $\delta$ = 1.26 and 4.43 ppm respectively. First order kinetic plots of $\ln([M]_0/[M]_t)$ against time reveal a linear correlation for both polymerisations, with apparent rate constants ($k_{app}$) of $1.41\times10^{-4} \pm 2\times10^{-6}$ $s^{-1}$ obtained for the polymerisation of MAC and $1.12\times10^{-4} \pm 3\times10^{-6}$ $s^{-1}$ for VDC. The similar $k_{app}$ values for the homopolymerisations demonstrate that both monomers are polymerised at a similar rate.

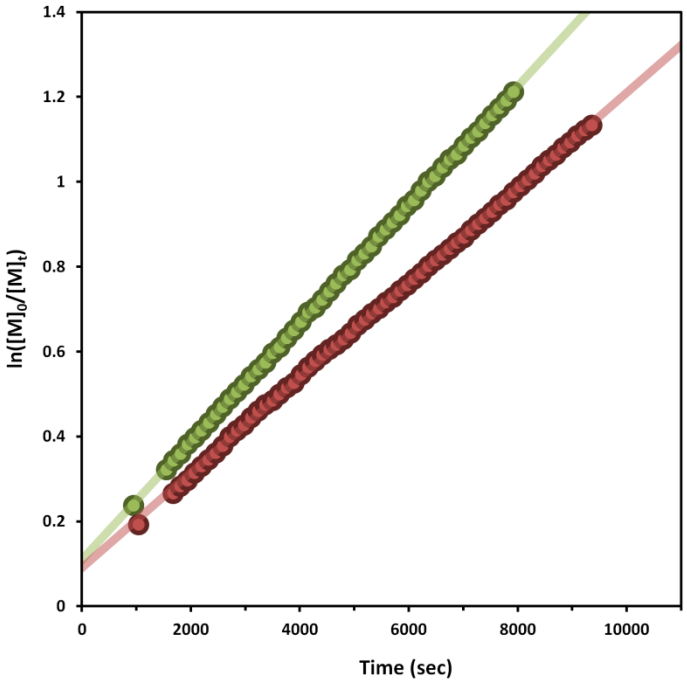


**Figure 4.1** $\ln([M]_0/[M]_t$ vs. time graph for separate homopolymerisations of VDC and MAC (Green = MAC; Red = VDC).

The copolymerisation of VDC and MAC (50:50 feed ratio) was undertaken using the same polymerisation conditions as those used for the homopolymerisations, aiming for a total DP of 20. The overall conversion could be monitored by the reduction in the monomer resonances at $\delta$ = 1.34 and 4.93 ppm for MAC and VDC and the growth of the PMAC and PVDC resonances at $\delta$ = 1.26 and 4.90 ppm respectively. After 90% overall monomer conversion a copolymer (DP = 21) was isolated with a $M_n$ of 4730 Da and $Đ_M$ of 1.09. MALDI-ToF MA analysis of the synthesised copolymer resulted in a single distribution. While copolymers usually exhibit a complicated distribution pattern, VDC and MAC have exactly the same molecular weight (200.2 m/z) and therefore the copolymer exhibits only a

single distribution (Figure 4.3). Spacings of 200 m/z were found between neighbouring peaks, with the peaks obeying the formula $M_n$ = DP(200.2) + 107.1 + 24, demonstrating that every polymer chain is initiated from benzyl alcohol and sodium charged. While VDC and MAC have the same molecular weight, they also have identical chemical formula ($C_9H_{12}O_5$) which results in the same isotope pattern for both homopolymers and copolymers (Figure 4.4). Although MALDI-ToF analysis does not provide further insight into the copolymer structure, the absence of secondary distributions shows that the excellent control observed for the homopolymerisations is maintained in the copolymerisation without the occurrence of side reactions.

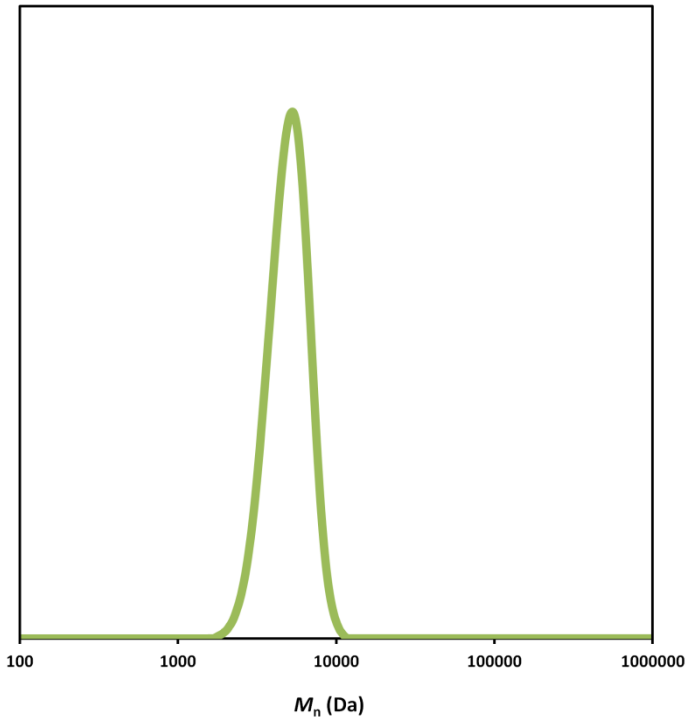


**Figure 4.2** GPC trace of VDC/MAC copolymer synthesised using a 50:50 feed of the two monomers. Initiated from benzyl alcohol ($[M]_0/[I]_0$ = 20). Analysed by chloroform GPC against PS standards.

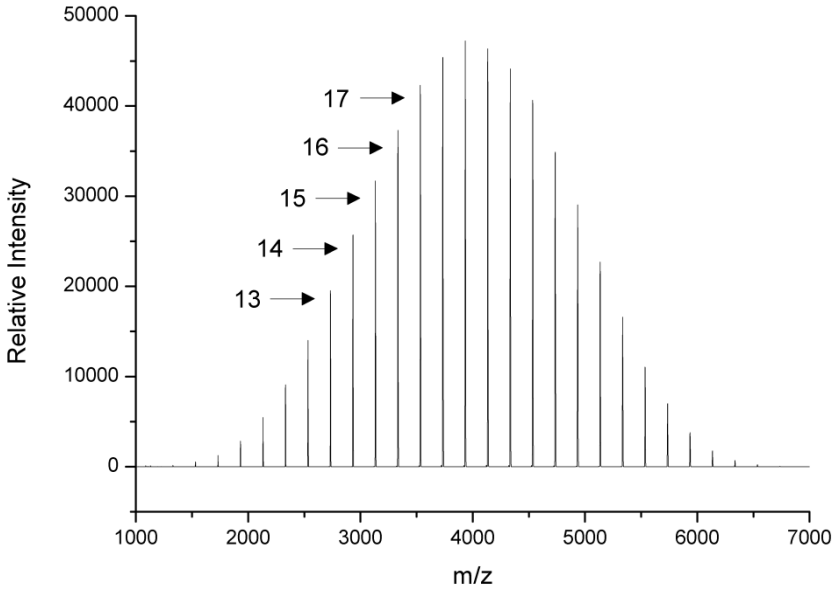


| x + y | Calc. m/z | Exp. m/z |
|---|---|---|
| 17 | 3534.5 | 3533.8 |
| 16 | 3334.3 | 3333.6 |
| 15 | 3134.1 | 3133.4 |
| 14 | 2933.9 | 2933.2 |
| 13 | 2733.7 | 2733.1 |

**Figure 4.3** MALDI-ToF MS of VDC/MAC copolymer (DP20) initiated from benzyl alcohol.

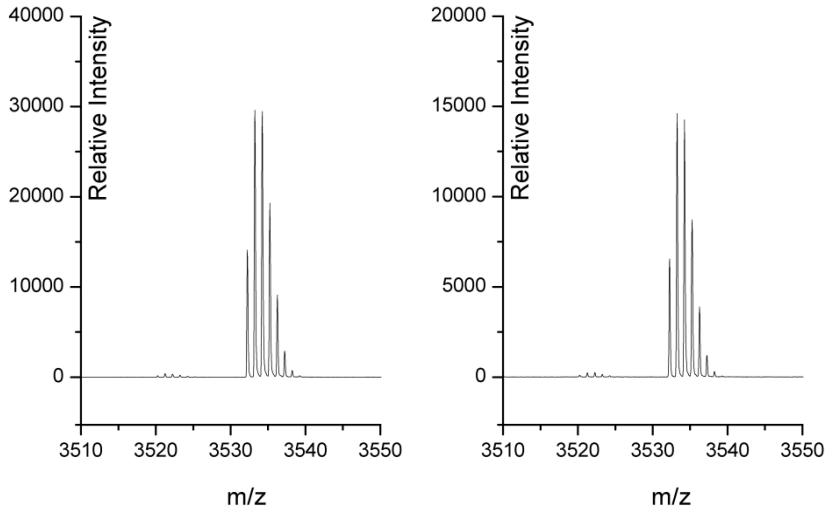


**Figure 4.4** MALDI-ToF MS in reflectron mode of a VDC/MAC copolymer and a VDC homopolymer initiated from benzyl alcohol. (Left): VDC/MAC copolymer; (Right): VDC homopolymer.

A representative $^{1}$H NMR spectrum of P(VDC-*co*-MAC) synthesised from a 50:50 monomer feed ratio is shown in Figure 4.5. While the alkene resonances of both monomers overlap, the remaining resonances show a clear separation which allowed for the easy calculation of monomer incorporation of the copolymer (50% for VDC and 50% for MAC). The respective incorporations were calculated using the PVDC $CH_2$ backbone resonance at $\delta$ = 4.45 ppm and the resonance resulting from the $CH_2$ adjacent to the pendant ester bond for PMAC at $\delta$ = 4.64 ppm. The $^{1}$H NMR spectrum reveals that at 90% monomer conversion, equal incorporation into the copolymer is achieved, however no further information about the structure of the polymer chains can be determined.

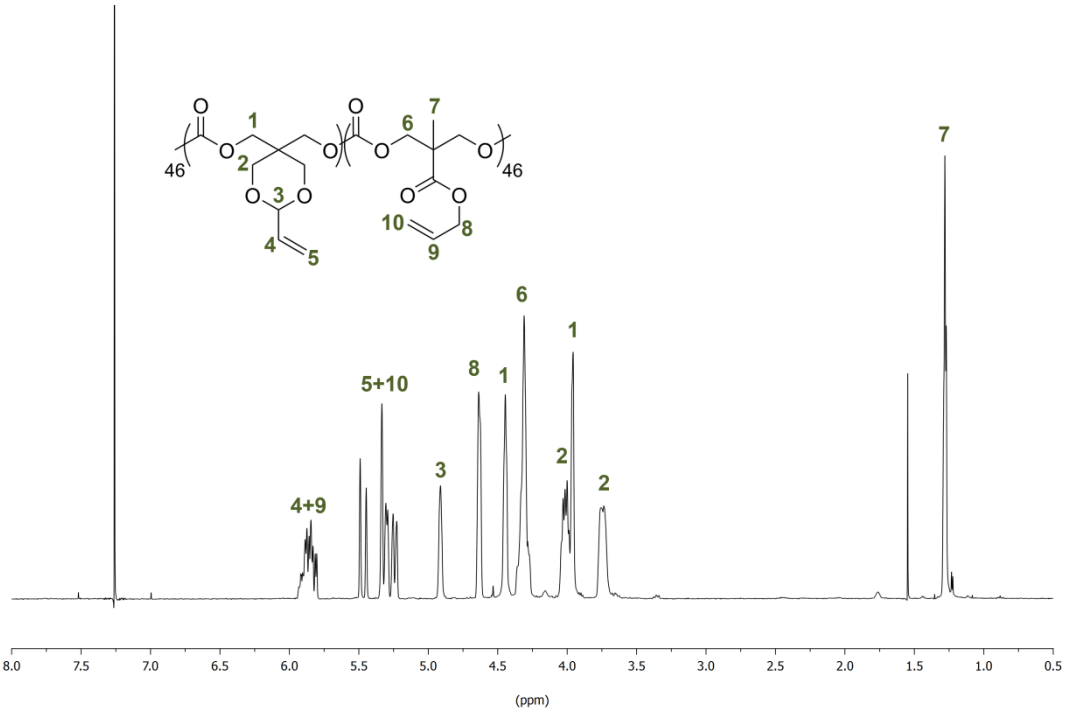


**Figure 4.5** $^{1}$H NMR spectrum ($CDCl_3$, 400 MHz) of the resulting copolymer synthesised from a 50:50 ratio of VDC and MAC.

### 4.2.2 Determinations of the Copolymer Structure

To further investigate the copolymers structure, a copolymerisation of VDC and MAC was monitored by $^{1}$H NMR spectroscopy. A polymerisation was performed with an equal feed of the two monomers utilising a reduced catalyst loading of 0.25 mol% DBU and 1.25 mol% TU (0.25 M) to allow for the copolymerisation to be followed from a low conversion. Plotting the individual monomer conversion versus time clearly shows similar incorporation of VDC and MAC into the resulting copolymer, suggesting that random copolymers are achieved with this system (figure 4.6). Further evidence of the random inclusion can be visualised in a plot of monomer incorporation in polymer versus overall conversion (Figure 4.7), where both monomers remain at approximately 50% incorporation throughout the copolymerisation.

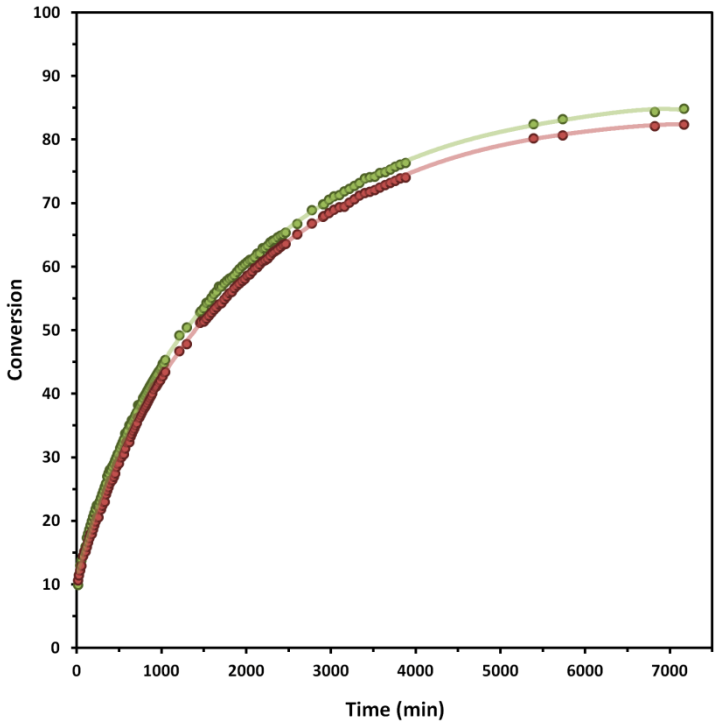


**Figure 4.6** Conversion *vs.* time graph resulting from the copolymerisation of VDC (green) and MAC (red) under reduced catalyst conditions (0.25 mol% DBU and 1.25 mol% TU).

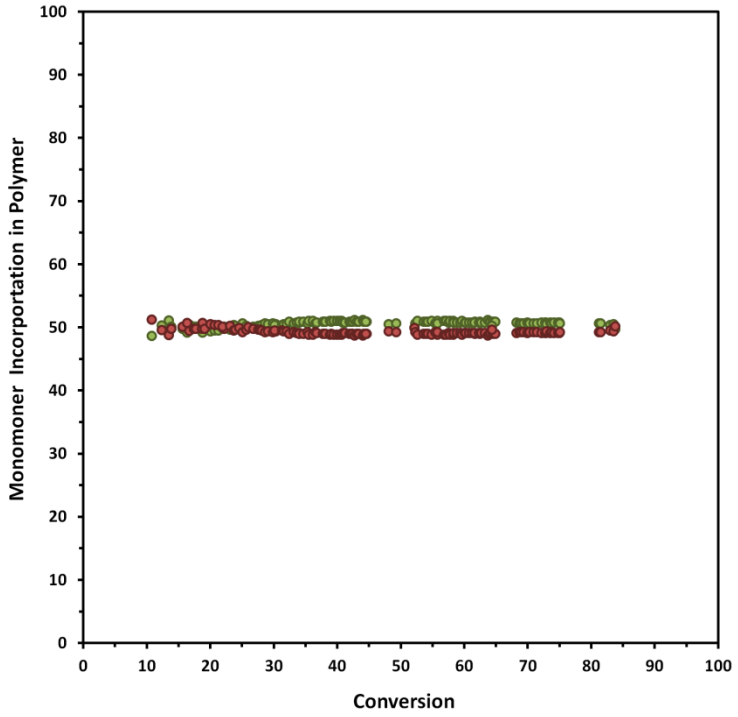


**Figure 4.7** Monomer incorporation in polymer *vs.* conversion graph for VDC/MAC copolymerisation (Green = VDC, Red = MAC).

Determination of the exact monomer feed ratio ($f_{VDC}$ and $f_{MAC}$) and monomer incorporation into the copolymer ($F_{VDC}$ and $F_{MAC}$) between 8-10% overall monomer conversion for a range of feed ratios (between 0.1 and 0.9) allowed for the reactivity ratios to be calculated. For each feed ratio the experiment was repeated in triplicate and the obtained values were averaged before calculation of the reactivity ratios using software designed by van Herk and co-workers.[6, 7] Reactivity ratios of 0.518 (± 0.071) for VDC ($r_{VDC}$) and 0.473 (± 0.059) for MAC ($r_{MAC}$) were calculated. Using the values for $f_{VDC}$ and $f_{MAC}$ calculated from $^{1}$H NMR spectroscopy along with the obtained reactivity ratios, a best fit curve can be plotted using the Mayo-Lewis equation:

$$F_{MAC} = 1 - F_{VDC} = \frac{r_{MAC}{f_{MAC}}^2 + f_{MAC}f_{VDC}}{r_{MAC}{f_{MAC}}^2 + 2f_{MAC}f_{VDC} + r_{VDC}{f_{VDC}}^2}$$

Plotting the averaged measured $F_{MAC}$ *vs.* $f_{MAC}$ values along with the best fit curve demonstrates that the experimental data matches closely with the reactivity ratios calculated by the software (Figure 4.8). The calculations undertaken assume that the rate of adding another monomer to the polymer chain only relies on the final chain end unit. The reactivity ratios obtained can therefore be related to the rate constants *via* the following formula:

$$r_{VDC} = \frac{\boldsymbol{k}_{VDC-VDC}}{k_{VDC-MAC}}$$

$$r_{MAC} = \frac{\boldsymbol{k}_{MAC-MAC}}{k_{MAC-VDC}}$$

As reactivity ratios of approximately 0.5 were determined for both monomers, it is therefore two times more likely that after the addition of a VDC or MAC monomer the next monomer will be the alternate monomer, resulting in statistical copolymers with an alternating tendency.

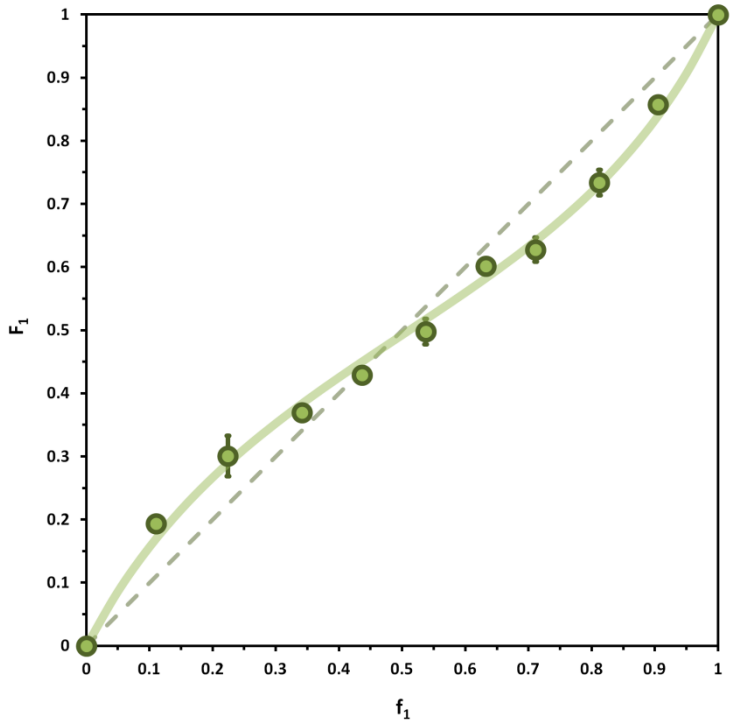


**Figure 4.8** $F_1$ vs. $f_1$ for VDC/MAC copolymerisation ($f_1$ = MAC, $f_2$ = VDC).

Further proof that a statistical copolymer was obtained was demonstrated by thermal analysis of the synthesised copolymers. For block like copolymers both glass transitions of the individual homopolymers should be present in the DSC thermogram, whereas in a statistical copolymer only one $T_g$ should be observed. In each case, copolymers synthesised using a range of monomer feeds were found to have a single $T_g$ by DSC analysis. The $T_g$ measured for P($VDC_{49}$-*co*-$MAC_{53}$) was not found to lie directly between that of the $T_g$ of PVDC and PMAC (73 °C and -11 °C respectively), but lower at 22.7 °C. The Fox equation[8-10] can be used to predict the $T_g$ of copolymers consisting of any ratio of two monomers as long as the $T_g$'s of the homopolymers are known and a statistical structure of the copolymer is obtained:

$$\frac{1}{T_g} = \frac{w_1}{T_{g,1}} + \frac{w_2}{T_{g,2}}$$

The Fox equation predicts a $T_g$ of 23.6 °C for P(VDC$_{49}$-*co*-MAC$_{53}$) which closely corresponds to the $T_g$ of 22.7 °C observed by DSC. In addition, $T_g$ values of other copolymers with varying ratios of VDC and MAC were found to match the $T_g$ values predicted by the Fox equation (Figure 4.9). Plotting $1/T_g$ versus weight percentage of MAC within the polymer chains yields a linear relationship, allowing for copolymers with targeted $T_g$ to be synthesised based on the monomer feed (Figure 4.10).

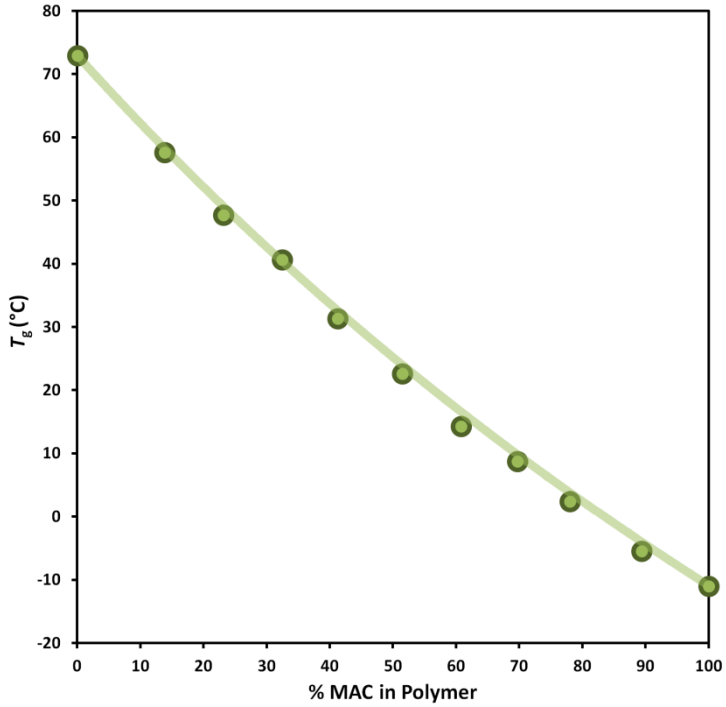


**Figure 4.9** $T_g$s of VDC/MAC copolymers vs. % MAC incorporated polymer graph. $T_g$s obtained by DSC analysis. Percentage of MAC incorporation calculated by $^1$H NMR spectroscopy. Predicted $T_g$s obtained by the Fox equation plotted as solid line.

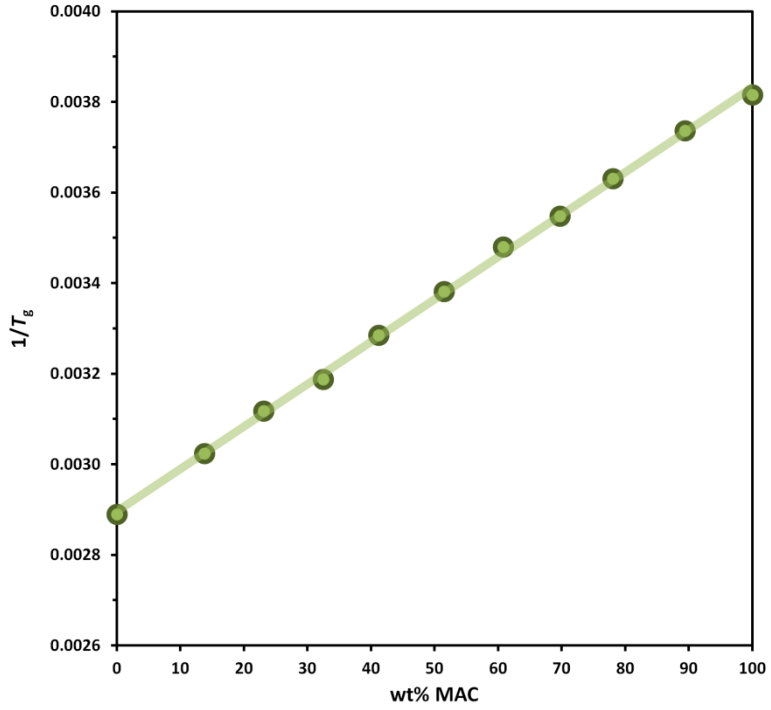


**Figure 4.10** $1/T_g$ of VDC/MAC copolymers vs. weight% MAC incorporated polymer. $T_g$s obtained by DSC analysis. Weight percentage of MAC incorporation calculated by $^1$H NMR spectroscopy.

**Table 4.1** P(VDC-*co*-MAC).

| Targeted VDC:MAC ratio | Copolymer VDC:MAC ratio[a] | DP (VDC:MAC)[a] | $M_n$ (g/mol)[b] | $Đ_M$[b] | $T_g$ (°C)[c] |
|---|---|---|---|---|---|
| 10:0 | 100:0 | 100:0 | 21,620 | 1.04 | 73.0 |
| 9:1 | 87:13 | 106:16 | 28,090 | 1.03 | 57.7 |
| 8:2 | 78:22 | 88:25 | 26,190 | 1.03 | 47.7 |
| 7:3 | 68:32 | 78:37 | 29,370 | 1.03 | 40.7 |
| 6:4 | 59:41 | 68:48 | 28,930 | 1.03 | 31.4 |
| 5:5 | 48:52 | 49:53 | 25,950 | 1.05 | 22.7 |
| 4:6 | 39:61 | 40:63 | 24,080 | 1.06 | 14.3 |
| 3:7 | 29:71 | 31:76 | 24,880 | 1.05 | 8.8 |
| 2:8 | 20:80 | 21:83 | 24,930 | 1.06 | 2.4 |
| 1:9 | 11:89 | 11:91 | 25,450 | 1.05 | -5.4 |
| 0:10 | 0:100 | 0:76 | 21,720 | 1.06 | -10.9 |

[a]Determined by $^1$H NMR spectroscopy. [b]Measured by chloroform GPC against polystyrene (PS) standards. [c]Measured by DSC.

Final confirmation of the statistical copolymer structure is provided by $^{13}$C NMR analysis of the synthesised copolymers. While the $^{13}$C NMR spectrum of the copolymers reveals the expected responses for both VDC and MAC repeat units, the three resonances between $\delta$ = 154.5 and 154.7 ppm yield important information about the copolymer structure. These resonances arise due to the different environments in which the carbonate carbonyls can exist in for VDC/MAC copolymers. Comparison with $^{13}$C NMR spectra for homopolymers of VDC and MAC show that the resonance at $\delta$ = 154.7 ppm corresponds to a carbonate carbonyl that exists between two VDC repeat units whereas the resonance at $\delta$ = 154.5 ppm corresponds to carbonate carbonyls with a MAC repeat unit either side. The third

resonance at $\delta$ = 154.6 ppm corresponds to a carbonate carbonyl with a VDC repeat unit on one side and a MAC repeat unit on the other. Further evidence for this was provided *via* the synthesis of a VDC-MAC block copolymer. Using PVDC (DP20, $M_n$ = 4470 Da, $Đ_M$ = 1.13) as a macroinitiator, ROP of MAC in $CDCl_3$ (0.5 M) was performed using DBU (1 mol%) and TU (5 mol%) as a binary catalyst system, targeting a DP of 20 and stopped upon reaching 90% monomer conversion. The increase in $M_n$ by GPC ($M_n$ = 6440 Da, $Đ_M$ = 1.10) along with the disappearance of the PVDC hydroxyl chain end response at $\delta$ = 4.53 ppm demonstrates the synthesis of a block copolymer. The same three resonances at $\delta$ = 154.7, 154.6 and 154.5 ppm were found for the $PVDC_{20}$-$PMAC_{16}$ block copolymer by $^{13}C$ NMR analysis. The resonance at $\delta$ = 154.6 ppm was only 1/20$^{th}$ the intensity of the PVDC resonance and 1/15$^{th}$ the intensity of the PMAC resonance, which is expected as only a single carbonate carbonyl positioned between a PVDC and PMAC unit exists in each polymer chain. Having demonstrated that the resonance at $\delta$ = 154.6 ppm results from this particular structure in the polymer chain, further information can be determined from the $^{13}C$ NMR spectrum of the copolymer (P($VDC_{49}$-*co*-$MAC_{53}$)) synthesised using an equal monomer feed. If it is assumed that both monomers have the same reactivity without any preference for the polymer chain end monomer unit, the expected intensity for each of the carbonate carbonyl resonances can be predicted. A ratio of 25:50:25 for the intensity of the VDC-VDC, MAC-VDC and MAC-MAC carbonate carbonyl resonances respectively. Only a slight divergence from this is measured experimentally (28:45:27) which suggests more of a random structure of the copolymer rather than a slightly alternating one, as the MAC-VDC signal would be higher if there was a tendency towards an alternating copolymer structure.

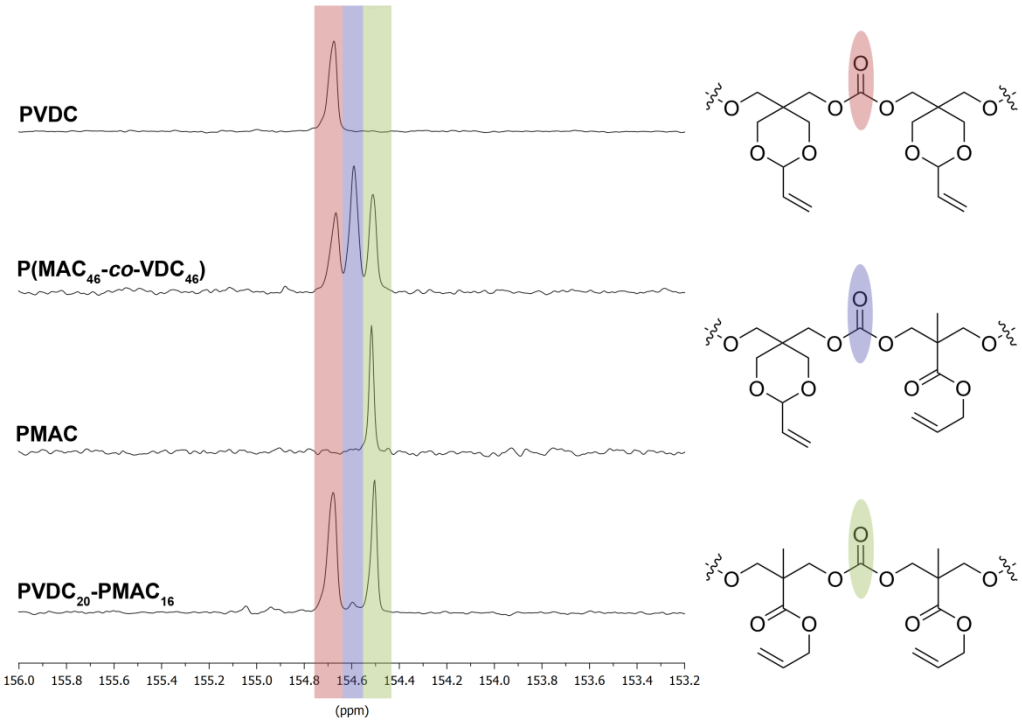


**Figure 4.11** $^{13}$C NMR spectra ($CDCl_3$) of PVDC, PMAC, P($MAC_{46}$-*co*-$VDC_{46}$) and $PVDC_{20}$-$PMAC_{16}$ focused on the carbonyl responses between 156.0 and 153.2 ppm.

A comparison of the $^{13}$C NMR spectra for copolymers synthesised using a range of monomer feeds shows a gradual change in the makeup of the polymer as the feed changes from 100% VDC to 100% MAC (Figure 4.12). Only a slight divergence from the predicted ratios is observed (assuming a random incorporation of each monomer), which could result from small differences in the actual monomer feed ratio compared to the targeted feed ratio. In each case the ratio of intensities match closely (maximum of 5% difference to predicted) and therefore firmly suggests that statistical copolymers with more random copolymer structures are synthesised, meaning a close reactivity of both monomers which is in contrast to the determined reactivity ratios.

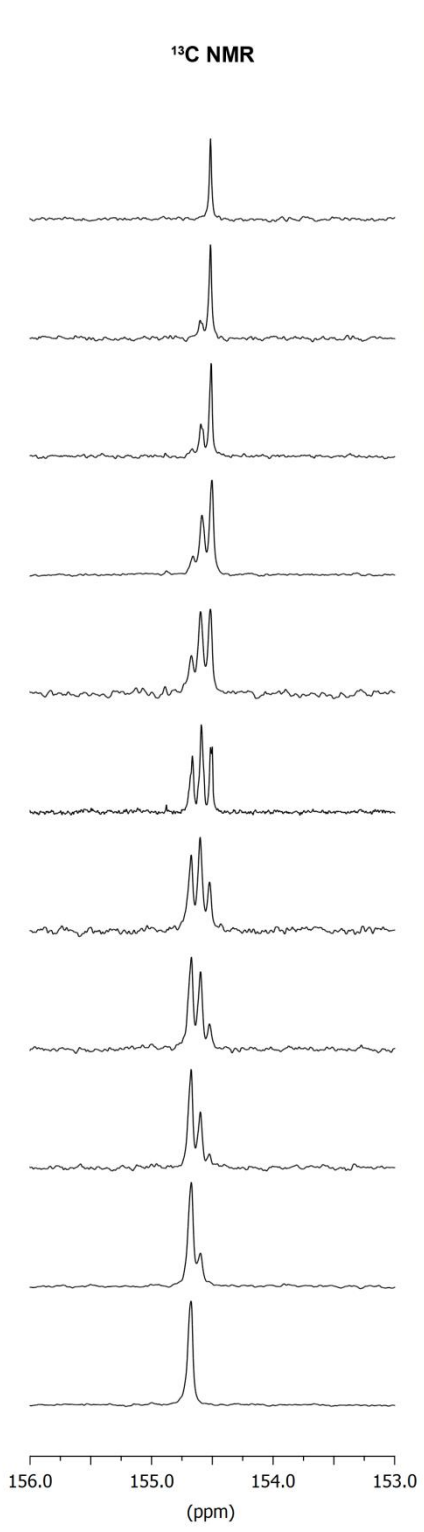


| $^{13}$C NMR | Monomer Feed Ratio VDC:MAC | Experimental Ratio (M-M):(V-M):(V-V) | Predicted Ratio (M-M):(V-M):(V-V) |
|---|---|---|---|
| | 0:100 | | |
| | 10:90 | 0:17:83 | 1:18:81 |
| | 20:80 | 5:29:66 | 4:32:64 |
| | 30:70 | 9:37:54 | 9:42:49 |
| | 40:60 | 17:43:40 | 16:48:36 |
| | 50:50 | 28:45:27 | 25:50:25 |
| | 60:40 | 37:43:19 | 36:48:16 |
| | 70:30 | 49:39:11 | 49:42:9 |
| | 80:20 | 63:32:5 | 64:32:4 |
| | 90:10 | 80:20:0 | 81:18:1 |
| | 100:0 | | |

**Figure 4.12** Comparison of experimental $^{13}$C NMR ($CDCl_3$) carbonate carbonyl resonances ratio of MAC/VDC copolymerisations to predicted ratio (assuming equal reactivity of both monomers).

### 4.2.3 Tuning Thermal Properties

The glass transition temperature of a VDC/MAC copolymer can be easily tuned by altering the ratio of each monomer, with the Fox equation having been shown to closely predict the resultant $T_g$ values of these copolymers. While this allows for the synthesis of alkene functional aliphatic polycarbonates with a $T_g$ anywhere between 73 and -11 °C, tailoring the $T_g$ of polycarbonates containing various added functionalities would provide access to a greater range of materials. As both monomers can be functionalised using the same thiol-ene reaction, the Fox equation can be utilised again to predict the $T_g$ of functionalised copolymers as long as the $T_g$ is known for the two functionalised homopolymers. The post-polymerisation functionalisation of PVDC has been previously demonstrated (Chapter Three) and the functionalisation of PMAC with a range of thiols has been reported in literature. However, to allow for a greater range of functionalities and a more accurate comparison, the synthesis and post-polymerisation functionalisation of PMAC were both undertaken using the same conditions as those reported in Chapter Three for PVDC.

To that end, PMAC was synthesised in $CDCl_3$ (0.5 M) using DBU (1 mol%) and TU (5 mol%) as the binary catalyst system, initiating from 1,4-butanediol ($[M]_0/[I]_0$ = 100). Precipitation into cold hexanes after 90% monomer conversion was reached. Analysis by chloroform GPC revealed a $M_n$ of 21,720 Da and a $Đ_M$ of 1.06 with a DP of 76 calculated by $^1$H NMR spectroscopy. Functionalistion of PMAC was achieved *via* the photoinitiated thiol-ene reaction as reported previously for PVDC (Chapter Three). As already determined for the thiol-ene functionalisation of PVDC, to achieve full conversion with 1-adamantylthiol, 2 mol% IRGACURE® 369 was required. GPC analysis of the functionalised polymers showed that in each

case a clear shift to lower retention time compared to the starting polymer GPC trace could be observed (Table 4.2). $^{1}$H NMR spectra for the 1-dodecanethiol, thioglycerol, mercaptoethanol and mercaptoacetic acid functionalised polymers matched those previously reported by Tempelaar *et al*. with the 1-adamantylthiol and 1-hexylthiol functionalised PMAC displaying resonances appropriate to their functional group.[11]

**Table 4.2** Post-polymerisation functionalisation of PMAC.

| Thiol added | Conversion (%) | $M_n$ (g/mol) | $Đ_M$ |
|---|---|---|---|
| - | - | 21,720[b] | 1.06[b] |
| 1-Adamantylthiol | >99 | 24,670[b] | 1.25[b] |
| 1-Dodecanethiol | >99 | 37,570[b] | 1.10[b] |
| 1-Hexylthiol | >99 | 30,410[b] | 1.08[b] |
| Thioglycerol | >99 | 38,780[c] | 1.13[c] |
| Mercaptoethanol | >99 | 34,840[c] | 1.10[c] |
| Mercaptoacetic acid | >99 | 33,470[c] | 1.11[c] |

[a]Determined by $^{1}$H NMR spectroscopy. [b]Measured by chloroform GPC against PS standards. [c]Measured by DMF GPC against PMMA standards.

Although only two functionalised homopolymers are required to predict the $T_g$ of a functionalised copolymer using the Fox equation, a VDC/MAC copolymer was functionalised with a range of thiols to confirm the correlation between experimental and theoretical values. The synthesis of P($VDC_{46}$-*co*-$MAC_{46}$) was achieved using the same conditions as for the synthesised PMAC homopolymer, with the post-polymerisation functionalisation undertaken using the same photoinitiator thiol-ene procedure. GPC analysis of the functionalised polymers

showed a clear shift to lower retention time compared to the starting copolymer GPC trace (Table 4.3).

**Table 4.3** Post-polymerisation functionalisation of P($VDC_{46}$-*co*-$MAC_{46}$).

| Thiol added | Conversion (%) | $M_n$ (g/mol) | $Đ_M$ |
|---|---|---|---|
| - | - | 22,320[b]/24,080[c] | 1.05[b]/1.05[c] |
| 1-Adamantyl thiol | >99 | 33,260[b] | 1.25[b] |
| 1-Dodecane thiol | >99 | 39,050[b] | 1.06[b] |
| 1-Hexylthiol | >99 | 31,630[b] | 1.06[b] |
| Thioglycerol | >99 | 39,030[c] | 1.14[c] |
| Mercaptoethanol | >99 | 35,410[c] | 1.09[c] |
| Mercaptoacetic acid | >99 | -[d] | -[d] |

[a]Determined by $^1$H NMR spectroscopy. [b]Measured by chloroform GPC against PS standards. [c]Measured by DMF GPC against (PMMA) standards. [d]No response observed by the refractive index detector of the DMF GPC even though the sample was completely soluble in the solvent system .

$^1$H NMR analysis of the functionalised copolymers revealed >99% monomer conversion for all samples. The conversion was determined by the disappearance of the alkene resonances between $\delta$ = 6.00 and 4.80 ppm and the appearance of resonances appropriate to the functional group of the thiol added. In case of the addition of 1-dodecanethiol, resonances corresponding to the added dodecyl chain can clearly be seen at $\delta$ = 2.50, 1.57, 1.36, 1.26 and 0.88 ppm, similar to the resonances observed for PVDC functionalised with 1-dodecanethiol (Figure 4.13). Resonances associated with the backbone peaks of the VDC and MAC repeat units exhibit a slight upfield shift after the thiol-ene functionalisation by a maximum of 0.05 ppm compared to the P($VDC_{46}$-*co*-$MAC_{46)}$ backbone resonances. Comparison

of the integral value of the methyl resonance resulting from the dodecyl group at $\delta$ = 0.88 ppm with integral values of the backbone resonances at $\delta$ = 4.14 ppm (VDC), $\delta$ = 4.29 and 4.24 ppm (MAC) further confirms that >99% of the repeat units are dodecane functionalised, demonstrating that undetectable amounts of crosslinking has occurred.

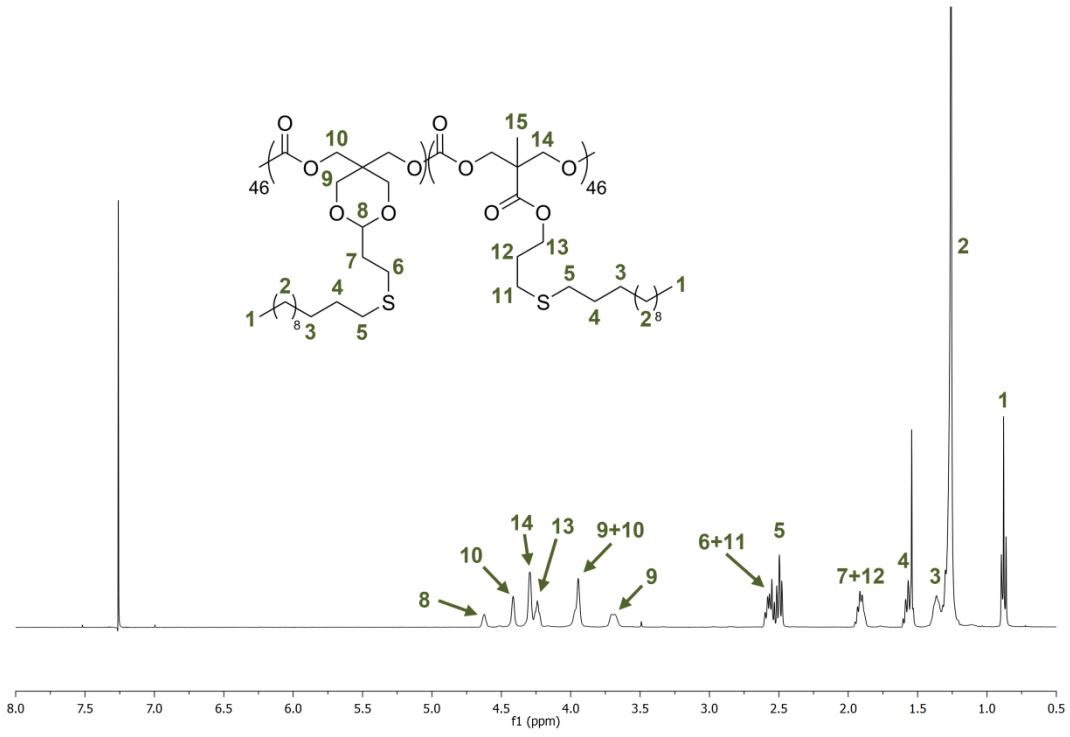


**Figure 4.13** $^{1}$H NMR spectrum ($CDCl_3$, 400 MHz) of dodecanethiol functionalised P($VDC_{46}$-*co*-$MAC_{46}$).

Thermal analysis was performed on a series of functionalised VDC and MAC homopolymers as well as functionalised P($VDC_{46}$-*co*-$MAC_{46}$) (Table 4.4). In each case, the $1/T_g$ vs. weight percentage of MAC plot resulted in a linear correlation between the three polymers, demonstrating that the $T_g$ of functionalised copolymers corresponds to the predicted values and therefore can be predicted based on the monomer incorporation into the copolymer (Figure 4.15).

**Table 4.4** Glass transition temperatures of functionalised PVDC, PMAC and P(VDC$_{46}$-*co*-MAC$_{46}$).[a]

| Thiol added | $T_g$ (°C) | | |
|---|---|---|---|
| | **PVDC** | **P(VDC-*co*-MAC)** | **PMAC** |
| - | 73.8 | 22.7 | -11 |
| 1-Adamantylthiol | 109.3 | 65.0 | 43.4 |
| 1-Dodecanethiol | 23.5 | -[b] | -[b] |
| 1-Hexylthiol | 7.7 | -21.9 | -47.0 |
| Thioglycerol | 40.6 | -24.4 | -3 |
| Mercaptoethanol | 43.4 | 18.9 | -15.0 |
| Mercaptoacetic acid | 48.3 | 25.1 | 3.0 |

[a]Measured by DSC. [b]$T_g$ obscured by melting point.

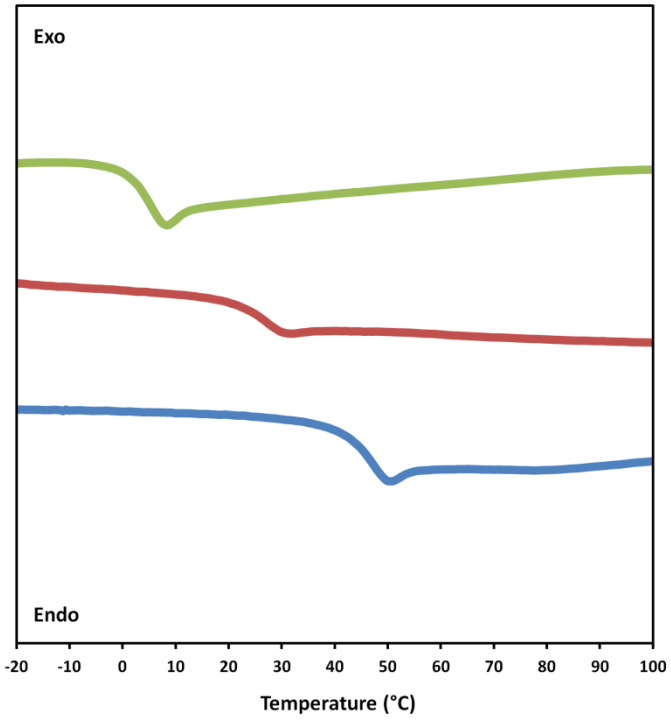


**Figure 4.14** DSC traces of mercaptoacetic acid functionalised PVDC (blue), P(VDC$_{46}$-*co*-MAC$_{46}$) (red) and PMAC (green) between -20 and 100 °C (taken from 4$^{th}$ heating cycle of each respective polymer).

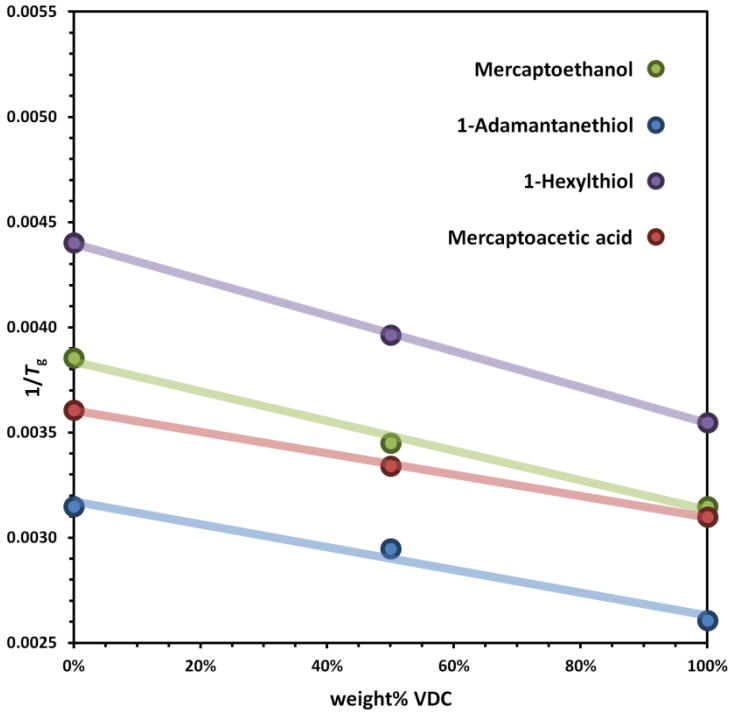


**Figure 4.15** $1/T_g$ vs. weight percentage of VDC incorporated into copolymer. Lines are of best fit between data points.

### 4.2.4 Targeting Thermal Properties

To verify that control over the $T_g$ is possible for polycarbonate copolymers after thiol functionalisation as well as before, copolymers were synthesised with the correct MAC/VDC ratio such that after post-polymerisation functionalisation a $T_g$ of 37 °C should be achieved. To achieve a $T_g$ of 37 °C for a mercaptoacetic acid functionalised VDC/MAC copolymer, a ratio of 23:77 MAC:VDC was required as predicted by the Fox equation using values for the respective functionalised homopolymers. To that end a copolymer initiated from 1,4-butanediol, with a final ratio of 24:76 of MAC and VDC respectively and an overall DP of 96 was utilised for post-polymerisation functionalisation with mercaptoacetic acid. Post-polymerisation functionalistion with mercaptoacetic acid was achieved using the

same thiol-ene conditions used previously (Chapter Three). $^{1}$H NMR analysis of the functionalised copolymer proves that >99% conversion was achieved as evident by the complete disappearance of resonances between $\delta$ = 6.00 and 5.00 ppm (Figure 4.15). Clear evidence of the incorporation of carboxylic acid functionality onto the copolymer is the acidic proton resonance at $\delta$ = 12.60 ppm. DMF GPC analysis reveals a $M_n$ of 32,000 Da and $Đ_M$ of 1.15 for the functionalised copolymer. More importantly DSC analysis of the functionalised copolymer yields a $T_g$ of exactly 37 °C.

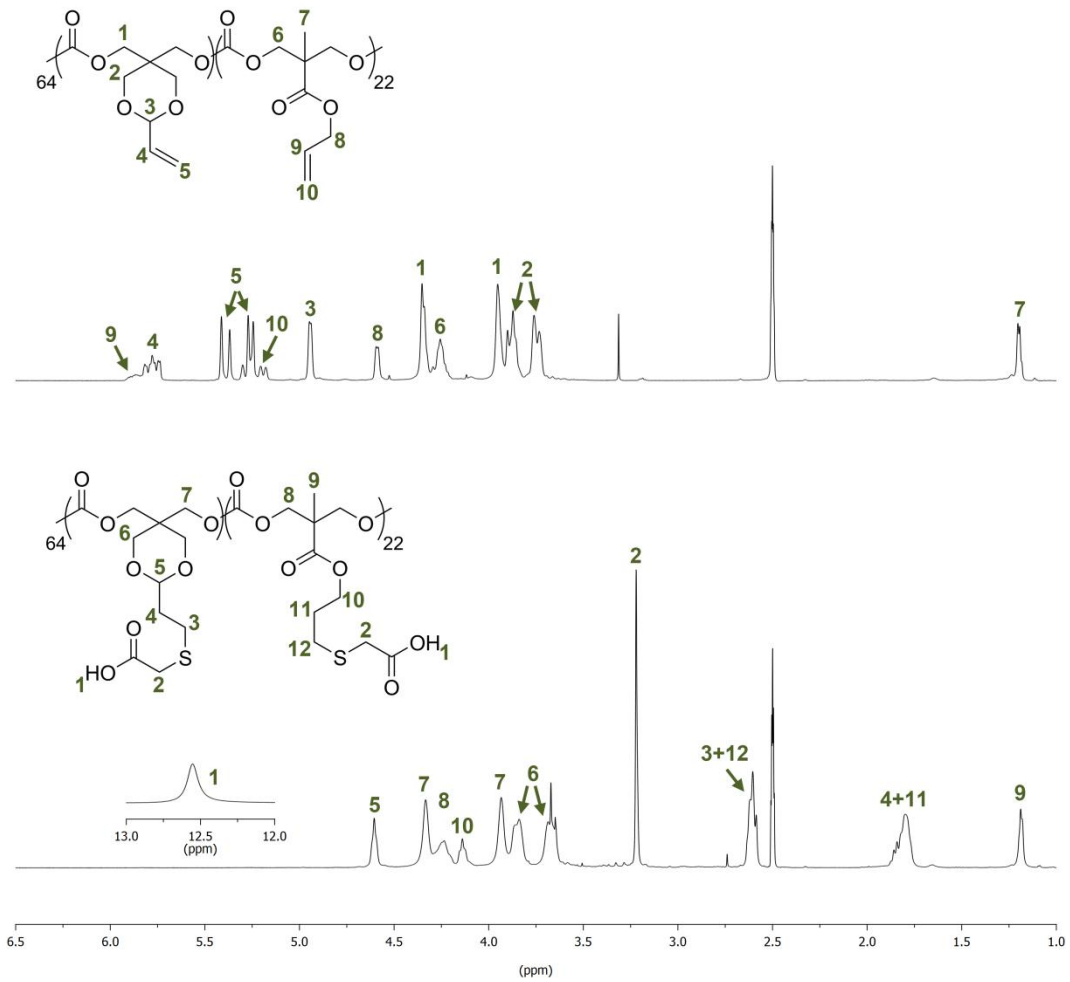


**Figure 4.16** $^{1}$H NMR spectra ($CDCl_3$, 400 MHz) of P($VDC_{64}$-*co*-$MAC_{22}$) and the same copolymer after functionalistion with mercaptoacetic acid.

The same procedure was repeated for a mercaptoethanol functionalised VDC/MAC copolymer, with a ratio of 14:86 (MAC:VDC) in the final copolymer required to achieve a $T_g$ of 37 °C as predicted by the Fox equation. The polymerisation of MAC and VDC using this ratio as the monomer feed was undertaken using the same polymerisation conditions as for the previous example resulting in a copolymer with an overall DP of 112 with a ratio of 16:84 of MAC and VDC and a $M_n$ of 21,750 Da with a $Đ_M$ of 1.08 (measured by DMF GPC). After post-polymerisation functionalisation with mercaptoethanol, $^1$H NMR analysis showed complete disappearance of the alkene resonances between $\delta$ = 6.0 and 5.0 ppm. Comparison of the integral intensity of the resonance at $\delta$ = 3.51 ppm ($SCH_2C\boldsymbol{H}_2OH$) to the copolymer backbone signals at $\delta$ = 1.19 ppm ($C\boldsymbol{H}_3$, PMAC) and $\delta$ = 4.03 – 3.77 ppm ($C\boldsymbol{H}_2$, PVDC) shows that every repeat unit was successfully functionalised with mercaptoethanol. Analysis by DMF GPC revealed an increase in molecular weight from 21,750 to 31,920 Da whilst maintaining a low dispersity ($Đ_M$ = 1.13). Furthermore, a glass transition temperature of 34 °C was measured by DSC.

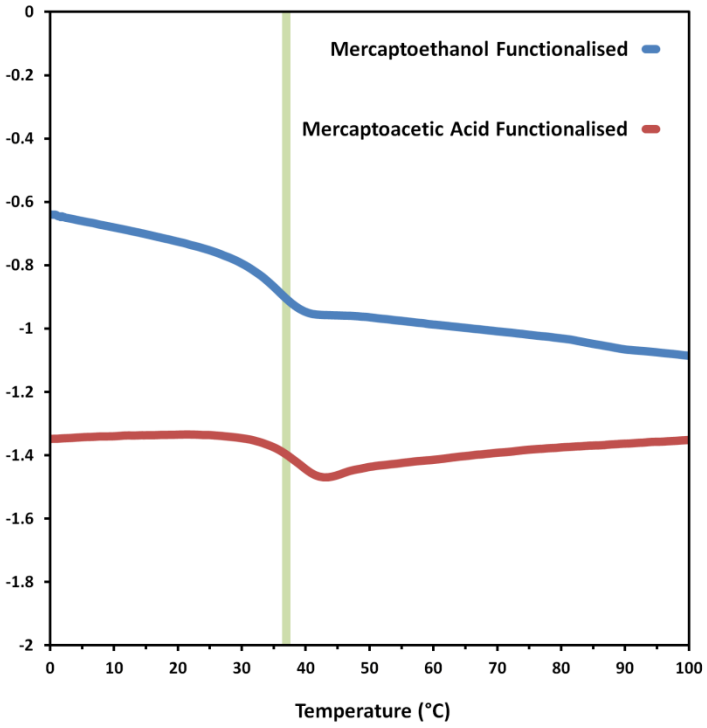


**Figure 4.17** DSC traces of mercpatoacetic acid and mercaptoethanol functionalised copolymers synthesised to target a glass transition temperature of 37 °C.

## 4.3 Conclusion

It has been clearly demonstrated that the copolymerisation of VDC and MAC using the binary catalyst system of DBU and TU results in the formation of a statistical copolymer structure by the calculation of reactivity ratios (*via* $^{1}$H NMR spectroscopy) and determination of the monomer distribution in the copolymer (*via* $^{13}$C NMR spectroscopy and DSC thermal analysis). While the calculation of the reactivity ratios suggests an alternating tendency in the copolymerisations ($r_{VDC}$ = 0.518 and $r_{MAC}$ = 0.473), investigation by $^{13}$C NMR spectroscopy of the final copolymers reveal a more random structure. Furthermore, $T_g$ values of VDC/MAC copolymers match closely to the values predicted by the Fox equation for statistical copolymers. Through the thiol-ene functionalisation of PMAC and P($VDC_{46}$-co-$MAC_{46}$) along with thermal data of the previously functionalised PVDC (Chapter Three), it was demonstrated that the functionalised copolymers also match $T_g$ values predicted by the Fox equation, with examples provided to show the successful synthesis of functionalised poly(carbonate)s with targeted glass transition temperatures.

## 4.4 References


1. S. Ramakrishna, J. Mayer, E. Wintermantel and K. W. Leong, *Compos. Sci. Technol.*, 2001, **61**, 1189-1224.
2. B. D. Ulery, L. S. Nair and C. T. Laurencin, *J. Polym. Sci. B Polym. Chem.*, 2011, **49**, 832-864.
3. A. S. Hoffman, *Adv. Drug Deliv. Rev.*, 2002, **54**, 3-12.
4. A.-C. Albertsson and I. K. Varma, *Biomacromolecules*, 2003, **4**, 1466-1486.
5. E. Vidović, D. Klee and H. Höcker, *J. Appl. Polym. Sci.*, 2013, **130**, 3682-3688.
6. A. M. van Herk, *J. Chem. Educ.*, 1995, **72**, 138.
7. B. G. Manders, W. Smulders, A. M. Aerdts and A. M. van Herk, *Macromolecules*, 1997, **30**, 322-323.
8. T. G. Fox and P. J. Flory, *J. Polym. Sci.*, 1954, **14**, 315-319.
9. J. Thomas G. Fox and P. J. Flory, *J. Appl. Phys.*, 1950, **21**, 581-591.
10. T. G. Fox, *Bull. Am. Phys. Soc.*, 1956, **1**, 123.
11. S. Tempelaar, L. Mespouille, P. Dubois and A. P. Dove, *Macromolecules*, 2011, **44**, 2084-2091.

# Chapter Five

## Conclusion

THE UNIVERSITY OF
WARWICK

## 5.1 Conclusion

The work discussed in this thesis demonstrates the synthesis of well defined biodegradable polymers with desirable properties through catalyst and/or monomer design. Initially this was demonstrated through the synthesis and subsequent application of a (-)-sparteine analogue, benzyl bispidine, for ring opening polymerisation in conjunction with hydrogen bond donor co-catalysts (such as 1-(3,5-bis(trifluoromethyl)phenyl)-3-cyclohexylthiourea (TU)). In particular, a thorough investigation into the benzyl bispidine/TU binary catalyst system revealed only a small reduction in ROP rate compared to that of (-)-sparteine/TU. $^{13}$C NMR spectroscopy, homonuclear decoupled $^{1}$H NMR spectroscopy and differential scanning calorimetry (DSC) analysis revealed little difference between the two binary systems. Undertaking ROP of *rac*-lactide by benzyl bispidine/TU yielded a probability of isotactic enchainment ($P_m$) of 0.74 which is identical to that observed for (-)-sparteine/TU. Benzyl bispidine/TU was shown to produce isotactic PLLA from *L*-LA with very few stereoerrors making it an efficient replacement for the now commercially unavailable (-)-sparteine. Additionally, a number of alternative hydrogen bond donor co-catalysts were investigated in conjunction with benzyl bispidine for the ROP of *L*-LA, but were not found to result in faster polymerisation rates compared to TU. The benzyl bispidine/TU system further proved a successful catalyst system for the ROP of cyclic carbonates.

The synthesis of well defined biodegradable polymers with desirable properties was further extended to the preparation of functional poly(carbonate)s, with post-polymerisation functionalisation providing access to functionalities not compatible with ROP. Literature studies have focused on the *bis*-MPA scaffold,

which results in poly(carbonate)s with relatively low glass transition temperatures, making them unsuitable for some applications. In this work the sterically bulky vinyl functional cyclic carbonate 9-vinyl-2,4,8,10-tetraoxaspiro[5.5]undecan-3-one (VDC) was synthesised and used to yield vinyl functional poly(carbonate)s with improved thermal properties. The binary catalyst system of 1,8-diazabicyclo[5.4.0]undec-7-ene (DBU)/TU was shown to efficiently polymerise VDC in a living manner, resulting in polymers with well defined properties. Functionalisation of PVDC (DP20) with a range of thiols using a UV active thiol-ene procedure resulted in full functionalisation with the polymers showing no sign of crosslinking. Unfortunately when the process was repeated for DP100 PVDC, the resultant GPC traces revealed small high molecular weight shoulders suggesting a low amount of crosslinking, even though no evidence of crosslinking was found by $^{1}$H NMR analysis. Functionalised PVDC samples analysed by differential scanning calorimetry (DSC) were found to exhibit increased thermal properties to that of the corresponding functionalised poly(allyl 5-methyl-2-oxo-1,3-dioxane-5-carboxylate) (PMAC).

To be able to achieve greater control over the glass transition temperature of functional poly(carbonate)s, copolymerisations of VDC and MAC were performed along with their subsequent thiol-ene functionalisations. Firstly, copolymers catalysed by DBU/TU were found to have a statistical structure which was determined *via* the calculation of the reactivity ratios and an in depth $^{13}$C NMR spectroscopy study. Although the reactivity ratios suggest a slight alternating tendency between the two monomers, $^{13}$C NMR analysis revealed a more random microstructure of the copolymers. The copolymers were shown to follow the Fox equation, allowing copolymers with a range of $T_g$s to be easily produced. Functionalisation of PMAC and PMAC$_{46}$-*co*-PVDC$_{46}$ with a range of thiols resulted

in full conversion, with the (co)polymers found to still follow the Fox equation. To demonstrate the ability to synthesise functional copolymers with a specific $T_g$, two separate copolymers were synthesised that after functionalistion with mercaptoacetic acid or mercaptoethanol would result in a $T_g$ of 37 °C. DSC analysis of the resulting functionalised copolymers resulted in $T_g$s close too or matching the targeted value.

In short, the work undertaken in this thesis provides the ability to synthesise polymers with desirable polymers, either through the development of a new organic catalyst that can produce highly isotactic PLLA or through the design and synthesis of a sterically bulky cyclic carbonate that can undergo ROP to yield functional poly(carbonate)s after post-polymerisation functionalisation with increased thermal properties.

# Chapter Six

Experimental

THE UNIVERSITY OF
WARWICK

## 6.1 Materials

Solvents were purchased from either Fisher or Sigma-Aldrich. Tetrahydrofuran and dichloromethane were purified over Innovative Technology SPS alumina solvent columns, degassed and stored under an inert atmosphere. Chemicals were purchased from Sigma-Aldrich or Alfa and used as received unless otherwise noted. $CDCl_3$ was dried over 4Å molecular sieves, collected *via* vacuum transfer and then stored under an inert atmosphere. (-)-Sparteine was dried over calcium hydride and then distilled under an inert atmosphere. Benzyl bispidine was dried over calcium hydride in THF, filtered under inert conditions and the solvent then removed under high vacuum. All hydrogen bond donor co-catalysts were prepared as reported in literature and either dried over 4Å molecular sieves in $CH_2Cl_2$, calcium hydride in THF or distilled over calcium hydride.[1-4] Lactide, kindly donated by PURAC, was purified using the following procedure: *L*- or *D*-Lactide was dissolved in $CH_2Cl_2$, passed through a silica plug and dried over magnesium sulphate, after which the solvent was removed. The lactide was dissolved in hot toluene which was removed before being transferred into a Schlenk flask under inert conditions. This procedure was repeated using dry toluene before further drying over 3Å molecular sieves in $CH_2Cl_2$ (×2). *rac*-Lactide was formulated by dissolving equal amounts of dried *L*-lactide and *D*-lactide in $CH_2Cl_2$ and removing the solvent.

## 6.2 General Experimental

All reactions with air and/or sensitive compounds were carried out under a dry nitrogen atmosphere using standard Schlenk line techniques or undertaken in a glovebox. $^{1}$H NMR and $^{13}$C NMR spectra were recorded using a Bruker AC-250, DPX-300, DPX-400, AV-400 "Ozric" DRX-500, AV III-600 or AV II-700 spectrometer at 293 K unless otherwise stated. Chemical shifts are reported as $\delta$ in parts per million (ppm) and referenced against reported chemical shifts of residual solvent resonances ($CHCl_3$: $^{1}$H $\delta$ = 7.26 ppm; $^{13}$C $\delta$ = 77.16 ppm). Gel permeation chromatography (GPC) analysis was used to determine the molecular weights and polydispersities of synthesised polymers using one of three systems. GPC in DMF was performed on an Agilent 1260 Infinity Multi-Detector GPC System fitted with differential refractive index (DRI) and ultraviolet detectors (UV) equipped with a guard column (PLgel 5 mm, 50 × 7.5 mm) and two mixed-C columns (PLgel 5 mm, 300 x 7.5 mm) and autosampler. A mobile phase of DMF with 1.06 g/litre of LiCl was used with the eluent flow rate set at 1.0 mL/min. Data generated by the GPC system was analysed using Cirrus v3.3 with calibration curves produced using Varian Polymer laboratories Easi-Vials linear poly(methyl methacrylate) standards (200–4.7 × $10^5$ g/mol). GPC in THF was performed on an Agilent 1260 Infinity Multi-Detector GPC System fitted with differential refractive index (DRI), light scattering (LS) and ultraviolet detectors (UV) equipped with a guard column (PLgel 5 mm, 50 × 7.5 mm) and two mixed-C columns (PLgel 5 mm, 300 × 7.5 mm) and autosampler. A mobile phase of THF with 5% triethylamine was used with the eluent flow rate set at 1.0 mL/min. Data generated by the GPC system was analysed using Cirrus v3.3 with calibration curves produced using Varian Polymer laboratories Easi-Vials linear poly(styrene) standards (162–3.7 × $10^5$ g/mol). GPC in

chloroform was performed on an Agilent 1260 Infinity Multi-Detector GPC System fitted with differential refractive index (DRI) equipped with a guard column (PLgel 5 mm, 50 × 7.5 mm) and two mixed-D columns (PLgel 5 mm, 300 × 7.5 mm) and autosampler. A mobile phase of chloroform was used with the eluent flow rate set at 1.0 mL/min. Data generated by the GPC system was analysed using Cirrus v3.3 with calibration curves produced using Varian Polymer laboratories Easi-Vials linear poly(styrene) standards (162–3.7 × $10^5$ g/mol). Differential scanning calorimetry (DSC) analyses run on a DSC1-STAR from Mettler Toledo in a T zero aluminium pan under a flow of nitrogen. MALDI-ToF (matrix-assisted laser desorption and ionisation time-of-flight) spectra were obtained using a Bruker Daltonics Ultraflex II MALDI-ToF mass spectrometer equipped with a nitrogen laser delivering 3 ns laser pulses at 337 nm. Solutions of trans-2-[3-(4-tertbutylphenyl)-2-methyl-2-propylidene]malonitrile (DCTB) as matrix, NaTFA as cationization agent and polymer were prepared by making $CH_2Cl_2$ solutions at a concentration of 10 g/litre. Aliquots (10 μl) of matrix, polymer and NaTFA solutions were applied sequentially to the target plate followed by solvent evaporation to prepare a thin matrix/analyte film. The samples were measured in linear ion mode unless otherwise stated and calibrated against poly(ethylene oxide) monomethyl ether standards (2 × $10^3$ and 5 × $10^3$ g/mol).

## 6.3 Experimental for Chapter Two

### 6.3.1 Synthesis of propane-1,1,3,3-tetracarboxylic acid tetramethylester:

Dimethylmalonate (80 g, 0.6055 mol, 4 eq.) and paraformaldehyde (4.6 g, 0.1514 mol, 1 eq.) were heated to 60 °C before potassium hydroxide (10% in ethanol) was added dropwise (1.5 g of the KOH solution), resulting in the mixture becoming clear. The temperature was increased to 95 °C and the solution stirred for 16 h. The excess dimethylmalonate was removed under vacuum before the product was dissolved in dichloromethane and filtered to yield a clear oil that crystallised on standing, (40 g, 0.145 mol, 96%). Characterizing data was consistent with those reported previously.[5]

$^{1}$H NMR (400 MHz, $CDCl_3$): $\delta$ = 3.69 (s, 12 H, C***H***$_3$), 3.46 (t, $^{3}J_{H\text{-}H}$ = 7.4 Hz, 2 H, C***H***), 2.42 (t, $^{3}J_{H\text{-}H}$ = 7.4 Hz, 2 H, C***H***$_2$); $^{13}$C NMR (100 MHz, $CDCl_3$): $\delta$ = 168.9 (***C***=O), 52.8 (***C***$H_3$), 49.0 (***C***H), 27.4 (CH***C***$H_2$CH).

### 6.3.2 Sythesis of 1,5-dihydroxy-2,4-di(hydroxymethyl)pentane:

$LiAlH_4$ (10.88 g, 0.2570 mol, 2 eq.) was suspended in dry THF (650 mL). The mixture was cooled to 0 °C before a solution of propane-1,1,3,3-tetracarboxylic acid tetramethylester (35.5 g, 0.1285 mol, 1 eq.) in THF (100 mL) was added dropwise over several hours and then refluxed for 16 hours. The solid was collected by filtration and the product extracted with soxhlet apparatus with THF as the solvent. The THF was removed under reduced pressure to yield white crystals, (8.52 g, 0.133 mol, 40%). Characterizing data was consistent with those reported previously.[5]

Mp: 130-132 °C (Lit: 130°C); $^{1}$H NMR (400 MHz, $CD_3OD$): $\delta$ = 3.59 (d, $^{3}J_{H\text{-}H}$ = 5.6 Hz, 8 H, C***H***$_2$O), 1.76 (m, 2 H, C***H***), 1.30 (t, $^{3}J_{H\text{-}H}$ = 6.9 Hz, 2 H, C***H***$_2$); $^{13}$C NMR (100 MHz, $CD_3OD$): $\delta$ = 64.0 (***C***$H_2$OH), 41.8 (***C***H), 27.4 (CH***C***$H_2$CH).

### 6.3.3 Synthesis of 1,5-dibromo-2,4-bis(bromomethyl)pentane:

1,5-Dihydroxy-2,4-di(hydroxymethyl)pentane (4.2 g, 0.0256 mol, 3 eq.) was heated to 80 °C with stirring before $PBr_3$ (4.8 mL, 0.0512 mol, 6 eq.) was slowly added dropwise. Fumes of HBr produced by the reaction were neutralized through a base scrubber prior to emission. After complete addition, the temperature was increased to 100 °C and left stirring for 16 hours. Careful addition of $H_2O$ was undertaken in small quantities to neutralise any remaining $PBr_3$ before the product was extracted with $CH_2Cl_2$ and passed through a silica plug. Removal of the solvent under reduced pressure yielded white crystals, (6.45 g, 0.016 mol, 61%).

Mp: 45-48 °C; $^{1}$H NMR (400 MHz, $CDCl_3$): $\delta$ = 3.6 (dd, $^{2}J_{H\text{-}H}$ = 10.5, $^{3}J_{H\text{-}H}$ = 4.0 Hz, 4 H, C***H***$_2$Br), 3.46 (dd, $^{2}J_{H\text{-}H}$ = 10.5, $^{3}J_{H\text{-}H}$ = 6.2 Hz, 4 H, C***H***$_2$Br), 2.08 (m, 2 H, C***H***), 1.64 (t, $^{3}J_{H\text{-}H}$ = 7.0 Hz, 2 H, C***H***$_2$); $^{13}$C NMR (101 MHz, $CDCl_3$): $\delta$ = 38.9 (C***H***), 35.62 (C***H***$_2$Br), 33.61 (C***H***$_2$); Elemental Analysis: % calcd (% found) for $C_7H_{12}Br_4$: C 20.2 (20.3), H 2.9 (2.8).

### 6.3.4 Synthesis of benzyl bispidine:

Under a nitrogen atmosphere, 1,5-dibromo-2,4-bis(bromomethyl)pentane (4.81 g, 0.01157 mol, 1 eq.) was transferred into an ampoule and dissolved in dry toluene (30 mL). Benzylamine (6 eq.) was added to the ampoule before it was sealed. The

solution was refluxed for three days resulting in the formation of a white solid. The mixture was washed with NaOH 15% in water (60 mL) and the aqueous phase re-extracted with toluene (2 × 50 mL). The organic phases were combined, and the solvent removed under reduced pressure to yield an oil. The crude product was purified by first passing through a silica plug using $CH_2Cl_2$:MeOH (90:10) to remove the impurities and then $CH_2Cl_2$:MeOH:$NEt_3$ (80:10:10) to obtain the product as a pure oil, (1.1 g, 0.004 mol, 31%). Spectroscopic data was found to be the same as previous literature reports for this compound.[6]

$^1$H NMR (400 MHz, $CDCl_3$) $\delta$ = 7.44 (d, $^3J_{H\text{-}H}$ = 7.4 Hz, 4H, C***H***$_{ortho}$), 7.31 (t, $^3J_{H\text{-}H}$ = 7.5 Hz, 4H, C***H***$_{meta}$), 7.23 (t, $^3J_{H\text{-}H}$ = 7.2 Hz, 2H, C***H***$_{para}$), 3.47 (s, 4H, PhC***H***$_2$), 2.80 (d, $^3J_{H\text{-}H}$ = 10.7 Hz, 4H, NC***H***$_{2(eq)}$CH), 2.33 (dd, $^2J_{H\text{-}H}$ = 10.8, $^3J_{H\text{-}H}$ = 4.0 Hz, 4H, NC***H***$_{2(ax)}$CH), 1.89 (m, 2H, C***H***), 1.55 (m, 2H, CHC***H***$_2$CH); $^{13}$C NMR (101 MHz, $CDCl_3$) $\delta$ = 139.95 (***C***), 128.97 (***C***H$_{meta}$), 128.16 (***C***H$_{ortho}$), 126.63 (***C***H$_{para}$), 63.49 (Ph***C***H$_2$), 58.06 (N***C***H$_2$CH), 31.10 (CH***C***H$_2$CH), 29.99 (***C***H***)***.

### 6.3.5 General lactide polymerisation procedure:

In a typical experiment, an alcohol initiator was weighed out in a vial, dissolved in chloroform and added to a vial containing the co-catalyst (for example 1-(3,5-bis(trifluoromethyl)phenyl)-3-cyclohexylthiourea (TU)) (10 mol% to monomer). Upon its dissolution, the ROH/co-catalyst solution was added to a vial containing *L*- or *rac*-lactide. In another vial the tertiary amine catalyst (benzyl bispidine, (-)-sparteine or $Me_6$TREN) (5 mol% to monomer) was weighed out and the lactide/ROH/co-catalyst solution added to it. The polymerisation was monitored by

$^{1}$H NMR spectroscopy and upon reaching 90% monomer conversion was precipitated into hexanes.

## 6.4 Experimental for Chapter Three

### 6.4.1 Synthesis of (2-vinyl-1,3-dioxane-5,5-diyl)dimethanol:

To a 500 mL flask was added pentaerythritol (50 g, 0.367 mol, 1 eq) and DMF (250 mL). The reaction mixture was heated at 120 °C until complete dissolution of pentaerythritol then cooled to 100 °C, before PTSA (2.5 g, 0.013 mol) was added followed by the slow addition of acrolein (25 mL, 0.367mol, 1 eq). The reaction was heated at 100 °C for three hours. After this time the reaction solution was allowed to cool and the DMF removed *in vacuo*. The crude mixture was dissolved in $CH_2Cl_2$ and unreacted starting material removed by filtration. Removal of the remaining solvent under vacuum yielded a yellow oil that was purified by passing through a plug of silica using $CH_2Cl_2$ as eluent, which was changed to diethyl ether after impurities were removed to obtain the desired product. Recrystallisation in toluene yielded white crystals (28.9 g, 0.166 mol, 45%).

Mp = 78-79 °C; $^1$H-NMR (*d*-DMSO, 400MHz) $\delta$ = 5.77 (ddd, $^3J_{H\text{-}H}$ = 17.4, 10.7, 4.5 Hz, 1H, $CH_2CH$), 5.36 (d, $^3J_{H\text{-}H}$ = 17.4 Hz, 1H, $CH_2CH$), 5.22 (d, $^3J_{H\text{-}H}$ = 10.7 Hz, 1H, $CH_2CH$), 4.83 (d, $^3J_{H\text{-}H}$ = 4.5 Hz, 1H, $CH_2CHCH$), 4.56 (t, $^3J_{H\text{-}H}$ = 5.3 Hz, 1H, OH), 4.47 (t, $^3J_{H\text{-}H}$ = 5.2 HZ, 1H, OH), 3.79 (d, $^2J_{H\text{-}H}$ = 11.5 Hz, 2H,$OCH_2C$ ), 3.62 (d, $^2J_{H\text{-}H}$ = 11.5 Hz, 2H, ,$OCH_2C$), 3.56 (d, $^3J_{H\text{-}H}$ = 5.4 Hz, 2H, $HOCH_2C$), 3.18 (d, $^3J_{H\text{-}H}$ = 5.2 Hz, 2H, $HOCH_2C$). $^{13}$C-NMR (*d*-DMSO, 101 MHz) $\delta$ = 135.35 ($CH_2CH$), 118.05 ($CH_2CH$), 99.90 ($CH_2CHCH$), 68.58 ($OCH_2C$), 61.05 ($HOCH_2C$), 59.47 (C); Elemental Analysis: % calcd (% found) for $C_8H_{14}O_4$: C 55.16 (55.26), H 8.10 (8.10); Mass Spec: Theoretical (Found) for $C_8H_{14}O_4Na$: 197.0784 (197.0782) m/z.

### 6.4.2 Synthesis of 9-vinyl-2,4,8,10-tetraoxaspiro[5.5]undecan-3-one (VDC):

To a 1 litre flask was added (2-vinyl-1,3-dioxane-5,5-diyl)dimethanol (20 g, 0.115 mol, 1 eq), ethyl chloroformate (31 g, 0.288 mol, 2.5 eq) and THF (600 mL). The stirred solution was cooled in an ice bath and then $NEt_3$ (29 g, 0.288 mol, 2.5 eq) in THF (100 mL) was added dropwise. After complete addition the ice bath was removed and the mixture stirred for a further three hours. The white precipitate was separated by filtration and the solvent removed on a rotary evaporator to yield an off-white solid. This solid was redissolved in $CH_2Cl_2$ and washed twice with water before drying with magnesium sulphate. The solvent was removed by vacuum and the crude product recrystallised in $CH_2Cl_2$/hexane to yield a white solid (17.0 g, 0.085 mol, 74%).

Mp = 118-119 °C; $^1$H-NMR ($CDCl_3$, 400 MHz) $\delta$ = 5.78 (ddd, $^3J_{H\text{-}H}$ = 17.4, 10.7, 4.5 Hz, 1H, $CH_2CH$), 5.43 (d, $^3J_{H\text{-}H}$ = 17.4 Hz, 1H , $CH_2CH$), 5.30 (d, $^3J_{H\text{-}H}$ = 10.7 Hz, 1H, $CH_2CH$), 4.88 (d, $^3J_{H\text{-}H}$ = 4.5 Hz, 1H, $CH_2CHCH$), 4.55 (s, 2H, $CH_2OC{=}O$), 4.02 (d, $^2J_{H\text{-}H}$ = 12.0 Hz, 2H, $CHOCH_2$), 3.96 (s, 2H, $CH_2OC{=}O$), 3.65 (d, $^2J_{H\text{-}H}$ = 12.0 Hz, 2H, $CHOCH_2$); $^{13}$C-NMR ($CDCl_3$, 101 MHz) $\delta$ = 148.01 (C=O), 133.42 ($CH_2CH$), 119.64 ($CH_2CH$), 101.35 ($CH_2CHCH$), 71.33 ($CH_2OC{=}O$), 70.33 ($CH_2OC{=}O$), 68.82 ($CHOCH_2$), 31.47 (***C***); Elemental Analysis: % calcd (% found) for $C_9H_{12}O_5$: C 54.00 (53.83), H 6.04 (6.02); Mass Spec: Theoretical (Found) for $C_9H_{12}O_5Na$: 223.0577 (223.0573) m/z.

### 6.4.3 General VDC polymerisation procedure:

In a typical experiment, an alcohol initiator was added to a solution of 1-(3,5-bis(trifluoromethyl)phenyl)-3-cyclohexylthiourea (5 mol% to monomer) and DBU (1 mol% to monomer) in chloroform. The resulting solution was then transferred into a separate vial containing a solution of VDC (final monomer concentration of 0.5 M). The polymerisation was followed by $^{1}$H NMR spectroscopy and then stopped after reaching 90% monomer conversion. The crude polymerisation solution was passed through a small column of silica using $CH_2Cl_2$ as eluent, followed by diethyl ether and then finally ethyl acetate. The ethyl acetate fraction was precipitated into hexanes to obtain pure PVDC.

Example: Initiated from benzyl alcohol ([M]/[I] = 20)

$^{1}$H NMR (400 MHz, $CDCl_3$) $\delta$ = 7.43 – 7.31 (m, C***H***$_{aromatic}$), 5.85 (ddd, $CH_2C$***H***CH), 5.47 (d, C***H***$_2$CHCH), 5.32 (d, C***H***$_2$CHCH), 5.16 (s, $(C_6H_5)C$***H***$_2$)), 4.92 (s, C***H***$CHCH_2$), 4.53 (s, C***H***$_2$OH), 4.46 (s, (C=O)OC***H***$_2$), 4.03 (d, CHOC***H***$_2$), 3.96 (s, (C=O)OC***H***$_2$), 3.81 – 3.67 (m, CHOC***H***$_2$); $^{13}$C NMR (101 MHz, $CDCl_3$) $\delta$ = 154.68 (C=O), 134.07 ($CH_2$***C***H), 128.78 - 128.63 (***C***H$_{aromatic}$), 119.55 (***C***$H_2$CH), 101.33 (***C***$HCHCH_2$), 68.63 (CHO***C***$H_2$C), 67.12 - 65.96 ((C=O)O***C***$H_2$ + $(C_6H_5)$***C***$H_2$), 37.48 ($CH_2$***C***); GPC (Chloroform, RI): $M_n$ ($Đ_M$) = 4,430 g/mol (1.13).

### 6.4.4 Synthesis of PEO-PVDC block copolymer:

Polymerisation was undertaken as described in **6.4.3** using commercially bought poly(ethylene oxide) methyl ether (Chloroform GPC: $M_n$ = 9,640, $Đ_M$ = 1.03) as a macroinitiator. The polymerisation was quenched by precipitation into diethyl ether.

$^{1}$H NMR (400 MHz, $CDCl_3$) $\delta$ = 5.85 (ddd, $CH_2C\boldsymbol{H}CH$), 5.47 (d, $C\boldsymbol{H}_2CHCH$), 5.32 (d, $C\boldsymbol{H}_2CHCH$), 4.92 (s, $C\boldsymbol{H}CHCH_2$), 4.53 (s, $C\boldsymbol{H}_2OH$), 4.46 (s, $(C=O)OC\boldsymbol{H}_2$), 4.03 (d, $CHOC\boldsymbol{H}_2$), 3.96 (s, $(C=O)OC\boldsymbol{H}_2$), 3.79 – 3.67 (m, $CHOC\boldsymbol{H}_2$), 3.64 (s, $C\boldsymbol{H}_2C\boldsymbol{H}_2O$), 3.37 (s, $CH_2CH_2OC\boldsymbol{H}_3$); $^{13}$C NMR (101 MHz, $CDCl_3$) $\delta$ = 154.56 ($(\boldsymbol{C}=O)_{PVDC}$), 133.94 ($CH_2\boldsymbol{C}H$), 119.39 ($\boldsymbol{C}H_2CH$), 101.19 ($\boldsymbol{C}HCHCH_2$), 70.58 ($C\boldsymbol{H}_2C\boldsymbol{H}_2O$), 68.49 ($CHO\boldsymbol{C}H_2C$), 66.76 - 66.12 ($(C=O)O\boldsymbol{C}H_2$), 37.33 ($CH_2\boldsymbol{C}$); GPC (Chloroform, RI): $M_n$ ($Đ_M$) = 15,840 g/mol (1.03).

### 6.4.5 Synthesis of PVDC-PCL-PVDC tri-block copolymer:

The polymerisation was undertaken as described in **6.4.3** using commercially bought poly(caprolactone) (Chloroform GPC: $M_n$ = 4,020, $Đ_M$ = 1.24) initiated from 1,4-butanediol as a macroinitiator. The polymerisation was quenched by precipitation into hexanes.

$^{1}$H NMR (400 MHz, $CDCl_3$) $\delta$ = 5.85 (ddd, $CH_2C\boldsymbol{H}CH$), 5.47 (d, $C\boldsymbol{H}_2CHCH$), 5.32 (d, $C\boldsymbol{H}_2CHCH$), 4.91 (s, $C\boldsymbol{H}CHCH_2$), 4.53 (s, $C\boldsymbol{H}_2OH$), 4.46 (s, $(C=O)OC\boldsymbol{H}_2CH_2$), 4.06 (t, $C\boldsymbol{H}_2O(C=O)$), 4.03 (d, $CHOC\boldsymbol{H}_2$), 3.96 (s, $(C=O)OC\boldsymbol{H}_2$), 3.80 – 3.68 (m, $CHOC\boldsymbol{H}_2$), 2.30 (t, $O(C=O)C\boldsymbol{H}_2CH_2$), 1.77 – 1.56 (m, $CH_2C\boldsymbol{H}_2CH_2C\boldsymbol{H}_2CH_2$), 1.47 – 1.31 (m, $CH_2CH_2C\boldsymbol{H}_2CH_2CH_2$); $^{13}$C NMR (101 MHz, $CDCl_3$) $\delta$ = 173.69 ($(\boldsymbol{C}=O)_{PCL}$), 154.68 ($(\boldsymbol{C}=O)_{PVDC}$), 134.00 ($CH_2\boldsymbol{C}H$), 119.51 ($\boldsymbol{C}H_2CH$), 101.33 ($\boldsymbol{C}HCHCH_2$), 68.63 ($CHO\boldsymbol{C}H_2C$), 67.10 - 65.85 ($(C=O)O\boldsymbol{C}H_2$), 64.29 ($CH_2\boldsymbol{C}H_2O(C=O)$), 37.50 ($CH_2\boldsymbol{C}$), 34.26 ($O(C=O)\boldsymbol{C}H_2CH_2$), 28.50 ($\boldsymbol{C}H_2CH_2O(C=O)$), 25.67 ($CH_2CH_2\boldsymbol{C}H_2CH_2CH_2$), 24.72 ($O(C=O)CH_2\boldsymbol{C}H_2$); GPC (Chloroform, RI): $M_n$ ($Đ_M$) = 8,420 g/mol (1.09).

### 6.4.6 General synthesis of block copolymers:

To a vial was added benzyl alcohol, 1-(3,5-bis(trifluoromethyl)phenyl)-3-cyclohexylthiourea (5 mol% to monomer) and DBU (1 mol% to monomer), which were then dissolved in $CDCl_3$. The contents of this vial were then added to a separate vial containing the monomer of the first block (*L*-lactide, VDC or TMC) dissolved in $CDCl_3$ (final monomer concentration of 0.5 M). The polymerisation was followed by $^1$H NMR spectroscopy and upon reaching 90% monomer conversion was divided into two portions. The first portion was precipitated in hexanes and the other portion was added to a separate vial containing the monomer for the second block (*L*-lactide, VDC or TMC). Upon 90% monomer conversion being reached by $^1$H NMR spectroscopy for the second block, the polymerisation was stopped by precipitating into hexanes. If necessary, further precipitations in hexanes or washing with diethyl ether were performed to obtain pure block copolymers.

#### 6.4.6.1 PVDC block:

$^1$H NMR (400 MHz, $CDCl_3$) $\delta$ = 7.42 – 7.31 (m, C***H***$_{aromatic}$), 5.84 (ddd, $CH_2C$***H***CH), 5.47 (d, C***H***$_2$CHCH), 5.32 (d, C***H***$_2$CHCH), 5.15 (s, ($C_6H_5$)C***H***$_2$)), 4.91 (s, C***H***$CHCH_2$), 4.53 (s, C***H***$_2$OH), 4.46 (d, (C=O)OC***H***$_2$), 4.02 (d, CHOC***H***$_2$), 3.96 (s, (C=O)OC***H***$_2$), 3.81 – 3.66 (m, CHOC***H***$_2$); $^{13}$C NMR (101 MHz, $CDCl_3$) $\delta$ = 154.66 (C=O), 134.05 ($CH_2$***C***H), 128.82 - 128.61 (***C***H$_{aromatic}$), 119.53 (***C***$H_2$CH), 101.30 (***C***$HCHCH_2$), 68.61 (CHO***C***$H_2$C), 67.08 - 65.97 ((C=O)O***C***$H_2$ + ($C_6H_5$)***C***$H_2$), 37.46 ($CH_2$***C***); GPC (Chloroform, RI): $M_n$ ($Đ_M$) = 7,220 g/mol (1.11).

### 6.4.6.2 PVDC-PTMC block copolymer:

$^{1}$H NMR (400 MHz, $CDCl_3$) $\delta$ = 7.39 - 7.34 (m, C***H***$_{aromatic}$), 5.84 (ddd, $CH_2C$***H***CH), 5.46 (d, C***H***$_2$CHCH), 5.31 (d, C***H***$_2$CHCH), 5.15 (s, $(C_6H_5)C$***H***$_2$), 4.91 (s, C***H***$CHCH_2$), 4.45 (s, (C=O)OC***H***$_2$), 4.23 (t, C***H***$_2CH_2C$***H***$_2$), 4.02 (d, CHOC***H***$_2$), 3.95 (s, (C=O)OC***H***$_2$), 3.81 – 3.64 (m, CHOC***H***$_2$), 2.04 (p, $CH_2C$***H***$_2CH_2$); $^{13}$C NMR (101 MHz, $CDCl_3$) $\delta$ = 155.00 ($(C=O)_{PTMC-PTMC}$), 154.83 ($(C=O)_{PTMC-PVDC}$), 154.64 ($(C=O)_{PVDC-PVDC}$), 134.04 ($CH_2$***C***H), 128.76 – 128.59 (***C***$H_{aromatic}$), 119.49 (***C***$H_2CH$), 101.28 (***C***$HCHCH_2$), 68.59 (CHO***C***$H_2C$), 67.06 – 65.78 ((C=O)O***C***$H_2$ + $(C_6H_5)$***C***$H_2$), 64.38 (***C***$H_2CH_2$***C***$H_2$), 37.44 ($CH_2$***C***), 28.14 ($CH_2$***C***$H_2CH_2$); GPC (Chloroform, RI): $M_n$ ($Đ_M$) = 10,540 g/mol (1.07).

### 6.4.6.4 PVDC-PLLA block copolymer:

$^{1}$H NMR (400 MHz, $CDCl_3$) $\delta$ = 7.42 – 7.31 (m, C***H***$_{aromatic}$), 5.84 (ddd, CHC***H***$CH_2$), 5.47 (d, C***H***$_2$CHCH), 5.32 (d, C***H***$_2$CHCH), 5.16 (q, C***H***$CH_3$), 4.91 (s, C***H***$CHCH_2$), 4.45 (s, (C=O)OC***H***$_2$C), 4.02 (d, CHOC***H***$_2$), 3.96 (s, (C=O)OC***H***$_2$C), 3.84 – 3.62 (m, CHOC***H***$_2$), 1.57 (d, C***H***$_3$); $^{13}$C NMR (101 MHz, $CDCl_3$) $\delta$ = 169.72 (***C***=OCH), 154.65 (O(***C***=O)O), 134.05 ($CH_2$***C***H), 128.82 – 128.60 (***C***$H_{benzene}$), 119.51 (***C***$H_2CH$), 101.29 (***C***$HCHCH_2$), 69.12 ($CH_3$***C***H), 68.60 (CHO***C***$H_2C$), 67.07 – 65.96 (C=OO***C***$H_2$ + (Benzene)***C***$H_2$), 37.45 ($CH_2$***C***), 16.76 (***C***$H_3$); GPC (Chloroform, RI): $M_n$ ($Đ_M$) = 12,870 g/mol (1.08).

### 6.4.6.5 PLLA block:

$^{1}$H NMR (400 MHz, $CDCl_3$) $\delta$ = 7.38 – 7.28 (m, C***H***$_{aromatic}$), 5.16 (q, C***H***$CH_3$), 4.39 – 4.29 (m, C***H***OH), 1.57 (d, C***H***$_3$); $^{13}$C NMR (101 MHz, $CDCl_3$) $\delta$ = 169.73 (***C***=O), 128.76 (***C***$H_{aromatic}$), 128.67 (***C***$H_{aromatic}$), 128.38 (***C***$H_{aromatic}$), 69.14 (***C***H), 67.35 (***C***$H_2$), 66.83 (***C***HOH), 16.77 (***C***$H_3$); GPC (Chloroform, RI): $M_n$ ($Đ_M$) = 9,000 g/mol (1.06).

### 6.4.6.6 PLLA-PVDC block copolymer:

$^{1}$H NMR (400 MHz, $CDCl_3$) $\delta$ = 7.39 – 7.28 (m, C***H***$_{aromatic}$), 5.84 (ddd, CHC***H***$CH_2$), 5.47 (d, C***H***$_2$CHCH), 5.32 (d, C***H***$_2$CHCH), 5.16 (q, C***H***$CH_3$), 4.91 (s, C***H***$CHCH_2$), 4.53 (s, C***H***$_2$OH), 4.45 (s, (C=O)OC***H***$_2$C), 4.02 (d, CHOC***H***$_2$), 3.96 (s, (C=O)OC***H***$_2$C), 3.81 – 3.67 (m, CHOC***H***$_2$), 1.57 (d, C***H***$_3$); $^{13}$C NMR (101 MHz, $CDCl_3$) $\delta$ = 169.72 (***C***=OCH), 154.65 (O(***C***=O)O), 134.05 ($CH_2$***C***H), 128.74 - 128.37 (***C***$H_{benzene}$), 119.53 (***C***$H_2$CH), 101.29 (***C***HCH$CH_2$), 69.12 ($CH_3$***C***H), 68.60 (CHO***C***$H_2$C), 67.07 - 65.08 (C=OO***C***$H_2$ + ($C_6H_5$)***C***$H_2$), 37.45 ($CH_2$***C***), 16.76 (***C***$H_3$); GPC (Chloroform, RI): $M_n$ ($Đ_M$) = 14,720 g/mol (1.09).

### 6.4.6.7 PTMC block:

$^{1}$H NMR (400 MHz, $CDCl_3$) $\delta$ = 7.40 – 7.32 (m, C***H***$_{aromatic}$), 5.15 (s, ($C_6H_5$)C***H***$_2$), 4.23 (t, C***H***$_2CH_2CH_2$C***H***$_2$), 3.73 (q, C***H***$_2$OH), 2.04 (p, $CH_2$C***H***$_2CH_2$), 1.91 (p, $CH_2$C***H***$_2CH_2$OH); $^{13}$C NMR (101 MHz, $CDCl_3$) $\delta$ = 155.03 (***C***=O), 128.75 - 128.49 (***C***$H_{aromatic}$), 65.15 (($C_6H_5$)***C***$H_2$), 64.41 (***C***$H_2CH_2$***C***$H_2$), 59.10 (***C***$H_2$OH) 31.77 ($CH_2$***C***$H_2CH_2$OH), 28.17 ($CH_2$***C***$H_2CH_2$); GPC (Chloroform, RI): $M_n$ ($Đ_M$) = 4,130 g/mol (1.06).

### 6.4.6.8 PTMC-PVDC block copolymer:

$^{1}$H NMR (400 MHz, $CDCl_3$) $\delta$ = 7.40 – 7.31 (m, C***H***$_{aromatic}$), 5.83 (ddd, CHC***H***$CH_2$), 5.45 (d, C***H***$_2$CHCH), 5.30 (d, C***H***$_2$CHCH), 5.13 (s, ($C_6H_5$)C***H***$_2$), 4.90 (s,C***H***$CHCH_2$), 4.51 (s, C***H***$_2$OH), 4.44 (s, (C=O)OC***H***$_2$C), 4.21 (t, C***H***$_2CH_2C$***H***$_2$), 4.01 (d, CHOC***H***$_2$), 3.94 (s, (C=O)OC***H***$_2$C), 3.72 (m, CHOC***H***$_2$), 2.03 (p, $CH_2$C***H***$_2CH_2$); $^{13}$C NMR (101 MHz, $CDCl_3$) $\delta$ = 154.96 ((C=O)$_{PTMC-PTMC}$), 154.78 ((C=O)$_{PTMC-PVDC}$), 154.60 ((C=O)$_{PVDC-PVDC}$), 134.00 ($CH_2$***C***H), 128.68 - 128.42 (***C***H$_{aromatic}$), 119.47 (***C***$H_2$CH), 101.23 (***C***$HCHCH_2$), 68.55 (CHO***C***$H_2$C), 67.01 - 65.73 ((C=O)O***C***$H_2$ + ($C_6H_5$)***C***$H_2$), 64.34 (***C***$H_2CH_2$***C***$H_2$), 37.39 ($CH_2$***C***), 28.10 ($CH_2$***C***$H_2CH_2$); GPC (Chloroform, RI): $M_n$ ($Đ_M$) = 10,770 g/mol (1.06).

### 6.4.7 General post-polymerisation functionalisation of PVDC procedure:

To a small vial was added PVDC (20 mg, either DP100 (Chloroform GPC: $M_n$ = 21,620, $Đ_M$ = 1.04) or DP20 (Chloroform GPC: $M_n$ = 4,430, $Đ_M$ = 1.13)) and a thiol (2 eq per vinyl group) which was then dissolved in 1,4-dioxane (0.20 mL). A stock solution containing Irgacure® 369 in 1,4-dioxane (0.2 M) was prepared and then 0.05 mL (0.01 eq per vinyl group) added to the original vial. The solution was exposed to UV light in a lightbox for two hours and precipitated in either hexanes, chloroform or methanol. In some cases a second precipitation was required to completely remove the excess thiol.

### 6.4.7.1 Functionalisation of PVDC (DP100) with 1-dodecanethiol:

$^1$H NMR (400 MHz, $CDCl_3$) $\delta$ = 4.63 (s, C***H***), 4.42 (s, (C=O)OC***H***$_2$C), 3.98 (s, CHOC***H***$_2$), 3.95 (s, (C=O)OC***H***$_2$C), 3.77 – 3.61 (m, CHOC***H***$_2$), 2.58 (t, $CHCH_2C$***H***$_2$), 2.50 (t, $CHCH_2CH_2SC$***H***$_2$), 1.91 (dd, CHC***H***$_2$), 1.64 – 1.51 (m, $CHCH_2CH_2SCH_2C$***H***$_2$), 1.43 – 1.32 (m, $SCH_2CH_2C$***H***$_2$), 1.26 (s, CH3(C***H***$_2)_8$), 0.88 (t, C***H***$_3$); GPC (Chloroform, RI): $M_n$ ($Đ_M$) = 35,340 g/mol (1.07).

### 6.4.7.2 Functionalisation of PVDC (DP100) with hexylthiol:

$^1$H NMR (400 MHz, $CDCl_3$) $\delta$ = 4.63 (s, OC***H***$CH_2$), 4.42 (s, (C=O)OC***H***$_2$C), 3.98 (s, CHOC***H***$_2$), 3.95 (s, (C=O)OC***H***$_2$C), 3.77 – 3.63 (m, CHOC***H***$_2$), 2.59 (t, $CHCH_2C$***H***), 2.50 (t, $CHCH_2CH_2SC$***H***$_2$), 1.91 (dd, CHC***H***$_2$), 1.65 – 1.51 (m, $CH_3(CH_2)_3C$***H***$_2$), 1.44 – 1.33 (m, $CH_3CH_2CH_2C$***H***$_2$), 1.33 – 1.22 (m, $CH_3C$***H***$_2C$***H***$_2$), 0.89 (t, C***H***$_3$); GPC (Chloroform, RI): $M_n$ ($Đ_M$) = 28,360 g/mol (1.07).

### 6.4.7.3 Functionalisation of PVDC (DP100) with 1-butylthiol:

$^1$H NMR (400 MHz, $CDCl_3$) $\delta$ = 4.63 (s, OC***H***$CH_2$), 4.42 (s, (C=O)OC***H***$_2$C), 3.99 (s, CHOC***H***$_2$), 3.95 (s, (C=O)OC***H***$_2$C), 3.78 – 3.62 (m, CHOC***H***$_2$), 2.59 (t, $CHCH_2C$***H***$_2$), 2.51 (t, $CHCH_2CH_2SC$***H***$_2$), 1.91 (dd, CHC***H***$_2$), 1.65 – 1.51 (m, $CH_3CH_2C$***H***$_2$), 1.49 – 1.35 (m, $CH_3C$***H***$_2$), 0.91 (t, C***H***$_3$); GPC (Chloroform, RI): $M_n$ ($Đ_M$) = 28,890 g/mol (1.08).

### 6.4.7.4 Functionalisation of PVDC (DP100) with 1-adamantylthiol:

(0.02 eq of Irgacure® 369 per vinyl group)

$^1$H NMR (400 MHz, $CDCl_3$) $\delta$ = 4.62 (s, OC***H***$CH_2$), 4.42 (s, (C=O)OC***H***$_2$C), 3.98 (s, CHOC***H***$_2$), 3.95 (s, (C=O)OC***H***$_2$C), 3.79 – 3.61 (m, CHOC***H***$_2$), 2.59 (t, C***H***$_2$S), 2.03 (s, C***H***$_{adamantyl}$), 1.91 – 1.87 (m, C***H***$_2$CH$_2$S), 1.85 (s, SCC***H***$_2$), 1.74 – 1.63 (m, SCH$_2$CHC***H***$_2$); GPC (Chloroform, RI): $M_n$ ($Đ_M$) = 29,900 g/mol (1.17).

### 6.4.7.5 Functionalisation of PVDC (DP100) with benzyl mercaptan:

(0.05 eq of Irgacure® 369 per vinyl group)

$^1$H NMR (400 MHz, $CDCl_3$) $\delta$ = 7.32 – 7.27 (m, C***H***$_{aromatic}$), 4.57 (s, OC***H***$CH_2$), 4.40 (s, (C=O)OC***H***$_2$C), 3.95 (s, CHOC***H***$_2$), 3.92 (s, (C=O)OC***H***$_2$C), 3.69 (s, ($C_6H_5$)C***H***$_2$), 3.67 – 3.57 (m, CHOC***H***$_2$), 2.50 (t, CHCH$_2$C***H***$_2$), 1.92 – 1.83 (m, CHC***H***$_2$); GPC (Chloroform, RI): $M_n$ ($Đ_M$) = 31,000 g/mol (1.55).

### 6.4.7.6 Functionalisation of PVDC (DP100) with 1-thioglycerol:

$^1$H NMR (400 MHz, *d*-DMSO) $\delta$ = 4.73 (d, CHO***H***), 4.61 (s, C***H***CH$_2$CH$_2$), 4.53 (t, CH$_2$O***H***), 4.34 (s, (C=O)OC***H***$_2$C), 3.94 (s, (C=O)OC***H***$_2$C), 3.86 (d, CHOC***H***$_2$), 3.68 (d, CHOC***H***$_2$), 3.54 (dq, C***H***OH), 3.34 (t,C***H***$_2$OH), 2.55 (t, CH$_2$C***H***$_2$S), 2.65 – 2.39 (m, SC***H***$_2$CH), 1.78 (s, SCH$_2$C***H***$_2$); GPC (Chloroform, RI): $M_n$ ($Đ_M$) = 40,200 g/mol (1.09).

### 6.4.7.7 Functionalisation of PVDC (DP100) with 2-mercaptoethanol:

$^1$H NMR (400 MHz, *d*-DMSO) $\delta$ = 4.74 (t, O***H***), 4.61 (s, C***H***), 4.34 (s, (C=O)OC***H***$_2$C), 3.94 (s, (C=O)OC***H***$_2$C), 3.86 (d, CHOC***H***$_2$), 3.68 (d, CHOC***H***$_2$), 3.51 (dd, C***H***$_2$OH), 2.57 – 2.52 (m, C***H***$_2$SC***H***$_2$), 1.78 (s, CHC***H***$_2$); GPC (Chloroform, RI): $M_n$ ($Đ_M$) = 34,840 g/mol (1.09).

### 6.4.7.8 Functionalisation of PVDC (DP100) with thioglycolic acid:

$^1$H NMR (400 MHz, *d*-DMSO) $\delta$ = 12.56 (s, COO***H***), 4.61 (s, C***H***), 4.34 (s, (C=O)OC***H***$_2$C), 3.94 (s, (C=O)OC***H***$_2$C), 3.86 (d, CHOC***H***$_2$), 3.67 (d, CHOC***H***$_2$), 3.22 (s, C***H***$_2$COOH), 2.61 (t, CHCH$_2$C***H***$_2$), 1.80 (s, CHC***H***$_2$).

## 6.5 Experimental for Chapter Four

### 6.5.1 Synthesis of MAC:

To a 1 L flask was added 3-hydroxy-2-(hydroxymethyl)-2-methylpropanoic acid (*bis*-MPA) (50 g, 0.373 mol, 1 eq), potassium hydroxide (23 g, 0.410 mol, 1.1 eq) and DMF (125 mL). This was stirred at 100 °C for 45 min and then allowed to cool to 60°C. Allyl bromide (35.5 mL, 0.410 mol, 1.1 eq) was added dropwise over a period of an hour and the reaction was then left to stir at 60 °C overnight. The solvent was remove by vacuum transfer and the crude mixture thoroughly washed with $CH_2Cl_2$. Removing the salt yielded a clear solution that once the solvent was removed produced allyl 3-hydroxy-2-(hydroxymethyl)-2-methylpropanoate as a yellow oil (45 g crude material, 0.258 mol, 69%). A proportion of this was then purified further by short path apparatus to yield a clear oil which was used in the next step.

$^1$H NMR (400 MHz, $CDCl_3$) $\delta$ = 5.91 (m, 1H, $CH_2C\boldsymbol{H}$), 5.33 (dq, $^3J_{H\text{-}H}$ = 17.2, $^4J_{H\text{-}H}$ = 1.5 Hz, 1H, $C\boldsymbol{H}_2CHCH_2O$), 5.24 (dq, $^3J_{H\text{-}H}$ = 10.5, $^4J_{H\text{-}H}$ = 1.2 Hz, 1H, $C\boldsymbol{H}_2CHCH_2O$), 4.65 (dt, $^3J_{H\text{-}H}$ = 5.6, $^4J_{H\text{-}H}$ = 1.4 Hz, 2H, $OC\boldsymbol{H}_2CH$), 3.80 (dd, $^2J_{H\text{-}H}$ = 76.5, $^3J_{H\text{-}H}$ = 11.2 Hz, 4H, $C\boldsymbol{H}_2C$), 2.84 (s, 2H, O***H***), 1.08 (s, 3H, $C\boldsymbol{H}_3$); $^{13}$C NMR (101 MHz, $CDCl_3$) $\delta$ = 175.70 (***C***=O), 131.89 ($CH_2\boldsymbol{C}H$), 118.53 ($\boldsymbol{C}H_2CHCH_2O$), 68.17 ($\boldsymbol{C}H_2C$), 65.64 ($O\boldsymbol{C}H_2$), 49.35 (***C***), 17.27 ($\boldsymbol{C}H_3$).

To a 1 L flask was added allyl 3-hydroxy-2-(hydroxymethyl)-2-methylpropanoate (28 g, 0.161 mol, 1 eq), ethyl chloroformate (43.66 g, 0.402 mol, 2.5 eq) and THF (600 mL). This stirred solution was cooled in an ice bath and then $NEt_3$ (40.71 g, 0.402 mol, 2.5 eq) in THF (100 mL) was added dropwise. After complete addition the ice bath was removed and the mixture stirred for a further three hours. The white

precipitate was separated by filtration and the solvent removed from the remaining solution on a rotary evaporator to yield an oil that solidified upon standing. The solid was dissolved in $CH_2Cl_2$ and washed twice with water before being dried with magnesium sulphate. The solvent was removed and the crude product recrystallised in hot toluene (×3) to yield a white solid (23.8 g, 0.119 mol, 74%). The spectroscopic data was found to be the same as previous literature reports for this compound.[7]

$^1$H NMR (400 MHz, $CDCl_3$) $\delta$ = 5.87 (m, 1H, $CH_2C\boldsymbol{H}$), 5.31 (dq, $^3J_{H\text{-}H}$ = 17.2, , $^4J_{H\text{-}H}$ = 1.3 Hz, 1H, $C\boldsymbol{H}_2CHCH_2O$), 5.26 (dq, $^3J_{H\text{-}H}$ = 10.4, $^4J_{H\text{-}H}$ = 1.0 Hz, 1H, $C\boldsymbol{H}_2CHCH_2O$), 4.67 – 4.62 (m, 2H, $CHC\boldsymbol{H}_2O$), 4.43 (dd, $^2J_{H\text{-}H}$ = 189.1, $^4J_{H\text{-}H}$ 10.8 Hz, 4H, $C\boldsymbol{H}_2C$), 1.30 (s, 3H, $C\boldsymbol{H}_3$); $^{13}$C NMR (101 MHz, $CDCl_3$) $\delta$ = 170.87 ($C(\boldsymbol{C}$=O)), 147.54 (O($\boldsymbol{C}$=O)O), 131.03 ($CH_2\boldsymbol{C}H$), 119.44 ($\boldsymbol{C}H_2CHCH_2O$), 73.00 ($\boldsymbol{C}H_2C$), 66.63 ($O\boldsymbol{C}H_2CH$), 40.26 ($\boldsymbol{C}$), 17.54 ($\boldsymbol{C}H_3$).

### 6.5.2 General synthesis of P(VDC-*co*-MAC):

In a typical experiment, 1,4-butanediol (1 mol% to monomer for DP100) and 1-(3,5-bis(trifluoromethyl)phenyl)-3-cyclohexylthiourea (5 mol% to monomer) were dissolved in chloroform and then added to a separate vial containing VDC. In a third vial MAC was dissolved in chloroform and added to the VDC/TU/ROH solution. DBU (1 mol% to monomer) was finally added to this solution (final monomer concentration = 0.5 M) to start the polymerisation. The copolymerisation was followed by $^1$H NMR spectroscopy and stopped after reaching 90% monomer conversion. The crude copolymerisation mixture was precipitated into hexanes and the polymer washed with diethyl ether.

Example using 50:50 VDC:MAC feed ratio:

$^{1}$H NMR (500 MHz, $CDCl_3$) $\delta$ = 5.97 – 5.77 (m, $CH_2C\boldsymbol{H}$), 5.47 (d, $C\boldsymbol{H}_2CHCH$), 5.36 – 5.28 (m, $C\boldsymbol{H}_2CHCH$ + $C\boldsymbol{H}_2CHCH_2O$), 5.23 (d, $C\boldsymbol{H}_2CHCH_2O$), 4.91 (s, $C\boldsymbol{H}CHCH_2$), 4.63 (s, $CHC\boldsymbol{H}_2O$), 4.44 (s, $(O(C=O)OC\boldsymbol{H}_2)_{VDC}$), 4.30 (s, $(O(C=O)OC\boldsymbol{H}_2)_{MAC}$), 4.08 – 3.98 (m, $CHOC\boldsymbol{H}_2$), 3.96 (d, $(O(C=O)OC\boldsymbol{H}_2)_{VDC}$), 3.80 – 3.68 (m, $CHOC\boldsymbol{H}_2$), 1.27 (d, $C\boldsymbol{H}_3$); $^{13}$C NMR (126 MHz, $CDCl_3$) $\delta$ = 171.88 ($C\boldsymbol{C}$=OO), 154.67 (VDC-O(*C*=O)O-VDC), 154.59 (VDC-O(C=O)O-MAC), 154.52 (MAC-O(***C***=O)O-MAC), 134.09 ($CH_2\boldsymbol{C}HCH$), 131.69 ($CH_2\boldsymbol{C}HCH_2$), 119.49 ($\boldsymbol{C}H_2CHCH$), 118.65 ($\boldsymbol{C}H_2CHCH_2O$), 101.28 ($\boldsymbol{C}HCHCH_2$), 68.72 $(O(C=O)O\boldsymbol{C}H_2)_{MAC}$, 68.61 ($CHO\boldsymbol{C}H_2C$), 67.10 - 66.00 ($(O(C=O)O\boldsymbol{C}H_2)_{VDC}$, 66.00 ($O\boldsymbol{C}H_2CH$) 46.68 $(CH_2\boldsymbol{C})_{MAC}$, 37.50 $(CH_2\boldsymbol{C})_{VDC}$, 17.62 ($\boldsymbol{C}H_3$); GPC (Chloroform, RI): $M_n$ ($Đ_M$) = 25,950 g/mol (1.05).

### 6.5.3 Synthesis of PVDC-PMAC:

PVDC (DP20, initiated from benzyl alcohol, $M_n$ = 4,430, $Đ_M$ = 1.13) was first dried over $P_2O_5$ for a week and then stored in a glovebox. In a glovebox TU (4.63 mg, 0.0125 mmol, 1 eq) was weighed and dissolved in $CDCl_3$ (250 µl). Separately, MAC (50 mg, 0.2498 mmol, 20 eq) was dissolved in $CDCl_3$ (230 µl). These two solutions were then added to a vial containing PVDC (51 mg). A DBU stock solution was prepared by weighing out 3.8 mg of DBU into a vial and then dissolving it in $CDCl_3$ (200 µl). To the vial containing the PVDC, MAC and TU solution was added 20 µl of the DBU stock solution to commence the polymerisation (final monomer concentration = 0.5 M). After reaching 90% monomer conversion by NMR analysis, the polymerisation was precipitated into hexanes and washed with diethyl ether.

$^{1}$H NMR (500 MHz, $CDCl_3$) $\delta$ = 7.41 – 7.32 (m, C$\boldsymbol{H}_{aromatic}$), 5.96 – 5.77 (m, $CH_2C\boldsymbol{H}$), 5.47 (d, C$\boldsymbol{H}_2$CHCH), 5.37 – 5.27 (m, C$\boldsymbol{H}_2$CHCH + C$\boldsymbol{H}_2$CHCH$_2$O), 5.23 (d, C$\boldsymbol{H}_2$CHCH$_2$O), 5.16 (s, ($C_6H_5$)C$\boldsymbol{H}_2$)), 4.92 (s, C$\boldsymbol{H}$CHCH$_2$), 4.62 (d, CHC$\boldsymbol{H}_2$O), 4.46 (s, (O(C=O)OC$\boldsymbol{H}_2$)$_{VDC}$), 4.30 (q, (O(C=O)OC$\boldsymbol{H}_2$)$_{MAC}$), 4.03 (d, CHOC$\boldsymbol{H}_2$), 3.96 (s, (O(C=O)OC$\boldsymbol{H}_2$)$_{VDC}$), 3.83 – 3.66 (m, CHOC$\boldsymbol{H}_2$), 1.27 (s, C$\boldsymbol{H}_3$); $^{13}$C NMR (126 MHz, $CDCl_3$) $\delta$ = 171.88 (C$\boldsymbol{C}$=OO), 154.68 (VDC-O(*C*=O)O-VDC), 154.60 (VDC-O(C=O)O-MAC), 154.50 (MAC-O(***C***=O)O-MAC), 134.07 ($CH_2\boldsymbol{C}$HCH), 131.69 ($CH_2\boldsymbol{C}HCH_2$), 128.77 - 128.63 ($\boldsymbol{C}H_{aromatic}$), 119.55 ($\boldsymbol{C}H_2$CHCH), 118.65 ($\boldsymbol{C}H_2CHCH_2O$), 101.32 ($\boldsymbol{C}$HCHCH$_2$), 68.72 (O(C=O)O$\boldsymbol{C}H_2$)$_{MAC}$, 68.63 (CHO$\boldsymbol{C}H_2$C), 67.10 - 66.00 ((O(C=O)O$\boldsymbol{C}H_2$)$_{VDC}$ + ($C_6H_5$)$\boldsymbol{C}H_2$), 66.00 (O$\boldsymbol{C}H_2$CH), 46.68 ($CH_2\boldsymbol{C}$)$_{MAC}$, 37.48 ($CH_2\boldsymbol{C}$)$_{VDC}$, 17.62 ($\boldsymbol{C}H_3$); GPC (Chloroform, RI): $M_n$ ($Đ_M$) = 6,440 g/mol (1.10).

### 6.5.4 Synthesis of PMAC for post-polymerisation functionalisations:

In a glovebox 1,4-butanediol (4.5 mg, 0.05 mmol, 1 eq) was dissolved in $CDCl_3$ (4 mL) and added to a vial containing TU (92.5 mg, 0.25 mmol, 5 eq). The solution was then transferred to a vial containing MAC (1 g, 5.00 mmol, 100 eq). Separately, DBU (7.6 mg, 0.05 mmol, 1 eq) was weighed out and dissolved in $CDCl_3$ (2 mL) before its addition to the monomer solution (final monomer concentration = 0.5M). The polymerisation was monitored by $^{1}$H NMR and upon reaching 90% monomer conversion was stopped by quenching with Amberlyst® 16 (acidic) ion exchange resin and precipitated into hexanes. Washing with diethyl ether yielded pure polymer.

$^1$H NMR (400 MHz, $CDCl_3$) $\delta$ = 5.88 (ddd, $CH_2C\boldsymbol{H}CH_2$), 5.31 (dd, $C\boldsymbol{H}_2CHCH_2O$), 5.24 (dd, $C\boldsymbol{H}_2CHCH_2O$), 4.63 (d, $CHC\boldsymbol{H}_2O$), 4.38 – 4.24 (m, $CC\boldsymbol{H}_2O$), 1.27 (s, $C\boldsymbol{H}_3$); $^1$H NMR (400 MHz, DMSO) δ = 5.86 (ddd, $CH_2C\boldsymbol{H}CH_2$), 5.27 (d, $C\boldsymbol{H}_2CH$), 5.18 (d, $C\boldsymbol{H}_2CH$), 4.58 (d, $CHC\boldsymbol{H}_2O$), 4.24 (q, $CC\boldsymbol{H}_2O$), 1.18 (s, $C\boldsymbol{H}_3$).$^{13}$C NMR (101 MHz, $CDCl_3$) $\delta$ = 171.89 ($C\boldsymbol{C}$=OO), 154.52 (O$\boldsymbol{C}$=OO), 131.71 ($CH_2\boldsymbol{C}HCH_2$), 118.66 ($\boldsymbol{C}H_2CHCH_2O$), 68.73 (O$\boldsymbol{C}H_2C$), 66.01 (O$\boldsymbol{C}H_2CH$), 46.70 ($CH_2\boldsymbol{C}$), 17.63 ($\boldsymbol{C}H_3$). GPC (DMF, RI): $M_n$ ($Đ_M$) = 21,720 g/mol (1.06).

### 6.5.5 PMAC post-polymerisation functionalisation procedure:

To a small vial was added PMAC (20 mg, DP76 (Chloroform GPC: $M_n$ = 21,720, $Đ_M$ = 1.06)) and a thiol (2 eq per vinyl group) which was then dissolved in 1,4-dioxane (0.20 mL). A stock solution containing Irgacure® 369 in 1,4-dioxane (0.2 M) was prepared and 0.05 mL (0.01 eq per vinyl group) added to the PMAC containing vial. The solution was exposed to UV light in a lightbox for two hours and then precipitated in either hexanes, chloroform or methanol. In some cases a second precipitation was required to completely remove the excess thiol.

#### 6.5.5.1 Functionalisation of PMAC (DP76) with 1-hexylthiol:

$^1$H NMR (400 MHz, $CDCl_3$) $\delta$ = 4.29 (s, 4H, $OC\boldsymbol{H}_2C$), 4.23 (t, $OC\boldsymbol{H}_2CH_2$), 2.55 (t, $OCH_2CH_2C\boldsymbol{H}_2$), 2.50 (t, $OCH_2CH_2CH_2SC\boldsymbol{H}_2$), 1.91 (p, $OCH_2C\boldsymbol{H}_2$), 1.63 – 1.52 (m, $CH_3CH_2CH_2CH_2C\boldsymbol{H}_2$), 1.44 – 1.34 (m, $CH_3CH_2CH_2C\boldsymbol{H}_2$), 1.33 – 1.28 (m, $CH_3C\boldsymbol{H}_2C\boldsymbol{H}_2$), 1.26 (s, $CC\boldsymbol{H}_3$), 0.89 (t, $C\boldsymbol{H}_3CH_2$); GPC (Chloroform, RI): $M_n$ ($Đ_M$) = 30,410 g/mol (1.08).

### 6.5.5.2 Functionalisation of PMAC (DP76) with 1-adamantylthiol:

(0.02 eq of Irgacure® 369 per vinyl group)

$^1$H NMR (400 MHz, $CDCl_3$) $\delta$ = 4.29 (s, OC***H***$_2$C), 4.22 (t, OC***H***$_2$CH$_2$), 2.55 (t, SC***H***$_2$), 2.04 (s, CH$_2$C***H***), 1.93 – 1.86 (m, CH$_2$C***H***$_2$CH$_2$), 1.85 (d, CC***H***$_2$CH), 1.75 – 1.63 (m, CHC***H***$_2$CH), 1.26 (s, C***H***$_3$); GPC (Chloroform, RI): $M_n$ ($Đ_M$) = 24,670 g/mol (1.25).

### 6.5.5.3 Functionalisation of PMAC (DP76) with 1-thioglycerol:

$^1$H NMR (400 MHz, *d*-DMSO) $\delta$ = 4.72 (d, CHO***H***), 4.53 (t, CH$_2$O***H***), 4.23 (dd, OC***H***$_2$C), 4.13 (q, OC***H***$_2$CH$_2$), 3.60 – 3.49 (m, C***H***OH), 3.34 (t, C***H***$_2$OH), 2.66 – 2.38 (m, SC***H***$_2$CH), 2.55 (t, CH$_2$C***H***$_2$S), 1.81 (p, CH$_2$C***H***$_2$CH$_2$), 1.18 (s, C***H***$_3$); GPC (DMF, RI): $M_n$ ($Đ_M$) = 38,780 g/mol (1.13).

### 6.5.5.4 Functionalisation of PMAC (DP76) with 2-mercaptoethanol:

$^1$H NMR (400 MHz, *d*-DMSO) $\delta$ = 4.73 (t, CH$_2$CH$_2$O***H***), 4.23 (dd, OC***H***$_2$C), 4.13 (t, OC***H***$_2$CH$_2$), 3.52 (dd, CH$_2$C***H***$_2$OH), 2.59 – 2.51 (m, C***H***$_2$SC***H***$_2$), 1.81 (p, CH$_2$C***H***$_2$CH$_2$), 1.18 (s, C***H***$_3$); GPC (DMF, RI): $M_n$ ($Đ_M$) = 34,840 g/mol (1.10).

#### 6.5.5.5 Functionalisation of PMAC (DP76) with thioglycolic acid:

$^1$H NMR (400 MHz, *d*-DMSO) $\delta$ = 12.57 (s, COO***H***), 4.23 (dd, OC***H***$_2$C), 4.13 (t, OC***H***$_2$CH$_2$), 3.21 (s, C***H***$_2$COOH), 2.61 (t, SC***H***$_2$CH$_2$), 1.84 (p, CH$_2$C***H***$_2$CH$_2$), 1.17 (s, C***H***$_3$); GPC (DMF, RI): $M_n$ ($Đ_M$) = 33,470 g/mol (1.11).

### 6.5.6 General post-polymerisation functionalisation of P(VDC-*co*-MAC) procedure:

To a small vial was added P(VDC-*co*-MAC) (20 mg, DP92 (Chloroform GPC: $M_n$ = 22,320 $Đ_M$ = 1.05)) and a thiol (2 eq per vinyl group) which was then dissolved in 1,4-dioxane (0.20 mL). A stock solution containing Irgacure® 369 in 1,4-dioxane (0.2 M) was then prepared and 0.05 mL (0.01 eq per vinyl group) added to the copolymer containing vial. The solution was exposed to UV light in a lightbox for two hours and then precipitated in either hexanes, chloroform or methanol. In some cases a second precipitation was required to completely remove the excess thiol.

#### 6.5.6.1 Functionalisation of P(VDC-*co*-MAC) (DP92) with 1-dodecanethiol:

$^1$H NMR (400 MHz, $CDCl_3$) $\delta$ = 4.62 (s, SCH$_2$CH$_2$C***H***), 4.41 (s, C***H***$_{2(\text{PVDC backbone})}$), 4.29 (s, C***H***$_{2(\text{PMAC backbone})}$), 4.24 (t, SCH$_2$CH$_2$C***H***$_2$O), 3.96 (s, CHOC***H***$_2$C), 3.95 (s, C***H***$_{2(\text{PVDC backbone})}$), 3.75 – 3.63 (m, CHOC***H***$_2$C), 2.62 – 2.53 (m, CHCH$_2$C***H***$_2$S + OCH$_2$CH$_2$C***H***$_2$S), 2.50 (t, SC***H***$_2$(CH$_2$)$_{10}$CH$_3$), 1.97 – 1.85 (m, C***H***$_2$CH$_2$S(CH$_2$)$_{11}$CH$_3$), 1.63 – 1.51 (m, C***H***$_2$(CH$_2$)$_9$CH$_3$), 1.43 – 1.33 (m, C***H***$_2$(CH$_2$)$_8$CH$_3$), 1.26 (s, (C***H***$_2$)$_8$CH$_3$ + C***H***$_3$C), 0.88 (t, C***H***$_3$CH$_2$); GPC (Chloroform, RI): $M_n$ ($Đ_M$) = 39,050 g/mol (1.06).

### 6.5.6.2 Functionalisation of P(VDC-*co*-MAC) (DP92) with 1-hexylthiol:

$^1$H NMR (400 MHz, $CDCl_3$) $\delta$ = 4.63 (s, $SCH_2CH_2C\boldsymbol{H}$), 4.42 (s, $C\boldsymbol{H}_{2(PVDC\ backbone)}$), 4.30 (s, $C\boldsymbol{H}_{2(PMAC\ backbone)}$), 4.24 (t, $SCH_2CH_2C\boldsymbol{H}_2O$), 3.98 (s, $CHOC\boldsymbol{H}_2C$), 3.95 (s, $C\boldsymbol{H}_{2(PVDC\ backbone)}$), 3.75 – 3.63 (m, $CHOC\boldsymbol{H}_2C$), 2.63 – 2.53 (m, $CHCH_2C\boldsymbol{H}_2S$ + $OCH_2CH_2C\boldsymbol{H}_2S$), 2.50 (t, $SC\boldsymbol{H}_2(CH_2)_4CH_3$), 1.99 – 1.85 (m, $C\boldsymbol{H}_2CH_2S(CH_2)_5CH_3$), 1.63 – 1.50 (m, $C\boldsymbol{H}_2(CH_2)_3CH_3$), 1.45 – 1.33 (m, $CH_3CH_2CH_2C\boldsymbol{H}_2$), 1.33 – 1.22 (m, $CH_3(C\boldsymbol{H}_2)_2$ + $C\boldsymbol{H}_3C$), 0.88 (t, $C\boldsymbol{H}_3CH_2$); GPC (Chloroform, RI): $M_n$ ($Đ_M$) = 31,630 g/mol (1.06).

### 6.5.6.3 Functionalisation of P(VDC-*co*-MAC) (DP92) with 1-adamantylthiol:

$^1$H NMR (400 MHz, $CDCl_3$) $\delta$ = 4.62 (s, $SCH_2CH_2C\boldsymbol{H}$), 4.42 (s, $C\boldsymbol{H}_{2(PVDC\ backbone)}$), 4.30 (s, $C\boldsymbol{H}_{2(PMAC\ backbone)}$), 4.23 (s, $SCH_2CH_2C\boldsymbol{H}_2O$), 3.97 (s, $CHOC\boldsymbol{H}_2C$), 3.95 (s, $C\boldsymbol{H}_{2(PVDC\ backbone)}$), 3.75 – 3.65 (m, $CHOC\boldsymbol{H}_2C$), 2.63 – 2.51 (m, $CHCH_2C\boldsymbol{H}_2S$ + $OCH_2CH_2C\boldsymbol{H}_2S$), 2.04 (s, $SC(CH_2C\boldsymbol{H})_3$), 1.95 – 1.81 (m, $SC(C\boldsymbol{H}_2)_3$), 1.76 – 1.62 (m, $SC(CH_2CHC\boldsymbol{H}_2)_3$), 1.27 (s, $C\boldsymbol{H}_3$); GPC (Chloroform, RI): $M_n$ ($Đ_M$) = 33,260 g/mol (1.25).

### 6.5.6.4 Functionalisation of P(VDC-*co*-MAC) (DP92) with 1-thioglycerol:

$^1$H NMR (250 MHz, *d*-DMSO) $\delta$ = 4.68 (t, $CHO\boldsymbol{H}$), 4.64 – 4.55 (m, $CH_2CH_2C\boldsymbol{H}$), 4.50 (t, $CHCH_2O\boldsymbol{H}$), 4.34 (s, $C\boldsymbol{H}_{2(PVDC\ backbone)}$), 4.24 (s, $C\boldsymbol{H}_{2(PMAC\ backbone)}$), 4.14 (t, $SCH_2CH_2C\boldsymbol{H}_2$), 3.94 (s, $C\boldsymbol{H}_{2(PVDC\ backbone)}$), 3.85 (d, $CHOC\boldsymbol{H}_2C$), 3.67 (d, $CHOC\boldsymbol{H}_2C$), 3.61 – 3.48 (m, $HOC\boldsymbol{H}$), 3.34 (td, $HOC\boldsymbol{H}_2CH$), 2.59 – 2.53 (m,

SC***H***$_2$CH$_2$), 2.67 – 2.37 (m, SCH$_2$C***H***), 1.91 – 1.71 (m, SCH$_2$C***H***$_2$), 1.19 (d, C***H***$_3$); GPC (DMF, RI): $M_n$ ($Đ_M$) = 39,030 g/mol (1.14).

### 6.5.6.5 Functionalisation of P(VDC-*co*-MAC) (DP92) with 2-mercaptoethanol:

$^1$H NMR (400 MHz, *d*-DMSO) $\delta$ = 4.73 (t, CH$_2$CH$_2$O***H***), 4.61 (t, CH$_2$CH$_2$C***H***), 4.33 (s, C***H***$_{2(\text{PVDC backbone})}$), 4.32 – 4.17 (m, C***H***$_{2(\text{PMAC backbone})}$), 4.14 (t, SCH$_2$CH$_2$C***H***$_2$), 3.93 (s, C***H***$_{2(\text{PVDC backbone})}$), 3.84 (d, CHOC***H***$_2$C), 3.67 (d, CHOC***H***$_2$C), 3.51 (p, CH$_2$C***H***$_2$OH), 2.60 – 2.52 (m, HOCH$_2$C***H***$_2$SC***H***$_2$), 1.88 – 1.72 (m, HOCH$_2$CH$_2$SCH$_2$C***H***$_2$), 1.18 (d, C***H***$_3$); GPC (DMF, RI): $M_n$ ($Đ_M$) = 35,410 g/mol (1.09).

### 6.5.6.6 Functionalisation of P(VDC-*co*-MAC) (DP92) with thioglycolic acid:

$^1$H NMR (400 MHz, *d*-DMSO) $\delta$ = 12.55 (s, COO***H***), 4.60 (s, CH$_2$CH$_2$C***H***), 4.33 (s, C***H***$_{2(\text{PVDC backbone})}$), 4.30 – 4.18 (m, C***H***$_{2(\text{PMAC backbone})}$), 4.14 (t, SCH$_2$CH$_2$C***H***$_2$), 3.93 (s, C***H***$_{2(\text{PVDC backbone})}$), 3.84 (d, CHOC***H***$_2$C), 3.67 (d, CHOC***H***$_2$C), 3.22 (s, SC***H***$_2$COOH), 2.68 – 2.54 (m, C***H***$_2$SCH$_2$COOH), 1.91 – 1.74 (m, SCH$_2$C***H***$_2$), 1.18 (d, C***H***$_3$).

## 6.6 References


1. S. Koeller, J. Kadota, F. Peruch, A. Deffieux, N. Pinaud, I. Pianet, S. Massip, J. M. Leger, J. P. Desvergne and B. Bibal, *Chem. Eur. J.*, 2010, **16**, 4196-4205.
2. S. Koeller, J. Kadota, A. Deffieux, F. Peruch, S. Massip, J. M. Leger, J. P. Desvergne and B. Bibal, *J. Am. Chem. Soc.*, 2009, **131**, 15088-15089.
3. A. Alba, A. Schopp, A. P. D. Delgado, R. Cherif-Cheikh, B. Martin-Vaca and D. Bourissou, *J. Polym. Sci. A Polym. Chem.*, 2010, **48**, 959-965.
4. R. C. Pratt, B. G. G. Lohmeijer, D. A. Long, P. N. P. Lundberg, A. P. Dove, H. B. Li, C. G. Wade, R. M. Waymouth and J. L. Hedrick, *Macromolecules*, 2006, **39**, 7863-7871.
5. A. Gogoll, C. Johansson, A. Axen and H. Grennberg, *Chem. Eur. J.*, 2001, **7**, 396-403.
6. L. Toom, A. Kutt, I. Kaljurand, I. Leito, H. Ottosson, H. Grennberg and A. Gogoll, *J. Org. Chem.*, 2006, **71**, 7155-7164.
7. X. Hu, X. Chen, Z. Xie, S. Liu and X. Jing, *J. Polym. Sci. A Polym. Chem.*, 2007, **45**, 5518-5528.